UNIVERSITY COLLEGE LONDON (UCL)

Genetic Control of MTOR to Improve Adoptive T Cell Therapy of Tumours

Mathias Zech

A thesis submitted to the

University College London (UCL)

for the degree of

DOCTOR OF PHILOSOPHY

Institute of Immunity and Transplantation

Division of Infection and Immunity

UCL Medical School (Royal Free Campus)

January 2014

I, Mathias Zech, confirm that the work presented in this thesis is my own. Where information has been derived from other sources, I confirm that this has been indicated in the thesis.

Dedicated to my parents,
Annerose and Herbert,
and Judith.

First thesis: *We know a great deal. And we know not only many details of doubtful intellectual interest but also things which are of considerable practical significance and, what is even more important, which provide us with deep theoretical insight, and with a surprising understanding of the world.*

Second thesis: *Our ignorance is sobering and boundless. Indeed, it is precisely the staggering progress of natural sciences (to which my first thesis alludes) which constantly opens our eyes anew to our ignorance, even in the field of natural sciences themselves. This gives us a new twist to the Socratic idea of ignorance. With each step forward, with each problem which we solve, we not only discover new and unsolved problems, but we also discover that where we believed that we were standing on firm and safe grounds, all things are, in truth, insecure and in a state of flux.*

Sir Karl R. Popper

Das schönste Glück des denkenden Menschen ist, das Erforschliche erforscht zu haben und das Unerforschliche ruhig zu verehren.

Johann Wolfgang Goethe

Abstract

Adoptive T cell therapy to treat cancer in combination with re-directing specificity through T cell receptor (TCR) gene transfer, represents an effective therapeutic option. However, reduced effector responses due to the immunosuppressive tumour microenvironment and insufficient long-term engraftment of transferred cells represent two potential limitations. Tumours often employ mechanisms to inhibit T cell responses including secretion of TGFβ and depleting the tumour microenvironment of amino acids. The main aim of this PhD project was to develop a strategy to enhance T cell function for tumour therapy. The mammalian target of rapamycin (mTOR) pathway regulates CD8 T cell differentiation such that high mTOR activation leads to enhanced effector whilst low mTOR activation leads to increased T cell memory formation. Two retrovirus constructs have been designed whereby one expresses the positive mTOR regulator Rheb and the other expresses the negative mTOR regulator Pras40. Rheb transduction into CD8 T cells resulted in enhanced activation of mTOR, increased effector functions and partial resistance to TGFβ and low arginine concentrations. Pras40 overexpression led to a decrease in the activation of mTOR and reduced effector functions. Rheb transduced CD8 T cells expanded efficiently upon antigen encounter *in vivo*, followed by pronounced T cell contraction. Pras40 transduced T cells were unable to expand *in vivo*, but persisted at low numbers and acquired a central memory phenotype. Tumour bearing mice treated with TCR re-directed CD8 T cells transduced with Rheb showed improved tumour protection. Pras40 overexpression resulted in the loss of the protective function of TCR re-directed T cells.

Together, the data show that gene transfer can be used to regulate mTOR activity in T cells. Enhancing mTOR activity led to improved tumour control despite reducing memory formation. Permanent mTOR inhibition, on the other hand, preserved some memory characteristcs of T cells but deteriorated their tumour protective functions.

Acknowledgments

First and foremost, I want to express my gratitude to my supervisor Professor Hans Stauss for the opportunity to work in his laboratory. I have benefitted a lot from his expertise, knowledge and clear thinking and he taught me some lessons I am never going to forget. In particular he kept reminding me that a scientific question has to be formulated in a way that it is concise and allows experimental and/or empirical approach. My gratitude extends to Professor Ronjon Chakraverty who has been crucial in guiding the recent developments in my project. The scientific discussions with him kept challenging me to re-think concepts and allowed me to accept results the way they were. Next, I want to thank Dr Pedro Velica, with whom I had the great chance to collaborate with. What Hans and Ron were on a theoretical level, Pedro was on a practical level. The discussions and experiments with him were inspiring, fun and very often did not even end when we were enjoying a beer or pizza together. Of great importance to me was Angelika Holler. She made my move from Austria to London easier in the beginning, introduced me to the very basics of tissue culture and molecular work, supported me wherever she could and without restrictions and spoiled me with a cup of coffee from Starbucks everyday. I am grateful for all their help and enduring friendship!

I also want to thank Sara Ghorashian, Sharyn Thomas, Cecile Voisine, Iggy Chua, Maryam Ahmadi, Lyn Ambrose, Rebecca Pike, James Griffin, Emma Nicholson, Benjamin Carpenter, Benjamin Uttenthal, Shao-An Xue, Liquan Gao and Graham Wright for their impeccable helpful hands. I must not forget to thank Mario Perro for his visionary approach to science which continues to have a big influence on me despite the big geographical distance between us. I also want to thank the whole EU Advanced Teaching and Training for Adoptive Cell Therapy (ATTRACT) consortium for giving young researchers like myself the great chance to gain in-depth knowledge into the field of tumour immunology. Not only did the regular meetings with supervisors and students provide a platform for collaborations and networking, they were also good fun and resulted in new friendships. In particular I am thankful to Dr Anna Mondino and Professor Wolfgang Uckert for letting me spend some time in their laboratories where I was taught new techniques.

Lastly, I want to mention the people who keep supporting me morally. I am thankful to my parents for their continuous support of my education and their visits to London. They have always promoted my interests and kept understanding that it is

Table of Contents

List of Abbreviations

AA	amino acid
αCD4/8/…	anti-CD4/8/…
ACT	adoptive (T) cell therapy
AICD	activation induced cell death
AIDS	acquired immunodeficiency syndrome
ALL	acute lymphatic leukemia
AMPK	adenosine monophosphate-activated protein kinase
APC	antigen presenting cell
APC (FACS)	allophycocyanin
ATF4	activating transcription factor 4
ATP	adenosine triphosphate
BCA	bicinchoninic acid
BCG	bacillus Calmette-Guerin
Bcl2	B cell lymphoma 2
BLI	bioluminescence imaging
Blimp1	B lymphocyte induced maturation protein 1
BM	bone marrow
2β-ME	2β mercaptoethanol
bp	base pair
BRDU	bromdesoxyuridin
BrefA	brefeldin A
BSA	bovine serum albumin
Cα/β	constant α/β TCR chain
CAR	chimeric antigen receptor
CCR7	chemokine receptor 7
cDNA	complementary DNA
CD4/8/…	cluster of differentiation 4/8/…
CFSE	carboxyfluorescein succinimidyl ester
CLL	chronic lymphatic leukemia
CHOP	C/EBP homology protein
cIg	control immunoglobulin
CMV	cytomegalovirus
ConA	concanavalin A
CPM	counts per minute

cSMAC	central supramolecular activation cluster
CTLA4	cytotoxic T-lymphocyte antigen 4
Ctrl	control
CTS	central termination site
DAG	diacylglycerol
DAMP	danger associated molecular pattern
DC	dendritc cell
DGK	diacylglycerol kinase
DMSO	dimethylsulfoxid
DNA	deoxyribonucleic acid
dNTP	deoxy-nucleoside triphosphate
dsRBD	double-stranded RNA binding domain
DTT	DL-dithiothreitol
EACR	extracellular acidification rate
4EBP1	4E binding protein 1
EBV	Ebstein Barr virus
EDTA	ethylenediaminetetraacetic acid
EIF2α	eukaryotic initiation factor 2α
EIF2αK4	eukaryotic initiation factor 2α kinase 4
ELISA	enzyme linked immunosorbent assay
Eomes	eomesodermin
ER	endoplasmatic reticulum
ERK	extracellular signal regulated kinase
F_{ab}	antibody binding fragment
FACS	fluorescence activated cell sorter
FCS	fetal calf serum
FITC	fluorescein isothiocyanate
FKBP12	12-kDa FK506-binding protein
FOXO1/3	forkhead box proteins O1/3
FSC	forward scatter
FSC-H	FSC height
Fw	forward
GAP	GTPase activating protein
GCN2	general control non-derepressible 2
GDP	guanosine diphosphate
GFP	green fluorescent protein
GLUT1	glucose transporter 1

GTP	guanosine triphosphate
GvHD	graft versus host disease
GvL	graft versus leukemia
Gy	gray
GZMB	granzyme B
HEV	high endothelial venules
HIF	hypoxia inducible factor
HIV	human immunodeficiency virus
HLA-A2	human leukocyte antigen A2
HPV	human papillomavirus
HRP	horse radish peroxidase
IDO	indoleamine-2,3-dioxygenase
IFNα/β/γ	interferon α/β/γ
IFNγR	interferon γ receptor
IL2/4/…	interleuking 2/4/…
i.p.	intraperitoneal
IP3	inositol trisphosphate
IRES	internal ribosome entry site
IRF4	interferon regulatory factor 4
ISR	internal stress response
ITAMs	immunoreceptor tyrosine based activation motifs
i.v.	intravenous
IVIS	intravenous immunoglobulin substitution
kbp	kilo base pair
KLF2	Kruppel like factor 2
KLRG1	killer cell lectin-like receptor G1
LAT	linker for the activation of T cells
LCMV	lymphocytic choriomeningitis virus
LDH	lactate dehydrogenase
LMO2	LIM domain only 2
LN	lymph node
LTR	long terminal repeat
LTS	leucyl-tRNA synthetase
mAb	monoclonal antibody
MACS	magnetic activated cell sorter
MAGEA1	melanoma antigen family A 1
MAPK	mitogen-activated protein kinases

MART1	melanoma antigen recognized by T cells 1
MCA	methylcholanthrene
MFI	median/mean fluorescence intensity
MHC	major histocompatibility complex
miRNA	micro RNA
MDSC	myeloid derived suppressor cell
MLR	mixed lymphocyte reaction
MLV	murine lentivirus
Mo-MLV	Moloney murine lentivirus
MOI	multiplicity of infection
mRNA	messenger RNA
MSC	myeloid suppressor cell
1-MT	1-methyl-tryptophan
mTOR	mammalian target of rapamycin
mTORC1/2	mTOR complex 1/2
MΦ	macrophages
NAD	nicotinamide adenine dinucleotide
NAPDH	nicotinamide adenine dinucleotide phosphate
NEB	New England biolab
NFAT	nuclear factor of activated T cells
NFκB	nuclear factor κ B
NK	natural killer
NKT	natural killer T cell
NKR	natural killer receptor
NMA	non myeloablative
NOS	nitric oxide synthetase
NP	nucleoprotein
ns	not significant
nt	nucleotide
OCR	oxygen consumption rate
OVA	ovalbumin
OXPHOS	oxidative phosphorylation
PAMP	pathogen associated molecular pattern
PBMC	peripheral blood mononuclear cell
PBS	phosphate buffered saline
PCR	polymerase chain reaction
PD1	programmed death receptor 1

pDC	plasmacytoid dendritc cell
PDK1	phosphoinositide-dependent kinase 1
PD-L1	programmed death ligand 1
PE	phycoerythrin
pEIF2α	phosphorylated eukaryotic initiation factor 2α
PI	propidium iodide
PI3K	phosphatidylinositol-3-OH kinase
PKCα/θ	protein kinase C α/θ
PLCγ1	phospholipase C γ 1
pMHC	peptide MHC
PMSF	phenylmethylsulfonylfluorid
PNAd	peripheral node addressins
PPT	polypurine tract
Pras40	proline-rich Akt substrate of 40 kDa
pri-miRNA	primary miRNA
pS6	phosphorylated S6
pSMAC	peripheral supramolecular activation cluster
PTK	protein tyrosine kinase
PVDF	polyvinylidenfluorid
Rag	recombination activating gene
Raptor	regulatory-associated protein of mTOR
RECIST	response evaluation criteria in solid tumors
Rev	reverse
Rictor	Raptor independent companion of TOR
Rheb	ras homolog enriched in brain
RISC	RNA induced silencing complex
RNA	ribonucleic acid
ROS	reactive oxygen species
RT	reverse transcriptase
s.c.	subcutaneous
Sca1	stem cell antigen 1
SCID	severe combined deficiency patients
SDS	sodium dodecyl sulphate
shRNA	short hairprin RNA
SH2	src homology 2
SLP76	SH2 domain–containing leukocyte phosphoprotein of 76 kDa
S.O.C.	super optimal broth with catabolite repression

SREBP1/2	sterol regulatory element-binding protein 1/2
SSC	side scatter
SSC-W	SSC width
Stat	signal transducers and activators of transcription
S6K1	S6 kinase 1
TAA	tumour associated antigen
TAM	tumour associated macrophage
TAP1	transporter associated with antigen processing 1
T-bet	T-box expressed in T cells
TBI	total body irradiation
TBS	Tris-buffered saline
TCR	T cell receptor
TD	transduction
TDLN	tumour draining lymph node
TGFβ	transforming growth factor β
tGFP	turbo GFP
TIL	tumour infiltrating lymphocyte
TNFα	tumour necrosis factor α
TOP	terminal oligopyrimidine
TRAIL	TNF related apoptosis inducing ligand
Treg	regulatory T cell
tRNA	transfer RNA
TSA	tumour specific antigen
TSC	tuberous sclerosis complex
TU	transducing unit
Vα/β	variable α/β TCR chain
VC	vector control
WB	western blot
WPRE	Woodchuck hepatitis posttranscriptional regulatory element
WT	wild type
WT1	wilms tumour 1
ZAP70	zeta associated protein 70
-/-	knock out

List of Figures

Chapter 1   Introduction

1.1 General Tumour Immunology

"It is by no means inconceivable that small accumulations of tumour cells may develop and because of their possession of new antigenic potentialities provoke an effective immunological reaction with regression of the tumour and no clinical hint of its existence (M. Burnet 1957)."

In the process of tumour evolution, six hallmarks have been postulated, all of which constitute the malignant transformation of cells (D Hanahan and Weinberg 2000) : 1) sustaining proliferative capacity, 2) evading growth suppressors, 3) resisting cell death, 4) replicative immortality, 5) induction of angiogenesis and 6) invasion and metastasis. Only recently, 2 other hallmarks have been added to this list (Douglas Hanahan and Weinberg 2011): 7) re-programming metabolism and 8) evasion of immune destruction. The idea that the immune system can act as an extrinsic form of tumour suppression (Vesely et al. 2011) – a process called "cancer immunosurveillance" – has been around for many years. In this chapter, a summary of the historical development as well as empirical evidence for its validity shall be given.

1.1.1 History of the immunosurveillance hypothesis

Already in 1893, William Coley made the interesting observation that some patients suffering from sarcoma are able to reject their tumour when they develop erysipelas infection which causes a strong systemic immunological reaction. He went on to design a mix of toxins, called Coley's toxins, consisting of killed cultures of streptococci and bacillus prodigiosus, as a treatment for sarcoma patients which occasionally showed success (Coley 1991). However, Coley did not anticipate an involvement of the immune system yet. Instead he assumed a direct anti-tumour effect by the toxins themselves.

The idea that the immune system can prevent the evolution as well as control the progress of tumours has first been explicitly expressed in 1909. Paul Ehrlich made the prediction that the frequency of observed carcinomas would be much higher if

the immune system did not constitute a level of control to carcinogeneis[1] (Dunn, Old, and Schreiber 2004). This concept was later revived by H. N. Green (1954) and the 1960 nobel prize winner in medicine Sir Frank Macfarlane Burnet (1957). Green (1954) already proposed a crude concept of immunosurveillance and immunoediting – the process of tumour escape from the immune system – related to experiments on carcinogen-induced tumourigenesis:

> *"The primary neoplastic change, preceding the appearance of a spontaneous tumour, appeared to be held in check. (…) it would seem that in the spontaneous development of' the C3H mouse breast carcinoma the 'pre-cancerous' cell was eliciting an immune reaction, which restrained its outgrowth for some time. (…)*
>
> *The antibody response thus elicited either destroys the precancerous cell at some stage, or continuous hyperplasia leads to an ever-increasing immune reaction which may finally induce an adaptation in the cell* [i.e. immunoediting]. *The adaptation involves the loss of 'identity-protein' complexes, and the neoplastic cell emerges (Green 1954)."*

The immunosurveillance hypothesis gained much popularity thanks to Burnet. F. M. Burnet (1970) gives a good account of his concept of cancer immunosurveillance, providing evidence for the hypothesis that tumour cells have a different antigenic make-up than the cells they arise from, allowing the immune system to mount a response against them. He has been aware that cancer can evolve when the immune system is repressed, be it due to age, genetic alterations or drugs and he predicted that spontaneous tumour regressions are associated with immunological responses. Shortly after this publication, however, the theory lost its popularity again, mainly due to observations made by Stutman (1974) that athymic nude mice which lack the thymus and therefore cannot develop mature T cells show no increased susceptibility to methylcholanthrene (MCA) induced tumours (Galon et al. 2013). Only later it was realized that these mice harbor high levels of innate immune cells, in particular natural killer (NK) cells which are powerful killers of tumour cells (Cerwenka and Lanier 2001). Nonetheless, encouraging evidence accumulated

---

[1] http://www.pei.de/SharedDocs/Downloads/institut/veroeffentlichungen-von-paul-ehrlich/1906-1914/1909-karzinomforschung.pdf

throughout the years which supported the idea of an inter-relationship between the immune system and tumours. For example the discovery of a serum factor in bacillus Calmette-Guerin (BCG) infected mice which can induce necrosis in transplantable tumours *in vivo* by Carswell et al. (1975), termed tumour necrosis factor (TNF). Or the discovery that protection against spontaneous leukemia can be conferred upon vaccination with mutagenic and hence immunogenic variants (Van Pel, Vessière, and Boon 1983). Later on, van der Bruggen et al. (1991) described the first antigen (melanoma antigen family A 1 [MAGEA1]), expressed on melanoma tumour cells that can be recognized by cytotoxic T lymphocytes. These and other discoveries gave reason to hope that vaccination and immune therapy strategies can be implemented to treat cancer but preliminary attempts with interferon (IFN) α and interleukin (IL) 2 were of limited benefit (Galon et al. 2013). It was only at the beginning of the new millennium that the field of tumour immunology experienced a new and lasting renaissance.

1.1.2 Immunosurveillance and immunoediting in animal models

Following the development of transgenic mouse models with defined molecular immunodeficiencies it was possible to demonstrate a direct link between the immune system and carcinogenesis (Dunn, Old, and Schreiber 2004). The current model of tumour evolution in the context of an intact immune system (immunoediting) postulates 3 phases, all of which could be demonstrated under experimentally defined conditions (see also Figure 1):

1) During the *elimination phase*, transformed cells are cleared by the immune system.

2) During the *equilibrium phase*, tumour cells are held in check by the immune system. This means that tumour cells are present but do not become clinically apparent.

3) In the last *escape phase*, tumours develop strategies to evade control by the immune system.

Immunoediting
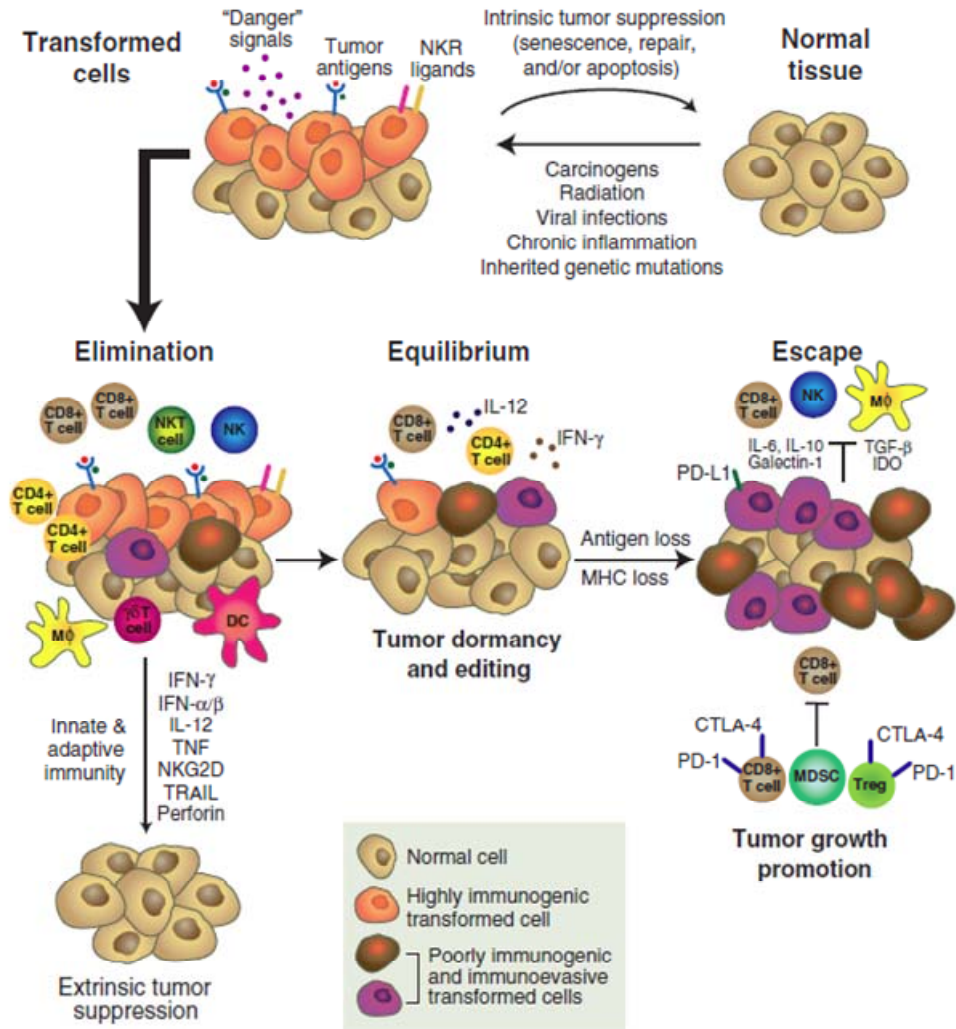
Figure 1: Immunosurveillance and immunoediting

The 3 phases of immunoediting are shown: On the left side of the picture, different components of the immune system contribute to the rejection of tumour. During the equilibrium phase in the middle, cancer cells are present but kept in check by T cells. And on the right hand side of the picture, the tumour has developed escape strategies to suppress and evade the immune response. Most of the components in the figure are discussed in more detail in the text, the abbreaviations of which can be found there. NKR=natural killer receptor. MΦ=Macrophages. TRAIL=TNF related apoptosis inducing ligand. Permission to reproduce this picture has been granted by Schreiber, Old, and Smyth (2011).

One milestone publication in the field of tumour immunology came out in 2001 by the group around Robert Schreiber at the Washington University School of Medicine. In a number of elegant experiments, the following observations were made (see also Figure 2) (Shankaran et al. 2001):

- Recombination activating gene 2 (Rag2) knock-out (-/-) mice which are unable to produce mature T, B and NKT cells as well as IFNγ receptor (IFNγR1)-/- and signal transducers and activators of transcription 1 (Stat1) -/- mice which are both insensitive to IFNγ and, finally, Rag2-/- X Stat1-/- (RkSk mice) develop significantly more sarcomas than wild type (WT) mice when injected subcutaneously with the carcinogen MCA.

- Rag2-/- and RkSk mice spontaneously develop significantly more neoplastic lesions of epithelial origin (intestine, mammary gland, lung) than WT mice.

- When MCA induced sarcomas isolated from either Rag2-/- or WT mice are injected into Rag2-/- mice, they grow progressively due to a lack of tumour control by the immune system. However, when injected into WT mice, 40 % of the tumours isolated from Rag2-/- mice are rejected whereas tumours isolated from WT mice grow progressively. This suggests that tumours isolated from immunocompromised hosts are more immunogenic than those from an immunocompetent host because they have not undergone immunoediting.

- Kaplan et al. (1998) have demonstrated the importance of IFNγ sensitivity of tumour cells for tumour surveillance. IFNγ boosts the antigen presentation machinery within cells, therefore rendering tumour cells more immunogenic. By overexpressing transporter associated with antigen processing 1 (TAP1) or H-2K^b, both of which are up-regulated by IFNγ in WT cells and involved in antigen presentation, in tumours derived from IFNγ insensitive mice, these tumours can suddenly be rejected when implanted into immunocompetent recipients. This rejection was shown to be dependent on CD4 and CD8 T cells as it is not observed when Rag2-/- mice are treated or when CD4 or CD8 T cells are depleted from WT mice.

Tumour elimination/escape
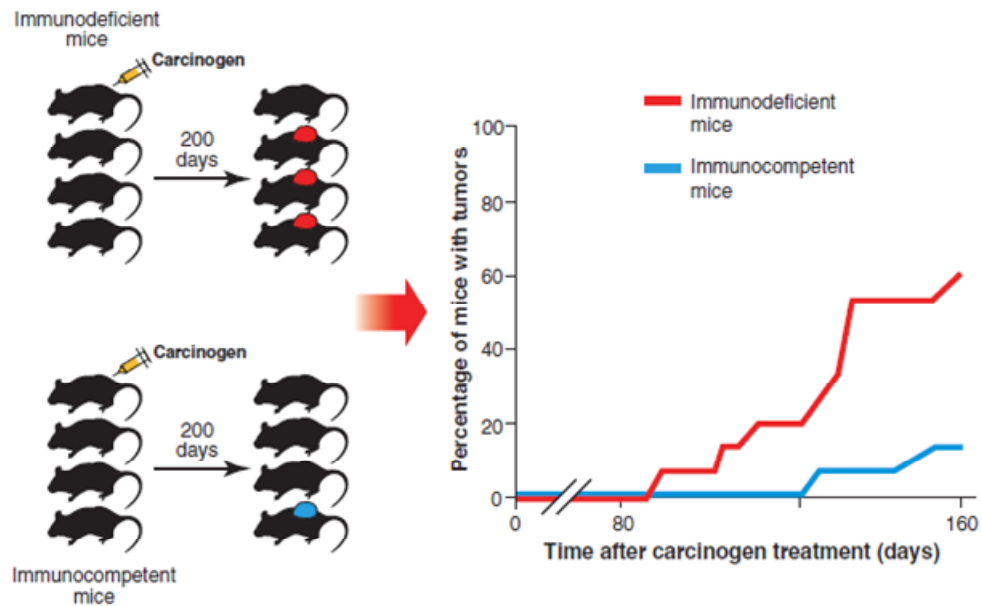
Figure 2: Tumour escape

Immunodeficient mice show increased susceptibility to carcinoge induced carcinogenesis. Permission to reproduce this picture has been granted by Schreiber, Old, and Smyth (2011).

In a follow-up paper by the same group, the postulated equilibrium phase could be demonstrated (Koebel et al. 2007). WT mice treated with MCA were observed for 200-230 days and the surviving subjects that did not develop tumour were injected with antibodies against CD4, CD8, IFNγ or IL12p40 (critical for IFNγ production). Sixty (60) % of the mice treated that way developed growing sarcomas, suggesting that microscopic malignant lesions are held in check by T cells in an IFNγ dependent fashion (see also Figure 3). Interestingly, NK cell depletion did not have any effect. Rag2-/- mice that did not form tumours after 200 days, on the other hand, did not develop *de novo* tumours when treated with the same antibodies, suggesting that tumour growth is not due to *de novo* formation in wild type mice. Additionally, stable masses could be detected in wild type mice treated with carcinogen – they revealed atypical histological characteristics – and cells of the immune system could be found within them (CD3+, B220+, F4/80+ cells). When isolated cells of these stable masses were transplanted into Rag-/- mice, they formed progressively growing tumours. Finally, it was shown that very late spontaneously arising sarcomas which have escaped control by the immune system reveal very low immunogenicity whereas stable masses maintain immunogenicity.
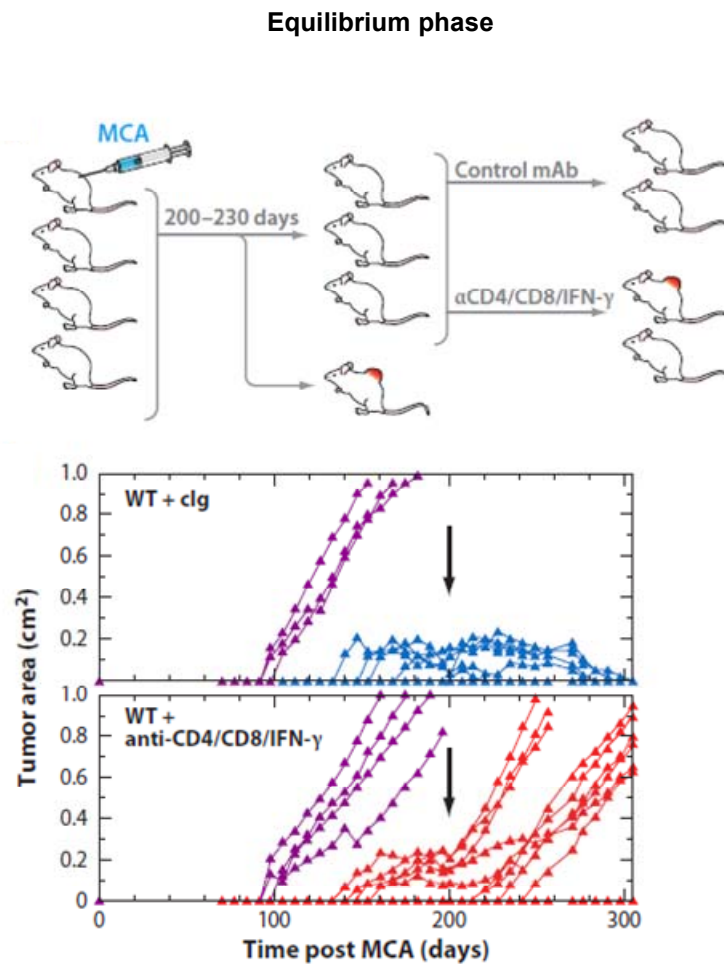
Equilibrium phase

Figure 3: Equilibrium phase

Many mice which are apparently unaffected by MCA treatment and show no clinical signs for tumour burden, develop outgrowing tumours upon CD4 and/or CD8 T cell or IFNγ depletion. mAb=monoclonal antibody. αCD4/8/IFNγ=anti-CD4/8/IFNγ antibody. cIg=control immunoglobulin. Permission to reproduce this picture has been granted by Annual Reviews, Inc. The picture was adopted from Vesely et al. (2011).

Through exome analysis, it could be demonstrated that T cells actively shape the immunogenicity of tumours. Whereas highly immunogenic cancer cells from MCA-induced tumours in Rag2-/- mice show tumour specific mutations which allow the mutated antigen (spectrin-β2) to be effectively presented by major histocompatibility complex class 1 (MHC 1) proteins to CD8 T cells, escape tumours following transplantation into WT mice do not show this phenomenon (Matsushita et al. 2012). In addition, CD8 T cells are able to change the biology of melanoma cells by inducing de-differentiation, allowing them to eventually escape the T cell response (Landsberg et al. 2012).

Antigen escape is not the only strategy allowing tumours to evade an immune response. T cells can also develop tolerance towards the tumour antigen they recognize (Willimsky and Blankenstein 2005), possibly already during the equilibrium phase (Willimsky et al. 2008). They are capable of developing a highly specified immunosuppressive microenvironment (Rabinovich, Gabrilovich, and Sotomayor 2007; Vesely et al. 2011). To name but a few strategies, tumours are able to recruit regulatory T cells (Tregs) (Terabe and Berzofsky 2004; Dürr et al. 2010), they can express the immunosuppressive cytokines transforming growth factor (TGF) β (Flavell et al. 2010; L Zhang et al. 2012) and IL10 (Aruga et al. 1997) and they can express programmed death ligand 1 (PD-L1) (Dong et al. 2002; Iwai et al. 2002). Additionally, they can express enzymes or recruit cells expressing these enzymes, which consume and thereby deplete amino acids, a process resulting in the inhibition of T cell responses, e.g. arginase 1 (consuming arginine) (Rodriguez et al. 2004; Zea et al. 2005) or indoleamine-2,3-deoxygenase (IDO) (consuming tryptophan) (Uyttenhove et al. 2003; Munn and Mellor 2007; Sharma et al. 2007). Recently it was shown that some of these immunosuppressive strategies (Treg infiltration, PD-L1, IDO up-regulation) are actively induced by tumour infiltrating CD8 T cells (Spranger et al. 2013). Some of these mechanisms are discussed in more detail further below.

In summary, it could be shown in a number of animal studies that the immune system, particularly T cells, can control the growth of tumours either by eliminating them or by keeping them in an equilibrium phase. The pro-inflammatory cytokine IFNγ plays a critical role in this process. During a process called "immunoediting", tumours can eventually escape control by the immune system by evading recognition, changing tumour biology and creating an immunosuppressive microenvironment.

1.1.3 Clinical evidence for immunosurveillance and immunoediting

In addition to evidence for immunosurveillance and immunoediting in animal studies, there is now a great deal of clinical data suggesting that tumour appearance is associated with a break-down of immune control (Vesely et al. 2011).

Patients suffering from immunodeficient conditions show increased susceptibility to tumours. Human immunodeficiency virus (HIV) patients with acquired immunodeficiency syndrome (AIDS) have a higher risk to develop virus associated malignancies, e.g. Ebstein Barr virus (EBV) associated lymphomas or human papilloma virus (HPV) related cervical carcinomas (Boshoff and Weiss 2002) but also to virus independent lung adenocarcinoma (Chaturvedi et al. 2007; Kirk et al. 2007). Furthermore, transplant patients have an increased risk of virus associated and virus independent malignancies (Vajdic et al. 2006; Vesely et al. 2011). Of note, kidney transplant patients have a 200-fold increased risk to develop non-melanoma skin cancer and a 2-10 fold risk to develop melanoma (Moloney et al. 2006).

Strong evidence for the intricate balance between T cell infiltration and colon cancer progress could be provided (Pagès et al. 2005; Galon et al. 2006). Excised colon cancer tissue samples from a large number of patients were examined. Immunostaining for CD3 and CD8 T cells, granzyme B (GZMB) and CD45RO (human T cell memory marker) revealed higher densities of immune cells within the center of the tumour as well as in the invasive margin in patients without compared to patients with tumour recurrence. Moreover, the level of T cell infiltration was shown to correlate with disease free survival in a way that allowed for stratification of patients into distinct groups with different prognoses. The predictive value of this method proved more accurate than the traditional pathological scoring system (TNM) that takes into account the level of local tissue infiltration of the tumour (T), lymph node (N) infiltration and the number of metastases (M). A strong immune cell infiltration was prognostically favorable even when the extent of tumour burden seemed big whereas low level immune cell infiltration proved prognostically bad, even when the tumour was localized and small (Galon et al. 2006). Similar results could be obtained for ovarian cancer (Lin Zhang et al. 2003) and melanoma patients (van Houdt et al. 2008).

The strongest evidence for immunological tumour elimination in humans, however, is the clonal expansion of T cells associated with the spontaneous regression of

melanoma lesions (Ferradini et al. 1993; Zorn and Hercend 1999; Vesely et al. 2011). This leads us to the next chapter. Because of the key role of T cells in eliminating and controlling tumours, can these cells be exploited for therapeutic purposes?

1.2 Adoptive T Cell Therapy

It has long been appreciated that T cells can effectively eliminate tumour cells. When leukemia patients receive a bone marrow transplant, the so called graft versus leukemia (GvL) effect of co-transferred donor T cells can result in the long term cure of patients (Horowitz et al. 1990). T cells can recognize and clear malignant cells very effectively due to an allogeneic mismatch between donor and recipient. The risk of graft versus host disease (GvHD), however, represents a major limitation to this therapeutic approach. GvHD is a systemic disease resulting in the destruction of healthy tissues and organs (e.g. skin, gut, liver) due to a wide-spread activation of co-transferred T cells (Ghorashian, Nicholson, and Stauss 2011). It would therefore be attractive to exploit the anti-cancerous effects of T cells in a way that does not cause harm to the patients. In addition, current endeavours are directed towards exploiting T cells for tumours other than haematological malignancies.

Two possible strategies to achieve these goals are:
1) The infusion of autologous tumour infiltrating lymphocytes (TILs) which have been expanded *ex vivo*.
2) The re-direction of autologous or allogeneic T cells towards tumour antigens by means of genetic modifications.

1.2.1 TIL trials

Rosenberg, Spiess, and Lafreniere (1986) described a method to isolate and expand TILs from excised tumours in mice *ex vivo* as early as in the mid 1980's. Mice suffering from tumour metastases which have been treated with a combination of the chemotherapeutic agent cyclophosphamide, TILs and IL2 showed a strong anti-tumour response. This technique was applied on 20 metastatic melanoma patients (S A Rosenberg et al. 1988). Eleven of them showed objective regression but most of them only for a limited period of time. The transferred cells persisted very poorly which is perhaps why the responses were not durable. Only with the advent of more elaborate pre-conditioning regimen before TIL transfusion it was possible to achieve better results. Pre-conditioning eliminates cells like Tregs and myeloid suppressor cells (MSCs) which can suppress T cell responses (Klebanoff, Khong, et al. 2005). It also allows the transferred cells to better compete for important cytokines by depleting endogenous T cells (Luca Gattinoni et al. 2005).

In 2002, Dudley et al. (2002) successfully expanded TILs from metastatic melanoma patients *ex vivo*. They were subsequently infused back into the patients after conditional non-myeloablative (NMA) lymphodepletion with cyclophosphamide and fludarabine which is now established as a standard pre-conditioning regimen resulting in good engraftment of transferred cells (Itzhaki et al. 2013). Although total body irradiation (TBI) can further enhance the therapeutic efficacy, this adds a level of toxicity which is not justifiable (Dudley et al. 2008; Steven A Rosenberg et al. 2011). Together with subsequent trials using the same strategy, up to this date 52 out of 93 patients (~56 %) have shown objective clinical responses (i.e. 30 % reduction in the sum of the longest diameters of measureable tumour lesions and no new lesions [Restifo, Dudley, and Rosenberg 2012]) according to the response evaluation criteria in solid tumors (RECIST), a clinical evaluation method taking into account objective measures of tumour shrinking, e.g. number of lesions disappearing, level of de-bulking etc. (Eisenhauer et al. 2009). Twenty (20) patients (~21 %) have presented with complete tumour regressions (no lesions detectable anymore) of which 19 (~20 %) are ongoing (Dudley 2011). In comparison, standard treatment with dacarbazine results in a clinical response rate of 16 % with short duration and IL2 treatment shows a 20 – 30 % objective response rate of which 5 – 7 % are durable complete responses (Atkins et al. 1999; Serrone et al. 2000; Itzhaki et al. 2013).

Even though adoptive cell therapy with isolated TILs is probably the best option for therapy resistant melanoma patients at the moment, there are several disadvantages related to this approach. The process of isolating and expanding TILs is laborious, expensive, and only available to patients with de-bulked tumour. In addition, to this date only melanoma patients were able to be treated that way. In the next chapters, the question of how to exploit T cells in a more efficient and global way will be addressed.

1.2.2 T cell receptor gene therapy

Pogulis and Pease (1998), Clay et al. (1999) and Kessels et al. (2000) made proof-of-principle experiments in which new T cell specificities were conferred through retrovirus transfer of the genetic codes of alpha (α) and beta (β) T cell receptor (TCR) chains of known antigen specificities. This opened the doors for the targeted re-direction of polyclonal T cells towards tumour antigens (see also Figure 4). Shortly thereafter it could be shown in mice that this method can indeed be used for the immunotherapy of tumours and viruses *in vivo* (Kessels et al. 2001).

TCR gene therapy
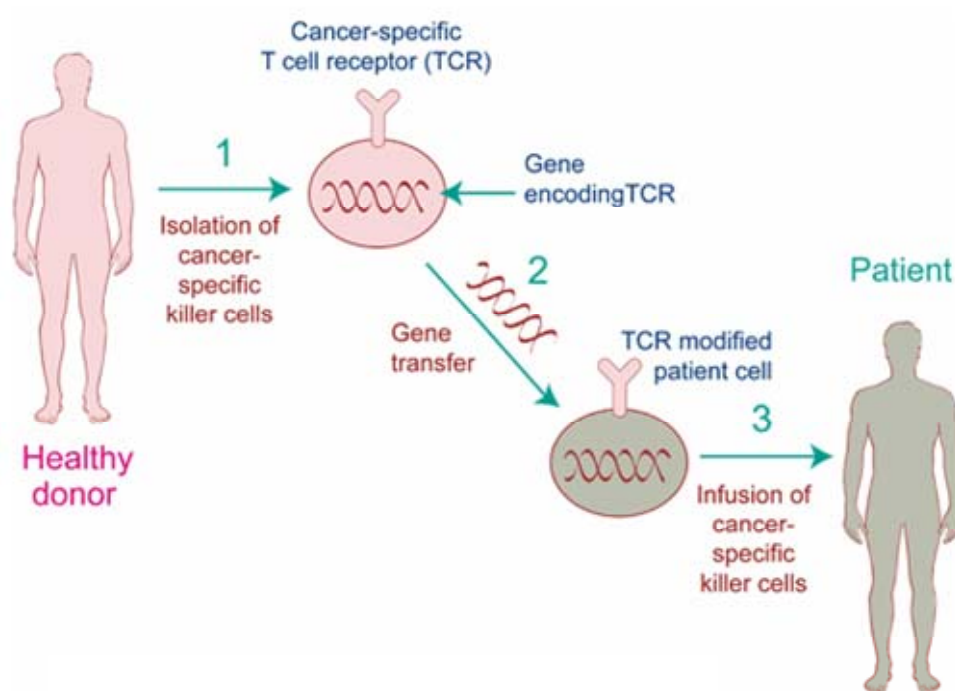
Figure 4: Principles of TCR gene therapy

Genes encoding for the α and β chains of a cancer specific TCR are isolated (1) and transferred through retrovirus transduction into patients T cells (2), enabling the patient to recognize and clear the tumour (3)[2].

---

[2] http://www.ucl.ac.uk/cancer/reshaematology/tumorimm

In 2006, Morgan et al. (2006) re-directed peripheral blood T cells from metastatic melanoma patients by means of T cell receptor (TCR) transduction post *ex vivo* activation. After conditional NMA lymphodepletion patients were treated with their own modified cells. The TCR used was derived from a responding T cell clone isolated from a patient reported in Dudley et al. (2002). It recognizes the immunogenic melanocyte differentiation antigen melanoma antigen recognized by T cells 1 (MART1) (Kawakami et al. 1994) in the context of human leukocyte antigen A2 (HLA-A2). In a follow-up trial in 2009 (Johnson et al. 2009), T cells isolated from patients were transduced with TCRs recognizing either MART1 or gp100 (another melanoma target) and expanded before they were re-infused back. So far, 13 out of 70 patients (~19 %) have shown objective clinical responses with a tendency to better response rates following TCR avidity optimization (Johnson et al. 2009). Recently, TCR gene therapy also showed efficacy in synovial cell sarcoma patients (4 out of 6 patients with objective clinical responses), where a TCR targeting the cancer testis antigen NY-ESO1 was used (Robbins et al. 2011). Additional TCRs in other tumour settings have been and are still being tested with different success rates (Kershaw, Westwood, and Darcy 2013).

The strategy of transferring TCR chains is restricted to antigens presented in the context of HLA. To circumvent this requirement, T cells can be re-directed towards tumour antigens through the transduction of so-called chimeric antigen receptors (CARs). In this case, the antigen binding moiety (F_{ab}) of an antibody recognizing a tumour antigen (not HLA restricted) is fused to TCR activation domains (Kochenderfer and Rosenberg 2013). When the CAR recognizes its cognate antigen, T cells are activated, kill targets and produce cytokines similar to conventional T cells.

Many leukemia types are derived from B cells which express the B cell specific marker CD19 (Gill and Porter 2013). A CAR was designed fusing the F_{ab} from a monoclonal anti-CD19 antibody with the TCR signaling domain CD3-zeta (CD3ξ) and the co-stimulatory signaling domain 4-1BB. Transduction of patient T cells with this receptor resulted in complete tumour remission in one lymphoma (Kochenderfer et al. 2010) and 2 out of 3 chronic lymphatic leukemia (CLL) patients (Porter et al. 2011; Kalos et al. 2011). More recently, also in 4 out of 5 adult patients with acute lymphoblastic leukemia (Brentjens et al. 2013) as well as 2 children suffering from acute lymphatic leukemia (ALL), one of which is ongoing (Grupp et al. 2013). This approach therefore represents a very promising treatment option for leukemia and lymphoma patients.

Even though these trials represent proof-of-principle that this strategy can potentially be applied to any type of cancer, there are certain challenges that need to be addressed and which are going to be discussed in more detail in the following chapter.

1.2.3 Challenges for T cell tumour therapy

Amongst the most important issues related to TCR gene therapy is the choice of the right target. Tumour antigens are divided into tumour specific antigens (TSAs) and tumour associated antigens (TAAs). TSAs are mutated antigens, exclusively found in tumour cells. They vary a lot between patients, making it very difficult to design TCRs which can be used in a large group of patients. Even though they would represent the best and safest types of antigens for TCR gene therapy, very few of them are known (Kunert et al. 2013).

TAAs are, ideally, antigens which are overexpressed on transformed cancer cells and expressed in limited amounts on non-transformed cells. For example, antigens expressed early during embryonic development or premature differentiation states can, in the course of carcinogenesis, be re-expressed and are usually not found on healthy tissues. Many of these are known and they are often shared within a group of patients, making them widely available for TCR targeting. So far, TCR gene therapy could only be achieved targeting TAAs. Examples are MART1, gp100 on melanoma cells and CD19 on leukemia cells. There is of course the risk of toxicity due to the potential of re-directed T cells to attack healthy cells which have not undergone malignant alteration (Hinrichs and Restifo 2013). Vitiligo (the destruction of normal melanocytes leaving behind white skin patches) is a common side effect resulting from the treatment of melanoma with TCR modified T cells but also toxicities in skin, eyes and ears are not uncommon. Patients treated with the CD19 CAR usually remain dependent on intravenous immunoglobulin infusions (IVIS) after treatment (Hinrichs and Restifo 2013). The goal for researchers is to design TCRs in a way that they are triggered only by the cells expressing high levels of these antigens, so the right activation threshold of TCRs is a matter of concern.

To avoid toxicities in future, other and potentially safer TAAs to target tumour cells are being tested. For instance the Wilms tumour antigen 1 (WT1) represents an attractive target for leukemia patients (Gao et al. 2000; Xue et al. 2004). WT1 is a transcription factor which plays a role in organ development during embryogenesis (Hohenstein and Hastie 2006) and was found to be highly expressed on leukemia

but not on normal haematopoietic cells (Martínez-Estrada et al. 2010; Xue et al. 2004). Another possibility to make TCR gene therapy safer is to define tumour cells based on a combination of antigens, rather than one antigen only. For example, a T cell can be equipped with 2 antigen recognizing receptors in a way that only ligation of both receptors allows the full activation of the T cells (one receptor providing the CD3, the other the co-stimulatory CD28 signal) (Wilkie et al. 2012). The inclusion of so-called safety switches, for instance suicide genes and antibody epitopes recognized by recombinant monoclonal antibodies are also strategies currently explored intensively (Kershaw, Westwood, and Darcy 2013). If transferred T cells cause overt toxicity, the cells can then either be instructed to undergo apoptosis or they are depleted through antibody treatment.

But even if a good target antigen has been found, other obstacles need to be overcome. It has already been mentioned that, as tumours evade immune responses through immunoediting, they acquire an immunosuppressive microenvironment. Amongst others, depletion of amino acids is a common strategy to inhibit T cell responses (Grohmann and Bronte 2010). Two enzymes were shown to be of significant importance in this context: IDO and arginase 1. IDO is a highly conserved L-tryptophan catabolizing enzyme catalyzing the first and rate limiting step in a chain of reactions resulting in the production of nicotinamide adenine dinucleotide (NAD) along the so-called kynurenine pathway (Grohmann and Bronte 2010). The immunoregulatory importance of IDO was first highlighted by Munn et al. (1998). They showed that IDO is crucial to prevent the T cell mediated rejection of the allogeneic fetus during pregnancy as the application of 1-methyl-tryptophan (1-MT) – a pharmacological inhibitor of IDO – results in the loss of fetus in WT but not in Rag1-/- mice. The same strategy, i.e. IDO expression, can be used by tumours to evade T cell responses directed against them. IDO was shown to be expressed either by tumour cells themselves (Uyttenhove et al. 2003) or by plasmacytoid dendritic cells (pDCs) in tumour draining lymph nodes (Munn et al. 2005). One way of how IDO is thought to exert its immunoregulatory function is by depleting the essential amino acid tryptophan from the microenvironment to starve T cells, as adding back tryptophan to *in vitro* co-cultures of T cells with IDO+ pDCs can reverse T cell inhibition (Munn et al. 2005). However, a possible contribution of kynurenines, metabolites of tryptophan resulting from IDO activity, is also debated (Grohmann and Bronte 2010).

Arginase 1, as the name indicates, catabolizes L-arginine to L-ornithine and urea and is constitutively expressed in the liver where the urea cycle is used for the

detoxification of ammonia. Arginase 1 expression can be induced in cells of the myeloid lineage by cytokines such as Interleukin 4 and 13 (IL4, IL13). Tumour associated macrophages (TAMs) and myeloid suppressor cells (MSCs), both of which are very common in the tumour microenvironment as well as in tumour draining lymph nodes and are known for their immunosuppressive functions (Gabrilovich and Nagaraj 2009), express high levels of arginase 1. Analogously to IDO, arginase 1 is thought to exert its inhibitory effect on T cells by depleting L-arginine which is a semi-essential amino acid as it cannot be synthesized in sufficient quantities under stressful conditions (Bronte and Zanovello 2005; Grivennikov, Greten, and Karin 2010; Rodriguez, Quiceno, and Ochoa 2007).

In addition to these metabolic challenges imposed on T cells, tumours can also secrete or express inhibitory signals. TGFβ and PD-L1 are amongst the most famous ones known to dampen T cell responses within tumours. TGFβ inhibits many effector functions of CD8 T cells, including the production of cytolytic agents (e.g. granzyme molecules) and cytokines (Flavell et al. 2010). PD-L1 can ligate the programmed death receptor 1 (PD1) on activated T cells and thereby negatively regulate their function (Iwai et al. 2002). Tregs (Spranger et al. 2013) are also very common and can exert their inhibitory functions through a number of mechanisms. For instance cytotoxic T-lymphocyte antigen 4 (CTLA4) is a crucial molecule for Treg function (Yong Zheng et al. 2008). It was shown to have a higher affinity for the co-stimulatory molecules B7.1 (CD80) or B7.2 (CD86) than CD28 on conventional T cells (Linsley et al. 1994). Tregs therefore compete better than conventional T cells for these co-stimulatory ligands which are expressed on antigen presenting cells (APCs), thereby preventing T cell activation (Qureshi et al. 2011). Ways to target these immunosuppressive evasion strategies are currently being developed and implemented in the clinical practice.

1.2.4 Immune modulatory strategies

Recently, two immune modulatory therapies have found their way into clinical practice. Treatment with the anti-CTLA4 antibody (Ipilimumab) showed some success for metastatic melanoma patients (Hodi et al. 2010). The median survival rate for patients receiving Ipilimumab with or without gp100 vaccination was ~10 months, as opposed to patients receiving vaccination only (~6.4 months median survival). Due to a lack of specificity associated with this treatment, most patients (60 %) suffered from immune related side effects (e.g. inflammation induced

diarrhea), as opposed to 32 % when patients received vaccination only. There are discussions of how this antibody exerts its function. It has recently been reported that treatment with anti-CTLA4 antibody can deplete Tregs from the tumour in a Fc dependent manner (Simpson et al. 2013). Consequently, Tregs cannot trans-endocytose B7 molecules from APCs, as this was reported by Qureshi et al. (2011), enabling them to provide a sufficient co-stimulatory signal to T cells.

Treatment with anti-PD1 (Lambrolizumab) (Hamid et al. 2012) or anti-PD-L1 (Brahmer et al. 2012) antibodies also holds promise for tumour patients. Advanced melanoma patients receiving Lambrolizumab showed a durable objective response rate of 38 % across all dose cohorts. Again in some cases, patients developed adverse reactions, most of them were mild but pneumonitis, renal failure and hypothyroidism were also observed and probably represent autoimmune manifestations. The mechanism of action is different compared to Ipilimumab. PD1 is up-regulated on activated T cells and serves as a negative feedback loop to control T cell activation. In other words, it serves as a T cell break to avoid uncontrolled T cell activation but can also cause loss of T cell function. Release of this break re-activates silenced T cells, enabling them to carry out their anti-tumour function (Iwai et al. 2002).

Combination therapy of melanoma patients with Ipilimumab and Nivolumab (another anti-PD1 antibody) at the maximum dose could further increase the objective response rate to 53 %, with all patients showing a tumour reduction of 80 % and more (Wolchok et al. 2013). However, also immune related side effects increased in this case.

With regards to amino acid consuming enzymes, inhibition of IDO by 1-MT was shown to result in the efficient rejection of IDO expressing tumours upon vaccination in mouse experiments. This rejection was T cell dependent as depletion of T cells with CD4 and CD8 antibodies could reverse the protective effects of 1-MT (Uyttenhove et al. 2003). There is currently a clinical trial underway looking at the effects of 1-MT treatement in patients with inoperable metastatic or refractory solid tumours[3].

Similarly, treatment with the phosphodiesterase 5 inhibitor Sildenafil was shown to interfere with immunosuppressive pathways exerted by tumour associated MSCs, particularly with arginase 1 and nitric oxide synthetase (NOS) enzymes, both of which use L-arginine as their substrate. Additionally, ACT with CD8 T cells

---

[3] http://clinicaltrials.gov/show/NCT00567931

combined with Sildenafil treatment could efficiently delay tumour outgrowth (Serafini et al. 2006).

These examples highlight the importance of boosting the immunity through an indirect way, i.e. by targeting components which impair T cell function. However, all of the just described strategies have 4 major disadvantages:

1) They rely on the fact that anti-tumour T cells are already present.
2) They are unspecific, enabling the activation not only of anti-tumour but also of potentially auto-reactive T cells, thereby causing toxicity.
3) Each of the just described interventions only target one immunosuppressive mechanism where most likely several are active at the same time, making a combination therapy unavoidable.
4) They rely on the transport of the drug to the right site.

It would therefore be highly attractive to design a strategy which overcomes some of these caveats at the same time. When T cells are re-directed towards tumour antigens (addressing the 1st and 4th point) it may be possible at the same time to modify them in a way that makes them resistant to a number of immunosuppressive tumour escape mechanisms (addressing the 3rd point). This would also enhance safety as only T cells specific for the tumour would be concerned (addressing the 2nd point). Transduction of a dominant negative TGFβ receptor mutant into tumour specific T cells represents an example of the feasibility of this approach (L Zhang et al. 2012). By interfering with TGFβ signaling in tumour specific CD8 and CD4 T cells, the therapeutic efficacy of these cells was shown to be dramatically improved.

Given that both tryptophan and arginine can be metabolized within the tumour by 2 different mechanisms and that most likely many other amino acids are depleted as well through a number of different enzymes (Cobbold et al. 2009), it would be highly attractive to design a strategy to maintain T cell effector functions under all of these conditions. To do so, it is necessary to know how low amino acid levels can be sensed by T cells and how this affects T cell biology. Historically, one kinase in particular has been suggested to play a key role in this process: general control non-derepressible 2 (GCN2).

1.3 GCN2

1.3.1 GCN2 signaling

GCN2, also called eukaryotic initiation factor 2 alpha kinase 4 (EIF2αK4), is a serine/threonine protein kinase activated by uncharged transfer ribonucleic acid (tRNA) molecules. Uncharged tRNAs accumulate in the absence of amino acids when tRNAs specific for any one amino acid cannot be loaded (Zaborske et al. 2009). GCN2 then activates the internal stress response (ISR) pathway, eventually resulting in the phosphorylation of eukaryotic initiation factor 2 alpha (eIF2α) (see also Figure 5). This causes a general stop of protein translation with the exception of activating transcription factor 4 (ATF4) which further contributes to the silencing of the cell (Kilberg, Shan, and Su 2009). ATF4, for instance, up-regulates C/EBP homology protein (CHOP) which itself is a transcription factor that controls stress induced target genes involved in apoptosis and cell regeneration (Harding et al. 2000). In the case of T cells, these effects are thought to prevent normal T cell function under amino acid starved conditions.

1.3.2 GCN2 in T cells

Munn et al. (2005) were the first ones to report that T cells from GCN2-/- mice are resistant to the effects of tryptophan starvation. They observed that in a mixed lymphocyte reaction (MLR), responder T cells are unable to proliferate in the presence of IDO expressing plasmacytoid dendritic cells (pDCs) which were isolated from tumour draining lymph nodes (TDLN). This can be reversed when either tryptophan is added in excess or when IDO is inhibited by 1-MT. They also found that stimulated T cells cultured in tryptophan free medium for 24 hours highly up-regulate CHOP, indicating that these cells activate the GCN2 pathway. T cells from GCN2-/- mice, on the other hand, do not upregulate CHOP. The same could be observed when the cells were cultured in the presence of IDO expressing pDCs. In addition, GCN2-/- T cells are able to proliferate in the presence of IDO expressing cells to the same extent as when 1-MT is added to the WT T cell cultures. This also proves to be the case *in vivo*. When mice are injected with OT-1 T cells lacking GCN2, they are still able to proliferate upon injection of IDO expressing and ovalbumin (OVA) loaded pDCs, as opposed to GCN2 competent T cells. The authors further argue that tryptophan starvation via the GCN2 pathway induces T cell anergy, as treatment with IL2 *in vitro* under normal culture conditions can rescue

the T cells in a way that they are responsive again whereas untreated T cells remain quiescent when the cells are stimulated.

The GCN2 pathway
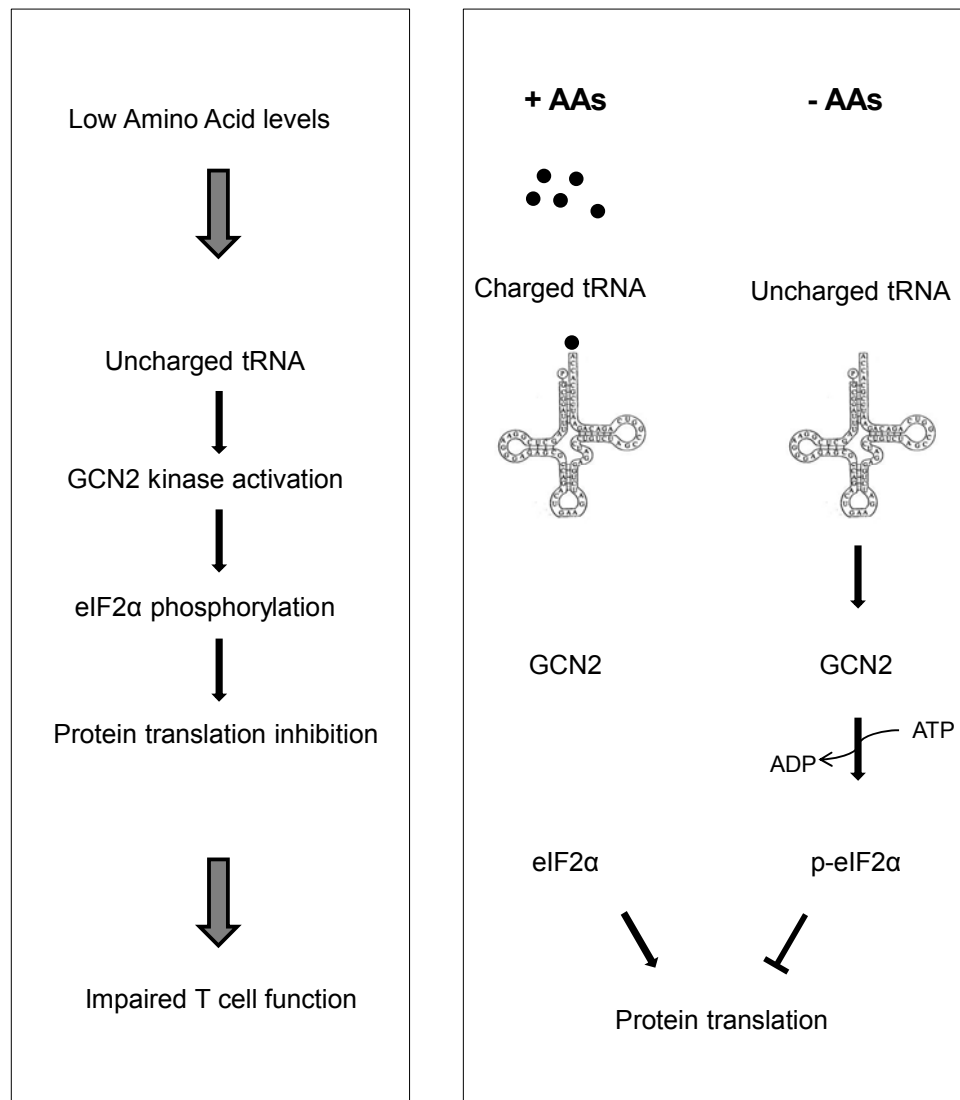
Figure 5: GCN2 pathway

Activation of GCN2 by uncharged tRNA molecules due to a lack of amino acids leads to the stop of protein translation. eif2α=eukaryotic initiation factor 2 α. p-eif2α=phosphorylated eukaryotic initiation factor 2 α. AAs=amino acids.

It is noteworthy to point out that GCN2-/- T cells were not tested in their ability to reject tumours that have employed an immune evasion strategy based on IDO expression.

Later on, similar results could be obtained by Rodriguez, Quiceno, and Ochoa (2007), this time in conjunction with arginine starvation. The authors show that arginine starvation arrests T cells in the G_0-G_1 phase of the cell cycle. They are unable to proliferate and up-regulate crucial cell cycle proteins like cyclin D3. The authors suggest an involvement of GCN2 in this inhibition as T cells from GCN2-/- mice can still proliferate in the absence of arginine as well as upregulate cyclin D3. In the discussion, they mention that T cells from GCN2-/- mice are also capable of proliferating in the presence of arginase expressing myeloid suppressor cells (MSCs) and that T cells maintain expression of the CD3ξ chain. CD3ξ chain down-regulation is one mechanism of how arginase expression and therefore arginine deprivation can impair T cell functions (Zea et al. 2005). However, they did not show these results.

Taken together, GCN2 represents an interesting target to enhance T cell effector functions under amino acid starved conditions.

The first aim of this PhD project was to develop a strategy to down-regulate GCN2 in T cells in order to make them resistant to the immunosuppressive effects of amino acid depletion within tumours.

1.4 The Choice of the Right Cell Type

Besides trying to design effective TCRs against safe and common tumour antigens, to develop safety switches for T cells and to explore strategies to overcome the immunosuppressive microenvironment, researchers are trying to use the right type of differentiated T cells to guarantee optimal therapeutic outcome by adoptive T cell therapy. For both, TIL as well as TCR gene therapy, high numbers of T cells are required. To this end, T cells are usually expanded by means of polyclonal stimulation with CD3 stimuli and IL2. Very often, this drives T cells into end stage effector cell differentiation. There is a risk, however, that these cells, despite their good effector potential *in vitro*, do not persist long enough to clear the tumour. Naïve and memory T cells may therefore harbor a higher therapeutic potential. However, in this case the problem prevails that due to the immunosuppressive microenvironment (discussed in more detail in chapter 1.2.3), the differentiation into effector cells cannot occur. A crucial question related to adoptive T cell therapy therefore is: are CD8 effector or memory T cells more powerful?

1.4.1 The linear T cell differentiation model

Classically, a T cell response is divided into 4 phases (Williams and Bevan 2007) (see also Figure 6):

1) The **expansion phase** in which a high number of effector T cells is being produced.
2) The **contraction phase**, in which most of the effector cells die off after the pathogen or the tumour has been cleared.
3) The **memory phase**, in which the cells which have been left behind pre-dominate.
4) The **re-call response** in which, upon re-encounter with the antigen, memory T cells mount another response which again results in the clearance of the pathological agent.

The T cell response
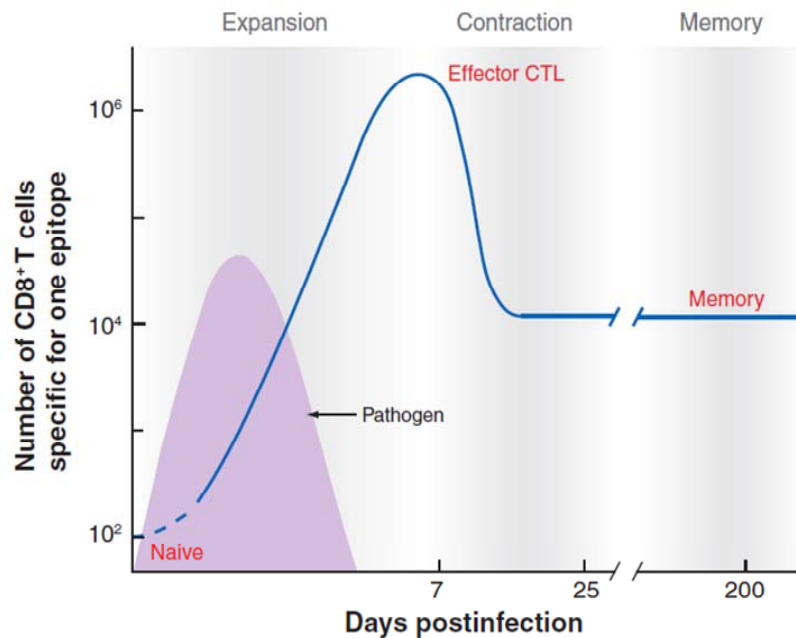
Figure 6: The T cell response

A typical T cell response consists of 1) an expansion phase, in which a high number of effector T cells is being produced; 2) a contraction phase, in which most of the effector cells die off after the pathogen or the tumour has been cleared; and 3) a memory phase, in which the cells which have been left behind pre-dominate.. Upon re-challenge with the same pathogen, memory T cells can mount an effective re-call response. Permission to reproduce this picture has been granted by Annual Reviews, Inc and Williams and Bevan (2007).

There are two main models of effector and memory T cell differentiation (see also Figure 7). The so called "On-Off-On" model predicts that memory T cells are derived from effector T cells (the "on" and "off" states refer to the phenotypic and metabolic effector and memory states on a per cell basis). The "Developmental Model" claims that effector T cells represent the end stage of a linear differentiation process that starts with naïve and goes through the stages of stem cell memory, central memory and effector memory T cells (Restifo and Gattinoni 2013). In this case, effector T cells would be unable to produce memory T cells whereas the opposite is possible.

T cell differentiation models
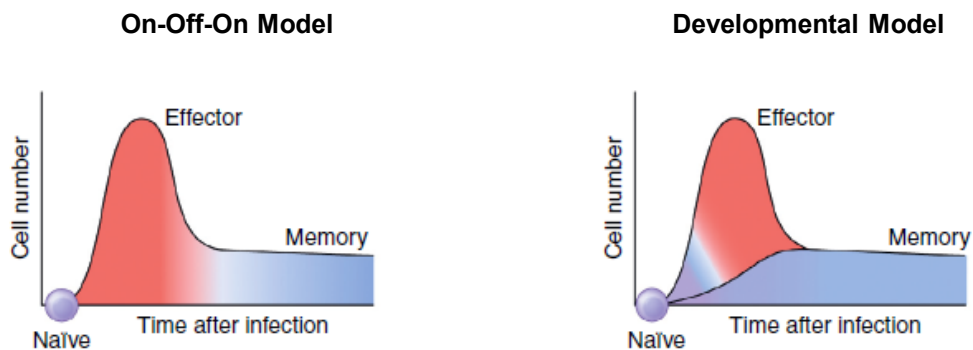
Figure 7: T cell differentiation models

The "On-Off-On model" (left picture) predicts the origin of memory out of effector T cells. The "Developmental model" (right picture) considers effector as more differentiated than memory T cells and therefore the latter as the origin of the former. Red represents effector, blue represents memory formation. Permission to reproduce this picture has been granted by Restifo and Gattinoni (2013).

Single cell transfer experiments demonstrated that one naïve T cell can give rise to all other types of differentiated T cells (Stemberger et al. 2007). However, Plumlee et al. (2013) showed that single cell transfer of naïve T cells mainly results in memory, while single cell transfer of memory T cells pre-dominantly results in effector T cell differentiation upon antigen encounter. In addition, single cell tracking of naïve monoclonal TCR transgenic T cells stimulated *in vivo* revealed that cells which pre-dominantly contribute to the initial expansion phase are not necessarily more likely to contribute to the memory T cell response later on. In fact, some of the T cell families that respond highly upon first antigen encounter, do not seem to take part in the memory re-call response at all. On the other hand, it was shown that those memory cells responding highly to re-challenge are likely to respond well to a 2nd re-challenge, suggesting that once memory is imprinted, it is permanent (Buchholz et al. 2013; Gerlach et al. 2013). In addition, effector cells were shown not to be able to differentiate into memory cells *in vitro* (Luca Gattinoni et al. 2011) and have shorter telomeres and less telomerase activity than memory T cells (Papagno et al. 2004). This is in contradiction with the "On-Off-On" model where one would expect that memory cells are mostly derived from effector cells (see also Figure 8). All of this strongly argues for the "Developmental Model" of T cell differentiation.

The linear differentiation model
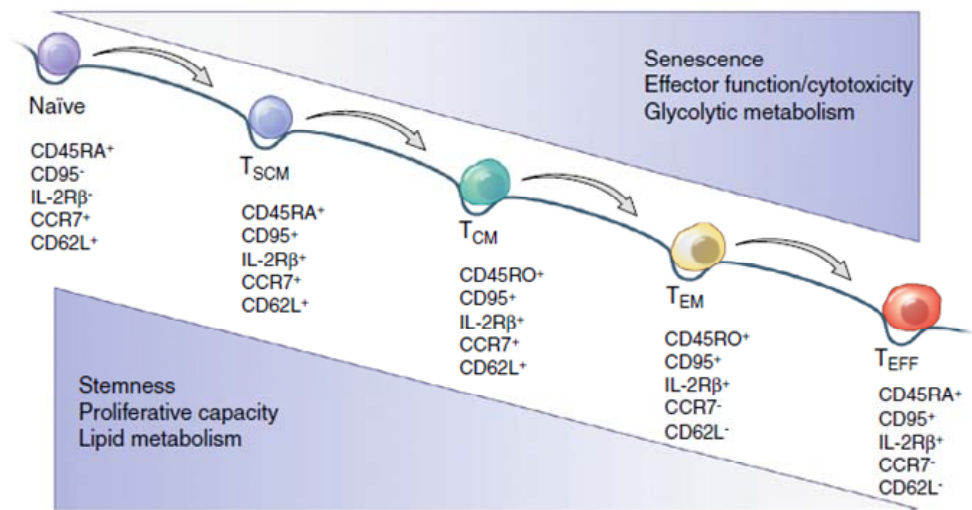
Figure 8: The linear differentiation model

T cell activation as a linear differentiation process. Once a naïve T cell get activated, it undergoes differentiation from stem cell memory to central and effector memory through to effector T cell. Each differentiation step is characterized by a distinct expression of markers. The combination of markers indicated in this diagram applies to human cells. SCM=stem cell memory. CM=central memory. EM=effector memory. EFF=effector. Permission to reproduce this picture has been granted by Restifo and Gattinoni (2013).

For adoptive T cell therapy, this means that the less differentiated the transferred T cells are, the more effector cells they should be able to produce without limitations. Consequently, it may seem beneficial for adoptive T cell therapy to transfer stem cell or central memory T cells in order to guarantee a robust and lasting effector response.

Indeed, Klebanoff, Gattinoni, et al. (2005) have shown that central memory confer better tumour protection than effector T cells upon adoptive T cell transfer into tumour bearing mice. In addition it could be demonstrated that the more differentiated T cells are, the better their function *in vitro* (effector>memory>naïve) but the worse their function *in vivo* (naïve>memory>effector) (L. Gattinoni 2005; Hinrichs et al. 2009; Hinrichs et al. 2011). Hence, one key goal to improve adoptive T cell therapy is to maintain T cells in a less differentiated state to improve adoptive T cell tumour therapy.

1.4.2 Strategies to promote T cell memory differentiation

Several strategies have been developed and suggested to increase the yield of memory T cells following *in vitro* culture or *in vivo* T cell stimulation. All of them seem to point in the same direction that high T cell stimulation, through a strong TCR signal and certain effector cytokines like IL2 and IL12 drives effector whereas T cells which show a reduced activation pattern preferentially differentiate into memory T cells.

Treatment of T cells with cytokines promoting memory, such as IL7 and IL15, were shown to drive differentiation of naïve T cells into stem cell memory T cells (Cieri et al. 2013). This may provide insights about culture requirements of, for example, TILs during *in vitro* expansion to maintain them in a less differentiated state before infusing them back into patients.

To avoid T cell activation and thereby maintain them in a fairly undifferentiated state in the process of TCR transduction, lentivirus transduction protocols have been developed. HIV-1 derived lentivirus, as opposed to other retrovirus systems such as the murine lentivirus (MLV) derived retrovirus, can infect quiescent and resting cells, including naïve T cells. Perro et al. (2010) succeeded in transducing human T cells with the WT1 TCR (Gao et al. 2000) in the presence of IL15 and IL21. This resulted in the production of multi-functional T cells *in vitro* which were superior to transduced cells which have been polyclonally activated prior to transduction.

Other strategies to promote differentiation into memory T cells are inhibition of Wnt (Luca Gattinoni et al. 2009) and mTOR signaling (Araki et al. 2009) during T cell activation. These two approaches may, in fact, be intricately related as Wnt was shown to activate mTOR signaling (Inoki et al. 2006). Inhibition of mTOR as a way to manufacture memory T cells will be further discussed in chapter 1.6. Since T cells, in the process of differentiating into effector T cells undergo a metabolic switch from lipid oxidation and oxidative phosphorylation to aerobic glycolysis (D. Finlay and Cantrell 2011), inhibiting this transition has recently emerged as another way to increase the yield of highly functional memory T cells (Sukumar et al. 2013).

1.4.3 Strategies to promote T cell effector responses

Even though memory cells may have the intrinsic potential to give an almost infinite rise to effector cells, the differentiation into effector cells still needs to take place for tumour therapy to be successful. Under certain conditions, however, this is not possible due to reasons listed in chapter 1.2.3. This is why strategies have been

developed to increase T cell effector functions, in particular under conditions where this is impaired.

One common and fairly simple strategy to enhance T cell activation is through TCR affinity maturation. This is expected to result in an enhanced TCR driven signal, allowing the T cell to mount a stronger response. Indeed, it could be shown that high affinity TCR – peptide MHC (pMHC) interactions lead to asymmetric T cell division, resulting in the production of potent effector cells which can infiltrate and destroy the pancreatic target tissue in a diabetic mouse model whereas low affinity TCRs were not able to cause this pathology and show a different division profile (King et al. 2012). However, increasing the affinity of TCRs, even though this may accelerate proximal signaling, does not necessarily increase the functional avidity of T cells (Thomas et al. 2011). The nature of T cell activation may require serial triggering by antigen which is only possible when the TCR occasionally releases its target (Rachmilewitz 2008). Increasing affinity may therefore only be beneficial when antigen load is saturating, as this occurs, for example, in virus infections but not when antigen is scarce, as this is often the case for tumours. In addition, there is the risk of so-called off-target toxicities by un-specifically increasing affinity for other antigens (Linette et al. 2013).

An alternative is to increase the functional avidity of tumour specific T cells through co-transfer of the TCR signaling molecule CD3. Together with the transduction of the nucleoprotein (NP) specific F5 TCR, which can recognize NP on stably transfected EL4 lymphoma cells, this was shown to result in a remarkable increase in T cell avidity *in vitro* and, consequently, improved tumour killing *in vivo* (Ahmadi et al. 2011). Supporting T cell signaling is also a common strategy to improve CAR-redirected T cell therapies. Different co-stimulatory domains attached to the CAR can confer multi-functionality. Carpenito et al. (2009), for example, report superior function of CAR T cells upon inclusion of a 4-1BB (CD137) in addition to a CD28 signaling domain. Also, pharmacological inhibition of diacylglycerol kinase (DGK) signaling which counteracts the diacylglycerol (DAG) and extracellular signal regulated kinase (ERK) signaling pathway triggered by the TCR can enhance effector functions and anti-tumour properties of CAR transduced T cells (Riese et al. 2013). However, it seems that a certain balance in overall signaling is crucial as Hombach, Rappl, and Abken (2013) have shown that when cytokine induced killer cells are armed with a CAR containing CD28 as well as OX40 domains, even though this results in enhanced IFNγ production *in vitro*, these cells are also more prone to activation induced cell death (AICD) and therefore perform worse in their ability to kill tumour *in vivo*.

Finally, T cells which have been equipped with the pro-inflammatory cytokine IL12 were shown to be more effective in their ability to reject tumour cells (Kerkar et al. 2010), again at the expense of long term persistence. IL12 acts in 2 ways:

1) It converts myeloid suppressor cells into stimulator cells (Kerkar et al. 2011) which either activate T cells or, through upregulation of Fas, kill tumour cells through Fas receptor binding (Kerkar et al. 2013).

2) It acts in an autocrine fashion on T cells to promote effector functions (Gerner et al. 2013). However, since IL12 is secreted and can gain access to the periphery, this approach may be toxic and needs further refinement. One such attempt has been to regulate IL12 expression through the use of a nuclear factor of activated T cells (NFAT) inducible expression cassette (Ling Zhang et al. 2011).

Taken together, it appears to be important to support both, long term engraftment of T cells as well as their ability to differentiate into potent effector cells, depending on the respective requirements in each situation. At present it is not known whether development of effector T cells or formation of T cell memory is a rate limiting step to achieve tumour immunity; this question will be further explored in this thesis.

One major signaling integrator determining whether a cell will become an effector or a memory T cell is the mTOR pathway (Delgoffe and Powell 2009) which therefore represents an interesting target for adoptive T cell therapy.

1.5 T Cell Signaling

T cell activation starts when antigen presenting cells (APCs), in particular dendritic cells (DCs) (Williams and Bevan 2007), which have been licensed by pathogen or danger associated molecular pattern signals (PAMPs/DAMPs) signals (Schenten and Medzhitov 2011), present a pathogen derived peptide in the context of MHC to a circulating antigen specific T cell carrying the right TCR to recognize this complex, an event which usually occurs in lymph nodes or mucosa associated lymphoid tissues (MALT). Depending on the type of MHC molecule (MHC class 1 or 2) either CD8 or CD4 molecules strengthen this binding and sustain a strong T cell signal. This would correspond to what is traditionally known as "signal 1" (Curtsinger and Mescher 2010). To avoid anergy, however, and consequently unresponsiveness, a co-stimulatory signal needs to accompany the TCR recognition process (Wells 2009). This is typically achieved through the interaction of CD28 on T cells and B7.1/2 on APCs ("signal 2"). Following these signals, T cells prepare to undergo massive clonal expansion. To guarantee and enable good T cell function and survival, cytokines are required. In the case of CD8 T cell effector production, IL2 is crucial in this context. This cytokine is either provided in an autocrine fashion or in a paracrine manner through CD4 T cell help (Boyman and Sprent 2012). Finally, to avoid overactivation of T cells, regulatory factors come into play. Next to autoinhibitory molecules on CD8 T cells, such as PD1, a T cell response can be regulated through Treg derived factors like TGFβ (Mueller 2010). The mTOR pathway has emerged as a converging node of T cell activation signals which helps to guide the differentiation of T cells, based on the availability of T cell signals and nutrients. Before this will be discussed in more detail, some general remarks about canonical T cell signaling elements are necessary.

1.5.1 TCR signaling cascade

Recognition of pMHC by a specific TCR needs to occur for a physiological T cell signal to be initiated. The mechanisms of early signaling initiation are still under debate and several models are currently being tested to explain how pMHC recognition can kick off the signaling cascade. TCR aggregation has long been thought to be important but this hypothesis has been confronted with the observation that TCR aggregates are pre-formed on nonactivated T cells (Smith-Garvin, Koretzky, and Jordan 2009). Because the TCR itself has no intracellular signaling domains, it is the CD3 co-receptor which serves as the key most proximal intracellular signaling molecule. Following TCR-pMHC binding, the CD3 molecule is

phosphorylated at so called immunoreceptor tyrosine based activation motifs (ITAMs) by the protein tyrosine kinases (PTKs) Lyn and Fck which are associated with either the TCR or the CD4 and CD8 co-receptors (Irving and Weiss 1991). This causes the recruitment of the 70 kDa zeta associated phosphoprotein (ZAP70) to the CD3ζ chain (Chan et al. 1992). ZAP70 can then phosphorylate the linker for the activation of T cells (LAT) (W. Zhang et al. 1998) as well as well as Src homology 2 (SH2) domain–containing leukocyte phosphoprotein of 76 kDa (SLP76) (Bubeck Wardenburg et al. 1996), both of which form a signaling complex to finally activate phospholipase C γ 1 (PLCγ1) (Smith-Garvin, Koretzky, and Jordan 2009). This enzyme produces inositol trisphosphate (IP3) and DAG, the latter of which initiates the Ras-Raf1 pathway, involving a number of MAP kinases as intermediate signaling steps. Ultimately this results in the extracellular signal regulated kinase 1 and 2 (ERK 1/2) dependent activation of the transcription factor ELK 1 which then activates the transcription factors Jun/Fos (activated protein 1 [AP1]) as well as Stat3 (Genot and Cantrell 2000). These factors then initiate the transcription of a myriad of molecules crucial for T cell activation. DAG is also involved in regulating the transcription factor nuclear factor κ B (NFκB) through protein kinase C θ (PKCθ) dependent phosphorylation and inactivation of the inhibitor of κB (IκB). IP3, on the other hand, is required for the activation of calcium influx from outside the cell as well as from the endoplasmic reticulum (ER). Intracellular rise of Ca^{2+} activates Ca^{2+} and calmodulin dependent transcription factors as well as the phosphatase calcineurin. Eventually, calcineurin dephosphorylates and thereby activates the nuclear factor of activated T cells (NFAT) which upon cooperation with AP1, Foxp3, and different Stat proteins determines the function of T cells through targeted activation of specific genes, e.g. Tbet or GATA3 (Smith-Garvin, Koretzky, and Jordan 2009). Co-stimulation through CD28 is aimed at a myriad of targets and mainly serves to strengthen and prolong the TCR signal, to promote survival and cytokine production (e.g. IL2) as well as to regulate T cell metabolism. It is thought to involve PI3K, PDK1, Vav1 and Akt which can all act on several target molecules (Smith-Garvin, Koretzky, and Jordan 2009), amongst which is also mTOR (Figure 9). Finally, integrin activation through so-called "inside-out" signaling from the TCR is meant to stabilize the interaction between T cells and APCs (Ménasché et al. 2007). This results in some distinct signaling complex patterns, including the central supramolecular activation cluster (cSMAC) which is TCR rich as well as the peripheral supramolecular activation cluster (pSMAC) which is integrin rich. Once the T cell is programmed to undergo expansion and exert effector functions, T cells depend on additional signals to maintain their function, one of which is IL2.
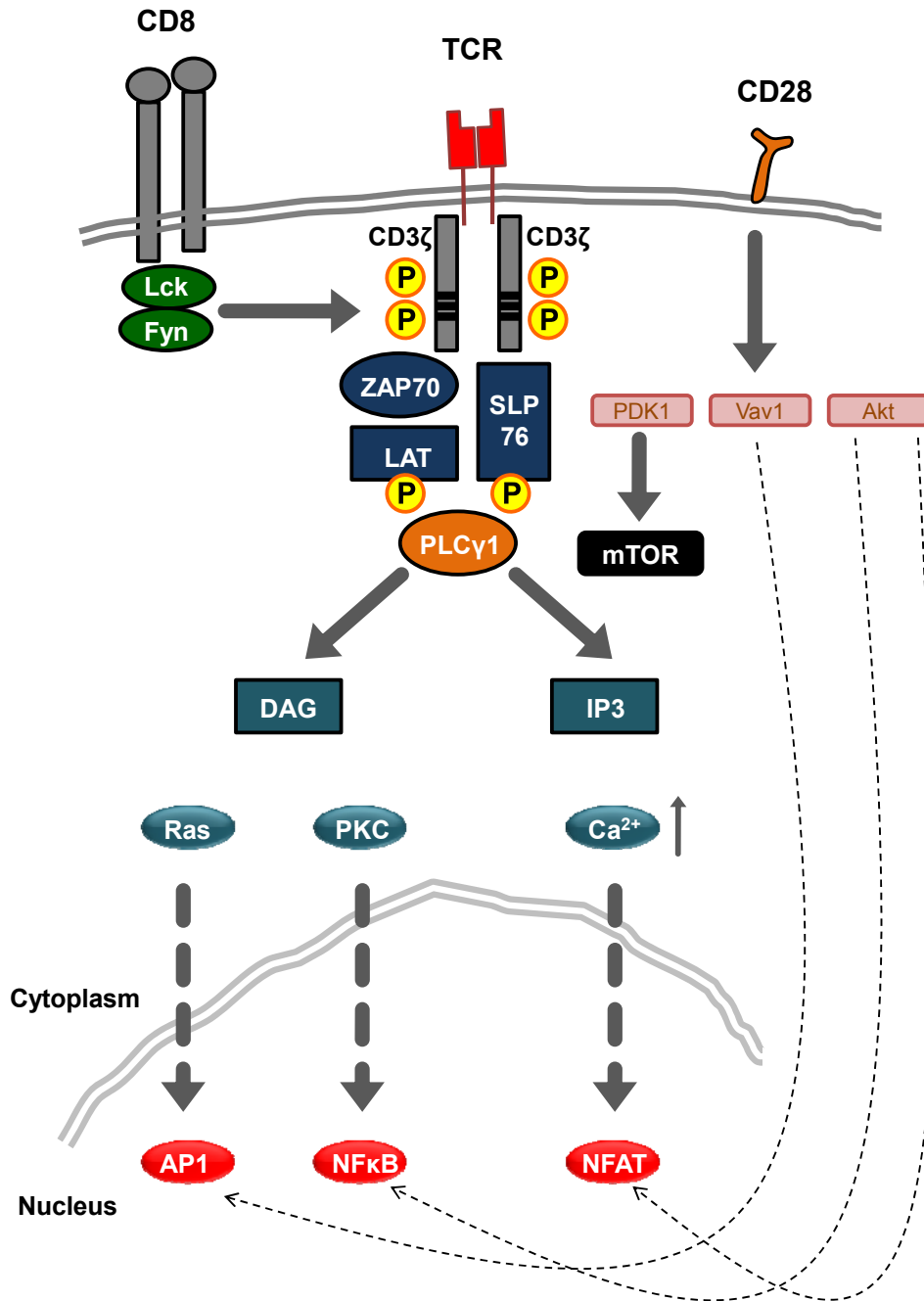
Figure 9: TCR signaling cascade

Following TCR-pMHC binding, the CD3 molecule is phosphorylated at so called ITAMs by Lyn and Fck which are associated with either the TCR or the CD8 co-receptor. This causes the recruitment of ZAP70 to the CD3ζ chain. ZAP70 then phosphorylates LAT as well as well as SLP76, both of which form a signaling complex to activate PLCγ1. This enzyme produces IP3 and DAG, the latter of which stimulates AP1 through the Ras-Raf1 pathway. DAG is also involved in regulating the transcription factor NFκB in a PKCθ dependent way. IP3 is required for the activation of calcium influx from outside the cell as well as from the ER. Intracellular rise of Ca^{2+} activates the phosphatase calcineurin which dephosphorylates and thereby activates NFAT. AP1, NFκB and NFAT initiate the transcription of a myriad of molecules which are crucial for T cell activation. Co-stimulation through CD28 mainly serves to strengthen and prolong the TCR signal, to promote survival and cytokine production as well as to regulate T cell metabolism. It is thought to involve PI3K, PDK1, Vav1 and Akt which can all act on several target molecules, amongst which is also mTOR.

1.5.2 IL2 signaling

IL2 is a growth and survival factor for T cells, produced predominantly by activated CD4 T helper and cytotoxic CD8 T cells. IL2 signaling was shown to be important during all phases of a T cell response, including the expansion, contraction, memory and recall phase, as shown by studies in CD25-/- and IL2-/- mice. Long and enhanced IL2 signaling favors the production of short-lived effector CD8 T cells. IL2 can bind to cells expressing either a low affinity dimeric or a high affinity trimeric receptor. The dimeric receptor consists of the IL2Rβ chain and the common cytokine receptor γ chain (IL2Rγ) which is also expressed by other cytokine receptors, such as those for IL4, IL7, IL9, IL15 and IL21. The dimeric receptor can be found in low quantities on naïve CD8 T cells and in high numbers on central memory CD8 T cells. It needs to be present in high numbers to be be stimulated by IL2. Upon T cell activation, IL2Rα (CD25) is transiently expressed and constitutes the 3rd chain of the trimeric IL2 receptor. CD25 does not contribute to signaling but can increase the affinity of the IL2 receptor, such that in this case low levels of IL2 are sufficient to initiate signaling (Boyman and Sprent 2012; Liao, Lin, and Leonard 2013). The expression of IL2 itself can be induced by NFAT, AP1 and NFκB upon T cell activation (Müller and Rao 2010) and is regulated by Blimp1 which acts as a repressor. Central memory T cells express low levels of Blimp1 and therefore maintain the ability to express IL2 whereas exhausted T cells express high levels of Blimp1, rendering them unable to express this cytokine. Binding to its trimeric receptor results in increased CD25 expression, IL2 thereby regulates its own action within a positive feedback loop. IL2 binding causes the activation of the Janus kinases (Jak) 1 and 3 which phosphorylate predominantly Stat5 and, in addition, provide a platform for MAPK signaling. Stat5 dimers and tetramers regulate the transcription of a number of important genes involved in cell growth, survival and effector functions of T cells, including for example CD25 (Boyman and Sprent 2012; Liao, Lin, and Leonard 2013). However, IL2 has also been shown to activate the mTOR pathway through PDK1 (D. K. Finlay et al. 2012), thereby mainly regulating the metabolic switch of T cells which will be discussed further below .

1.5.3 TGFβ signaling

In order to avoid inflammation related organ and tissue damage due to an uncontrolled immune response, regulatory mechanisms have evolved which help to restrict and contain activated T cells. One crucial factor in that respect is TGFβ. This cytokine exists in 3 highly homologous isoforms (TGFβ1, 2 and 3), of which TGFβ1

represents the most important one in an immune context (Travis and Sheppard 2013). The TGFβ receptor is a tetrameric complex consisting of a TGFβRI and a TGFβRII homodimer (Kang, Liu, and Derynck 2009). Both dimers are serine/threonine kinases and upon binding of TGFβ1, Smad2 and Smad3 are recruited and phosphorylated. Phosphorylated Smad2 and 3 then form a trimer with Smad4 which can translocate to the nucleus to initiate or repress the transcription of target genes. Next to this classical activation cascade, TGFβ has recently been shown to also activate PI3K, MAPK and Rho GTPase (Travis and Sheppard 2013). In addition, a link to the mTOR pathway could be established as Smad3-/- CD4 T cells show normal mTOR activation in the presence of TGFβ whereas WT cells show a decreased signal (Delisle et al. 2013).

Lack of TGFβ1 in TGFβ1-/- mice results in excessive lymphoproliferation causing severe inflammation induced organ damage and mice die either *in utero* or shortly after birth (Kulkarni et al. 1993). Because these overt effects could be recapitulated in mice lacking the TGFβRI or TGFβRII in T cells (Cre recombinase expression under CD4 promoter), it was clear that TGFβ must have a profound regulatory effect on these cells. TGFβ was shown to inhibit T cell proliferation (Kehrl et al. 1986) by downregulating IL2, c-myc and cyclin dependent kinases (Travis and Sheppard 2013). In addition, it was shown to promote apoptosis in short lived effector CD8 T cells by downregulating bcl2 (Sanjabi, Mosaheb, and Flavell 2009). Finally, TGFβ can inhibit perforin as well as IFNγ production and interference with TGFβ signaling was shown to increase cytotoxic activity (M. O. Li et al. 2006).

Next to the canonical pathways described for TCR, IL2 and TGFβ signaling, mTOR always seems to be involved as well. In the presence of positive stimuli (TCR, IL2), mTOR gets activated and in the presence of TGFβ, it is inhibited. This pathway therefore appears to be an indicator of the activation status of T cells and, as will be discussed now, is located in the centre of a signaling process regulating the outcome of T cell differentiation.

1.6 mTOR

1.6.1 mTOR signaling pathway

mTOR, like GCN2, is a highly conserved serine/threonine protein kinase, and the pharmacological target of the immunosuppressant rapamycin (Brown et al. 1994; Sabatini et al. 1994). It occurs in 2 different complexes: mTOR complex 1 (mTORC1) contains the scaffolding protein regulatory-associated protein of mTOR (Raptor) whereas mTOR complex 2 (mTORC2) is characterized by the scaffolding protein raptor-independent companion of TOR (Rictor). mTOR is considered to be a key integrator of growth stimuli and other environmental cues, such as amino acid, energy (adenosine triphosphate or ATP) and oxygen availability. It is thought to keep a balance between anabolic and catabolic processes based on the requirements and availabilities of the cell. Whereas upstream activators and regulators for mTORC1 are fairly well known, this is less the case for mTORC2 (Laplante and Sabatini 2012). The following paragraph therefore mainly focuses on mTORC1.

mTORC1 in T cells is activated by TCR ligation (D. K. Finlay et al. 2012), engagement of CD28 as well as other co-stimulatory receptors (ICOS and OX40) and binding of IL2 to its receptor. IL7, IL4, IL12, TNFα and IFNγ were also shown to promote mTORC1 activity (Delgoffe and Powell 2009; Laplante and Sabatini 2012; Waickman and Powell 2012). Eventually, this leads to the phosphorylation and inactivation of the tuberous sclerosis complex (TSC) as well as of proline-rich Akt substrate of 40 kDa (Pras40), most likely along the phosphoinositide-dependent kinase 1 (PDK1) in CD8 T cells (D. K. Finlay et al. 2012). TSC is a GTPase-activating protein (GAP) complex regulating the activity of the GTPase ras homolog enriched in brain (Rheb). Upon TSC inhibition, GTP bound Rheb accumulates, leading to the activation of mTORC1 through physical interaction (Delgoffe and Powell 2009). Pras40 is a Raptor binding protein, hence an integral component of mTORC1 and serves as an auto-inhibitory mTOR kinase regulator (Sancak et al. 2007). Upon phosphorylation, Pras40 is repressed and mTOR kinase activity is released. Negative T cell signals, such as those resulting from PD1 ligation (Patsoukis et al. 2012) and TGFβ receptor binding (Delisle et al. 2013) counteract mTORC1 activation.

Rheb is a protein located in the endosomal and lysosmal membranes of the cell. Co-localization of mTORC1 and Rheb is only possible in the presence of enough amino

acids through a mechanism involving v-ATPase, Rag GTPase heterodimers and a protein complex called Ragulator (Sancak et al. 2008). This represents an additional level of regulation next to CD28 engagement and different cytokines. Even in the presence of these stimuli, mTORC1 will not be fully activated under amino acid low conditions. Activation of the adenosine monophosphate-activated protein kinase (AMPK) by hypoxia and a low ATP/ADP ratio reflecting a low energy state adds an additional level of mTOR regulation. AMPK can phosphorylate TSC2 and thereby increase GAP activity towards Rheb (Laplante and Sabatini 2012).

Two key targets of mTORC1 – when activated – are the S6 kinase 1 (S6K1) and the 4E binding protein 1 (4E-BP1). S6K1 phosphorylates the ribosomal protein S6 and thereby controls protein production on a translational level. 4E-BP1 inhibits protein translation by binding eukaryotic initiation factor 4 (eIF4) and is released when phosphorylated by mTORC1, allowing protein translation to take place. mTORC1 pre-dominantly regulates translation of mRNA molecules with so-called transcripts with established 5' terminal oligopyrimidine (TOP) motifs. These mRNAs encode for many components of the translational machinery (Thoreen et al. 2012). Whereas the S6K1-S6 axis is known to regulate cell growth, translation induced by eIF4 mainly affects cell proliferation (Dowling et al. 2010). mTORC1 also regulates lipid synthesis which is crucial for proliferating cells, pre-dominantly through sterol regulatory element-binding protein 1/2 (SREBP1/2) transcription factors (Laplante and Sabatini 2009). Another key function of mTORC1 is to initiate a metabolic switch in cells. Once activated, mTORC1 induces the expression of glycolytic genes through the transcription factor hypoxia inducible factor 1 α (HIF-1α) (Brugarolas et al. 2003; Düvel et al. 2010). Due to its role as an anabolic switch, mTORC1 also inhibits recycling of its own organelles and cell components, a process called autophagy (Koren, Reem, and Kimchi 2010). The most important components of mTORC1, their inter-connections as well as the effects on CD8 T cell function, which are going to be discussed in further detail in chapter 1.6.3, are summarized in Figure 10.
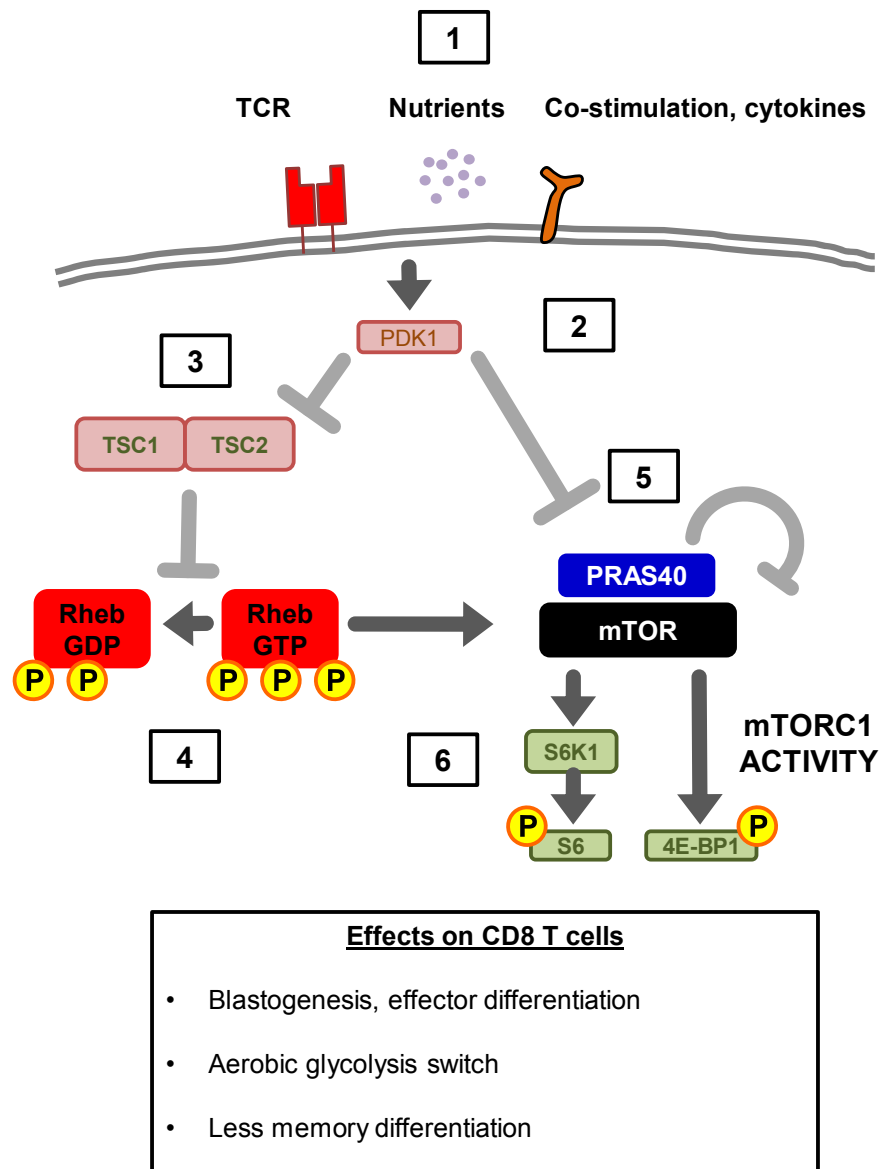
Figure 10: Regulation and components of the mTORC1 pathway

Signals, such as those from the TCR, co-stimulatory molecules and cytokines (1), eventually activate mTOR through activation of the PDK1 pathway (2), which then leads to the inhibition of the TSC 1/2 (3). TSC1/2 acts as a GAP that regulates the GTPase activity of the mTOR activator Rheb. Activated by TSC1/2, Rheb is constantly repressing itself by converting GTP to GDP (4). Once TSC1/2 is inhibited, Rheb is de-repressed and can therefore activate the mTOR kinase. The mTOR kinase is embedded within a whole complex of proteins (mTORC1). One protein within this complex is Pras40 which serves as an endogenous inhibitor of mTOR. Upon T cell activation, Pras40 is inhibited (5). Once mTOR kinase activity is released, the target proteins S6 kinase and 4E binding protein (4E-BP1) are phosphorylated (6). S6 kinase then phosphorylates the ribosomal protein S6 and phosphorylated 4E-BP1 is released from the eukaryotic translation initiation factor 4E, both of which eventually results in increased protein translation. For T cells, the net result consists in cell growth (blastogenesis), effector differentiation, including expression of effector molecules and proliferation, metabolic switch to aerobic glycolysis and less memory differentiation.

The main substrate of mTORC2 is Akt. Once activated, Akt regulates cell growth, proliferation, metabolism and apoptosis. mTORC2 also serves as a regulator of cell shape by affecting the actin cytoskeleton through activation of protein kinase C α (PKCα) and other proteins (Laplante and Sabatini 2012). It is also noteworthy that mTORC2 induced phosphorylation of Akt results in the suppression of the forkhead box proteins O1 (FOXO1) and FOXO3. If phosphorylated by Akt, these 2 transcription factors are repressed from inducing the expression of apoptosis related genes. mTORC2 signaling, therefore, promotes cell survival (Zoncu, Efeyan, and Sabatini 2011).

When a naïve T cell gets activated, a switch from catabolic to anabolic metabolism and from oxidative phosphorylation and fatty acid metabolism to aerobic glycolysis occurs (D. Finlay and Cantrell 2011; Wang and Green 2012). The reason for these key changes are that upon antigen encounter, T cells get ready to undergo massive clonal expansion as well as to produce a myriad of effector molecules, processes which cannot be accomplished unless cells adapt their metabolism. Even though oxidative phosphorylation yields more ATP molecules – the molecular carriers of energy – than aerobic glycolysis (30 versus 2), glucose represents a good carbon source for the synthesis of nucleic acids and phospholipids which are required for proliferation and expansion (D. Finlay and Cantrell 2011). Once T cells have cleared the pathogen, they can re-tune their metabolism back to oxidative phosphorylation and fatty acid metabolism, both of which are the preferred metabolic pathways used by memory T cells.

Since mTOR is probably the most important factor regulating this metabolic switch, inhibition of mTOR during the initial antigen encounter is expected to result in the inhibition of T cell functions. Indeed, rapamycin is primarily known as an effective agent to suppress the immune system, in particular T cells, e.g. to prevent allograft organ rejection in kidney transplant patients (Kreis et al. 2000). It could also be shown that anergic T cells are metabolically incompetent, in that they show reduced mTORC1 activation accompanied by a lack of up-regulation of the amino acid transporter CD98 and the transferrin receptor CD71 as well as reduced glycolytic activity. Vice versa, inhibition of metabolic activity renders T cells anergic (Yan Zheng et al. 2009). As simple as that may seem, in recent years, mTOR has emerged as a more complex player in T cell biology than expected. The multifaceted effects of mTOR on T cell differentiation and function are going to be summarized in the following 2 chapters.

1.6.2 CD4 T cell differentiation and mTOR

The development of transgenic mouse models with targeted genetic knock-outs of key components of either mTORC1, mTORC2 or both allowed a detailed insight in the requirements of CD4 T cell subtype differentiation. The following models were used:

1) **TSC1-/-:** Mice carrying loxP-flanked TSC1 alleles as well as Cre-recombinase under the CD4 promoter show conditional deletion of TSC1 as early as in the double positive (CD4+CD8+) stage of T cell development in the thymus. This results in a constitutive activation of mTORC1 due to a lack of GAP activity towards Rheb, leading to the accumulation of Rheb-GTP and consequently mTORC1 activation. This causes a loss of quiescence in the peripheral T cell pool with reduced CD4 and CD8 T cell numbers. The cells produce an excess of reactive oxygen species (ROS) and have an increased susceptibility to apoptosis, in particular because of decreased B cell lymphoma (bcl2) protein expression. They are larger, have an activated phenotype (CD25$_{hi}$, CD69$_{hi}$) and are dysfunctional, i.e. *in vivo* antibacterial responses are impaired (Yang et al. 2011). In addition, they seem to be resistant to anergy, i.e. these cells are less dependent on co-stimulatory signals (Xie et al. 2012). In terms of CD4 T cell differentiation, mTOR signaling due to loss of TSC1 in CD4 T cells impairs the development of Foxp3 expressing Tregs as well as their suppressive function when activated under polarizing conditions. On the other hand, it promotes differentiation into Th1 and Th17 cells to an extent that this can cause severe autoimmune pathology (Park et al. 2013).

2) **mTOR-/-:** Mice carrying loxP-flanked Frap1 alleles (Frap1 is the gene encoding for mTOR) as well as Cre-recombinase under the CD4 promoter show conditional deletion of mTOR as early as in the double positive (CD4+CD8+) stage of T cell development in the thymus. This results in a lack of both, mTORC1 as well as mTORC2. CD4 Tcells lacking mTOR, even though they show normal T cell activation (CD25 and CD69 upregulation), IL2 secretion and reduced but not abolished proliferation, these cells are unable to differentiate into Th1, Th2 or Th17 T cells under the respective skewing conditions but they show an increased susceptibility to commit to the Treg lineage (Delgoffe et al. 2009).

3) **Rheb-/-:** Mice carrying loxP-flanked Rheb alleles as well as Cre-recombinase under the CD4 promoter show conditional deletion of Rheb as

early as in the double positive (CD4+CD8+) stage of T cell development in the thymus. This results in a lack mTORC1 but not mTORC2 activation. CD4 T cells preferentially differentiate into Th2 subtypes but not Th1 or Th17 under the respective skewing conditions, highlighting the importance of mTORC2 for Th2 lineage commitment (Delgoffe et al. 2011).

4) **Rictor-/-:** Mice carrying loxP-flanked Rictor alleles as well as Cre-recombinase under the CD4 promoter show conditional deletion of Rictor as early as in the double positive (CD4+CD8+) stage of T cell development in the thymus. This results in a lack mTORC2 but not mTORC1 activation. CD4 T cells preferentially differentiate into Th1 and Th17 but not Th2 subtypes under the respective skewing conditions, highlighting the importance of mTORC1 for Th1 and Th17 lineage commitment (Delgoffe et al. 2011).

In summary, high mTORC1 activation promotes Th1 and Th17, high mTORC2 promotes Th2 differentiation and an overall reduced mTOR signal enhances Foxp3+ Treg development. Concomitant with this result is the observation that Treg differentiation can be facilitated in the presence of rapamycin (Haxhinasto, Mathis, and Benoist 2008; Sauer et al. 2008). Furthermore, when CD4 T cells are activated under amino acid low conditions, they are more likely to differentiate into Tregs due to a weaker mTOR signal (Cobbold et al. 2009). Tregs were also shown to be metabolically less active compared to other CD4 T cell subsets. More precisely, Tregs do not show high expression of the glucose transporter 1 (GLUT1), they have less glycolytic activity and high lipid oxidation rates (Michalek et al. 2011).

1.6.3 CD8 T cell differentiation and mTOR

In contrast to CD4 T cells, CD8 T cells show reduced differentiation heterogeneity. The effects of mTOR are therefore more limited.

Araki et al. (2009) made the unexpected observation that mice infected with the lymphocytic choriomeningitis virus (LCMV), when treated with rapamycin in low doses, show enhanced CD8 T cell responses compared to untreated mice (high doses, on the other hand, suppress T cell functions as anticipated). When they examined this phenomenon in more detail, they found that T cells from rapamycin treated mice yield the same number of effector cells at the peak of the response but the cells contract to a reduced extent due to an enhanced survival potential. In addition rapamycin treated mice have more cells with a central memory phenotype

(CD62L$_{hi}$, CD127$_{hi}$, bcl2$_{hi}$ KLRG1$_{lo}$) and are more potent in mounting a re-call response upon re-infection. When the T cells are isolated and transferred into secondary hosts, they persist better than isolated cells from untreated mice, suggesting that these cells are indeed not only phenotypically but also functionally genuine memory cells.

Early rapamycin treatment during infection (days – 1 to 8) accounted for the reduced contraction whereas late treatment (days 8 to 35) was responsible for the phenotypic transition of the cells. In addition, rapamycin treatment could enhance the re-expression of CD62L on previously CD62L negative cells.

As treatment of rapamycin can affect not only T cells but also other cells of the immune system, for instance macrophages or dendritic cells (Weichhart et al. 2008) as well as Tregs (Haxhinasto, Mathis, and Benoist 2008; Sauer et al. 2008), the authors went on to examine whether the observed phenomena can be assigned to a CD8 T cell intrinsic inhibition of mTOR. They designed retroviruses encoding shRNA against mTOR and Raptor and found that virus infected mice treated with cells harboring low mTOR and Raptor re-capitulate the phenotypes observed when mice are treated with rapamycin, suggesting that the effects of rapamycin on CD8 T cell memory differentiation are in fact cell intrinsic. However, they did not comment on whether these cells are equally effective in their ability to clear virus.

Vice versa, because rapamycin exerts its function on mTOR through binding to 12-kDa FK506-binding protein (FKBP12), this protein was knocked-down in T cells, rendering them insensitive to this drug. Rapamycin resistant cells do not show the same memory transition compared to rapamycin sensitive cells.

All of this strongly indicates that mTOR inhibition in CD8 T cells during a virus response increases the yield, phenotype and function of central memory cells.

Sinclair et al. (2008) made the intriguing observation that mTOR, next to phosphatidylinositol-3-OH kinase (PI3K), can affect the migratory properties of T cells. TCR activation induces early proteolysis and shedding of CD62L through PI3K and its inhibition by LY294002 can prevent this process. IL2 induced mTOR activation represses the transcription of CD62L and chemokine receptor 7 (CCR7) by down-regulating the Kruppel like factor 2 (KLF2). KLF2 induces expression of these 2 molecules on a transcriptional level in naïve and memory T cells (Bai et al. 2007). Consequently, treatment with rapamycin can maintain expression of CD62L and CCR7. In addition, D. K. Finlay et al. (2012) were able to show that HIF1β-/- CD8 T cells maintain high expression of CD62L after peptide specific stimulation *in*

vitro. Since HIF activity is regulated by mTOR, CD62L expression can also be influenced through the mTOR-HIF axis.

Circulating T cells bind, through CD62L, to peripheral node addressins (PNAd) on high endothelial venules (HEV) which represent entry ports of lymph nodes. CCR7 then arrests T cells and enables their transendothelial migration, mainly through ligation by CXCL19 and CXCL21 (Förster, Davalos-Misslitz, and Rot 2008). Lymph nodes are residing sites of naïve and central memory T cells. Upon CD62L down-regulation, T cells enter circulation again and infiltrate peripheral tissues (Weninger et al. 2001).

It therefore seems that through activation signals mediated by PI3K and mTOR, effector functions and migration of T cells to peripheral target tissues are synchronized.

How exactly mTOR induces effector functions in CD8 T cells has been a key question for years. Rao et al. (2010) reported that the transcription factors T-box expressed in T cells (T-bet) and eomesodermin (Eomes) are differentially regulated by mTOR. T-bet is thought to promote $CD127_{lo}$ and killer cell lectin-like receptor G1 $(KLRG)_{hi}$ effector T cells (Joshi et al. 2007) while Eomes favors memory differentiation (Intlekofer et al. 2005). Therefore, high T-bet:Eomes ratios are a signature of effector while low T-bet:Eomes ratios are a signature of memory CD8 T cells (Takemoto et al. 2006). mTOR was shown to be a key factor in regulating these ratios such that high mTOR tips the balance towards the former while low mTOR favors the latter. In addition, they were the first to show that priming of tumour specific T cells in the presence of rapamycin *in vitro* results in greater tumour protection upon adoptive transfer *in vivo* through preserving memory characteristics. mTOR was also shown to sustain expansion of CD8 T cells by inducing the expression of interferon regulatory factor 4 (IRF4). IRF4 is not required for the early phases of T cell activation and expansion but it becomes necessary to sustain proliferation through induction of T-bet and B lymphocyte induced maturation protein 1 (Blimp1), transcription factors highly expressed by end stage effector T cells, and through promoting T cell survival as well as repressing cell cycle arrest genes. It also engages the IFNγ and granzyme B promoters. This effect was shown to be TCR driven and dependent on a functional mTOR signal (Yao et al. 2013).

Further, it was reported that upon T cell activation, mTOR induces HIF-1α and β expression (D. K. Finlay et al. 2012). This ultimately causes a switch in metabolism from oxidative phosphorylation to aerobic glycolysis by up-regulating enzymes

involved in glycolysis, such as hexokinase 2, pyruvate kinase 2, phosphofructokinase, and lactate dehydrogenase. It could also be shown that the HIF complexes regulate the expression of perforin and granzyme molecules, as T cells from HIF-1β knock-out mice had lost expression of these molecules. Perforin and granzymes are key cytolytic factors produced by activated CD8 T cells. Perforin, through multimerisation, can plunge holes into target cells recognized by T cells and granzyme molecules are secreted through these holes to initiate the apoptotic program inside of the cell. Interestingly, other effector molecules, e.g. IFNγ, T-bet and Blimp1, were not affected by HIF-1. However, it is conceivable that mTOR affects IFNγ production through direct and indirect ways. For example, Chang et al. (2013) showed that glycolytic enzymes such as nicotinamide adenine dinucleotide phosphate (NAPDH) can regulate IFNγ messenger RNA (mRNA) translation. By inducing the metabolic switch, mTOR might play a role in this post-transcriptional regulation. The same holds true for the NFAT induced up-regulation of IL2 and subsequent proliferation which was shown to be dependent on ROS produced by mitochondria (Sena et al. 2013).

mTORC1 and CD8 T cells
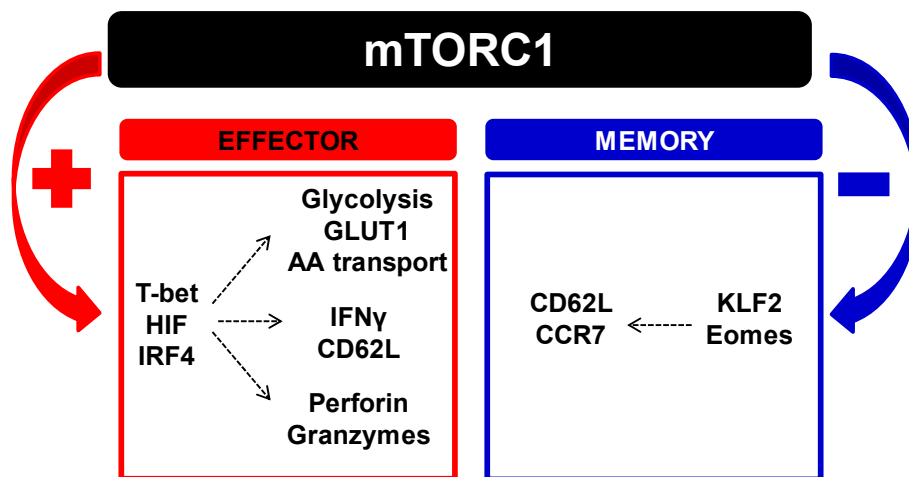
Figure 11: mTORC1 and CD8 T cells

A summary of the effects of mTORC1 activation on important CD8 T cell components regulating effector versus memory differentiation is given. mTORC1 was shown to positively influence T-bet, HIF and IRF4 (indicated in red) and to negatively regulate KLF2 and Eomes (indicated in blue). These molecules can affect the expression of a multitude of factors which are involved in the differentiation of effector and memory T cells on a transcriptional as well as on a post-transcriptional level. Dotted arrows represent positive influence. AA=amino acid.

The importance of metabolism in T cell differentiation and function is also highlighted by other recent reports. Fatty acid metabolism is a major metabolic pathway used by central memory T cells and impairing this metabolic route results in a severe dysfunction in memory formation (Pearce et al. 2009). In addition, inhibition of glycolysis through the glucose analogue 2-Deoxyglucose (DG) was shown to drive T cells towards memory rendering them superior in their ability to protect from tumour. Vice versa, promoting glycolysis through overexpression of the glycolytic enzyme phosphoglycerate mutase-1 impaired T cell memory formation (Sukumar et al. 2013). Lastly, Sinclair et al. (2013) have shown that T cell activation requires excessive supply of amino acids. This is achieved through the up-regulation of respective transporters, enabling the activation of mTORC1 and thereby normal T cell function.

In summary, it can be concluded that mTOR is a key player not only in regulating cell growth and proliferation but also in inducing the metabolic switch from oxidative phosphorylation to aerobic glycolysis which is an integral component of T cell activation. By doing so, mTOR can drive T cell effector functions through an indirect way. Next to that, mTOR can also directly induce CD8 T cell effector molecules. Because effector and memory T cells have an opposite metabolic make-up, it comes with no surprise that mTOR is an important regulator of effector versus memory differentiation. mTOR therefore represents an attractive target to manufacture effector and/or memory T cells.

The second aim of this PhD project was to develop a strategy to tune mTOR in a way to manufacture potent effector and or memory T cells.

1.7 Goals of PhD Project

1) To establish a strategy rendering tumour specific T cells resistant to an amino acid low condition by interfering with the GCN2 pathway.

2) To design a strategy which allows manufacturing potent effector and memory T cells by tuning the mTOR pathway.

3) To combine these approaches with a TCR transfer strategy to improve current tumour therapies based on the re-direction of T cells to tumours.

Chapter 2   Material and Methods

2.1 Molecular Cloning

2.1.1 Isolation of RNA and reverse transcription

Splenocytes from a C57BL/6 mouse were activated with CD3/28 bead antibodies for 24 hours after red blood cells lysis (see 2.2.4). Ribonucleic acid (RNA) extraction was done on 7×10^6 cells after beads removal, following the instructions of the Qiagen RNeasy Mini Kit (Qiagen 74104). RNA was eluted in 40 µl of Nuclease free water (H_2O) and frozen at -80° Celsius (C). RNA concentration was determined using Nanodrop technology. For the reverse transcriptase (RT) reaction, 440 ng of the sample was heated for 10 minutes at 65°C on a heat plate in a volume of 15 µl (in an 1.5 ml Eppendorf tube), pulsed down and put on ice. The RT reaction mix contained the following reagents (per reaction): 3 µl nuclease free H_2O, 6 µl 2.5 mM deoxyribonucleotide triphosphates (dNTPs), 7 µl 5x buffer (Invitrogen Y00146), 1 µl 0.1M DL-Dithiothreitol (DTT) (Invitrogen Y00147), 1 µl Random Hexamers (500 ng/µl), 1 µl RNAse inhibitor (Promega 14422705), 1 µl M-MLV RT 200 U/µl (Invitrogen 29025-013). This master mix was added to the RNA and the reaction was allowed to take place at 37°C in an Eppendorf tube on a heat plate for 2 hours. The complementary deoxyribonucleic acid (cDNA) was pulsed down and stored at -20°C.

2.1.2 Design of primers

Rheb cDNA (mus musculus) sequence was identified using the Pubmed database[4]. Based on this information, the following primers were designed in the DNA analysis program "pDRAW32" (primers produced by Invitrogen):

Forward (Fw) primer (5'-3'):

5'-TCGAGCGGCCGCAAGATGCCTCAGTCCAAGTC-3'

Reverse (Rev) primer (5'-3'):

5'- CGTCGAGTCGACTTGTCACATCACCGAGCACG -3'

Primers were designed such as to include a Not 1 restriction site (GCGGCCGC) at the 5' and a Sal 1 restriction site (GTCGAC) at the 3' end of the expected 585bp

---

[4] http://www.ncbi.nlm.nih.gov/

fragment. Polymerase chain reaction (PCR) was done using 2.5 µl of cDNA solution in a total volume of 5 µl which was added to a master mix containing the following reagents (Qiagen Taq polymerase kit, Cat. No. 201203) (per reaction): 2 µl 10x buffer, 0.4 µl 10 mM dNTPs, 0.1 µl Fw primer (10 mM), 0.1 µl Rev Primer (10 mM), 0.1 µl Polymerase, 12.3 µl nuclease free H_2O. PCR settings were as follows (30 cycles): 3 minutes initial denaturation at 94°C, 0.5 minute denaturation at 94°C per cycle, 1 minute annealing at 55°C, 1 minute elongation at 72°C, 5 minutes elongation in last cycle at 72°C. PCR product was purified with QIA Quick PCR purification kit (Qiagen 28106). DNA was eluted in 32 µl of nuclease free H_2O.

2.1.3 Restriction digestion

25 µl of the PCR product was digested with 1 µl Not 1 (NEB R0189L) restriction enzyme, 1 µl Sal 1 (NEB R0138L) enzyme and 3 µl 10x buffer 3 (NEB B7003S) (total volume = 30 µl). To acquire the according MP71 vector backbone, a known in-house vector (*Gcn2dn.Ires.Gfp*) containing a construct with the right restriction sites (Not 1and Sal 1) was digested the following way: 1 µl vector (1 ug/µl), 1 µl NEB Not1 restriction enzyme, 1 µl NEB Sal 1 enzyme and 2 µl NEB 10x buffer 3 in a total volume of 20 µl. Digestion reactions were allowed to take place in an incubator at 37°C for 1 hour. Thereafter, digestion products were analyzed using gel electrophoresis (1% agarose gel, 0.5x Tris/Borate/EDTA [TBE] buffer + 0.5x H_2O, ethidium bromide 1:1.000) after addition of Gel Loading Solution (Sigma G2526) in an end dilution of 1:5, alongside 5 µl of Hyper Ladder 1 (Bioline 33025) to determine the fragment size. Gel was analyzed using Ultrospec 1100 Pro (Amersham Biosciences). The 585 bp Rheb fragment as well as the 7 kbp vector backbone were extracted with QIAquick Gel Extraction Kit (Qiagen 28704), following the kit's instructions, and eluted in 50 µl of nuclease free H_2O.

2.1.4 Ligation

The ligation reaction was carried out in an Eppendorf tube at room temperature for 10 minutes, containing the following reagents: 10 µl 2x Quick Ligase Buffer (NEB B2200S), 3 µl digested vector backbone, 4 µl digested Rheb insert, 1 µl Quick T4 DNA Ligase (NEB M2200L), 2 µl H_2O. After the reaction, Max Efficiency DH5α bacteria (Invitrogen 18258-012) were transformed (see 2.1.6). DNA was isolated from bacteria using QIAPrep Spin Miniprep kit (Qiagen 27106). DNA was sent for sequencing to Eurofins MWG Operon.

2.1.5 Site directed mutagenesis

Stratagene QuikChange II XL Site-Directed Mutagenesis Kit (Cat.No.: 200521) was used to create the constitutively active Rheb mutant (hereby referred to as RQ64L) and the manufacturer's instructions were followed. Primers were designed using the company's online programme[5]:

Fw primer (5'–3'):

5'-TAGACACAGCGGGGCTGGATGAATATTCCATTT-3'

Rev primer (5'–3'):

5'-AAATGGAATATTCATCCAGCCCCGCTGTGTCTAC-3'.

The following mix was prepared (per reaction): 23 µl H_2O, 3 µl 10x Buffer, 0.6 µl dNTP mix, 1.8 µl Quick solution, 0.6 µl Fw primer (0.2 ug/µl), 0.6 µl Rev

primer (0.2 ug/µl), 1 µl *Rheb.Ires.Gfp* vector, 0.6 µl PFU Polymerase. PCR settings were as follows (18 cycles): 1 minute initial denaturation at 95°C, 50 seconds denaturation per cycle at 95°C, 50 seconds annealing per cycle at 60°C, 8 minutes and 40 seconds elongation per cycle at 68°C (=1 minute/kbp).

After PCR, 1 µl of Dpn 1 (10 U/µl) enzyme was added and the samples were incubated at 37°C for 1 hour to digest the wild type plasmid. After 1 hour, transformation was done with 6 µl of the digested product using the provided XL10 Gold bacteria (see 2.1.6). Bacteria were spun down in a microcentrifuge at 8.000 rotations per minute (rpm) for 3 minutes. DNA was isolated using Qiagen MiniPrep Kit and eluted in 1:10 LCTE elution buffer. A test digestion with Not 1 and Sal 1 as described above (2.1.3) was done to identify correct samples (see 2.1). All acquired DNA samples were sent to Eurofins MWG Operon to confirm the introduced mutation. DNA concentration was determined using Nanodrop technology.

2.1.6 Transformation

Subcloning Efficiency DH5α (Invitrogen 18265-017) or Max Efficiency DH5α bacteria (Invitrogen 18258-012) were used for transformation of conventional plasmids and ligation reactions, respectively. 20 µl of the subcloning efficiency or 50 µl of the Max Efficiency bacteria were dispensed into Eppendorf tubes and 20 ng of conventional plasmids or 2 µl of the ligation mix was added to the bacteria. Bacteria were put on ice for 30 minutes, after which they were subjected to heat shock for 30 seconds at

---

[5]

http://www.genomics.agilent.com/CollectionSubpage.aspx?PageType=Tool&SubPageType=ToolQCPD&PageID=15

42°C on a heat plate, followed by 2 minutes incubation on ice. 5x volume of super optimal broth with catabolite repression (S.O.C.) medium (Invitrogen 15544-034) was added and bacteria were put into shaking incubator at 37°C for 1 hour (225 rpm). Bacteria were spread on Ampicillin treated LB agar plates (0.1 mg/ml, Sigma-Aldrich) and incubated overnight at 37°C. Colonies were inoculated in 5 ml of Ampicillin containing LB Broth medium (0.1 mg/ml, Sigma-Aldrich), put into a shaking incubator at 37°C (225 rpm) either overnight for 12-16 hours (for MiniPrep) or for 8 hours, after which they were diluted 1:500-1:1.000 in 100 ml of LB Broth to further expand the bacteria (MaxiPrep). Bacteria were spun down either in a microcentrifuge at 8.000 rpm for 3 minutes (MiniPrep) or in a Sigma 4K15 centrifuge at 4.500 rpm for 15 minutes at 6°C (MaxiPrep). DNA was isolated either by Mini- or Maxiprep, following the kit's instructions. For the site-directed mutagenesis, XL10 Gold bacteria provided with the kit were thawed on ice and 25 µl were transferred into an Eppendorf tube. 1.2 µl of provided 2-β-Mercaptoethanol were added, the tube was swirled and put on ice for 10 minutes. Tube was swirled every 2 minutes during that time. Thereafter, 6 µl of the digested PCR product were added to the bacteria and the same steps as above were followed.

2.2 Cell Culture

2.2.1 Cell counting

Twenty (20) µl of cell suspension was mixed with an equal volume of Trypan Blue (Life Technologies 15250-061) and loaded onto a Haemocytometer. Viable cells were identified under light microscope as cells that have not taken up the dye. Cells within 2 large grids (each containing 3x3 squares) were counted and the count (=n) was multiplied by 10^4. This final number represented the concentration of the cell suspension (n x10^4/ml).

All tissue culture work was carried out in Biohit Biological Safety Cabinet Class 2 hoods. A Labcare CR422 centrifuge was used for spinning the cells down.

2.2.2 Cell lines

293 cells and Phoenix eco cells: The 293 line is a standard transfection line (He et al. 1998) used for the production of lentivirus/retrovirus. Phoenix eco cells are 293 cells stably transfected with DNA encoding for the gag-pol proteins as well as the ecotropic virus envelope, thereby facilitating the production of retrovirus by providing structural components. Cells were grown in Tissue Culture Flaks 75 qcm (TPP 90076) with Isocove's Modified Dulbecco medium (IMDM) (Lonza BE12722F), supplemented with 10 % Fetal Calf Serum (FCS) (Biosera), 1 % L-glutamine 200mM (GIBCO 25030) (2 mM) and 1 % Penicillin/Streptomycin (GIBCO 15070) (100 U/ml). Cells were detached by treating them with 3 ml of 0.05 % Trypsin-EDTA (GIBCO 25300) for 1 minute before neutralization with normal medium. Cells were sub-cultured every 2 days when the cells were 90 % confluent or above.

BW5154 cells: A murine thymoma cell line isolated from spontaneously evolved tumour in AKR/J mice (Ralph 1973). Cells were kept in RPMI 1640 medium (Lonza BE12-167F), supplemented with 10 % Fetal Calf Serum (FCS) (Biosera), 1 % L-glutamine (2 mM) and 1 % Penicillin/Streptomycin (100 U/ml). Cells were transferred into fresh medium every 2 days.

EL4 cells: A murine T lymphoblast lymphoma cell line derived from a C57BL/6 mouse treated with the carcinogen 9,10-dimethyl-1,2-benzanthracene (Herberman 1972). Cells were kept in RPMI 1640 medium (Lonza BE12-167F), supplemented with 10 % Fetal Calf Serum (FCS) (Biosera), 1 % L-glutamine (2 mM) and 1 %

Penicillin/Streptomycin (100 U/ml). Cells were transferred into fresh medium every 2 days.

EL4-NP cells: Gift from Professor Brigitta Stockinger (National Institute for Medical Research, London). EL4 cells which have been stably transfected with the influenza A nucleoprotein (NP) and present this peptide in the context of H-2D^b. Transfected cells also carry a resistance gene against the antibiotic Geneticin (Sigma G418 disulfate salt solution 50 mg/ml A1720). Cells were cultured the same way as conventional EL4 cells and were subjected to Geneticin once a week in an end concentration of 1 mg/ml.

2.2.3 Human and murine T Cell culture

RPMI 1640 medium was supplemented as for BW cells. 2-β-Mercaptoethanol in an end concentration of 50 μM was added for the culture of murine cells. For culture in arginine limited medium, custom made RPMI 1640 arginine free medium (PAA T1090, 2500) was used and supplemented with arginine in powder form relative to the standard concentration of 200 mg/l in normal RPMI medium. All cells were grown under humidified conditions at 37°C and 5 % CO_2.

2.2.4 Murine T Cell selection

Magnetic activated cell sorter (MACS) buffer was made up of phosphate buffered saline (PBS) containing 0.5 % bovine serum albumin (BSA) and 2 mM Ethylendiamintetraacetat (EDTA), de-gassed and filter sterilized.

CD3 T cell selection: Miltenyi Pan T cell isolation kit II (Cat.No. 130-095-130) for mouse cells was used. Mouse splenocytes were extracted and prepared as described in chapter 2.2.5, re-suspended in 40 μl MACS buffer and 10 μl of biotin-antibody cocktail per 10^7 and then incubated at 4°C for 10 minutes. Afterwards, 30 μl of MACS buffer and 20 μl of anti-biotin beads per 10^7 cells were added and cells were incubated for another 15 minutes at 4°C. In the meantime, MS (Miltenyi 130-042-201) or LS (Miltenyi 130-042-401) magnetic separation columns were rinsed with either 500 μl or 3 ml MACS buffer, respectively. After incubation, cells were washed with 5x MACS buffer and re-suspended in 500 μl (up to 10^8 cells) or 3 ml (>10^8 cells) MACS buffer. Cells were transferred to the separation column, column

was washed 3 times and flow-through contained CD3 T cells. Sort purity was checked by fluorescence-activated cell sorting (FACS).

CD8 T cell selection: Miltenyi CD8a (Ly-2) MicroBeads (Cat.No. 130-049-401) were used. Splenocytes were prepared as described above, re-suspended in 90 µl MACS buffer and 10 µl microbeads per 10^7 cells and incubated at 4°C for 20 minutes. Afterwards, cells were washed and placed onto a column as above. After the 3rd wash of the column, cells were flushed off the column into a 15 ml Falcon tube with 1ml (MS) or 3 ml (LS) MACS buffer. Sort purity was checked by FACS.

2.2.5 Murine T Cell Activation

Mice were culled according to Schedule 1 home office requirements (CO_2 suffocation and cervical dislocation). Spleens and inguinal lymph nodes were extracted, mashed through a cell strainer (BD Falcon 352340) into a 50 ml Falcon centrifuge tube (TPP) and washed with autoclaved PBS. Red blood cell lysis was done with ammonium-chloride-potassium (ACK) lysing buffer (Lonza 10-548E). A volume equal to the cell pellet was added to the cells, tube was swirled for 30 seconds, then RPMI medium was added to stop lysis and cells were spun down. Either bulk splenocytes, sorted CD3 or sorted CD8 T cells (see 2.2.4) were re-suspended in T cell medium to a final concentration of $1-1.5 \times 10^6$ cells/ml.

Bead activation: Twenty-five (25) µl of dynabeads mouse T-activator CD3/28 (Invitrogen 114.53D) (hereby referred to as CD3/28 bead antibodies) were used to activate 1×10^6 T cells. Beads were washed with the same volume or at least 1 ml PBS and collected with a magnet before adding them to the T cells.

Antibody coated plates activation: BD anti-CD3 (Cat.No. 553057) was diluted to an end concentration of 2.5 ug/ml and BD anti-CD28 (Cat.No. 553294) to an end concentration of 1.25 ug/ml in PBS. Non tissue culture treated 96 flat well plates were coated with 200 µl of this antibody solution for 2 hours in a cell culture incubator at 37°C, after which plates were washed twice with PBS and were then ready for use.

ConA + interleukin 7 (IL7) activation: For transduction, T cells were usually activated with concanavalin A (ConA) (2 ug/ml final concentration) and IL7 (1 ng/ml final concentration) unless when stated otherwise. Where indicated, T cells received

either Chiron (100 u/ml) or Roche IL2 (20 u/ml) every 2 days together with fresh medium.

2.2.6 Retrovirus production and transduction

A standard retrovirus spin transduction protocol which has been established in our lab was followed (Ahmadi et al. 2011). All murine transductions have been carried out with a MP71 Moloney murine leukemia virus (Mo-MLV) based vector (Engels et al. 2003) and under level 2 containment conditions.

Transfection: 1.5×10^6 Phoenix eco packaging cells were plated out on a 60.1 qcm tissue culture dish (TPP 93100) (day 1) in 8 ml of IMDM medium (see 2.2.1) and grown overnight. Medium was replaced 4 hours before transfection (8 ml $\rightarrow$ 5 ml) (day 2). Fugene HD Transfection Reagent (Roche 04709713001) was used. 10 µl Fugene HD was added to 75 µl OPTI-MEM (GIBCO 31985) in a 1.5 ml Eppendorf tube. DNA mix was separately prepared in an Eppendorf tube containing 4.6 µg vector DNA and 3 µg p-eco DNA in a total volume of 40 µl H_2O. DNA was carefully added to the Fugene mix and incubated under the hood for 15 minutes before adding all of it drop-wise to the Phoenix eco cells. On the next day (day 3), medium was replaced with T cell medium (5 ml $\rightarrow$ 5 ml) and cells were incubated for another night. On day 4, virus supernatant was collected from Phoenix eco cells and spun down to remove cell debris and either stored at -80°C (up to 3 months) or used for transduction.

Mouse T cell transduction: T cells were activated as described above (see 2.2.5). 6×10^6 activated T cells were re-suspended in 1.5 ml of virus supernatant and transferred onto a non-tissue-culture treated 6 well plate that has been coated with 2 ml RetroNectin (Takara T100B) either overnight at 4°C or for 2 hours at room temperature, blocked with filter sterilized 2 % BSA/PBS for 30 minutes and washed twice with PBS to facilitate the infection of T cells with virus. With regards to double transductions, cells were re-suspended in 1.5 ml of each virus supernatant (total volume 3 ml). The plate was then centrifuged at 2.000 rpm for 90 minutes at 32°C before incubation under standard conditions. On the following day, medium was topped up to a full volume of 6 ml/well and either Chiron or Roche IL2 was added (see 2.2.5).

BW cell transduction (for validation): $5x10^4$ cells were transduced with 100 µl of virus supernatant, transferred onto a tissue culture treated 96 well round bottom plate (TPP 92697) and spin transduced as described above. Straight after the spin, cells were transferred into a tissue culture flask 25 qcm (TPP 90026) containing 10 ml of medium and further expanded for 4 days before they were analyzed.

2.2.7 Human T cell activation

Peripheral blood mononuclear cells (PBMCs) were obtained from healthy volunteers by the National Blood Service (Colindale, London, UK). PBMCs were isolated by gradient separation. Addition of lymphoprep^{TM} (Fresenius Kabi) to whole blood results in the aggregation of erythrocytes which increases their sedimentation rate. A 50 ml tube was filled with 15 ml of lymphoprep^{TM}, 30 ml of whole blood was carefully layered on top of it. After 20 minutes of centrifugation at 1.600 rpm without breaks, the buffy coat layer is visible and can be aspirated. PBMCs were washed once with PBS, cells were counted and then aliquoted at a concentration of 5-$10x10^6$ cells/ml in 1 ml cryotubes. Freezing medium was normal T cell medium supplemented with 10 % dimethylsulfoxid (DMSO). Cells were stored overnight at -80°C before they were transferred into liquid nitrogen.

For experimental purposes, cells were quickly thawed by transferring them into a 37°C water bath. DMSO was washed out of the cells by drop-wise addition of pre-warmed T cell medium. Cells were counted to evaluate viability and re-suspended in T cell medium at a concentration of $1x10^6$ cells/ml. PBMCs were activated with either anti-CD3 antibodies (Okt3) 30 ng/µl and Chiron IL2 300U/ml or human CD3/28 bead antibodies (Invitrogen 111.32D) (25 µl per $1x10^6$ cells corresponds to a cell:beads ratio of 1:1) and 20U/ml of Roche IL2. Cells were plated 6 ml/well on a 6 well plate (Bobisse et al. 2009).

2.2.8 Lentivirus production and transduction

A standard lentivirus transduction protocol which has been established in our lab was followed (Perro et al. 2010). In collaboration with Thermo Scientific Open Biosystems, UCL established a lentiviral short hairpin RNA (shRNA) library which contains a big selection of shRNA sequences that targets a broad range of human and murine proteins. Using a UCL open source database, the right shRNA to target mouse as well as human GCN2 was chosen (anti-sense sequence: 5'-TTTCTTGCCACATATCTTG-3'). The so-called GIPZ shRNA lentivirus vector

contains green fluorescent protein (GFP) as a marker of transduction as well as a puromycin resistance gene that allows for the pharmacological selection of transduced cells. All work was carried out under level 2 containment conditions.

Transfection: 293 cells were cultured in 75 qcm tissue culture flaks and when confluent, half of the cells were transferred into a 150 qcm flask (day 1). On the next day, 30 ml of old medium was replaced with 25 ml of fresh medium and 4 hours later transfection was carried out (day 2). For this, 40 µl of Fugene was slowly added to 300 µl of OPTI-MEM medium in a 1.5 ml Eppendorf tube. In seperate Eppendorf tubes, the DNA mixes were prepared: 4.6 µg of plasmid DNA, 3 µl of p8.91 (=gag/pol structural genes) and 3µug of pMDP (=VSV-G envelope gene) were added into 39.4 µl H_2O to make up a total volume of 50 µl. This DNA mix was then carefully mixed together with the DNA/OPTI-MEM mix. This transfection solution was incubated at room temperature for 15 minutes before it was added drop-wise to the cells. On the next day (day 3) medium was replaced with an equal amount of fresh medium. Another 2 days later (day 5), virus was harvested and frozen at -80°C.

Lentivirus concentration: A 20 % sucrose H_2O solution was prepared. Centrifuge tubes (Beckman Coulter) were washed with 70 % ethanol before use. They were filled with virus supernatant which had been thawed beforehand. Two ml of the sucrose solution was carefully transferred onto the bottom of the tubes. Virus was spun at 25.000 rpm for 2 hours at 10°C in an ultracentrifuge. After that, supernatant was disposed and virus pellet was re-suspended in 300 µl of T cell medium (~1:100 concentration), aliquoted into cryotubes and transferred into –80° C freezer.

293 cell transduction (for virus titration): 0.5×10^6 293 cells/well were plated out on a 6 well plate and 2 ml of medium (see 2.2.2) was added (day 1). On the next day (day 2), cells were transduced with different volumes (2, 4 and 8 µl) of 100-fold concentrated virus (srambled [vector control] or GCN2 shRNA) in a total volume of 1 ml. Polybrene (stored at -20°C) in an end concentration of 8 µg/ml was added. Medium was changed on the following day (day 3) and cells were transferred into fresh medium every 2 days. Transduction efficiency (% GFP+ cells) was determined on day 5. Up to a transduction efficiency of 30%, it could safely be assumed that 1 virus particle infects one cell, allowing for the determination of the virus titer (transducing units [TU]/ml) by using the following formula:

$$\frac{(\% \text{ GFP+ cells}) \times (\text{transduced cells})}{\text{volume of virus (ml)}}$$

The multiplicity of infection (MOI) is defined as the ratio of virus particles to cells. If cells were transduced with a MOI of 30, this means that 30 times more virus particles than cells were used. The required volume could be calculated by virus titer.

Puromycin selection: The toxic concentration of puromycin for un-transduced 293 cells and 2 days activated PBMC's was determined by culturing these cells in increasing concentrations of puromycin (0-4 µg/ml). The selection of transduced cells was done in the lowest toxic concentration. This concentration was determined to be 1 µg/ml for both, 293 as well as PBMCs.

Human T cell transduction: Due to low virus titers, the transduction protocol had to be optimized. Instructions from the publication by Bobisse et al. 2009 were followed. PBMCs were activated as previously described (day 0) (2.2.7). Two days after activation, 2×10^6 PBMCs were transduced with either scrambled (vector control) or GCN2 shRNA with a MOI between 20 and 50. Protamine Sulfate (stock concentration 1 µg/µl) in an end concentration of 8 µg/ml was added. This transduction suspension was transferred onto a 24 well plate and incubated for 1 hour at 37°C. Thereafter, fresh medium was added to a make up a total volume of 2 ml (= conc. of 1×10^6 cells/ml) and Chiron IL2 was added in an end concentration of 100 u/ml. Cells were incubated for another 2 days and analyzed on day 5. They were re-stimulated with CD3/28 beads in the presence of puroymcin in an end concentration of 1 µg/ml to select for the transduced population.

2.3 Flow Cytometry

2.3.1 Surface staining

Between 1×10^5 and 1×10^6 cells were used for FACS analysis. The cells were washed once with PBS before treating them with 50 µl of 1% FCS/PBS FACS buffer containing the monoclonal antibodies of interest in the appropriate dilutions (see Table 1). Cells were incubated in the dark on ice for 20 minutes, washed twice and re-suspended in 250-300 µl of FACS buffer, after which they were ready for analysis.

2.3.2 Intracellular staining

BD cytofix/cytoperm kit (BD Biosciences 554714) was used. After surface staining, cells were fixed in 50 µl of the fixation solution on a 96 well plate and incubated on ice for 15 minutes. After that, they were washed in 150 ul of 1x perm/wash solution, followed by 15 minutes of incubation with the intracellular antibodies in the right dilutions (diluted in perm/wash buffer). They were then washed again once in perm/wash and once in PBS before the cells were analyzed.

FACS analysis was done on either the BD LSR 2 or the Fortessa FACS machine. FACS sorting was done using the FACSAria. All the antibodies used with the appropriate dilutions are summarized in a table at the end of the Material & Methods chapter.

2.4 Functional Assays

2.4.1 Proliferation assays

Thymidine incorporation assay: $2x10^5$ T cells were activated with plate-bound anti-CD3 and anti-CD28 antibodies as described in 2.2.5. Cells were plated out in triplicates on 96 well plates in 200 µl of the indicated type of medium. Two (2) days after activation, 3-H Thymidine (Perkin Elmer 201112) was added to the cells in an end dilution of 1:400 (= 0.5 µCi) and cells were incubated overnight under standard culture conditions. On the following day, cells were harvested onto a printed filtermat A (Perkin Elmer 1205-401) using a 96 well plate harvester (TOMTEC). After addition of 10 ml betaplate scint (Perkin Elmer 1205-440) scintillation fluid and sealing the filter into a plastic bag, 3-H decay was determined using a beta-plate liquid scintillation counter (Perkin Elmer). Results are presented as counts per minute (CPM).

Non-radioactive proliferation assays: Cells were labeled with either CellTrace™ carboxyfluorescein succinimidyl ester (CFSE) cell proliferation kit (Invitrogen C34554) or cell proliferation dye eFluor® 670 (eBioscience 65-0840-85). A CFSE stock of 5 mM was made up by adding 18 µl of DMSO to the CFSE in powder form. Up to $1x10^7$ cells were labeled with 1 ml PBS containing CFSE in a final concentration of 1 uM (= 1:5.000 dilution of stock) and incubated at 37°C for 3 minutes under gentle agitation every 60 seconds. Cells were then washed once with 4 ml of ice-cold 8 % FCS/PBS and twice with ice-cold 2 % FCS/PBS. Cells were spun down at 4°C. Rate of proliferation was determined by FACS analysis of the diluted CFSE on the fluorescein isothiocyanate (FITC) channel. Labeling cells with eFluor670 follows the same principle as labeling with CFSE, except that eFluor670 was added to the cells in an end concentration of 5 uM and that the FACS analysis was done on the allophycocyanin (APC) channel.

2.4.2 Intracellular cytokine staining

NP peptide specific stimulation: Five days post transduction, T cells transduced with a T cell receptor (TCR) that can recognize the NP peptide in the context of H-$2D^b$ and which has been cloned from TCR transgenic mice designed by Mamalaki et al. (1992) (from now on referred to as F5 TCR), were stimulated with EL4-NP cells which had been irradiated for 14 minutes, in an effector to target (E:T) ratio of 1:3. Two hours after re-stimulation, brefeldin A was added in an end concentration of 5

µg/ul. Brefeldin A blocks the transport of cellular proteins to the Golgi apparatus, preventing them from being secreted, and henceforth traps the cytokines inside of the cell, making them available for intracellular staining. After another 2 hours of incubation, cells were collected, surface stained and fixed (see 2.3.2). Fixed cells were stained for IFNγ, IL2 or TNFα.

Alternatively, cells were re-stimulated overnight, after which brefeldin A was added for 2 hours and processed as before. In this case, IL2 and TNFα could not be detected anymore as opposed to IFNγ.

Polyclonal stimulation: TCR un-transduced T cells were re-stimulated with CD3/28 bead antibodies as described in 2.2.5 and 2.2.7. When indicated, cells were re-stimulated either under normal conditions, in the presence of TGF-β1 (PeproTech 100-21) or under arginine deprived conditions. Other than that, they were treated in the same way as F5 TCR transduced T cells stimulated with EL4-NP cells.

2.4.3 Enzyme-linked immunosorbent assay

$2x10^5$ and $1x10^5$ T cells were activated or re-stimulated either with plate bound anti-CD3 and anti-CD28 antibodies or with CD3/28 bead antibodies in triplicates (see 2.2.4). 50 µl of supernatant was collected on day 2 and 3 after activation, respectively, diluted in 150 µl of PBS and frozen at -20°C for later analysis. IL2 and IFNγ enzyme linked immunosorbent assay (ELISA) was done using BD OptEIA kit 555418 and 555138, respectively. 50 µl of capture antibody, diluted 1:250 in coating buffer, was coated onto 96 well ELISA plates, sealed and incubated at 4°C overnight. On the next day, plates were washed 3 times with wash buffer, wells were blocked with 200 µl of assay diluent and incubated at room temperature for 1 hour. Plates were washed 3 times and were then ready to be loaded with 50 µl of samples as well as IL2 and IFNγ standards. Plates were sealed and incubated at room temperature for 2 hours, after which they were washed 5 times. Then 50 µl of the working detector solution was added which was made up of assay diluent containing biotin linked detection antibody (IL2: 1:1.000; IFNγ: 1:250) and the avidin-horse radish peroxidase (HRP) reagent (1:250). Plates were sealed and incubated for 1 hour at room temperature, washed 7 times and 50 µl of substrate solution was added, containing substrate reagent A and substrate reagent B in equal amounts (1:1). Plates were incubated in the dark for 30 minutes (unsealed). Thereafter, 50 µl of stop solution was added and absorbance rate at 450 nm was determined on an

ELISA plate reader. Standard curves were prepared in Excel and concentrations of samples were calculated relative to these curves.

2.4.4 Western Blot

Celly lysis: Six days after transduction and 4 days after puroymcin selection (~99 % GFP+ cells), $2x10^6$ 293 cells which have been transduced with either scrambled (vector control) or GCN2 shRNA were lysed with 10x Cell Lysis Buffer (stored at - 20°C) (Cell Signalling 9803). Buffer was thawed on ice, 200 µl were mixed with 1800 µl of autoclaved H_2O and 20 µl of phenylmethylsulfonylfluorid (PMSF) (= 1%) was added which serves as an inhibitor of proteinases. Cells were then taken up in 200 µl of this solution, transferred into an Eppendorf tube and spun for 10 minutes at 13.000 rpm in a micro-centrifuge before the supernatant was collected into a fresh Eppendorf tube and frozen at -80°C.

Protein quantification: Thermo Scientific Pierce™ BCA™ protein assay kit (23225) was used. Protein lysates were thawed on ice. Standard dilutions (BSA 0-200 µg/ml) and working reagent (WR) were prepared according to manufacturer's recommendations. Twenty-five (25) µl of standard and protein lysate samples were transferred into 200 µl of WR. The assay is based on a reduction of Cu2+ to Cu1+ by protein in an alkaline medium. Addition of bicinchoninic acid (BCA) results in reaction with Cu1+. The chelate complex of 2 BCA molecules with 1 Cu1+ ion absorbes light at 560 nm which can be detected by a standard plate reader. Hence, the level of absorbance correlates with the amount of protein present in the solution.

Gel preparation: A two-layer gel was prepared (bottom 15 % acrylamide, top 8 % acrylamide). Five ml was enough to make one gel which was made up of the following components: 1.3 (8 %) or 2.5 (15 %) ml of 30 % acrylamide mix, 1.3 ml of 1.5 mM Tris (pH 8.8), 0.05 ml of 10 % sodium dodecyl sulphate (SDS), 0.05 ml of 25 % ammonium persulfate (APS), 0.03 ml TEMED and 2.7 (8 %) or 1.2 ml (15 %) H_2O, respectively. One (1) ml of stacking gel was made up of the following components: 0.17 ml of 30 % acrylamide mix, 0.13 ml of 1.0 mM Tris (pH 6.8), 0.01 ml of 10 % sodium SDS, 0.01 ml of 25 % APS, 0.001 ml TEMED and 0.68 ml H_2O. Gel mix was poured between two thin glass plates while still soluble. Isopropanol was added carefully on top and as soon as gel was polymerized it was removed again. Remaining traces were washed off with H_2O. Stacking gel was poured on top of polymerized gel and comb was put on top. Gel was either stored in at 4° C or used immediately.

Protein separation: Protein lysates were thawed on ice. Five times (5x) Laemmli sample buffer contained the following components: 60 mM Tris-Cl pH 6.8, 2 % SDS, 10 % glycerol and 0.01% bromophenol blue. 2β-mercaptoethanol was added in an end dilution of 1:20 (5 %) just before use. Sample buffer was diluted 1:5 in protein lysate solution and incubated at 95°C for 5 minutes. A quick pulse spin was done before 10 µg of protein was loaded onto the gel. Five (5) µl of a Protein Ladder (10-250 kDa) (NEB P7703S) was also added to determine the correct size of the protein of interest (GCN2: 187 kDa, GAPDH: 35.9 kDa). Protein electrophoresis was done at 70 volts for 3 hours in running buffer which was made up in H_2O containing the following components (pH 8.3): 25 mM Tris base 190 mM glycine and 0.1% SDS.

Protein transfer: Polyvinylidenfluorid (PVDF) (BioRad 162-0175) membrane was activated in methanol before being transferred into transfer buffer which was made up in H_2O of the following components (total volume: 1 litre): 3.03 g Tris, 14.4 g Glycine, 200 ml methanol. Filter papers (BioRad 170-3932) were soaked in Transfer buffer, 2 layers were put onto semi-wet transfer machine, PVDF membrane was put on top, followed by the gel and 2 more layers of filter paper. Transfer was done at 12 volts for 1 hour.

Antibody staining: After 1 hour of transfer, membrane was incubated for 5 minutes in 1x Tris-buffered saline (TBS) buffer which was made up of the following components: 200 ml of 5x TBS (1 litre: 25 ml 2 M Tris (pH 8), 150 ml 5 M NaCl, 2.5 ml Tween-20, H_2O to 1 litre) and 800 ml H_2O. Membrane was then blocked under shaking for 1 hour in the following blocking solution: 5 % milk powder, 1x Tris-Buffered Saline (TBS), 0,1 % Tween. It was then washed 3 times in 1x TBS + 0,1 % Tween. Thereafter, lower part of membrane was cut off and transferred into a 50 ml Falcon tube, containing a 1:5.000 dilution of rabbit anti-GAPDH antibody (Cell Signaling 2118) (5 % BSA, 1xTBS , 0,1 % Tween, 7 ml H_2O). The upper part was transferred into a 50 ml Falcon tube, containing a 1:1.000 dilution of rabbit anti-GCN2 antibody (Cell Signaling 3302) (5 % BSA, 1xTBS , 0,1 % Tween, 7 ml H_2O). Membranes were incubated overnight under gentle agitation. On the next day, membranes were washed 3 times as described above. Afterwards, they were transferred into a 50 ml Falcon tube containing a 1:2.000 dilution of secondary horse radish peroxidase (HRP)-linked anti-rabbit IgG antibody (Cell Signalling 7074) (5 % BSA, 1xTBS , 0,1 % Tween, 10 ml H_2O) and incubated for 1 hour at room temperature under gentle agitation. Finally, membranes were washed again 3 times.

Development and visualization: 20X LumiGLO® Reagent and 20X Peroxide (Cell Signalling 7003) were diluted 1:20 in H_2O (same solution). This solution was carefully poured over the membrane. Membrane was wrapped into silo foil after 1 minute of incubation and transferred into a photo plate containing X-ray film where it was kept for 1-3 minutes (in dark room). Film was then developed manually or automatically.

2.5 In Vivo Experiments

2.5.1 Mice

C57BL/6 mice were obtained from the in-house animal facility at the Royal Free Hospital. B6.129S6-Eif2ak4<tm (GCN2-/-) mice were shipped from the Jackson Laboratory in the US and breeders were established at our local site. C57BL/6 mice or GCN2-/- mice were used as tissue donors for *in vitro* experiments. For the *in vivo* experiments, Thy1.1 C57BL/6 mice, aged between 8 and 12 weeks, were used as donors and age-matched Thy1.2 mice as recipients unless when stated otherwise. All experiments were carried out under a home office license (project license numer 70/7300).

2.5.2 Genotyping

Flow through from an untouched CD3 WT and GCN2-/- T cell selection was used for genotyping. At first, red blood cells were lysed, remaining cells were spun down and 5 ml of cell lysis solution (Quiagen 1045723) was added. 1 ml of protein precipitation solution (Quiagen 1045701) was added and the whole mix was vortexed for 20 seconds to get a homogeneous suspension, after which the mix was put into a centrifuge at 3.500 rpm for 30 minutes. Supernatant was transferred into a fresh tube, 1x volume of isopropanol was added and this mix was put into a centrifuge at 3.500 rpm for 20 minutes. Five (5) ml of 70 % ethanol was added and tube was put into a centrifuge for 5 minutes at 3.500 rpm. All spins were carried out at 4°C. DNA pellet was air dried and dissolved in 150-200 µl of H_2O. DNA was quantified on a spectrophotometer and diluted such as to get a concentration of 100 ng/µl. Primers were designed and PCR was carried out according to the online recommendations of the Jackson laboratory[6].

2.5.3 Engraftment experiments

A CD8 sort on Thy1.1 splenocytes was done, the cells were activated with ConA and IL7 and doubly transduced with F5 TCR + GFP vector control (VC) and F5 TCR + Rheb 24 hours later. On the day of injection (= day 3 after transduction), Thy1.2

---

[6]

http://jaxmice.jax.org/protocolsdb/f?p=116:2:3546024893428046::NO:2:P2_MASTER_PROT OCOL_ID,P2_JRS_CODE:1841,008240

recipients (n=3 per group) were irradiated with 5.5 Gray 4 hours before T cell administration to enhance engraftment of the transferred population. 0.5×10^6 Vβ11/GFP double positive cells were injected intravenously in a total volume of 200 µl PBS.

2.5.4 Competition experiments

Mice from different congenic backgrounds were used as T cell donors and recipients. For example, CD8+Thy1.1+CD45.2+ T cells from C57BL/6 mice were doubly transduced with either the F5 TCR + Rheb or the F5 TCR + Pras40 and CD8+Thy1.2+CD45.2+ T cells from C57BL/6 mice were doubly transduced with the F5 TCR + VC. F5+GFP+ cells from these two transductions were mixed in a ratio of 1:1 and were then injected intravenously into CD45.1 C57BL/6 recipients (n=4 per group). Transferred cells could be detected using the CD45.2 marker while the change of the cell ratio could be monitored with the help of the Thy1.1 marker. A total of 4×10^5 cells were injected on day 3 post transduction. Two days later, a tail-bleed was carried out to confirm the 1:1 mix before the mice were vaccinated with 1×10^6 irradiated EL4-NP cells intraperitoneally (i.p.). The T cell response (expansion and contraction) was monitored by weekly tailbleeds over a course of 130 days. To test the functional memory capacity of the transferred cells, mice were re-challenged with the same dose of irradiated EL4-NP cells on day 41 post transfer. Upon termination of the experiment, spleens, lymph nodes and bone marrow were collected for a detailed analysis of the transferred cells.

2.5.5 Tumour protection experiments

One million (1×10^6) EL4-NP cells were re-suspended in 50 µl of PBS mixed together with 50 µl of Matrigel (BD Biosciences) which serves as a stabilizing matrix, allowing the tumour to grow uniformly which is crucial to take exact size measurements. Mice were weighed, shaved on their right flank and irradiated with 5.5 Gray. 4 hours later, 100 µl of the tumour suspension was injected subcutaneously. Tumour size was manually measured in 2 dimensions (a,b) with a standard caliber and the mice were monitored over time. The formula used to calculate tumour surface is as follows: $\frac{a \times b \times \pi}{4}$. Mice were taken down when tumour size exceeded 15 mm in any dimension, when mice got sick or when they lost more than 20 % of their original weight. In the latter case, mice were excluded from analysis as the cause of death

was uncertain. Mice received F5 TCR transduced T cells that were co-transduced with either VC, Rheb or Pras40 between 1 and 9 days post tumour challenge.

2.5.6 Bioluminescence imaging

To look at *in vivo* infiltration of mTOR modified CD8+ F5 TCR transduced T cells, Thy1.1+ luciferase transgenic mice were used as donors (described by Zeiser et al. [2007]). CD8 T cells were transduced with VC, Rheb and Pras40 and a FACS sort for GFP+ cells was done prior to injection. A total of 0.03×10^6 F5+ T cells were injected into mice bearing 5 days old EL4-NP tumours (see 2.5.5). Eight days post adoptive cell therapy (ACT), mice were subjected to bioluminescence imaging (BLI). They received 100 µl of filter sterilized luciferin 15 mg/ml (PerkinElmer 122796) i.p. and were anaesthesized with isofluran (Baxter 10019-360-60) for 10 minutes in an oxygenized chamber before they were exposed under the BLI camera for 5 minutes. The enzyme luciferase which is expressed by the transferred T cells oxidizes the substrate luciferin in an ATP dependent manner into a bluish-green light emitting product which can be detected by the BLI camera. Data were analyzed using the software "Living Image 3.2".

2.5.7 Isolation of tumour infiltrating lymphocytes

A standard tumour infiltrating lymphocytes (TIL) extraction protocol from the laboratory of Dr Sergio Quezada from the UCL Cancer Institute was followed.

One vial of liberase 1 (Roche 05401020001) was re-suspended in 1 ml of RPMI (5 mg/ml end concentration), aliquots of 330 µl were prepared and frozen at -80°C. Each aliquot is enough to treat 5 tumour samples. Liberase consists of a mix of collagenase 1, 2 and the protease thermolysin, allowing for an effective enzymatic digestion of the extracellular matrix in order to liberate the entrapped T cells. One vial of DNase 1 grade 2 (Roche 10104159001) was re-suspended in 5 ml of distilled water (20 mg/ml end concentration), aliquots of 50 µl were prepared and frozen at -80°C. Each aliquot is enough to treat 5 tumour samples. DNase breaks down the DNA released from dead cells and decreases the viscosity of the samples. After mice were killed, tumours were carefully removed and put into 3 ml of plain RPMI. They were then cut up into small pieces with a scalpel and transferred into a 50 ml Falcon tube. Tumour pieces from one tumour were then immersed in 1 ml of a solution containing 330 µl liberase, 50 µl DNase, and 4620 µl plain RPMI and

incubated in a 37°C water bath for 30 minutes. During this incubation, tubes were carefully mixed every 10 minutes. Thereafter, tubes were immediately put on ice and samples were further processed with PBS containing 5 mM EDTA. Live cells were counted and further analyzed by FACS.

2.5.8 Ex vivo tumour cell isolation

To explore the possibility of antigen escape of mice which succumbed to a secondary tumour outgrowth after an apparent first rejection, EL4 tumours from these mice were isolated, mashed through a cell strainer and cultured in normal EL4 tumour cell medium (see 2.2.2). After one week of culture, F5 transduced CD8 T cells were mixed together with these cells as described in 2.4.2, next to *in vitro* cultured EL4-NP cells as a positive control.

Alternatively, cells were cultured for 2 days with G418 after which cells were counted. Only cells carrying the NP expression cassette should be resistant to this antibiotic (see also 2.2.2).

2.6 Analysis and Statistical Tests

FCS flow cytometry files were analyzed using FloJo 7.6.4 software. Raw data were predominantly transferred into Microsoft Excel 2010 where they were further processed. Arithmetic means, standard deviations, ratios and unpaired as well as paired students t-tests were calculated in Excel (normally distributed data), Mann-Whitney and Wilcoxon matched-pairs signed rank tests were done in GraphPad Prism6 (not normally distributed data).

To calculate significance of the deviation from a certain ratio, either a one sample t-test (normally distributed data) or a Wilcoxon signed rank test (not normally distributed data) was carried out in GraphPad Prism6.

Survival curves were created in GraphPad Prism6 and a log rank test was done to calculate the p-values.

Differences were considered statistically significant when p value was <0.05 (* <0.05, ** <0.01, *** <0.001, **** <0,0001).

Antibody specificity	Fluorochrome	Manufacturer	Dilution
CD3 (FACS)	FITC	BD Bioscience	1:100
CD3 (Activation)	/	BD Bioscience	1:400
CD8 (FACS)	V450	BD Bioscience	1:250
CD16/32 (Fc block)	/	eBioscience	1:50
CD19 (FACS)	APC	eBioscience	1:200
CD19 (FACS)	PerCP-Cy5	eBioscience	1:100
CD28 (Activation)	/	BD Bioscience	1:800
CD44 (FACS)	PE	BD Bioscience	1:400
CD45.1 (FACS)	APC-eFluor 780	eBioscience	1:100
CD45.2 (FACS)	PerCP-Cy5.5	eBioscience	1:400
CD62L (FACS)	APC	BD Bioscience	1:400
CD62L (FACS)	PE	BD Bioscience	1:400
CD127 (FACS)	eFluor 660	eBioscience	1:100
GAPDH (WB)	/	Cell Signaling	1:5000
GCN2 (WB)	/	Cell Signaling	1:1000
GCN2 (FACS)	/	Cell Signaling	1:25
H-2D^b (FACS)	PE	eBioscience	1:100
IFNγ (FACS)	APC	BD Bioscience	1:100
IFNγ (FACS)	PE	BD Bioscience	1:100
IL2 (FACS)	APC	BD Bioscience	1:100
pS6 (FACS)	Alexa 647	Cell Signaling	1:100
Q8 (FACS)	Biotin	Biolegend	1:100
Rabbit IgG (FACS)	PE	eBioscience	1:12.5
Streptavidin	PE	eBioscience	1:200
Thy1.1 (FACS)	Pe-Cy7	eBioscience	1:10.000
Thy1.2 (FACS)	Pe-Cy7	eBioscience	1:12.500
Vβ11 (FACS)	PE	BD Bioscience	1:200

Table 1 Table of mouse antibodies used. Applications are indicated in brackets. WB=Western Blot.

Chapter 3 GCN2 as a Potential Target to Improve Cancer Immunotherapy

GCN2 has been suggested to mediate T cell inhibition under tryptophan (Munn et al. 2005) and arginine low conditions (Rodriguez, Quiceno, and Ochoa 2007). Absence of GCN2 in T cells, as is the case in GCN2-/- mice, was therefore expected to make them resistant to the effects of amino acid deprivation, as reported by Munn et al. (2005) and Rodriguez, Quiceno, and Ochoa (2007). It would therefore be attractive to design strategies, based on genetic modifications, which interfere with the GCN2 pathway in order to render T cells resistant to an amino acid low tumour microenvironment. The aims of the following experiments were to:

1) Establish such a strategy.
2) Show that this results in a functional advantage of the T cells under arginine deprived conditions.

3.1 shRNA Transduction Results in a Decrease of GCN2

One common strategy to reduce the expression of a protein by means of genetic interference is the use of short hairpin ribonucleic acid (shRNA). The principles of physiological micro RNA (miRNA) mediated down-regulation of proteins, upon which this technique relies, are outlined in Figure 12 which was adopted from Bushati and Cohen (2007).

In collaboration with Thermo Scientific, UCL established a lentivirus plasmids library offering shRNAs targeting a broad range of murine as well as human proteins. The shRNA transcribed from the so-called GIPZ vector is embedded in the backbone of the primary miR-30 miRNA (Zeng, Wagner, and Cullen 2002; Silva et al. 2005). The transcript consists of 22 nucleotides (nt) of double stranded (ds) RNA, a 19 nt loop from human miR-30 as well as 125 nt of miR-30 flanking sequences on either side (see also Figure 13). This allows for the expression of a whole length pri-miRNA, resulting in a natural and effective processing of the shRNA of interest, in contrast to traditional expression systems that are based on the more mature pre-miRNA configuration which occurs more distal in the physiological miRNA processing pathway. Using this system, a reduction of up to 80 % (theoretical maximum) of the target mRNA can be achieved (Silva et al. 2005). Figure 13 describes other features of the GIPZ vector in detail.
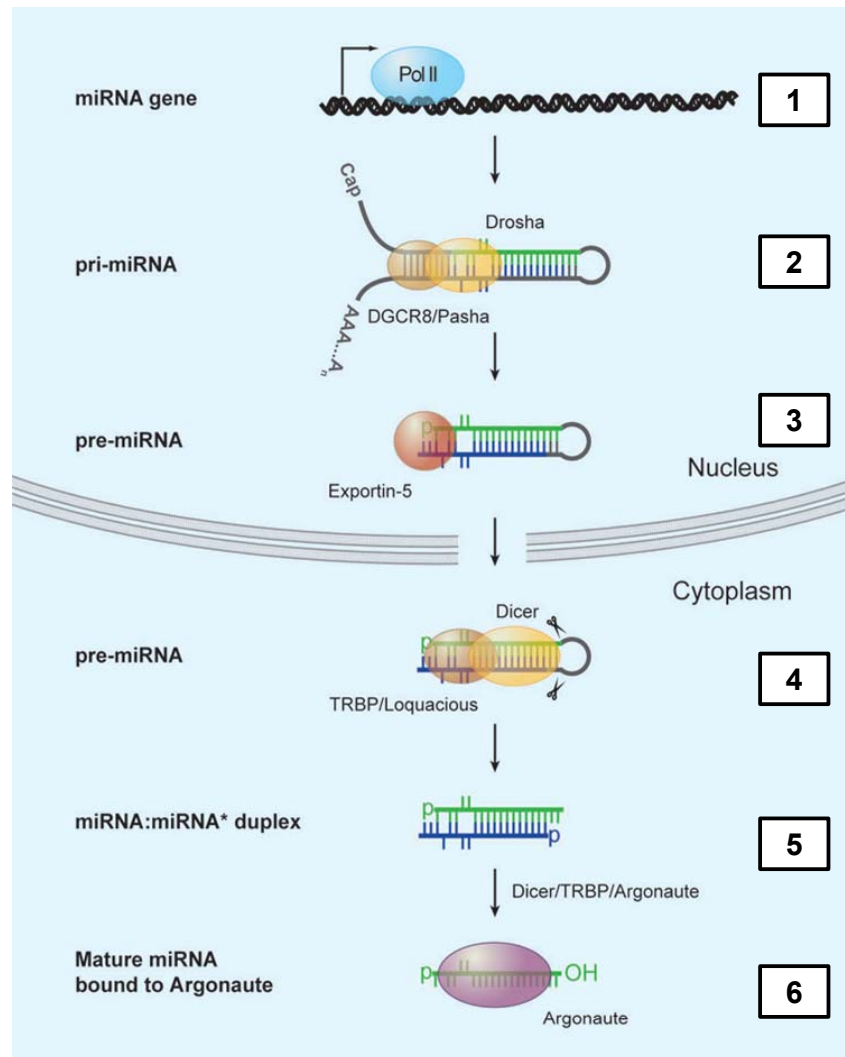
miRNA: How does it work?

Figure 12: The miRNA pathway

Most miRNA genes are transcribed by RNA Polymerase 2 (Pol II), producing a stemloop primary miRNA (pri-miRNA) transcript (1). This transcript is recognized within the nucleus by the protein complex "Microprocessor" which contains as key components Drosha, a RNase 3 enzyme, and the double-stranded RNA binding domain (dsRBD) protein DGCR8/Pasha (2), resulting in the cleavage of pri-miRNA into a ~70 nucleotides (nt) hairpin-precursor miRNA (pre-miRNA) (3). Thanks to a 2-nt 3' overhang, this product can be recognized by the protein Exportin-5 which is responsible for the transport from the nucleus into the cytoplasm where pre-miRNA is further cleaved into a ~22-nt miRNA:miRNA* duplex by the RNase 3 enzyme Dicer (4). Together with Dicer, the dsRBD protein TRBM/Loquacious recruits a so-called Argonaute protein, forming a trimeric protein complex which initiates the assembly of the protein complex RNA induced silencing complex (RISC) (5). miRNA is incorporated into RISC whereas miRNA* is degraded (6). The whole complex is guided by miRNA through base-pair binding to its complementary target RNA which is subsequently either cleaved or translation is repressed. Permission to reproduce this picture has been granted by Bushati and Cohen (2007).

At first, a potential shRNA targeting both murine as well as human GCN2 was identified in the UCL GIPZ online databank. As a control, a so-called "scrambled" vector was used which encodes for a shRNA that does not target any of the known naturally occurring mRNAs. Transduction of 293 cells with 100-fold concentrated virus resulted in good GFP expression, allowing for the determination of the virus titer (see Figure 14).

Figure 13 Vector used for shRNA expression

Schematic representation of vector. The viral sequences of the GIPZ vector include the following components: 1) 5'LTR (long terminal repeat) and 3'LTR mark the beginning and the end of the virus genome, respectively. The 3'LTR lacks enhancer elements located in the U3 region (ΔU3), thereby preventing the native transcriptional activity from the viral LTR, making it a so-called self-inactivating (SIN) vector. 2) The primer binding site (PBS) complementary to tRNA^{Lys3} marks the initiation site of the reverse transcription (resulting in minus-strand DNA synthesis). 3) ψ (Phi) represents the HIV-1 packaging signal, allowing for the assembly of the virus genome with its viral envelope. Attached to it is the 5' gag sequence, as well as the env fragment which includes the Rev response element (RRE), both of which further facilitate packaging. 4) The FLAP fragment contains a central polypurine tract (cPPT) and a central termination site (CTS) which enable translocation of the pre-integration complex into the nucleus. 5) The polypurine tract (PPT) facilitates the initiation of the plus strand DNA synthesis. The non-viral and hence transgene components contain the following sequences: 1) The cytomegalovirus (CMV) promoter enables strong transcription of turbo green fluorescent protein (tGFP) which serves as a marker of transduction. 2) Thanks to an internal ribosome entry site (IRES), the puromycin resistance gene (puro) can be co-expressed on the same transcript as tGFP, allowing for the pharmacological selection of transduced cells. 3) The Woodchuck hepatitis posttranscriptional regulatory element (WPRE) enhances transgene expression in the target cells. Information was adopted from the Resources section of the ThermoScientific homepage[7]. Permission to reproduce this picture has been granted by Thermo Fisher Scientific Biosciences Inc.
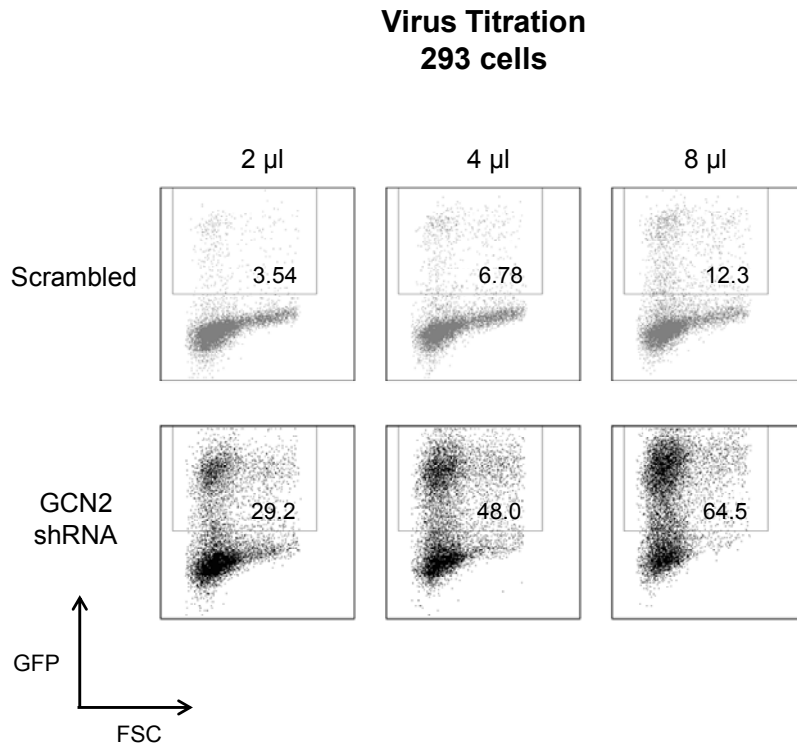
---

[7] http://www.thermoscientificbio.com/shrna/gipz-lentiviral-shrna-libraries/

Virus Titration
293 cells

Figure 14: Virus titration

GCN2 shRNA encoding as well as control ("scrambled") lentivirus was produced and concentrated by means of ultracentrifugation. Thereafter, a titration on 293 cells was carried out with 2, 4 and 8 µl of virus solution. Assuming that up to a transduction efficiency of 30 % one virus transduces one cell, the titer was calculated according to the following formula:

$$\frac{(\% \text{ GFP+ cells}) \times (\text{transduced cells})}{\text{volume of virus (ml)}}.$$

Given that 3.54 % (scrambled) and 29.2 % (GCN2) of 1×10^6 transduced 293 cells expressed GFP when transduced with 2 µl of virus, the virus titers were calculated to be 35.4×10^6 (scrambled) and 292×10^6 (GCN2) transducing units (TU)/ml, respectively, for this round of transduction. Numbers inside of gates represent percentage (%) of GFP+ cells of total cells.

Before transduced cells could be treated with puroymcin to select for cells that have been successfully infected by virus, the right concentration of puroymcin for this procedure had to be determined. Puromycin killing curves were done on un-transduced 293 cells as well as PBMCs which have been activated for 2 days with anti-CD3 antibodies (Okt3) 30 ng/µl and Chiron IL2 300 U/ml. Cells were activated in order to mimic the situation for transduced cells which also undergo activation to guarantee a good transduction efficiency. The right concentration in each case was established to be 1 µg/ml (Figure 15A).

A)

B)
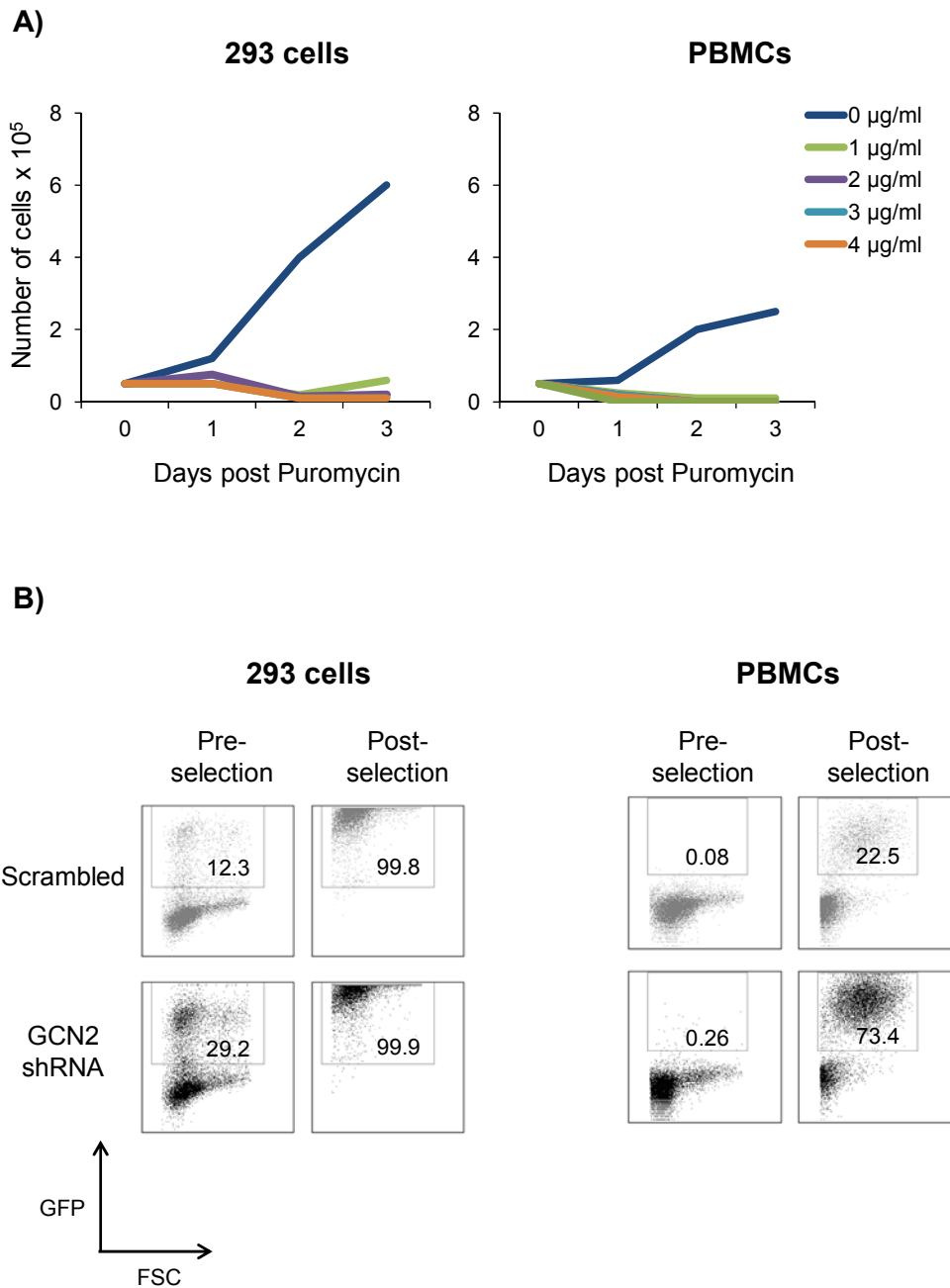
Figure 15: Selection with puroymcin

A) To determine the toxic concentration threshold for un-transduced cells, 293 and activated PBMCs (2 days post Okt3 and IL2 activation) were cultured with different concentrations (0-4 μg/ml) of puroymcin and the cells were counted over the following days. In each case, as little as 1 μg/ml was enough to kill all cells.

B) GCN2 shRNA and control ("scrambled") transduced 293 cells (left) from Figure 14 were cultured for 10 days in the presence of 1 μg/ml of puroymcin to increase the yield of GFP+ cells. PBMCs (right) were transduced with GCN2 shRNA and control ("scrambled") lentivirus with a multiplicity of infection (MOI) of 30 one day post CD3/28 bead antibodies and IL2 activation. They were purified 3 days post transduction by treating them again with CD3/28 bead antibodies and puroymcin (1 μg/ml) to increase the yield of GFP+ cells. Numbers inside of gates represent percentage (%) of GFP+ cells.

Thereafter, transduced 293 cells as well as transduced PBMCs were subjected to a puroymcin treatment using the above determined concentration. Because the expression of GFP was very low in PBMCs (<0.5 % for both scrambled and GCN2 shRNA), these cells were re-stimulated with human CD3/28 bead antibodies in the presence of puroymcin to enrich for the transduced population. Transduced 293 cells could be successfully enriched, such that >99 % of the cells expressed GFP after 10 days of culture in puroymcin enriched medium (change of medium every 2 days). Interestingly, despite the low initial transduction efficiency, also transduced human T cells showed enrichment after 2 days of re-stimulation, albeit in a reduced manner (22.5 % - 74.4 %) compared to 293 cells and with a lower yield of live cells.

Because of the high efficiency of Puroymcin selection of transduced 293 cells, these cells could be used for a Western Blot to determine the down-regulation of GCN2 on a protein level. Transduction with GCN2 shRNA resulted in a visible down-regulation of the protein of interest (Figure 16A), suggesting that this vector can potentially be used to render T cells resistant to amino acid deprivation.

Because of the lower selection rate in PBMCs and a low yield in cell numbers post treatment with puroymcin, these cells could not be used for a Western Blot. It was therefore necessary to establish another test to evaluate the effects of GCN2 shRNA transduction in primary human T cells. One possibility was to do an intracellular staining for GCN2 for a FACS analysis. Because no FACS antibody against GCN2 was commercially available, a double layered staining had to be performed. To these ends, 293 cells were at first subjected to a fixation and permeabilization procedure. Cells were incubated with a rabbit anti-human GCN2 Western Blot antibody for 1 hour before they were exposed to a secondary anti-rabbit IgG FACS fluorochrome (Phycoerythrin [PE]) attached antibody that binds the primary antibody and should hence enable the detection of GCN2 attached antibody.

A)

Western Blot 293 cells
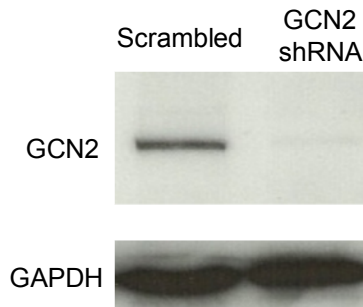
B)

GCN2 FACS staining 293 cells
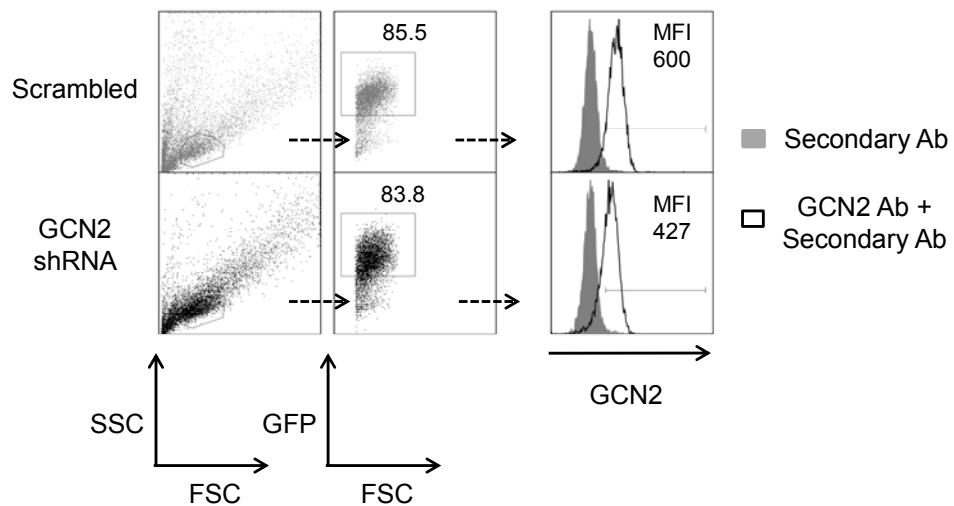
Figure 16: GCN2 detection

A) GCN2 shRNA and control ("scrambled") transduced as well as puromycin (1 µg/ml) purified 293 cells were lysed and a Western Blot was carried out to determine the level of GCN2 down-regulation. GAPDH=house keeping protein control.

B) Intracellular FACS staining for GCN2 on GCN2 shRNA and control ("scrambled") transduced 293 cells. Because the cell number of transduced human PBMCs was too low to do a Western Blot, a staining assay for GCN2 was established. Here, transduced and purified 293 cells were fixed and then incubated with the Western Blot antibody (rabbit origin) before a secondary staining with a PE-conjugated anti-rabbit antibody could be done. Arrows in plots show gating. Numbers inside of gates represent percentage and, where indicated, mean fluorescence intensity (MFI). Grey filled histograms show staining with secondary anti-rabbit antibody only (=background). One representative example of 2 independent experiments is shown.

As shown in Figure 16B, 293 cells transduced with the GCN2 shRNA show a down-regulation of ~29 % compared to cells transduced with the scrambled vector. This result does not contradict the Western Blot result which suggests a greater down-regulation at first sight but does not provide any information about the quantitative level of protein reduction. In this case, the amount of protein loaded as well as the exposure time of the immunoblot membrane to the X-ray film significantly influenced the visualization of the GCN2 protein (result not shown). Hence, GCN2 could also be seen in significant amounts when more protein was used or when the exposure time was extended, also when cells were transduced with GCN2 shRNA. Nonetheless, even in this case it was visible that when cells were transduced with GCN2 shRNA, the expression of the targeted protein was reduced. The advantage of the FACS staining for GCN2 is that it also provides an idea about the quantitative level of down-regulation.

Afterwards, the same staining was done on transduced and puromycin selected T cells to confirm a similar level of down-regulation in these cells of primary interest. As shown in Figure 17, GCN2 shRNA transduced T cells exhibit a down-regulation of about 43 % compared to cells transduced with the scrambled vector, hence confirming that also in these cells, GCN2 could be successfully targeted.

GCN2 FACS staining PBMCs
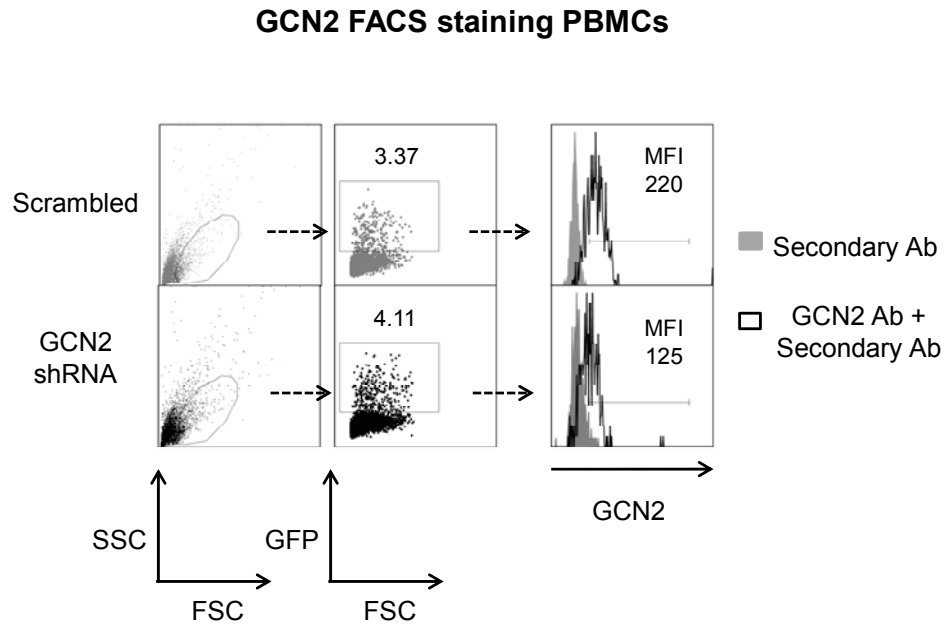
Figure 17: GCN2 staining of transduced human T cells

PBMCs were transduced with GCN2 shRNA and control ("scrambled") lentivirus with a multiplicity of infection (MOI) of 30 one day post CD3/28 bead antibodies and IL2 activation. They were purified 3 days post transduction by treating them again with CD3/28 bead antibodies and puroymcin (1 µg/ml) to increase the yield of GFP+ cells. Two days post purification, cells were fixed and then incubated with the Western Blot antibody (rabbit origin) before a secondary staining with a PE-conjugated anti-rabbit antibody could be done. Arrows in plots show gating. Numbers inside of gates represent percentage and, where indicated, mean fluorescence intensity (MFI). Grey filled histograms show staining with secondary anti-rabbit antibody only (=background). One representative example of 2 independent experiments is shown.

3.2 GCN2 shRNA Transduction Does Not Provide a Proliferative Advantage

The next logical step was to see if the shRNA mediated down-regulation of GCN2 in human T cell results in any functional advantage under amino acid low conditions. Rodriguez, Quiceno, and Ochoa (2007) reported that T cells (CD3+) from GCN2-/- mice are able to proliferate to a full extent in arginine free medium, while T cells from wild type (WT) mice show an almost complete lack of proliferation. Therefore, GCN2 shRNA transduced and puroymcin selected human T cells were stained with the red fluorescent cell proliferation dye eFluor670 which binds to cellular proteins containing primary amines. Upon cell division, the dye is equally distributed to daughter cells, therefore the level of signal loss correlates with the rate of proliferation. Cells treated that way were stimulated with CD3/28 bead antibodies in either normal medium or arginine free medium. As shown in Figure 18, GCN2 shRNA transduced CD8 T cells do not show any proliferative advantage in arginine free medium compared to T cells transduced with the scrambled vector, particularly not to the extent reported in the above mentioned publication. Both, scrambled as well as GCN2 shRNA transduced cells show reduced (2 cell divisions as the two peaks indicate) but not completely abrogated proliferation on day 4 post stimulation in arginine free medium.

However, this negative result could be due to the fact that GCN2 down-regulation is not complete and that the residual GCN2 expression mediates the inhibitory effects of arginine deprivation on T cell proliferation. In addition, the results reported only apply to mouse T cells and the possibility remains that human and mouse T cells behave in different ways. Hence, before other functional experiments and optimizations of GCN2 down-regulation were to be done, it was necessary to show that absolute lack of GCN2 does indeed provide functional benefits.

Proliferation of transduced CD8+ T cells
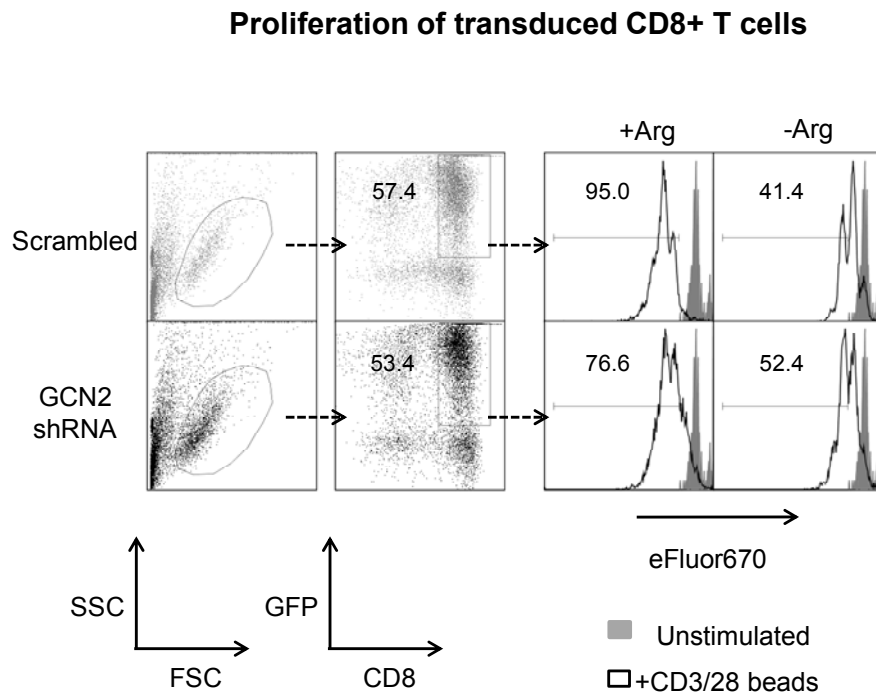
Figure 18: Proliferation of shRNA transduced T cells in arginine free medium

PBMCs (right) were transduced with GCN2 shRNA and control ("scrambled") lentivirus with a multiplicity of infection (MOI) of 30 one day post CD3/28 bead antibodies and IL2 activation. They were purified 3 days post transduction by treating them again with CD3/28 bead antibodies, IL2 and puroymcin (1 µg/ml) to increase the yield of GFP+ cells. Five days later, they were stained with the cell proliferation dye eFluor670 and re-stimulated with CD3/28 bead antibodies in normal or arginine free medium. FACS was done 4 days later. Arrows in plots show gating. Numbers inside of gates represent percentage. Grey filled histograms show cells that were left un-stimulated. One representative example of 2 independent experiments is shown.

3.3 GCN2-/- T Cells Do Not Proliferate under Arginine Low Conditions

In a first instance, it was crucial to re-produce the results upon which the aims of this project were based. B6.129S6-Eif2ak4<tm (GCN2-/-) mice were shipped from the Jackson Laboratory in the US and breeders were established at our local animal facility site. The first author of Rodriguez, Quiceno, and Ochoa (2007) was contacted to get detailed information about the experimental setup with GCN2-/- T cells in addition to the information listed in the "Material & Methods" section. In order to reproduce and confirm the published data, an untouched CD3 T cell sort was carried out on splenocytes from GCN2-/- and wild type C57BL/6 mice. CD3 sort purity was >95 %. T cells were activated with plate bound anti-CD3 and anti-CD28 antibodies the same way as reported. Cells were re-suspended in medium containing different amounts of arginine, ranging from "normal" arginine concentrations of 200 mg/l in conventional 1640 RPMI medium to no arginine at all. On day 2 after activation, supernatant was harvested to determine cytokine production and 3-H Thymidine was added to analyze the proliferative capacity of the cells. As shown in Figure 19A, both wild type and GCN2-/- T cells show reduced proliferation as arginine levels decrease. The same is true for IFNγ production: under sub-optimal arginine availability, T cells secrete less of this cytokine.

To confirm these results using an additional proliferation assay, T cells were stained with CFSE before activation and analyzed 3 days later (principles the same as staining with eFluor670). Lack of CFSE dilution under arginine low conditions further supported and confirmed the Thymidine incorporation results (Figure 20A).

Due to these un-expected results, the genetic disruption of the GCN2 locus in GCN2-/- mice had to be confirmed. Genomic DNA was isolated from flow-through cells that were left over from the untouched CD3 T cell sort on WT and GCN2-/- mice. PCR genotyping revealed a 603 base pair (bp) long fragment for the mutant and a 375 bp long fragment for the wild type mice which is in accordance with the PCR genotyping instructions of the Jackson Laboratory[8] and therefore confirmed the knock-out status of the mice (Figure 20B).

---

[8]

http://jaxmice.jax.org/protocolsdb/f?p=116:2:2697141884681567::NO:2:P2_MASTER_PROT OCOL_ID,P2_JRS_CODE:1841,008240

A)

CD3 T cell sort

B)
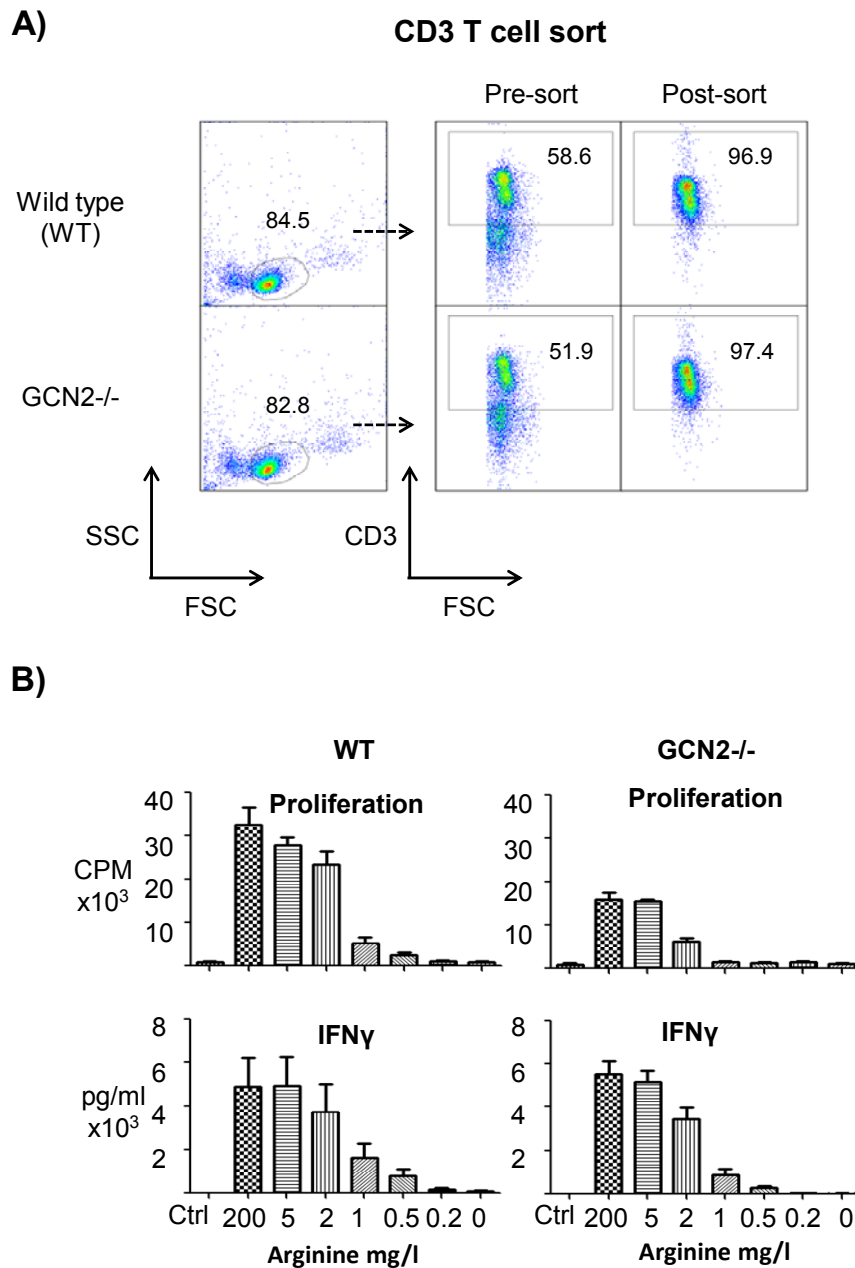
Figure 19: Proliferation of GCN2-/- T cells in arginine free medium

A) An untouched CD3 T cell sort was carried out on splenocytes from GCN2-/- and wild type C57BL/6 mice and sort purity was confirmed. Arrows in plots show gating. Numbers inside of gates represent percentage.

B) CD3 sorted T cells were activated with plate bound anti-CD3 and anti-CD28 antibodies after re-suspension in medium containing different amounts of arginine. On day 2 after activation, supernatant was harvested to determine cytokine production and 3-H Thymidine was added to analyze the proliferative capacity of the cells. Controls (Ctrl) were left un-stimulated. CPM=counts per minute. One representative example of 3 independent experiments is shown.

A)

CFSE Proliferation WT vs GCN2-/- T cells

Concentration of arginine in medium (mg/l)
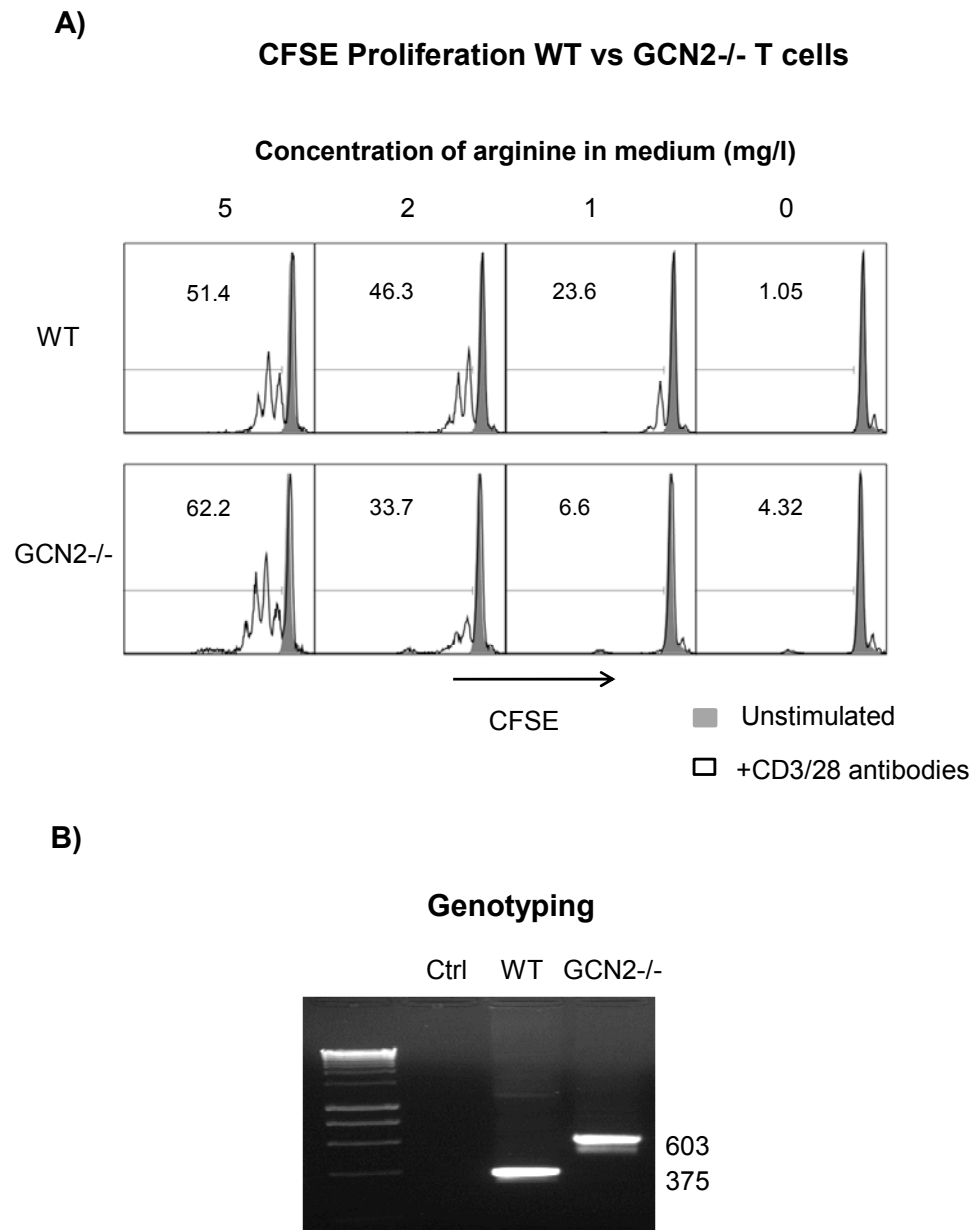
Figure 20: CFSE proliferation and genotyping of GCN2-/- T cells

A) T cells were stained with CFSE before activation with plate bound anti-CD3 and anti-CD28 antibodies in medium containing different amounts of arginine. FACS analysis was done 3 days post stimulation. It was gated on FSC/SSC live cells. Numbers inside of gates represent percentage. Grey filled histograms show cells that were left un-stimulated. One representative example of 3 independent experiments is shown.

B) To confirm the genetic disruption of the GCN2 locus, mice were genotyped. The PCR revealed a 603 base pair (bp) long fragment for the mutant and a 375 bp long fragment for the wild type mice and confirmed the genetic deletion of GCN2. Ctrl = no DNA added to PCR reaction mix.

3.4 Summary and Conclusion

In summary, it was possible to develop a strategy based on shRNA interference to down-regulate GCN2 in 293 as well as primary human T cells. This modification, however, did not result in any proliferative advantage of human T cells in arginine free medium as this would have been expected according to previously published reports. When it was attempted to re-produce the published data, it was not possible to detect any functional advantage of T cells lacking GCN2 when stimulated under arginine low conditions. This is not in accordance with the published data. There are several explanations for this unexpected result:

1) Small experimental deviations as well as the usage of slightly different reagents from different companies can have a significant impact on experimental outcomes. However, the experiments were carefully repeated in the same manner as reported. The first author of Rodriguez, Quiceno, and Ochoa (2007) was contacted to ensure that the same plates were used, the cells were sorted in a similar manner, that the same activation antibodies were used in the same concentrations and that an equal number of cells was plated out. Nonetheless, different batches of fetal calf serum (FCS) used to supplement the medium as well as arginine free RPMI 1640 medium from different companies may still account for the observed differences.

2) It cannot be excluded that the here reported data are false negative. However, much care was taken to confirm the results: a) experiments were repeated independently 3 or more times, b) additional experimental tests (e.g. CFSE proliferation staining in addition to 3-H Thymidine incorporation assay) were carried out and c) besides doing the standard experiments as reported in the publications, the experimental setup was also slightly modified to test the hypothesis under conditions other than reported in publications (e.g. stimulation of cells with CD3/28 bead instead of plate bound antibodies – results not shown). Lastly, only the situation for arginine deprivation was examined, GCN2-/- T cells may still be functional in the absence of other amino acids, as this was reported by Munn et al. (2005) in the case of tryptophan depletion by the enzyme IDO.

3) Published data are false positive. Another group reported difficulties in reproducing the data on GCN2-/- T cells (Cobbold et al., 2009). They managed to show that the internal stress response (ISR) is initiated by GCN2 because GCN2-/- T cells did not up-regulate gene transcripts downstream of the ISR such as CHOP and myd116 (GADD34) under amino

acid starvation whereas T cells from wild type mice did. However, this lack of activation made the cells more sensitive to cell death, especially when they were previously activated and then re-stimulated in amino acid deprived medium. Another publication also suggests that lack of GCN2 exacerbates the detrimental effects of amino acid depletion by Asparaginase on cells of the immune system – including T cells – rather than helping them to overcome these conditions (Bunpo et al. 2010). In addition, based on the idea that lack of GCN2 in T cells can render T cells resistant to the tryptophan consuming effects of IDO within tumours, Metz et al. (2012) failed to show any advantage of GCN2-/- T cells to protect from tumour while lack of IDO did provide such a protection. Two of these publications point out the importance of low mTOR signaling in mediating T cell inhibition under amino acid deprivation.

Whatever the reason, in conclusion we decided to look out for other strategies to improve adoptive T cell tumour therapy.

Chapter 4   MTOR Tuning as a Strategy to Improve Cancer Immunotherapy

The Mammalian Target of rapamycin (mTOR) is a central regulator of cell growth and division by integrating both extrinsic growth factor stimuli as well as intrinsic energy and nutrient availability (Zoncu, Efeyan, and Sabatini 2011). The mTOR complex 1 (mTORC1) gets activated by the TCR, co-stimulatory molecules, such as CD28, and cytokines, for instance IL2, along the phosphoinositide-dependent kinase 1 (PDK1) (D. K. Finlay et al. 2012) axis whereas regulation of mTORC2 is less clear. The following investigations are therefore restricted to mTORC1. For simplification reasons mTORC1 will from now on be referred to as mTOR unless when stated otherwise. Major components as well as the regulation of mTOR are summarized in Figure 10.

mTOR is critical in determining effector versus memory CD8 T cell differentiation, as summarized in detail in Chapter 1. As both of these subsets are crucial for a successful adoptive T cell tumour therapy, it would be attractive to design strategies to guarantee optimal development of both, effector as well as memory T cells, based on differential mTOR signaling. In close collaboration with Dr. Pedro Velica and Professor Ronjon Chakraverty (UCL) from the UCL Research Department of Haematology, these possibilities were further explored. While they were focusing on manufacturing memory cells through the inhibition of mTOR, the aims of the following experiments were to:

1) Establish a strategy to increase mTOR signaling in CD8 T cells.
2) Explore the functional effects of this modification *in vitro.*
3) Explore the behavior of modified cells under suboptimal T cell activation conditions.
4) Combine this strategy with a TCR gene therapy approach.
5) Compare the *in vitro* function of CD8 T cells with high mTOR ($mTOR_{hi}$) to cells with low mTOR ($mTOR_{lo}$) activity.

It is expected that enhancing mTOR signaling in CD8 T cells leads to improved effector functions while inhibiting mTOR results in increased CD8 T cell memory differentiation.

## 4.1 Arginine Deprivation Inhibits MTOR Singaling

The activation of mTOR can easily be monitored through FACS by staining for phosphorylated S6 (pS6). However, S6 can also be phosphorylated by mTOR independent pathways, such as the mitogen-activated protein kinases (MAPK) pathway (Roux et al. 2007) which, in T cells, is triggered through the TCR (Smith-Garvin, Koretzky, and Jordan 2009). Therefore it was necessary to confirm that the pS6 signal pre-dominantly correlates with mTOR activity and no other pathway. In addition, because of the highly dynamic character of mTOR signaling, it was essential to get an idea about its kinetics.

A CD8 magnetic beads selection was performed on splenocytes from a normal C57BL/6 mouse. CD8 purity was confirmed before the cells were activated with CD3/28 bead antibodies in the presence or without rapamycin (250 nM). Rapamycin is the most common mTOR inhibitor (giving mTOR its name), therefore if any residual pS6 can be detected in the presence of this drug, this signal probably stems from a mTOR independent source. The cells were collected at different time points (0-44h) post activation, fixed and permeabilized before they were treated with an intracellular pS6 FACS antibody. Hardly any pS6 signal could be detected in cells activated in the presence of rapamycin, suggesting that mTOR is the primary kinase responsible for the phosphorylation of S6. Cells with no rapamycin, however, showed the strongest signal between 4 and 24 hours post stimulation. The signal was gone after 48 hours (Figure 21).

It was already shown that T cell inhibition by arginine deprivation is most likely not mediated by GCN2 activity (see 3.2). Several reports have suggested a role for reduced mTOR signaling in T cell inhibition due to absence of amino acids (e.g. Cobbold et al. 2009). To explore a possible role of GCN2 in the decreased activation of mTOR under arginine low conditions, T cells from wild type and GCN2-/- mice were activated as described in the previous chapter. Because of a slightly different activation regime as shown in Figure 21 – plate bound anti-CD3/anti-CD28 instead of CD3/28 bead antibodies – which results in delayed mTOR activation, the time point of staining had to be postponed to 44 hours instead of 24 hours. Cells were fixed, permeabilized and stained for pS6. Figure 22 shows that, as arginine levels drop, pS6 decreases dramatically in both, WT as well as GCN2-/- T cells. Therefore, GCN2 does not contribute to the decreased activation of mTOR under amino acid low conditions and mTOR seems to be a plausible cause for the observed T cell inhibition (low proliferation and IFNγ production) reported in the previous chapter. This also raises the question if increased mTOR signaling can rescue T cells from the negative effects of arginine depletion.

A)

CD8 sorted murine T cells
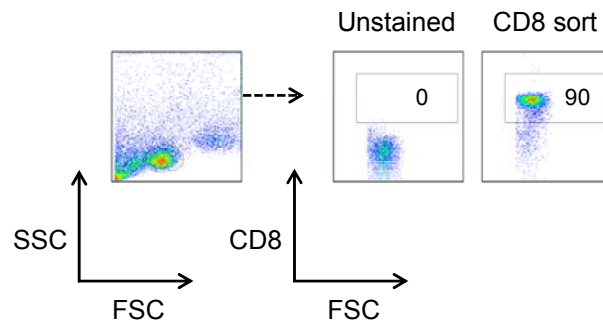
B)

mTOR kinetics activated primary mouse CD8+ T cells

Hours post activation
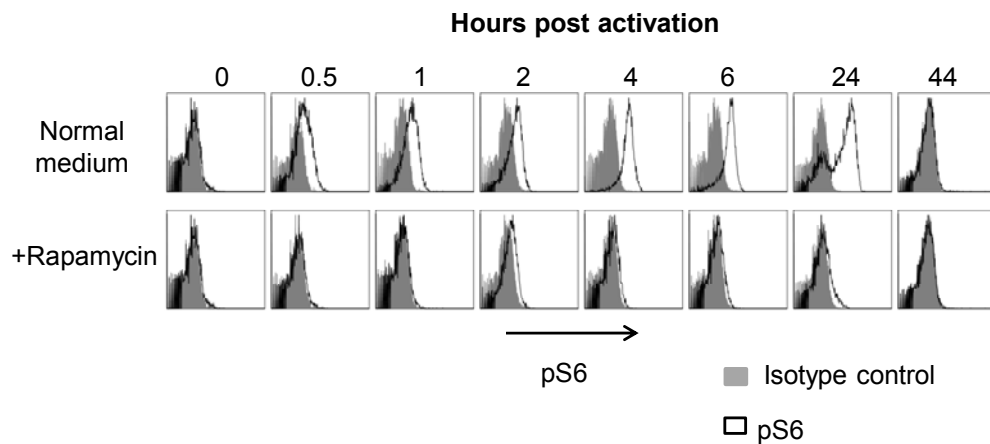
Figure 21: mTOR activation kinetics

A) Sort purity post CD8 T cell selection on murine C57BL/6 splenocytes. Arrow indicates gating strategy. Numbers inside of gates represent percentage.

B) S6 phosophorylation on sorted CD8 T cells at different time points after activation with CD3/28 bead antibodies in the presence or absence of rapamycin (250 nM). Because of pure CD8 population, no other staining was included, it was gated on live cells only (FSC/SSC). Grey filled histograms represent staining with an isotype antibody control (background). One of 3 independent experiments is shown.

mTOR inhibition by arginine deprivation
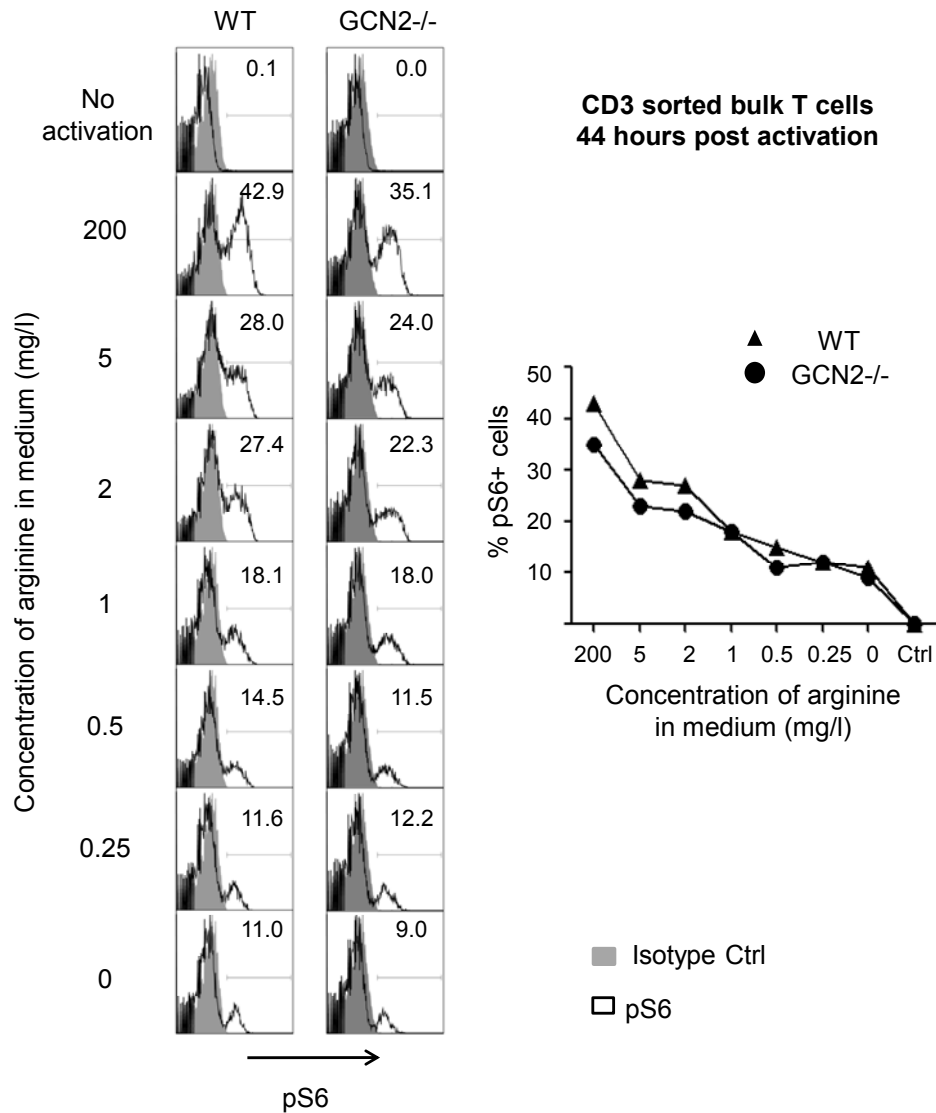
Figure 22: mTOR inhibition by low arginine

CD3 sorted T cells from wild type and GCN2-/- mice were activated in different arginine containing medium with plate bound anti-CD3 and anti-CD28 antibodies as described in chapter 3.3. Cells were fixed and permeabilized 44 hours later and stained for pS6. Because of pure CD3 population, no other staining was included, it was gated on live cells only (FSC/SSC). Grey filled histograms represent staining with an isotype antibody control (background). Numbers in FACS plots represent percentages. Controls (Ctrl) were left un-stimulated. One of 2 independent experiments is shown.

4.2 Cloning of Rheb and RQ64L

One strategy that emerged early on as a potential way to modify mTOR signaling was to over-express the positive mTOR regulator Rheb while over-expressing the negative regulator Pras40 should result in the opposite effect, i.e. mTOR inhibition. Rheb overexpression is a common strategy used by molecular biologists to study the effects of mTOR signaling and has also been shown to confer resistance to the effects of amino acid deprivation (Saucedo et al. 2003; Stocker et al. 2003; Roccio, Bos, and Zwartkruis 2005; Long et al. 2005) while Sancak et al. (2007) identified Pras40 as a powerful inhibitor of mTOR. As a basic orientation, transductions with **Rheb** or its mutated version (see below) are highlighted in red, transductions with **Pras40** are highlighted in blue and control transductions with **vector control** (**VC**) (containing spacer DNA instead of an insert) are highlighted in grey.

At first, RNA from activated splenocytes (24 hours) was extracted and cDNA was produced through a reverse transcriptase reaction. Rheb was PCR amplified using the primers listed in chapter 2.1.1. Two unique restriction sites were added on either end of the Rheb DNA molecule, a Not 1 restriction site on the 5' and a Sal 1 restriction site on the 3' end. Using an in-house MP71 vector from our lab which contained an insert with the same restriction sites (5' Not 1 – insert – Sal 1 – IRES - GFP), this vector as well as the PCR fragment were digested with Not 1 and Sal 1 enzymes. The vector backbone and the PCR fragment were gel extracted, ligated with each other and bacteria were transformed. A PCR colony screen was done to identify the bacterial colonies that took up the plasmid. Ligation efficiency was very high: 100 % of the picked colonies revealed the correct PCR fragment size. After further expansion of the bacteria, plasmids of 7 bacterial colonies were purified by MiniPrep, they were test digested with Not 1 and Sal 1 to confirm proper integration into the vector backbone, again 100 % presented with the correct fragment and vector backbone size. A selection of these was sent off for sequencing to confirm the correct Rheb sequence and one plasmid was then chosen for future usage of transfection and transduction.

In addition to normal WT Rheb, through a simple PCR mutagenesis reaction inducing a point mutation at position 191 (A→T), it was possible to create a mutant Rheb protein - from now on referred to as RQ64L which indicates the amino acid change (glutamine [Q] → leucine [L]) at the amino acid position 64 – that is not subject to TSC1/2 inhibition anymore (Long et al. 2005). This mutant was reported to have increased binding of GTP (90 % GTP binding) compared to WT Rheb (50 %

GTP binding) due to the substitute of a highly conserved glutamine with a hydrophobic leucine (Long et al. 2005). Eventually, this results in a constitutive activation of mTOR (Long et al. 2005; Ohtani et al. 2008) as opposed to a simple over-activation of mTOR through WT Rheb as soon as a T cell gets stimulated by TCR, co-stimulation etc. The process of Rheb and RQ64L cloning as well as the principles behind are summarized in Figure 23 to Figure 25.

A)

Cloning of Rheb

Splenocytes +
CD3/28 beads 24h

↓

RNA extraction

↓

Reverse
transcription

↓

PCR

B)

Digest of vector backbone and Rheb

Restriction enzyme
digestion

↓

Gel extraction

↓

Ligation
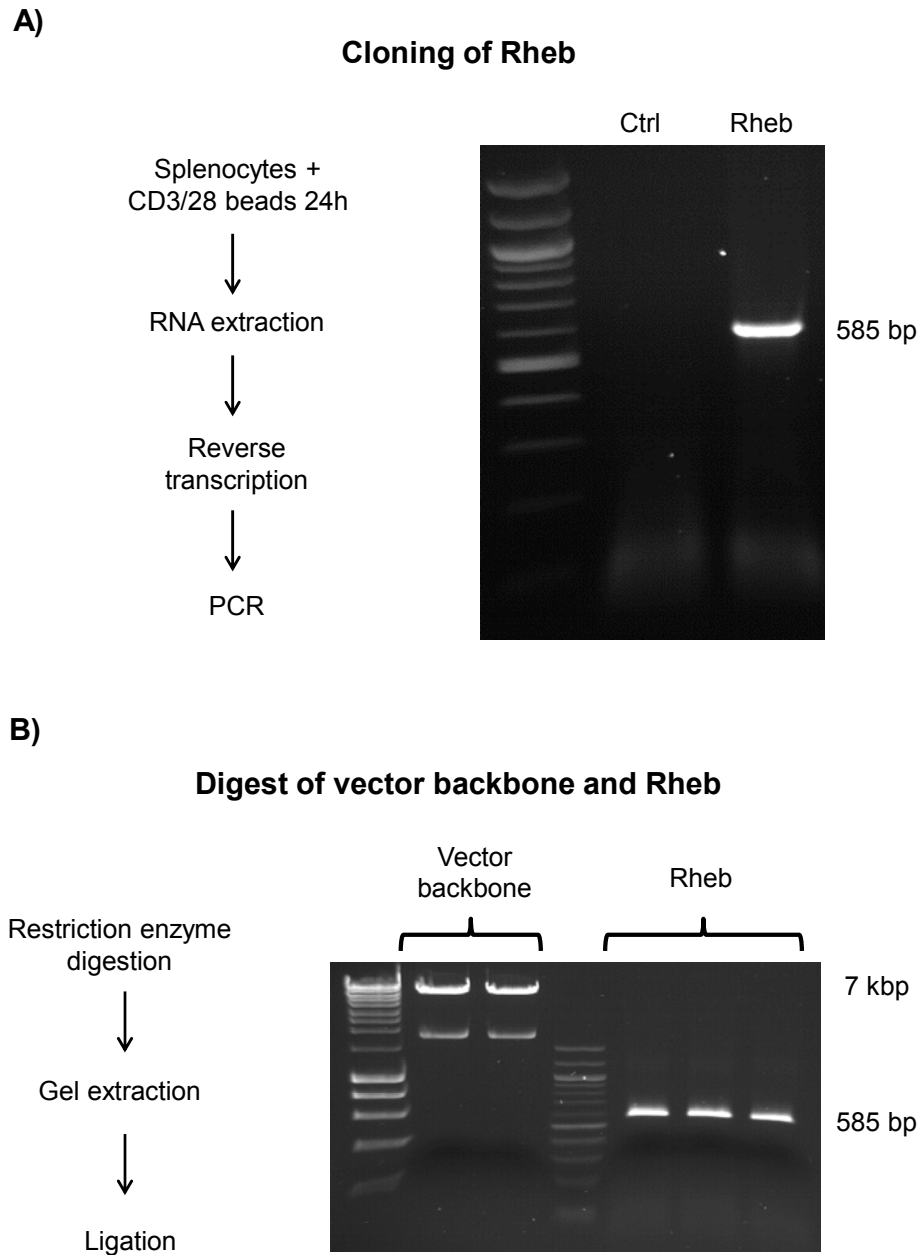
Figure 23: Cloning of Rheb (1)

A) RNA from activated splenocytes was extracted, cDNA was produced and Rheb was PCR amplified (fragment size 585 bp). Two unique restriction sites were included on either end (Not 1 on the 5' and Sal 1 on the 3' end). Ctrl=No template.

B) In-house vector as well as the PCR fragment were digested with Not 1 and Sal 1 enzymes, the vector backbone (7 kbp) and the Rheb PCR fragment (585 bp) were gel extracted, ligated with each other and bacteria were transformed.

A)

PCR colony screen

Controls

Colonies 1-17

-    +

585 bp

B)

Test digestion of purified plasmids 1-7

Digested plasmids 1-7

Undigested

7 kbp

585 bp

Figure 24: Cloning of Rheb (2)

A) PCR colony screen. Single bacterial colonies were picked and a PCR for Rheb expression was carried out. Negative control (-Ctrl)=No template. Positive control (+Ctrl)=cDNA template

B) Test digestion with Not 1 and Sal 1 enzymes on purified plasmids. A selection of positive samples was sent off for sequencing.

Construction of constitutively active Rheb (RQ64L)

Introduction of point mutation **A → T** (position 191)

```
  1 ATGCCTCAGT CCAAGTCCCG GAAGATCGCC ATCCTGGGCT ACCGGTCTGT
 51 GGGAAAGTCC TCGTTGACAA TTCAGTTTGT TGAAGGCCAA TTTGTTGATT
101 CCTACGGTCC AACCATAGAG AACACGTTCA CCAAGTTGAT CACGGTAAAT
151 GGTCAAGAGT ATCATCTTCA GCTTGTAGAC ACAGCGGGGC AGGATGAATA
201 TTCCATTTTT CCTCAGACAT ACTCCATAGA TATTAATGGT TATATTCTTG
251 TGTATTCTGT TACATCAATC AAAAGTTTTG AAGTAATTAA AGTTATCCAT
301 GGCAAGTTGT TGGATATGGT GGGGAAAGTG CAGATACCTA TTATGTTGGT
351 TGGAAATAAG AAGGACCTGC ATATGGAAAG GGTGATCAGC TATGAAGAAG
401 GAAAGGCTTT GGCAGAATCT TGGAATGCAG CTTTTTTGGA ATCTTCTGCT
451 AAAGAAAATC AAACTGCTGT TGATGTTTTT AAAAGGATAA TTTTGGAAGC
501 AGAAAAGATT GATGGAGCAG CTTCACAAGG AAAGTCTTCG TGCTCGGTGA
551 TGTGA
```

Fw primer: 5'-GTAGACACAGCGGGGC*T*GGATGAATATTCCATTT-3'

Rev primer: 5'-AAATGGAATATTCATCC*A*GCCCCGCTGTGTCTAC-3'

Figure 25: Cloning of RQ64L
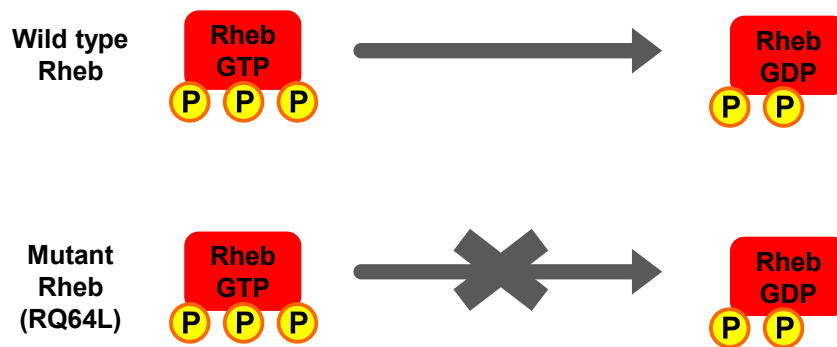
Rheb cDNA sequence highlighting the locus of the introduced mutation (position 191) in red is displayed. Primers are designed such that the daughter plasmids carry a mutation at position 191. This will result in the exchange of glutamine with leucine at position 64 (Q64L), which eventually leads to an increased binding of GTP, rendering Rheb constitutively active. Fw=Forward, Rev=Reverse.

4.3 In Vitro Validation of Rheb and RQ64L in BW Cells

An initial validation was done on cells that are easy to expand and transduce. BW5147 (hereby referred to as BW) cells (see chapter 2.2.2) were transduced with Rheb, RQ64L and VC. GFP could be detected in all 3 cases (Figure 26A). When the cells were stained for pS6 after 24 hours of incubation in normal medium or medium with reduced arginine concentrations, it is clearly visible that Rheb and RQ64L transduced cells show increased mTOR signaling compared to cells transduced with VC in all conditions (gated on GFP+ cells) (RQ64L>Rheb>VC). This difference is gone when the gate is put around the GFP- cells (result not shown). However, even Rheb and RQ64L transduced cells show a loss in pS6 expression when arginine gets scarce, suggesting that mTOR signaling cannot be rescued completely (Figure 26B).

In addition to increased mTOR signaling, Rheb and RQ64L transduced BW cells show an overall increased cell size (RQ64L>Rheb>VC) (see Figure 27). mTOR is an important regulator of cell growth which can therefore be considered an indicator for the level of mTOR activation (Saucedo et al. 2003; Stocker et al. 2003).

A)

Validation of Rheb: GFP expression in BW cells

B)
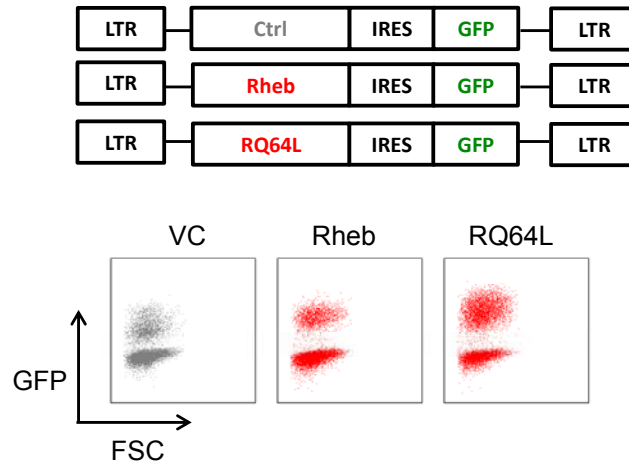
Validation of Rheb: mTOR activation in BW cells
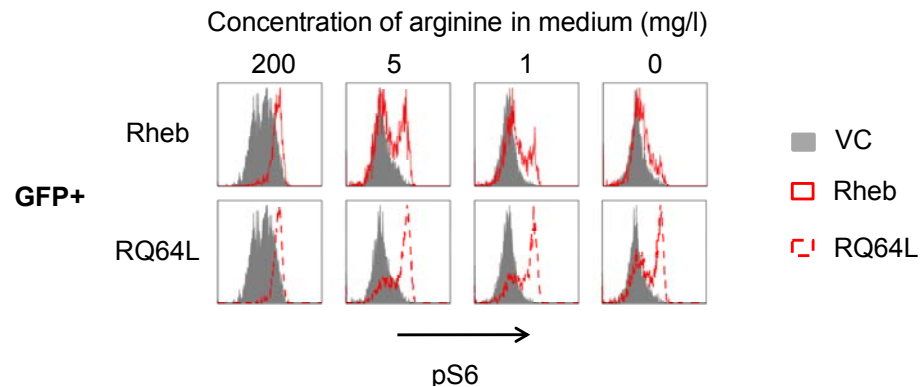
Figure 26 BW cells: Transduction with Rheb, RQ64L and VC

A) MP71 retrovirus vectors were used for the following transduction (see chapter 2.2.6). Linking the inserts via an internal ribosome entry site (IRES) sequence (Ngoi, Chien, and Lee 2004), the vectors also carry green fluorescent protein (GFP) as a marker to track transduced cells. Transcription is regulated by the U3 region in the long terminal region (LTR) and IRES regulates translation of GFP post-transcriptionally. Dot plots show representative examples of GFP expression upon transduction. It was gated on FSC/SSC live cells.

B) BW cells were transduced with VC, Rheb or RQ64L. Several days later, they were fixed, permeabilized and stained for pS6 24 hours after *in vitro* culture in medium containing different concentrations of arginine. It was gated on GFP+ cells. Grey filled histograms represent VC, red line represents Rheb and red dotted line represents RQ64L. One of 2 representative experiments is shown.

Validation of Rheb: Cell size BW cells

Figure 27 BW cells: cell size of transduced cells

BW cells were transduced with VC, Rheb or RQ64L. Several days later, a FACS analysis was carried out after 48 hours of *in vitro* culture in medium containing different concentrations of arginine. Forward Scatter (FSC) is an indicator of cell size. It was gated on GFP+ cells. Grey filled histograms represent VC, red line represents Rheb and red dotted line represents RQ64L. One of 2 representative experiments is shown.
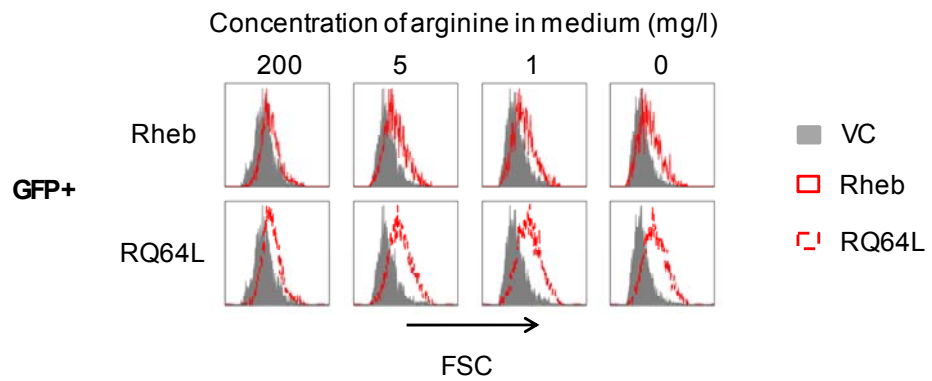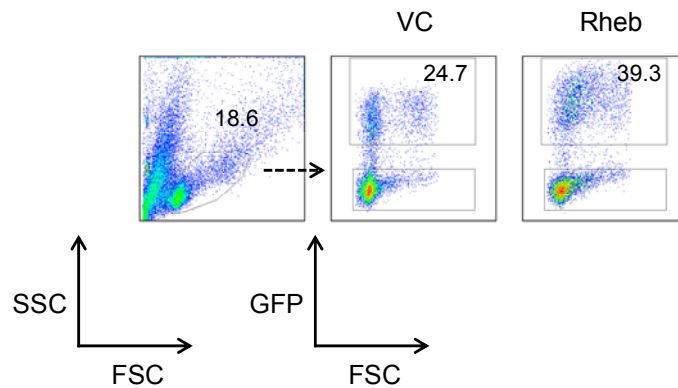
4.4 In Vitro Validation of Rheb and RQ64L in Primary Mouse T Cells

Bulk T cells from a C57BL/6 mouse were activated with CD3/28 bead antibodies and IL2, transduced 24 hours later with Rheb and VC, expanded with IL2 one day after transduction and stained for pS6 on day 3 post transduction (i.e. day 4 post activation). As for the BW line, cells showed high GFP expression (Figure 28A). In contrast to BW cells which do not depend on any growth signal other than sufficient nutrients, T cells need to be activated or stimulated with cytokines in order to grow and proliferate. At the time point of analysis, 4 days have passed since the initial activation and 2 days have passed since they have last received IL2. It was interesting to see that cells transduced with VC control did not show any pS6 staining - as expected according to Figure 21 where pS6 was gone 48 hours post activation - while Rheb transduced cells still presented with a strong signal. In addition, Rheb transduced cells were much larger than VC transduced cells (Figure 26B). In a follow-up experiment, bulk T cells were transduced with VC, Rheb and RQ64L, cells received IL2 on days 1 and 3 post transduction to extend culture time and were analyzed on day 5 post transduction (i.e. day 6 post activation). Figure 29A shows the gating strategy (GFP+CD8+ cells). Figure 29B shows that both, VC and Rheb transduced cells have lost the pS6 signal whereas RQ64L transduced cells still stained positively. Interestingly, Rheb transduced cells were larger than VC transduced cells despite no difference in pS6 expression. RQ64L transduced cells had the largest phenotype.

This initial validation data suggests that transduction with Rheb and RQ64L can prolong mTOR signaling beyond its physiological activation kinetics as shown in Figure 21. However, while it may be attractive to increase mTOR signaling in a controlled and timely restricted manner, such as in Rheb transduced T cells, detrimental effects of a constitutively active mTOR pathway have been reported in TSC1-/- mice (Yang et al. 2011; O'Brien et al. 2011). These mice show a selective deletion of TSC1 in T cells from an early stage onwards, they respond to TCR stimulation in a hyperactive way and show a more activated phenotype but are also more sensitive to cell death and less capable of mounting an effective immune response in mice infected with Listeria monocytogenes. Transduction with RQ64L very much resembles the situation in these TSC1-/- T cells. Henceforth, we decided to continue experiments using Rheb only to benefit from an increased mTOR while reducing the negative effects of an over-activated mTOR signaling pathway.

A)

Validation of Rheb: GFP expression in murine T cells

B)

Validation of Rheb: mTOR and cell size in murine T cells
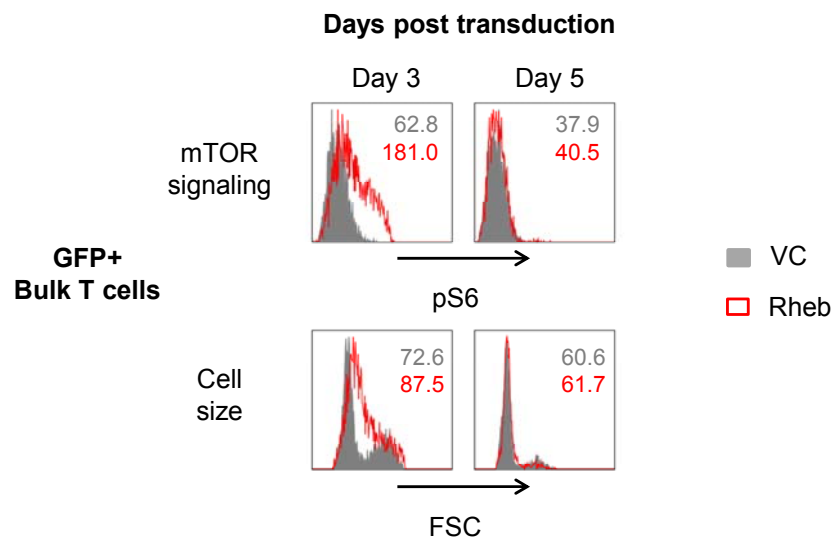
Figure 28: mTOR signaling of Rheb transduced bulk T cells

A) C57BL/6 bulk T cells were activated with CD3/28 bead antibodies and IL2, transduced 24 hours later with Rheb and VC and expanded with IL2 one day after transduction. Cells were analyzed 3 days post transduction. Arrow shows gating. Numbers inside of gates represent percentage.

B) Transduced cells were analyzed for pS6 3 (i.e. 4 days post activation) and 5 (i.e. 6 days post activation) days post transduction. It was gated on GFP+ cells. Grey filled histograms represent VC, red line represents Rheb. Numbers inside of plots represent pS6 median fluorescence intensity (MFI) x10^3 of GFP+ cells and, respectively, median of FSC index x10^3.

A)
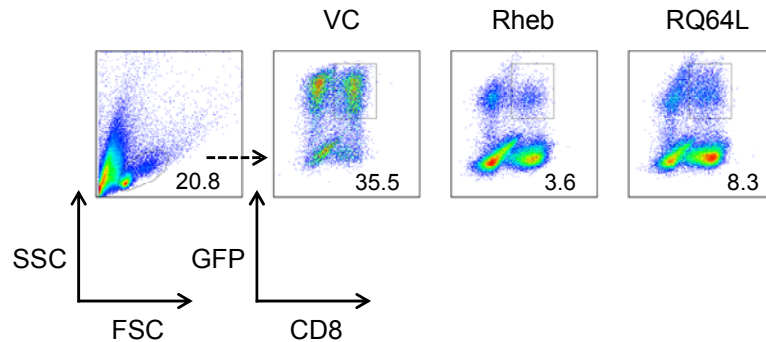
B)

Prolonged mTOR signaling in RQ64L transduced CD8 T cells

Day 5 post transduction
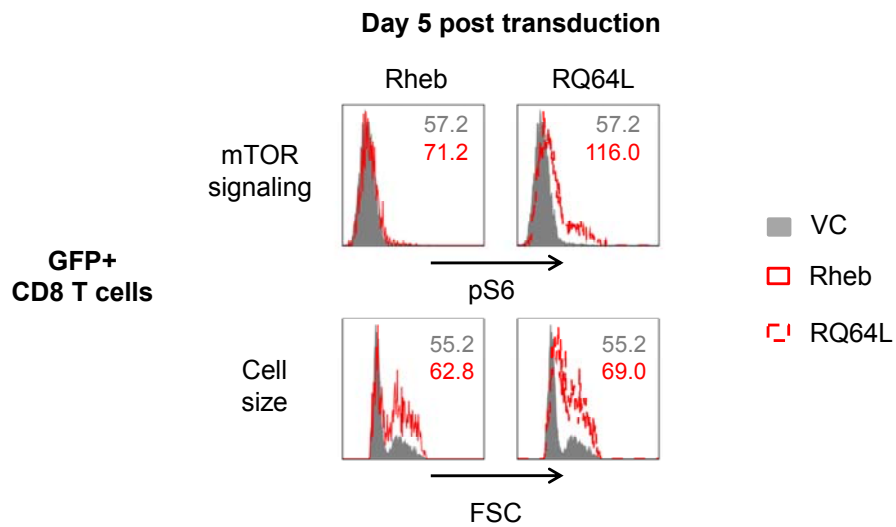
Figure 29 mTOR signaling of Rheb and RQ64L transduced CD8 T cells

A) C57BL/6 bulk T cells were activated with CD3/28 bead antibodies and IL2, transduced 24 hours later with Rheb, RQ64L and VC, expanded with IL2 on days 1 and 3 after transduction and stained for pS6 on day 5 post transduction (i.e. day 6 post activation). Arrow shows gating. Numbers inside of gates represent percentage.

B) Five days post transduction, cells were analyzed for pS6. It was gated on GFP+CD8+ cells. Grey filled histograms represent VC, red line represents Rheb and red dotted line represents RQ64L. Numbers inside of plots represent pS6 median fluorescence intensity (MFI) x10^3 and, respectively, median of FSC index x10^3 of GFP+ cells.

4.5 Function of Rheb Transduced Cells under Suboptimal Activation Conditions

It is crucial that T cells carry out their protective effector functions under conditions when this becomes difficult. For example, lack of nutrients as well as the presence of inhibitory signals can impair T cell responses (Rabinovich, Gabrilovich, and Sotomayor 2007). mTOR integrates environmental and internal stimuli to fine tune T cell responses according to these inputs (Delgoffe and Powell 2009; Powell et al. 2013), such that a low mTOR net result impairs effector differentiation while at the same time promoting tolerogenic and T cell memory responses. A high mTOR net result, on the other hand, favors effector differentiation at the expense of T cell memory formation. By increasing mTOR signaling in T cells under situations where effector functions are normally impaired (e.g. arginine deprivation, presence of TGFβ) it may still be possible to elicit good effector responses.

Rheb and VC transduced cells were re-stimulated with CD3/28 bead antibodies in medium with limited arginine (0 – 200 mg/l) and analyzed 6 and 24 hours post stimulation. The highest mTOR signal is seen 6 hours post stimulation in normal medium. As arginine levels drop, S6 phosphorylation decreases. In nearly all conditions (except of 6 hours post stimulation in 5 mg/l arginine medium), Rheb transduced cells overall express more pS6 compared to VC transduced cells but the signal decreases proportionally the same in both groups (Figure 30).

To investigate the proliferative performance of transduced T cells under arginine limiting conditions, cells were stained with eFluor670 (see also chapter 3.2) before re-stimulation with CD3/28 bead antibodies in medium with limited arginine (0 – 200 mg/l). Two days post stimulation, Rheb transduced cells present with a larger phenotype under all conditions, suggesting that blastogenesis in preparation for cell division is increased in Rheb compared to VC transduced cells (Figure 31).

Indeed, when cells are analyzed 5 days post stimulation, Rheb transduced bulk T cells proliferated to an increased extent than VC transduced T cells when cultured in 200 and 5 mg/l arginine concentrated medium. As arginine levels drop, the level of proliferation decreases and hardly any differences between VC and Rheb transduced cells can be detected when cells are cultured in 1 and 0 mg/l arginine concentrated medium (Figure 32).

mTOR signaling of Rheb transduced CD8 T cells
6 and 24 hours post re-stimulation with low arginine
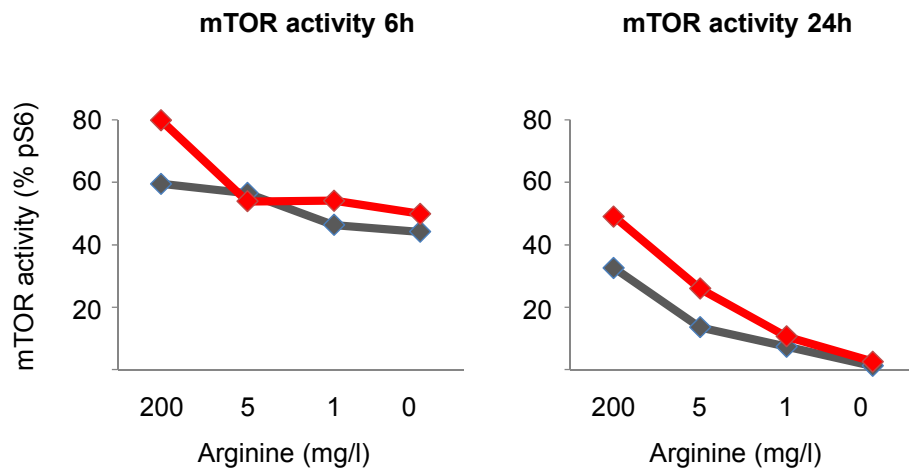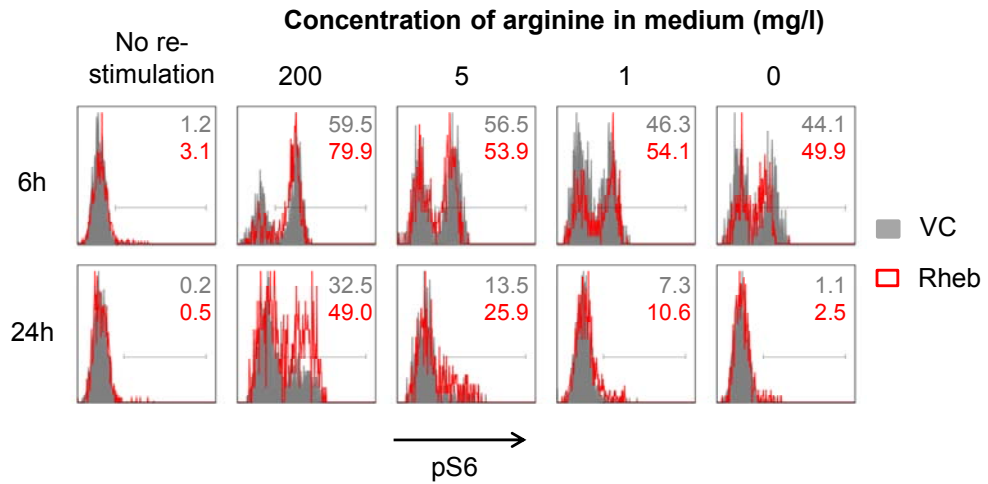
Figure 30: pS6 of re-stimulated CD8 T cells in arginine limited medium

Rheb and VC transduced cells were re-stimulated with CD3/28 bead antibodies in medium with different concentrations of arginine 5 days after transduction. A pS6 FACS analysis was carried out 6 and 24 hours post stimulation. It was gated on CD8+GFP+ cells. Numbers inside of plots represent percentage. The data are summarized below the plots. Grey filled histograms and lines represent VC, red line represents Rheb. One of 2 representative experiments is shown.

**Blastogenesis of Rheb transduced bulk T cells
2 days post re-stimulation with low arginine**
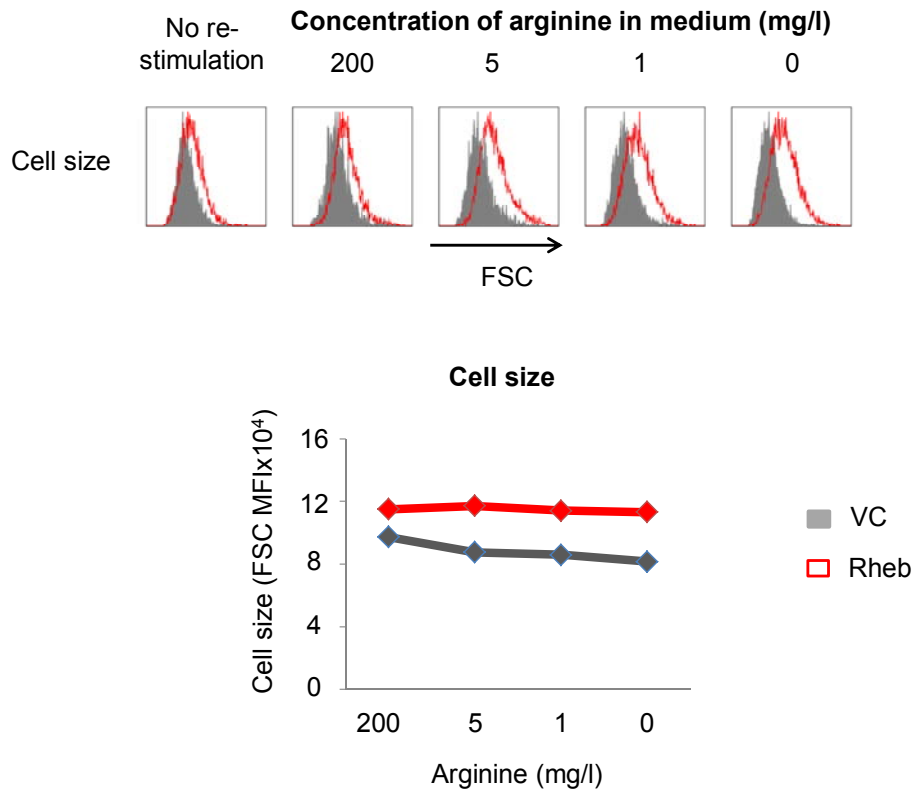
Figure 31: Cell size under arginine low conditions day 2

Five days after transduction, Rheb and VC transduced cells were re-stimulated with CD3/28 bead antibodies in medium with different concentrations of arginine. A FACS analysis was carried out on day 2 post stimulation. It was gated on bulk GFP+ T cells. Numbers inside of plots represent median of FSC index $x10^3$. The data are summarized below the plots. Grey filled histograms and lines represent VC, red line represents Rheb. One of 2 representative experiments is shown.

**Proliferation of Rheb transduced bulk T cells
5 days post re-stimulation**
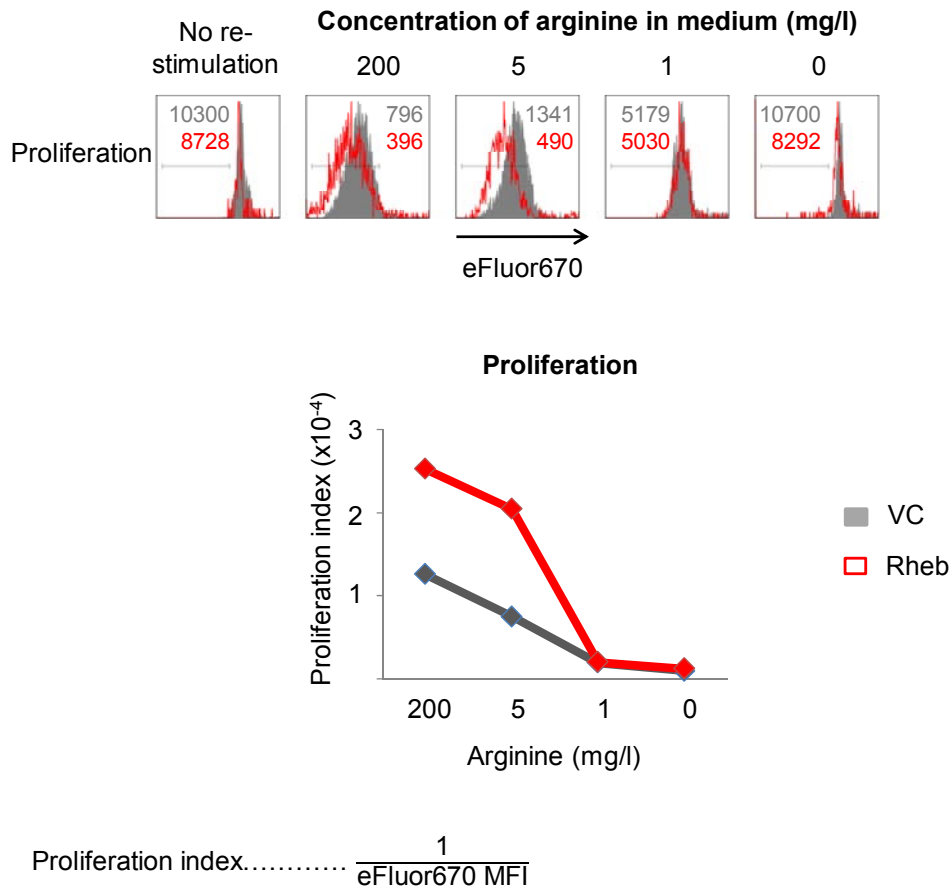
Figure 32: Proliferation under arginine low conditions day 5

Five days after transduction, Rheb and VC transduced cells were stained with eFluor670 before re-stimulation with CD3/28 bead antibodies in medium with different concentrations of arginine. A FACS analysis was carried out on day 5 post stimulation. It was gated on bulk GFP+ T cells. The data are summarized below the plots. Grey filled histograms and lines represent VC, red line represents Rheb. Numbers inside of plots represent median fluorescence intensity (MFI). The MFI of the proliferation dye eFluor670 correlates inversely with proliferation rate, therefore the proliferation index was defined as: $\frac{1}{eFluor670\ MFI}$. One of 2 independent experiments is shown.

TGFβ has been shown to inhibit CD8 T cell responses in tumours (Flavell et al. 2010; L Zhang et al. 2012) and, amongst other mechanisms, can exert its inhibitory effects through mTOR inhibition (Delisle et al. 2013). To see if Rheb transduction can partially rescue T cells from these inhibitory effects, cells were stained with eFluor670 before re-stimulation in the presence of TGFβ at different concentrations (0 – 10 ng/ml). Four days post stimulation, cells were analyzed. With increasing concentrations of TGFβ, VC transduced CD8 T cells proliferate less and present with a smaller phenotype whereas Rheb transduced cells show increased proliferation in all conditions where TGFβ is present as well as larger cell size.

In this experiment, Rheb transduced cells are also larger when TGFβ is absent but do not show increased proliferation (Figure 33). This is not in contrast to the experiment shown in Figure 32 as in this case, cells have been analyzed on day 5, not on day 4 post stimulation. In fact, the increased cell size observed on day 4 may put the cells in a position to undergo further rounds of cell division, leading to the increase in proliferation observed on day 5 post stimulation.

In summary, Rheb transduction into T cells can enhance mTOR signaling, blastogenesis and their proliferative function under normal (200 mg/l arginine) and arginine low (5 mg/l) conditions but it cannot completely rescue them at very low arginine concentrations (0 – 1 mg/l). Furthermore, Rheb transduction into T cells can enhance blastogenesis and their proliferative function in the presence of TGFβ (1 – 10 ng/ml). This makes Rheb an attractive tool to combine with TCR gene therapy approaches.

Proliferation and blastogenesis Rheb transduced CD8 T cells

4 days post re-stimulation in presence of TGFβ
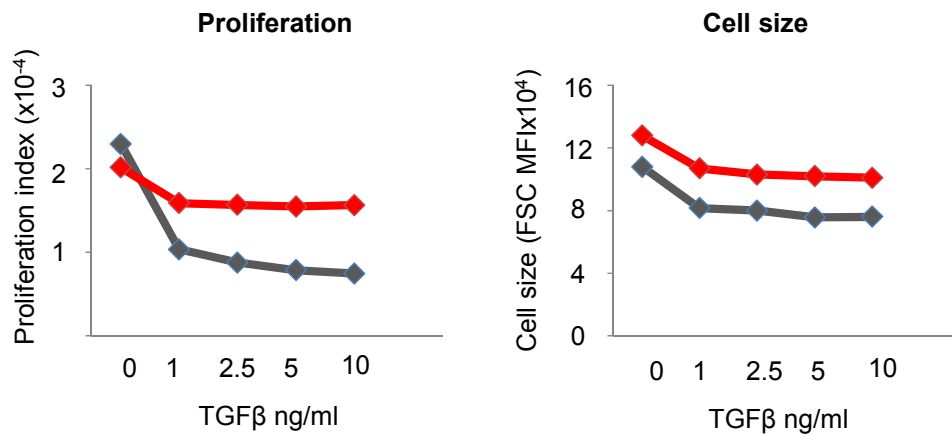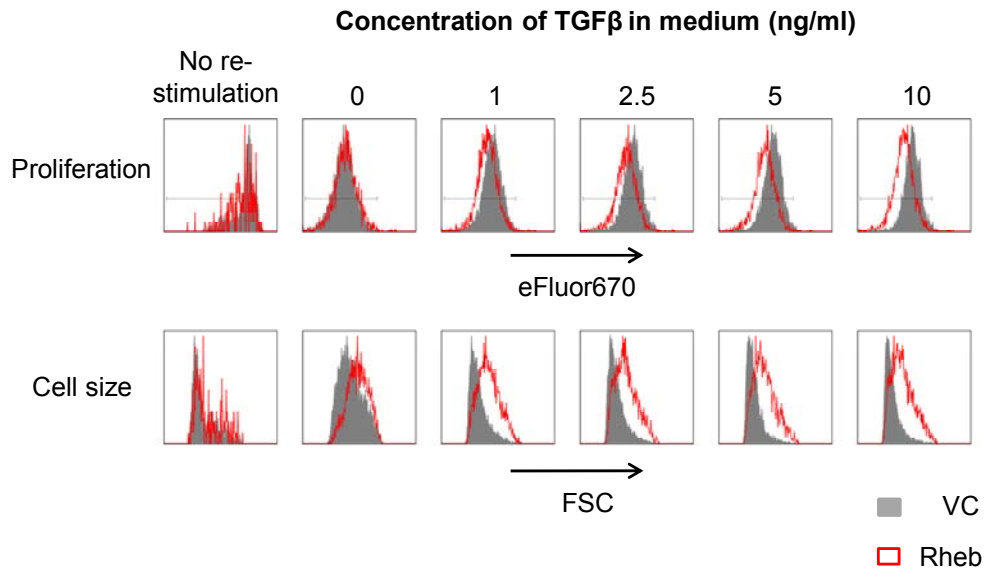
Figure 33: Proliferation and cell size in the presence of TGFβ day 4

Five days after transduction, Rheb and VC transduced cells were stained with eFluor670 before re-stimulation with CD3/28 bead antibodies in medium with different concentrations of TGFβ. They were analyzed on day 4 post stimulation. It was gated on CD8+GFP+ T cells. The data are summarized below the plots: proliferation index and median of FSC index x10³ are shown. Grey filled histograms and lines represent VC, red line represents Rheb. One of 2 independent experiments is shown.

4.6 TCR Gene Therapy with MTOR Modified T cells

The tumour model used in the following experiments is introduced in Figure 34 and is also described by Ahmadi et al. (2011). In short, CD8 T cells transduced with the so-called F5 TCR (see chapter 2.4.2) which, through IRES, also carries a truncated CD19 (tCD19) as a marker, can recognize the NP peptide presented in the context of H-2D^b on the T cell lymphoma cell line EL4-NP and thereby elicit an effector response resulting in proliferation, cytokine production and killing of the tumour.

This strategy of F5 TCR transduction was combined with Rheb and Pras40 transduction to investigate the effects of mTOR modification on adoptive T cell therapy. The Pras40 encoding vector was constructed and validated by Dr Pedro Velica from the UCL Research Department of Haematology and transduction results in an inhibition of mTOR activation. It is expected that CD8 T cells transduced with this vector preferentially differentiate into memory T cells. As control, we used CD8 T cells transduced with the F5 TCR and VC. CD8 sorted T cells were co-transduced with F5 TCR and Rheb, Pras40 or VC as described in 2.2.6. In each case, most of the cells expressing the F5 TCR (tCD19+) also express GFP (Figure 35A). When co-cultured with plain EL4 cells that do not express the NP peptide, no IFNγ or pS6 is produced by the F5+GFP+ CD8 T cells (Figure 35B). When co-cultured with EL4-NP, however, the F5+GFP+ CD8 T cells clearly elicit a tumour specific response, resulting in an up-regulation of pS6 and IFNγ, a key cytokine involved in the protection from tumour (Shankaran et al. 2001). Rheb transduced cells produce more while Pras40 transduced cells express less pS6 and IFNγ compared to VC transduced cells. In addition, the fraction of pS6+IFNγ+ cells is higher for Rheb and respectively lower for Pras40 transduced cells (Figure 36A). Surprisingly, relative to VC, IFNγ production by Rheb transduced cells does not turn out to be increased with statistical significance, even though these cells consistently show a trend to more IFNγ production (Figure 36B). However, the observations could nonetheless be of biological significance, as this is going to be discussed later on (chapter 6.3).

In Figure 36, cells were treated with brefeldin A 2 hours before staining to prevent the release of cytokines, making them available for intracellular staining (see also chapter 2.4.2). There have been reports that brefeldin A can interfere with mTOR activation (Buerger, DeVries, and Stambolic 2006). Indeed, when re-stimulated cells were not treated with brefeldin A, mTOR activity was much higher in all 3 groups, such that the difference between Rheb and VC disappeared while Pras40 produced less pS6 but still more than when treated with brefeldin A (Figure 37A).

A)

F5 TCR transduction of CD8 T cells
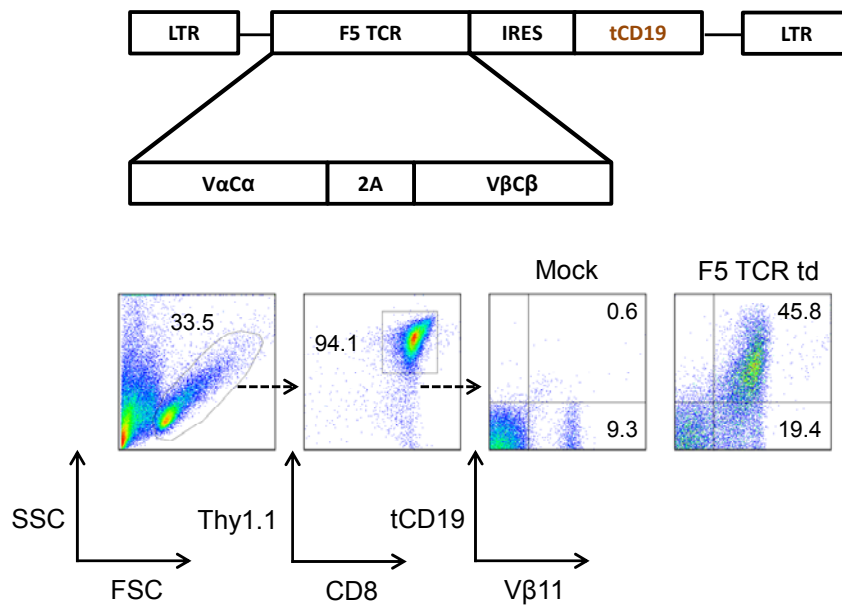
B)

The EL4-NP tumour model
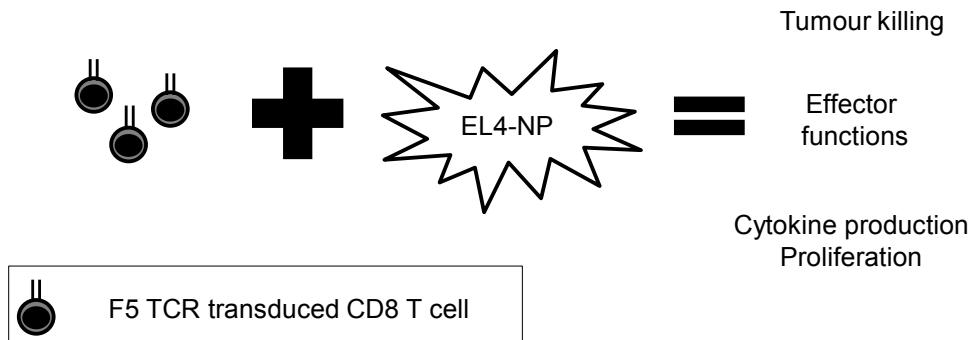
Figure 34: The F5 TCR/EL4-NP tumour gene therapy model

A) Schematic representation of the F5 TCR vector and example transduction. Variable and constant alpha (VαCα) and VβCβ chains of the TCR are connected through a self-cleaving 2A sequence (Holst et al. 2006). Through IRES, the TCR is connected to a truncated CD19 (tCD19) which is used as a marker of expression (Tey et al. 2007). The TCR expresses the Vβ11 chain which can be stained with a commercial antibody. The Vβ11 antibody stains about 9 – 10 % of mock transduced cells. Upon transduction, all tCD19+ CD8 T cells are Vβ 11 positive. Arrows in plots show gating. Numbers inside of gates represent percentage. LTR=long terminal repeat. td=transduced

B) CD8 T cells transduced with the F5 TCR recognize the NP peptide presented in the context of H-2D^b on the T cell lymphoma cell line EL4-NP and thereby elicit an effector response resulting in proliferation, cytokine production and killing of the tumour.

107

A)

Double transduction F5 + VC/Rheb/Pras40

B)

Re-stimulation with EL4 tumour cells (no NP)
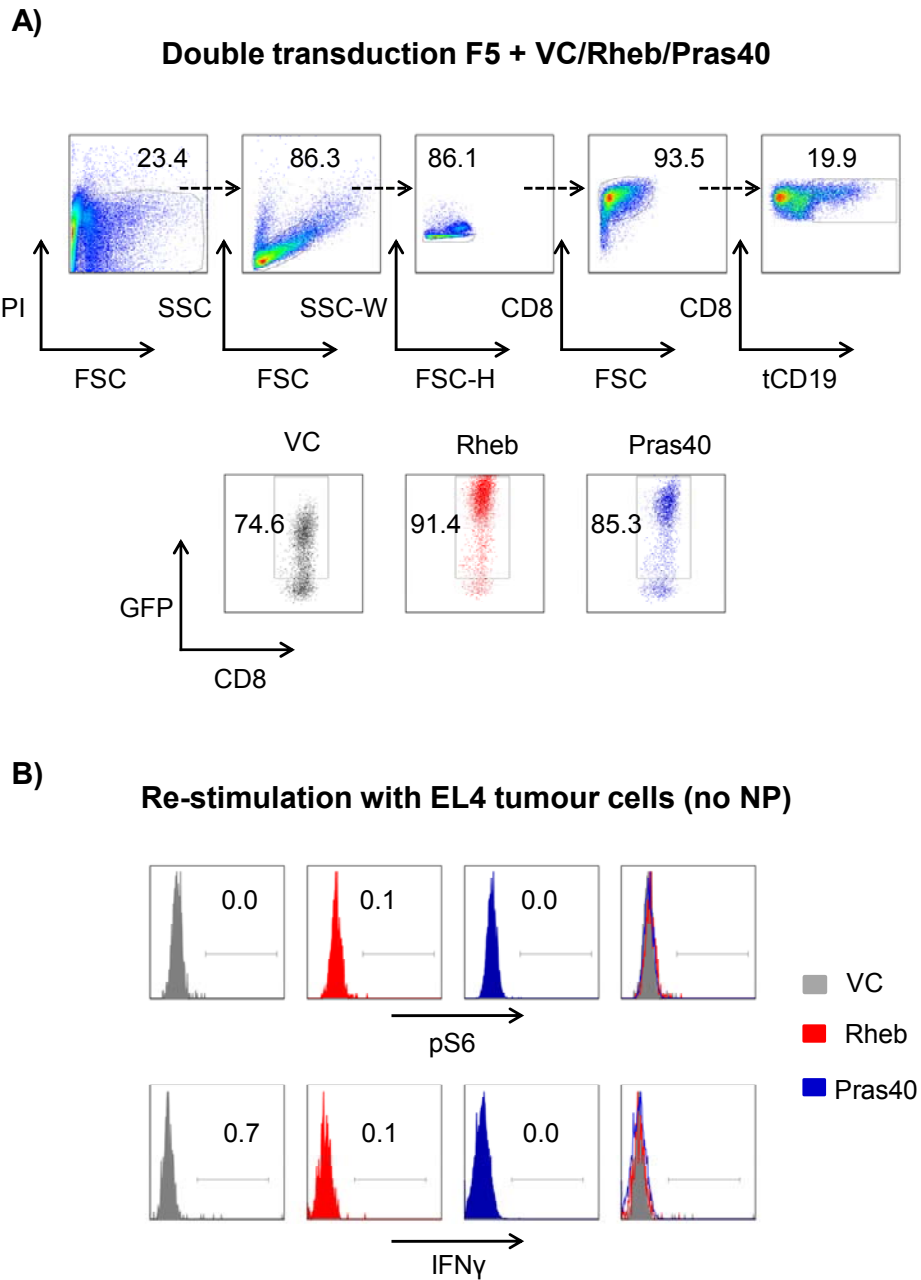
Figure 35: Co-transduction F5 + VC/Rheb/Pras40

A) CD8 T cells were co-transduced with the F5 TCR and Rheb, Pras40 or VC. Cells were analyzed on day 3 post transduction. Arrows in plots show gating. Numbers inside of gates represent percentage. Next to a propidium iodide (PI) negative live gate (PI is only taken up by dead cells), a lymphocyte gate (FSC/SSC) as well as a singlets gate (FSC-H/SSC-W) was made. VC, Rheb and Pras40 dot plots are all of gated tCD19+ cells. Grey plots represent VC, red plots Rheb and blue plots Pras40. FSC-H=FSC Height. SSC-W=SSC Width.

B) Co-culture of double transduced cells with EL4 cells. Cells were analyzed for IFNγ 24 hours later. It was gated on tCD19+GFP+ cells. Grey plots represent VC, red plots Rheb and blue plots Pras40.

A)

Re-stimulation with EL4-NP tumour cells

pS6

IFNγ

VC

Rheb

Pras40

IFNγ

pS6

B)

Summary data IFNγ

24h post stim.
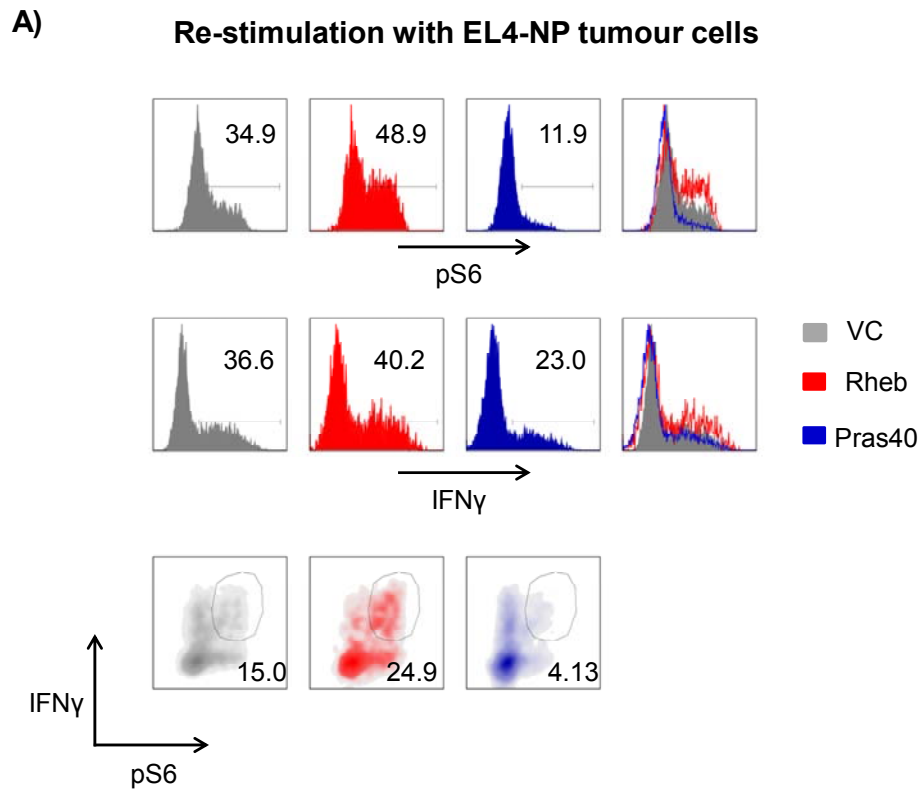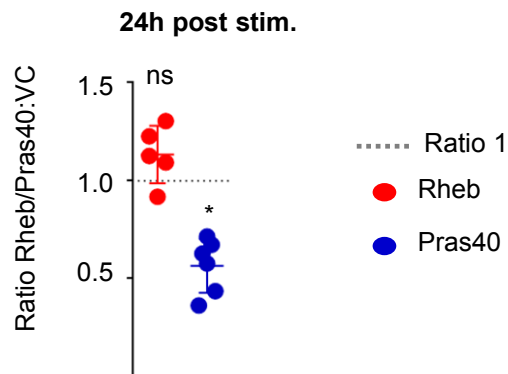
Figure 36: pS6 and IFNγ production by F5 + VC/Rheb/RQ64L transduced cells

A) Co-culture of double transduced cells with EL4-NP cells. Cells were analyzed for IFNγ 24 hours later. It was gated on tCD19+GFP+ cells. Numbers inside of gates represent percentage. Density plots show correlation between pS6 and IFNγ. Grey plots represent VC, red plots Rheb and blue plots Pras40.

B) Summary data IFNγ production relative to VC, including mean and standard deviation. Red filled circles represent Rheb, blue filled circles represent Pras40. Grey dotted line marks the hypothetical ratio of 1, everything above means cells have produced more, everything below means cells have produced less IFNγ than VC. Statistical test: Wilcoxon Signed Rank test (calculates p-value of the difference from the hypothetical value 1). Statistical significance is defined as p-value < 0.05. ns=not significant.

Brefeldin A inhibits mTORC1 signaling

B)
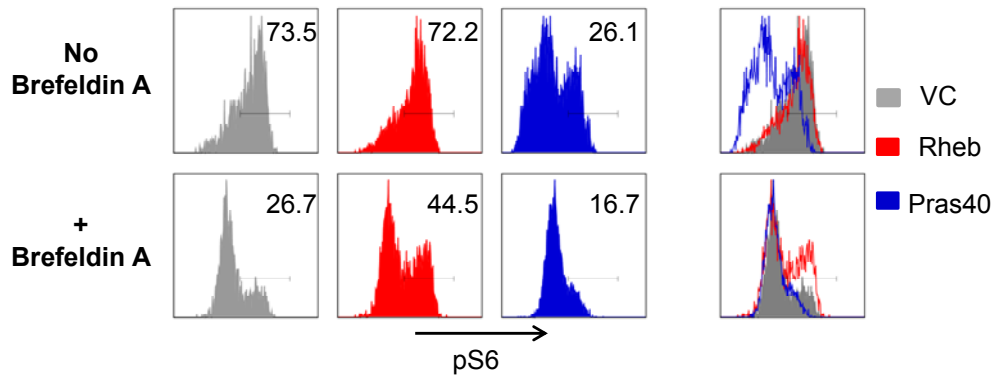
Summary data cell size and mTOR activity
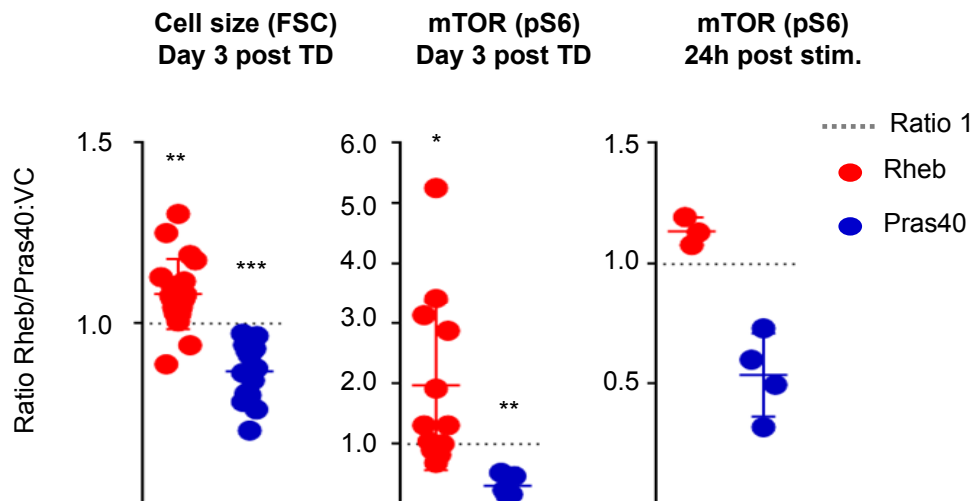
Figure 37: Brefeldin A blocks mTOR

A) Co-culture of double transduced cells with EL4-NP cells without or in the presence of brefeldin A. Cells were analyzed for pS6 24 hours later. It was gated on tCD19+GFP+ cells. Numbers inside of gates represent percentage. Grey plots represent VC, red plots Rheb and blue plots Pras40.

B) Summary data cell size (FSC) 3 days post transduction, mTOR activity (pS6) 3 days post transduction as well as 24 hours post re-stimulation relative to VC, including mean and standard deviation. Red filled circles represent Rheb, blue filled circles represent Pras40. Grey dotted line marks the hypothetical ratio of 1, everything above means that cells have produced more pS6 or were larger, everything below means cells have produced less pS6 or were smaller than VC. Statistical test: Wilcoxon Signed Rank test (calculates p-value of the difference from the hypothetical value 1). Statistical significance defined as p-value < 0.05. TD=Transduction. Stim=Stimulation.

110

The summary data shown in Figure 37B shows the change in cell size and pS6 production of Rheb and Pras40 transduced cells relative to VC in the absence of brefeldin A. Rheb transduced cells are larger and produce more pS6 while Pras 40 transduced cells show exactly the opposite. Interestingly, the difference in pS6 expression by Rheb transduced cells is most pronounced 3 days post transduction (hence before re-stimulation) (see also Figure 28) and becomes less when re-stimulated. The mode of re-stimulation, of course, is different to chapter 4.5 where cells were stimulated with CD3/28 beads whereas in the current case, they are stimulated through a peptide-MHC complex. Also, 24 hours post stimulation the mTOR signal may be saturated so that differences between Rheb and VC cells are small. The advantages of Rheb may therefore be particularly obvious only under suboptimal conditions of T cell stimulation and during late phases of T cell activation.

This question has been addressed in Figure 38 where CD8 sorted T cells were co-transduced with F5 TCR and VC, Rheb or Pras40. They were re-stimulated with EL4-NP tumour cells under normal conditions, in the presence of TGFβ or with only 5 mg/l arginine. In the presence of TGFβ or low arginine, cells produce less pS6. Rheb transduced cells always produce most pS6 but the difference is most obvious under arginine low conditions. Pras40 transduced cells always produce the least pS6.

**Re-stimulation with EL4-NP tumour cells
in the presence of TGFβ and low arginine conditions**
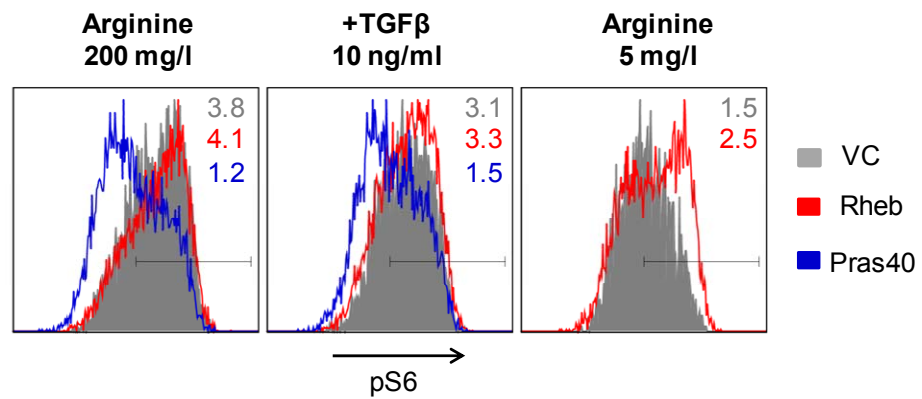
Figure 38: pS6 expression of F5 + VC/Rheb/RQ64L transduced cells under suboptimal T cell activation conditions

Co-culture of double transduced cells with EL4-NP cells under normal conditions, in the presence of TGFβ (10 ng/ml) and under low arginine concentration (5 mg/l). Cells were analyzed 24 hours later for pS6. It was gated on tCD19+GFP+ cells. Numbers inside of gates represent median fluorescence intensity (MFI) x10^3. Grey filled histograms represent VC, red lines Rheb and blue lines Pras40.

4.7 Summary and Conclusion

In summary, it was possible to establish strategies that enable tuning of the mTOR pathway in T cells. While transduction with Rheb results in increased mTOR signaling, Pras40 transduction inhibits the mTOR pathway. Rheb transduced cells show enhanced proliferation and blastogenesis under arginine low conditions as well as in the presence of TGFβ. When combined with a TCR gene therapy approach, Rheb transduced cells show a trend towards enhanced IFNγ production, even though this was not statistically significant. Rheb transduced cells can sustain a better mTOR activation signal under arginine low conditions as well as in the presence of TGFβ. Pras40 transduced cells, on the other hand, show suppressed mTOR activity, cell growth and IFNγ production.

It has to be mentioned that even though so far Rheb has only been associated with the regulation of mTOR activity, it cannot be excluded that its overexpression affects other signaling pathways as well. Rheb is a Ras like GTPase and hardly any GTPase known to this day carries out one single function only. Despite significant structural differences between Rheb and conventional small GTPase proteins (Yu et al. 2005), it still seems unlikely that Rheb represents an exception in this respect. Nonetheless, given the current evidence, it is safe to assume that mTOR signaling can be increased in a fairly specific and effective way through overexpression of Rheb. The same considerations apply to Pras40. Even though described thus far only in the context of negatively regulating mTOR kinase activity, it cannot be excluded that other signaling cascades are affected following Pras40 transduction.

Monitoring mTOR activity by staining for phosphorylated S6 only is not unproblematic. S6 phosphorylation can also occur through mTOR independent pathways, such as TCR driven MEK/ERK MAPK as well as PI3K activity (Salmond et al. 2009). By focusing on S6 phosphorylation as a read out for mTOR activity, it is therefore not possible to distinguish between direct effects of Rheb and Pras40 overexpression on mTOR activity and secondary, mTOR independent effects of these modifications which may be related to tuning MAPK or PI3K activity. It is also conceivable that the impact of Rheb or Pras40 overexpression are underestimated as the convergence of different signals towards one single target might overshadow the effects of Rheb and Pras40 transduction through a saturation of the response. However, FACS monitoring of S6 phosphorylation proved to be the most effective and practical method to assess the effects of Rheb and Pras40 overexpression on mTOR activity as it results in a strong and clean staining. As opposed to other

approaches involving the investigation of the phosphorylation status of S6K and 4EBP1, both of which are specific and direct targets of the mTOR kinase, no Western Blot had to be carried out which would have required FACS sorting of transduced cells. In addition, a high number of transduced cells is required to carry out these tests, whereas FACS staining is possible with lower cell numbers and allows a quick and uncomplicated analysis. Finally, in our hands S6 phosphorylation following T cell activation was predominantly associated with mTOR activity as this is suggested by Figure 21. In this case, the addition of rapamycin resulted in a nearly complete loss of the signal. Taken together, FACS monitoring of the S6 phosphorylation status was specific enough and proved to be the most effective method to assess the effects of Rheb and Pras40 transduction into CD8 T cells for the purposes of this thesis.

mTOR is very sensitive to nutrient availability and can easily be inhibited by depriving cells of either amino acids (Cobbold et al. 2009) or glucose (Yan Zheng et al. 2009). T cell activation is associated with a strong upregulation of the single system L amino acid transporter Slc7a5 in a calcineurin dependent way as cyclosporin A was shown to inhibit this event. This is followed by an increased amino acid influx into the cells which can then regulate the activity of mTOR. One amino acid is particularly important in the regulation of mTOR activity: leucine. Leucine deprivation results in an almost immediate inhibition of mTOR whereas the absence of glutamine was shown to inhibit mTOR only after 1 hour (Sinclair et al. 2013). In addition, leucyl-tRNA-synthetase (LTS) has recently been identified as an important leucine sensor involved in the regulation of mTOR activity (Han et al. 2012). It is known that for mTOR activity to occur, Rheb and mTOR have to co-localize at endosomal and lysosomal membranes (Sancak et al. 2010). It is exactly this phenomenon which is guided by amino acid availability, involving a number of molecules such as ragulator, rag GTPases (Sancak et al. 2010) and v-ATPase (Zoncu et al. 2011). If leucine is one key player in regulating this whole complex of molecules to guide Rheb and mTOR co-localization, the question arises what happens when other amino acids are deprived. Or in other words: does arginine deprivation directly inhibit mTOR activity? The fact that leucine deprivation results in an almost instantaneous inhibition of mTOR whereas lack of arginine causes mTOR inhibition only at later stages as shown in Figure 22 (48 hours post stimulation) and Figure 30 (24 hours post simulation) does not suggest so. As an alternative explanation, it is possible that through arginine deprivation, not enough c-myc protein can be produced. This protein has been described as an important metabolic

switch next to mTOR, especially during early phases of T cell activation (Wang et al. 2011). Lack of c-myc which has a short half life requiring constant *de novo* production (Sinclair et al. 2013) would be followed by a decrease in the expression of amino acid transporters and the uptake of glutamine. Glutamine, on the other hand, is required for the import of leucine through Slc7a5 as this transporter acts as an amino acid exchange antiporter. In the end, this would then result in delayed mTOR inhibition due to lack of leucine. Alternatively, because c-myc controls glucose influx through upregulating GLUT1, low glucose can impair mTOR activation (Yan Zheng et al. 2009). Finally, it is also possible that lack of arginine deprivation results in a lack of IL2 receptor expression or other growth factor and stimulation receptors which are involved in the activation of mTOR. However, this would occur through a c-myc independent way as lack of c-myc has not been shown to be associated with a reduction in the expression of T cell activation markers, including CD25. Whatever the true reason for the observed mTOR inhibition following retrieval of arginine, the question arises: how can Rheb transduction help to maintain mTOR activity and rescue T cell function under these conditions? In the case of glucose absence, it is likely that Rheb overexpression would not help at all. Ultimately, this would result in the activation of the AMP kinase which can enhance the GAP activity of the TSC complex resulting in a wide-spread inactivation of Rheb. Furthermore, with the absence of glucose, the most important substrate of activated T cells is gone and Rheb overexpression would in no way help to overcome this situation. With regards to absolute amino acid deprivation, including leucine, it has been extensively shown in other publications that Rheb overexpression can help to overcome these conditions (Saucedo et al. 2003; Stocker et al. 2003). Although co-localization of Rheb and mTOR would still not occur to a 100 %, overexpressing Rheb would by itself increase the chance of intracellular mTOR and Rheb encounter, enabling mTOR activation even under these circumstances. This would go along with the here observed subtle increase in mTOR activity under low arginine concentrations. Finally, lack of mTOR stimulating receptors such as IL2 would also cause a reduction in mTOR activity. More Rheb may help rendering T cells fitter under this condition because the ratio of Rheb:TSC is increased in transduced cells, so less Rheb molecules can be targeted by TSC. If less TSC complexes are repressed due to reduced IL2 receptor expression, Rheb overexpression may pose an advantage in this case. All of these questions require further and deeper clarification to better understand the effects of Rheb transduction into CD8 T cells under different conditions.

Higher IFNγ due to enhanced mTOR activity would be in accordance with reports by Powell et al. (2013) as well as a recent publication by Park et al. (2013). However, this applies to CD4 T cells only. For CD8 T cells there is no direct link between high mTOR activity and IFNγ production (D. K. Finlay et al. 2012). mTOR has been shown to regulate the expression of T-bet (Rao et al. 2010). Although T-bet can regulate transcription of IFNγ, this is only true for CD4, not for CD8 T cells (Szabo et al. 2002). Recently, it has been reported that IRF4, which is dependent on mTOR, can induce IFNγ expression, albeit only during late phases of the T cell response (Yao et al. 2013). But since mTOR regulates the switch from oxidative phosphorylation to aerobic glycolysis as reported by Finlay et al. (2012) and others (Sukumar et al. 2013; Chang et al. 2013), the effects of this change may result in increased effector functions, including IFNγ production. Chang et al. (2013) reported that GAPDH as a glycolysis enzyme can regulate the expression of IFNγ on a post-transcriptional level. It is therefore likely that by enhancing mTOR activity in CD8 T cells, more IFNγ is produced through post-transcriptional regulatory mechanisms due to an increase in glycolytic metabolism.

Overall, Rheb transduction enhances effector T cell responses *in vitro*, particularly under suboptimal stimulation conditions, while Pras40 transduction suppresses such a response. It is now necessary to investigate if this holds true for *in vivo* T cell responses.

Chapter 5   In Vivo Validation of Rheb and Pras40 transduced CD8 T Cells

5.1 Engraftment of Rheb Transduced CD8 T Cells

In a first instance, it was important to know how Rheb transduced CD8 T cells behave *in vivo* when there is no antigen present. The principles of the following experiment are schematically outlined in Figure 39. In short, C57BL/6 mice which have been sub-lethally irradiated with 5.5 Gray (Gy) to favor T cell engraftment and homeostatic proliferation by creating an immunodepleted microenvironment, received 0.5×10^6 F5+GFP+ transduced CD8 T cells. One group received F5 T cells co-transduced with Rheb, another group received F5 T cells co-transduced with VC. Three weeks later, mice were culled and their spleen, lymph nodes (inguinal, axial, brachial, cervical and para-mesenterial) and bone marrow (femur and tibia from one leg) were collected to evaluate numbers of transferred F5+GFP+ T cells as well as their CD8 T cell memory phenotype (CD62L/CD44). To detect transferred cells, Thy1.1 congenic T cells were injected into Thy1.2 recipients.

Figure 40A shows the pre-injection profile and gating strategy *ex vivo* to detect transferred cells. CD8 T cells from Thy1.1 congenic mice have been co-transduced with the F5 TCR and either Rheb or VC. Expression of Vβ11 indicates F5 TCR expression and does not differ between the 2 groups (46.6 % for F5+VC and 47.5 % for F5+Rheb). 78.1 % of the F5+Rheb and 52.9 % of the F5+VC transduced cells express GFP.

Based on the expression of the markers CD62 L-selectin (CD62L) and CD44, three to four distinct T cell subsets can be distinguished: CD62L+CD44- cells are considered naïve, CD62L+CD44+ cells are classified as central memory and CD62L-CD44+ cells are either effector or effector memory T cells. When previously activated (CD44+) T cells express CD62L, a lymph node homing molecule also expressed by naïve T cells, this is a sign that those cells have undergone differentiation towards a central memory phenotype. It is self-evident that this is an over-simplified way of looking at T cells that ignores functional aspects as well as other markers which further help sub-classifying the cells, such as the IL7 receptor (CD127), stem cell antigen 1 (Sca1), bcl2, chemokine receptor 7 (CCR7) etc (Restifo, Dudley, and Rosenberg 2012). For the current purposes, however, it was an easy way of looking at the effects of mTOR modification, in particular on the

expression of CD62L as a marker which has been reported to be down-regulated by mTOR (Sinclair et al. 2008).

Gating on GFP+ cells, the percentage of CD62L+CD44+ double positive cells does not differ too much between the 2 groups before injection (84.1 % for F5+Rheb and 82.6 % for F5+VC). However, F5+Rheb transduced cells present with slightly more CD62L-CD44+ cells (8.6 %) than F5+VC transduced cells (4.8 %), already indicating a potential effect on CD62L expression.

Figure 40B shows that the absolute numbers of F5+GFP+ cells do not differ between the two groups in any of the 3 lymphoid compartments (spleen, lymph node, bone marrow). Numbers have been pooled from 2 independent experiments and are wide spread, especially for the F5+Rheb group. Therefore, the change of F5+GFP+ cells relative to pre-injection has been calculated which resulted in less variation. Again, no differences between the Rheb and the control group could be detected in spleen and lymph node. However, in bone marrow it appeared that Rheb transduced cells engrafted better than VC transduced cells.

With regards to the CD62L/CD44 profile of transferred cells, F5+Rheb transduced cells showed a general trend towards less CD62L+CD44+ central memory like T cells and more CD62L-CD44+ effector or effector memory like T cells in all 3 compartments compared to F5+VC transduced T cells. However, this difference became only statistically significant in spleen (Figure 42). Less expression of CD62L due to increased mTOR activation is in accordance with previously published data (Sinclair et al. 2008) and will be further discussed later (see chapter 5.2, Figure 48).

In conclusion, F5+Rheb transduced CD8 T cells show equal engraftment in spleen and lymph nodes and slightly better engraftment in bone marrow compared to F5+VC transduced cells. In addition they show an increased trend to spontaneous differentiation towards an effector or effector memory like phenotype (CD62L-CD44+). As a next step, we wanted to address the question, how F5+Rheb and F5+Pras40 transduced cells behave in direct comparison to F5+VC transduced cells when mice are challenged with antigen.

Experimental layout:
Engraftment of cells without vaccination

3 weeks post injection
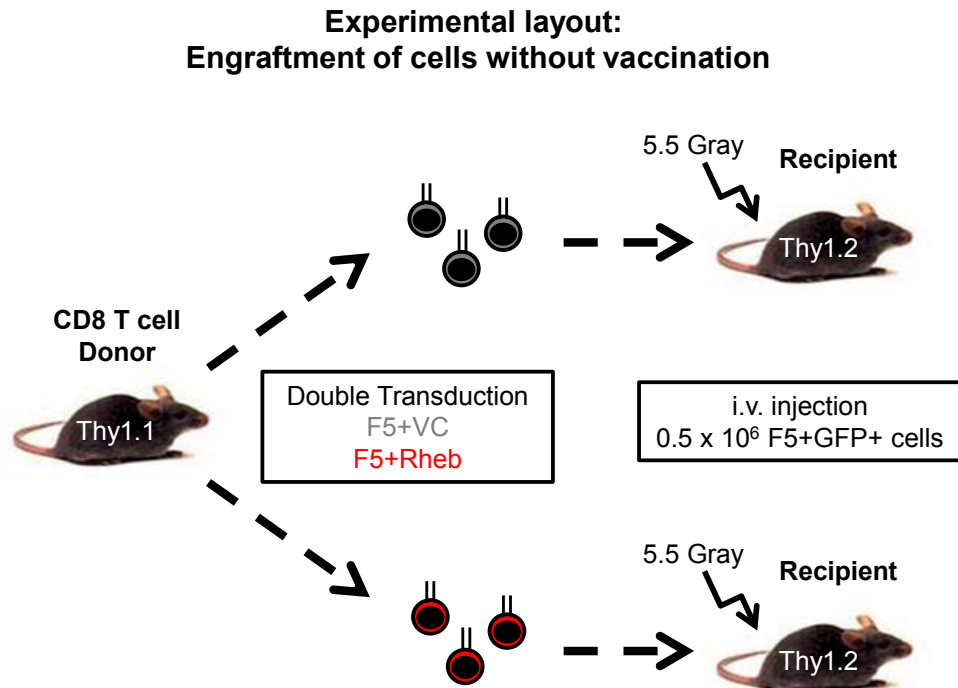
- Take down: spleen, lymph nodes, bone marrow

- Cell counts double positive cells

- Phenotyping: CD62L/CD44

Figure 39: *In vivo* engraftment of Rheb transduced CD8 T cells

C57BL/6 (Thy1.2) mice have been sub-lethally irradiated with 5.5 Gray to favor T cell engraftment and homeostatic proliferation. Four hours later, they received 0.5×10^6 F5+GFP+ transduced CD8 T cells from a Thy1.1 congenic background through intravenous injection. One group (n=5) received F5 TCR+ T cells co-transduced with Rheb, another group (n=6) received F5 TCR+ T cells co-transduced with VC. Three weeks later, mice were culled and their spleen, lymph nodes and bone marrow (femur and tibia from one leg) were collected. Cells were counted and stained for CD62L and CD44 as markers of central memory T cells. Mice losing >20 % of their original weight after irradiation were culled and excluded from analysis. i.v.=intravenous.

A)

**Transduction efficiency and CD62L/CD44 profile
Pre-injection**

B)   Engraftment: Absolute cell number F5+GFP+ cells
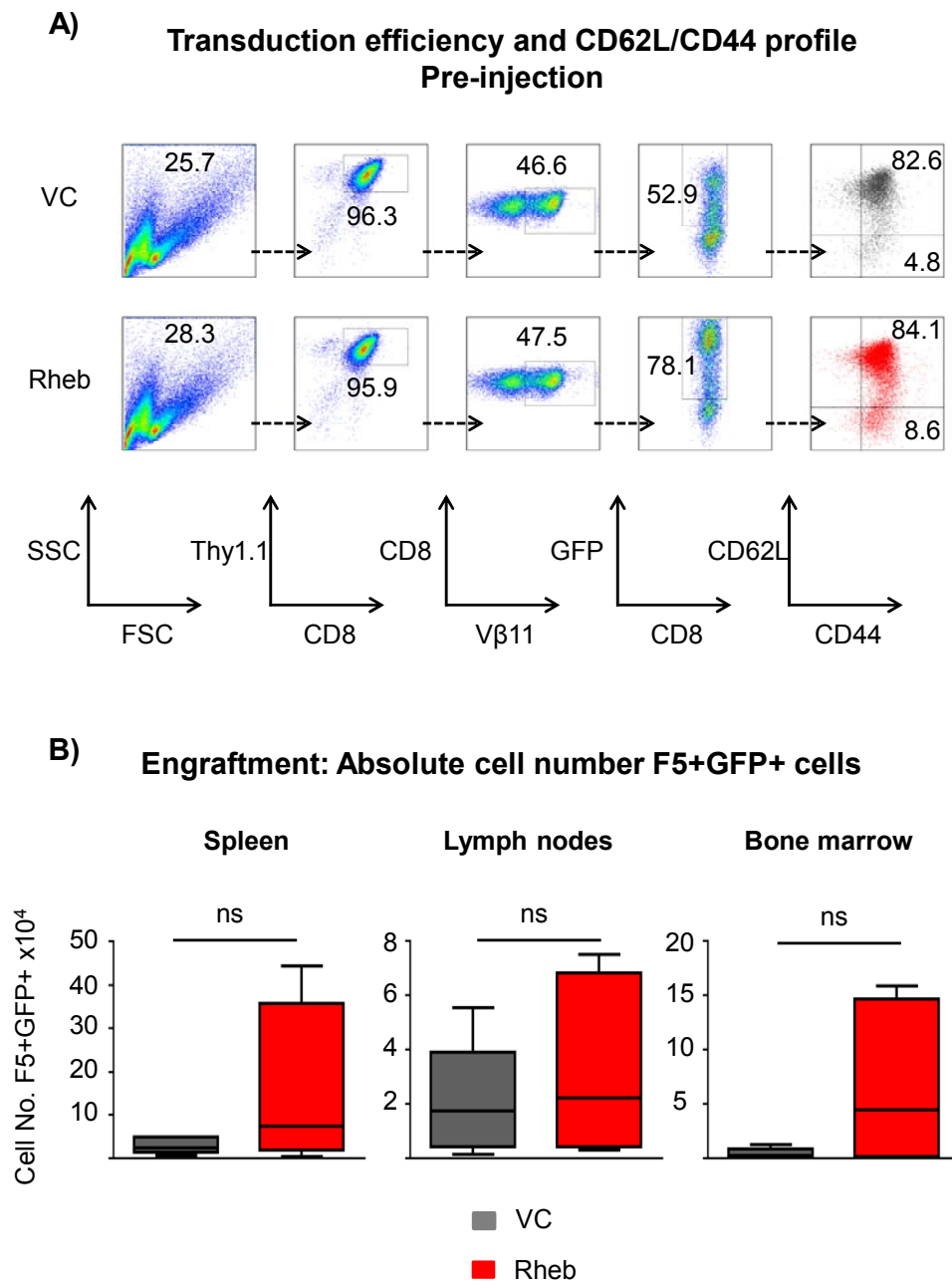
Figure 40: Pre-injection profile and engraftment in lymphoid organs

A) Pre-injection FACS profile. CD8 sorted Thy1.1 congenic T cells were co-transduced with the F5 TCR and either Rheb or VC. F5 TCR expression was determined by staining for the Vβ11 chain. CD62L/CD44 profile of GFP+ cells is shown. 0.5×10^6 F5+GFP+ cells were injected i.v. into Thy1.2 recipients irradiated with 5.5 Gy which were culled 3 weeks later. Numbers and CD62L/CD44 profile were determined and compared to pre-injection profile in spleen, lymph nodes (LN) and bone marrow (BM). Arrows in plots show gating. Numbers inside of gates represent percentage. Grey plots represent VC, red plots represent Rheb.

B) Absolute numbers of F5+GFP+ cells in spleen, lymph nodes and bone marrow, including median and range, pooled from 2 independent experiments are shown (Rheb n = 6; VC n = 5). Statistical test: Mann-Whitney U test. Statistical significance defined as p-value < 0.05. Grey Box & Whiskers bars represent VC, red Box & Whiskers bars represent Rheb. Cell No.=Cell number. ns=not significant.

A) **Change of F5+GFP+ profile (relative to pre-injection)**
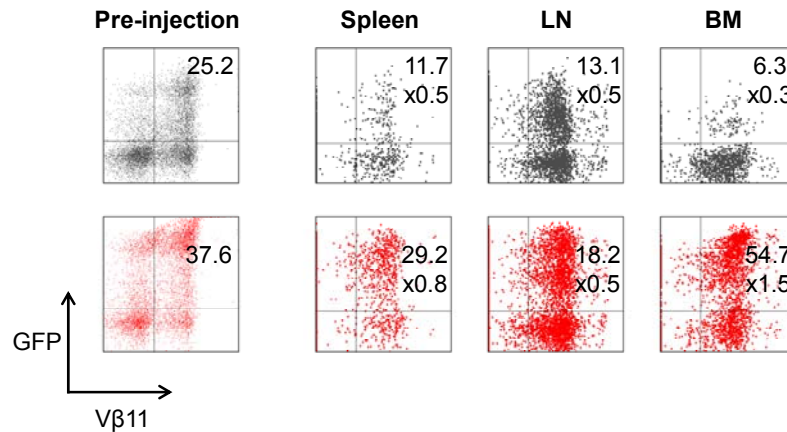
B)
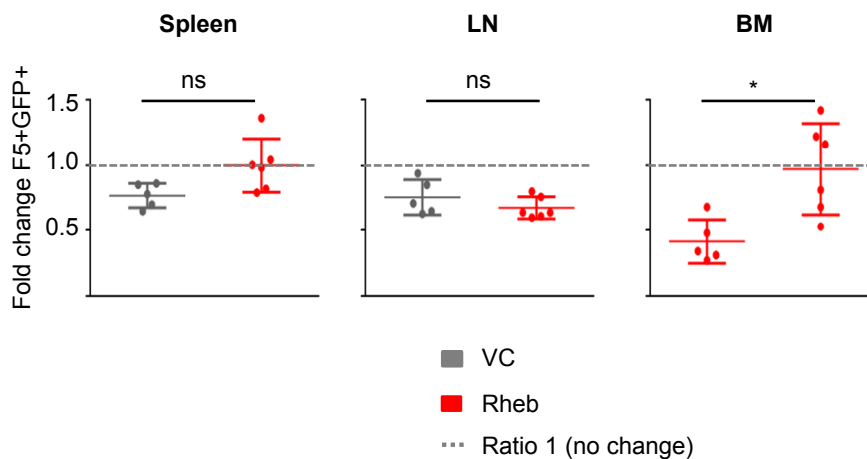
Figure 41: Change of F5+GFP+ frequency relative to pre-injection

A) Vβ11/GFP profile before injection and on the day of take down in the different immune compartments is shown. Numbers inside of gates represent percentage of double positive (Vβ11+GFP+) cells (gated on CD8+Thy1.1+ transferred cells) as well as the relative change compared to pre-injection. Grey plots represent VC, red plots represent Rheb.

B) Summary of the relative change of Vβ11+/GFP+ percentage compared to the pre-injection profile is shown, including median and standard deviation. Pooled data from 2 independent experiments (Rheb n = 6; VC n = 5). Grey dotted line represents the hypothetical relative change of 1 (= no change). Everything above means that cells have expanded, everything below means that cells have contracted relative to pre-injection. Grey filled circles represent VC, red filled circles represent Rheb. Statistical test: Mann-Whitney U test. Statistical significance defined as p-value <0.05. LN=lymph nodes; BM=bone marrow; ns=not significant.
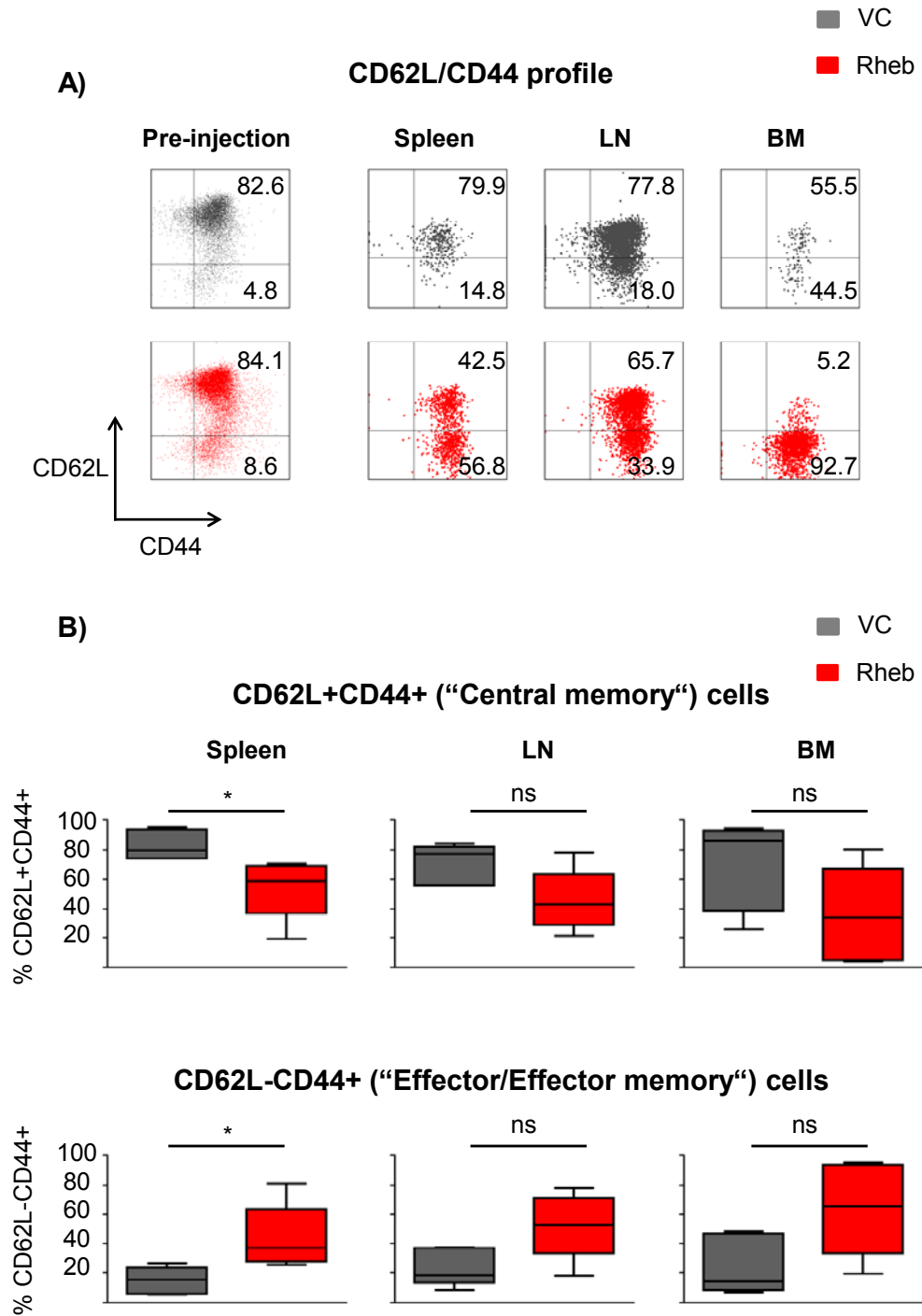
Figure 42: CD62L/CD44 profile

A) C62L/CD44 profile before injection and on the day of take down is shown. Numbers inside of gates represent percentage of double positive (CD62L+CD44+) and CD62L-CD44+ cells. It was gated on F5+GFP+ cells. Grey plots represent VC, red plots represent Rheb.

B) Summary central memory (CD62L+CD44+) and effector/effector memory (CD62L-CD44+) like profiles of F5+Rheb and F5+VC, including median and range. Pooled data from 2 independent experiments (Rheb n = 6; VC n = 5). Grey filled circles represent VC, red filled circles represent Rheb. Statistical test: Mann-Whitney U test. Statistical significance defined as p-value < 0.05. Grey Box & Whiskers bars represent VC, red Box & Whiskers bars represent Rheb. LN=lymph nodes; BM=bone marrow; ns=not significant.

5.2 Immunological Response of MTOR Modified CD8 T Cells Over Time

Figure 43 schematically shows the set-up of the following experiment. In short, CD8 T cells from mice with different congenic backgrounds were co-transduced with F5 TCR and either Rheb or Pras40 as well as F5 TCR and VC. Mice from yet another congenic background were irradiated with 4 Gy and were injected with a mix of cells consisting of an equal number of F5+Rheb (or F5+Pras40) and F5+VC transduced cells. The different congenic background allowed for 1) the detection of transferred cells and 2) for distinguishing VC from mTOR modified (Rheb or Pras40 transduced) T cells. Two days after injection, mice received an intraperitoneal vaccination boost with growth-incompetent (irradiated) EL4-NP cells to initiate an immunological response. This response was monitored through weekly tailbleeds, including the expression of CD62L. A typical CD8 T cell response consists of an expansion (~weeks 1-2 post antigen challenge), a contraction (~weeks 3-8 post antigen challenge) and a memory phase (Williams and Bevan 2007). Mice were re-challenged after 6 weeks to investigate the F5 T cell memory re-call response. After 3-4 months, mice were culled and their lymphoid organs were collected to look at numbers as well as phenotype of the cells. The advantage of this experiment is that mTOR modified and VC transduced cells were injected into the same mouse which allowed to look at the behavior of the cells over a certain time course within the same animal.

Figure 44A shows the pre-injection profile which, at the same time, represents the gating strategy for detecting the transferred cells. It was gated on PI negative lymphocytes (defined by FSC/SSC profile) to detect the CD45.2+ cells in the CD45.1 recipient mice. Then the tCD19+ cells (= F5 TCR+) were selected to look at GFP expression. mTOR modified (Rheb or Pras40 transduced) and VC transduced cells could be distinguished by the expression of Thy1.1. Rheb and Pras40 transduced cells expressed Thy1.1, VC transduced cells did not express Thy1.1 (they were of Thy1.2 origin). Pre-injection, the ratios of mTOR modified cells to VC were as follows: Rheb:VC = 52:46 (~1.12) and Pras40:VC = 52:45 (~1.14). When looking at the MFI of CD62L, Rheb transduced cells expressed slightly less while Pras40 cells expressed a little bit more CD62L on a per cell basis. This becomes more evident when looking at the summarized and pooled data: the difference in CD62L expression is always significantly lower (Rheb) or higher (Pras40) relative to VC. As already shown in Chapter 4, Rheb transduced cells are larger and Pras40 transduced cells are smaller compared to VC transduced cells (Figure 44B).

Experimental layout:
Immunological response of mTOR modified CD8 T cells
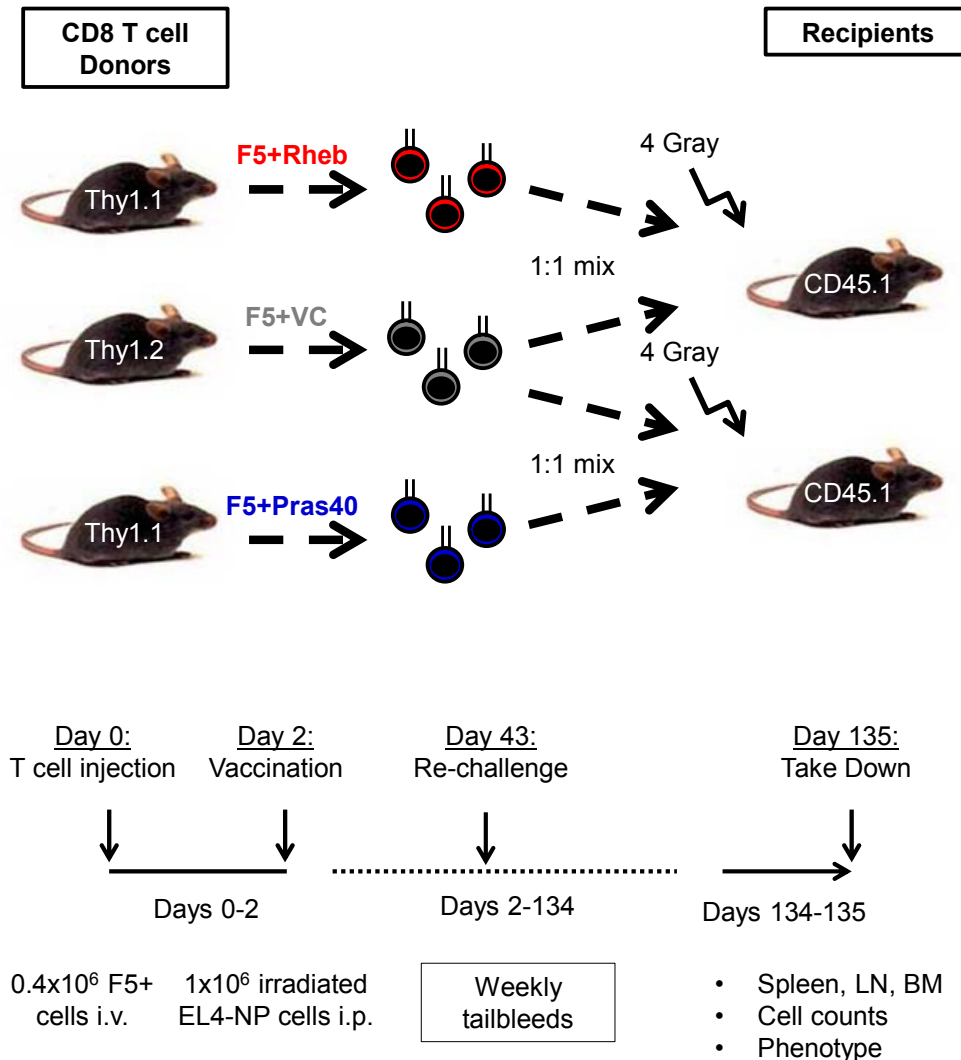
Figure 43: Immunological response of mTOR modified CD8 T cells

Schematic representation of the experimental set-up. CD8 T cells from Thy1.1 congenic mice were co-transduced with the F5 TCR and either Rheb or Pras40. CD8 T cells from Thy1.2 mice were co-transduced with the F5 TCR and VC. Three days post transduction, F5+Rheb or F5+Pras40 transduced cells were mixed with F5+VC transduced cells in a ratio as close as possible to 1. CD45.1 congenic mice were conditioned with 4 Gy and received the mix of cells i.v (0.4×10^6 total F5 TCR+ cells). Two days after injection, mice were vaccinated with 1×10^6 irradiated EL4-NP cells i.p. The immunological response (expansion-contraction-memory) was monitored, including the memory-re-call response ~40 days post ACT, through weekly tail-bleeds, including expression of CD62L. After 3-4 months, mice were culled and their lymphoid organs were collected to look at numbers as well as phenotype of the cells. LN=lymph nodes. BM=bone marrow. i.v.=intravenous. i.p.=intraperitoneal.

A)

**Transduction efficiency and CD62L profile
Pre-injection**

B)
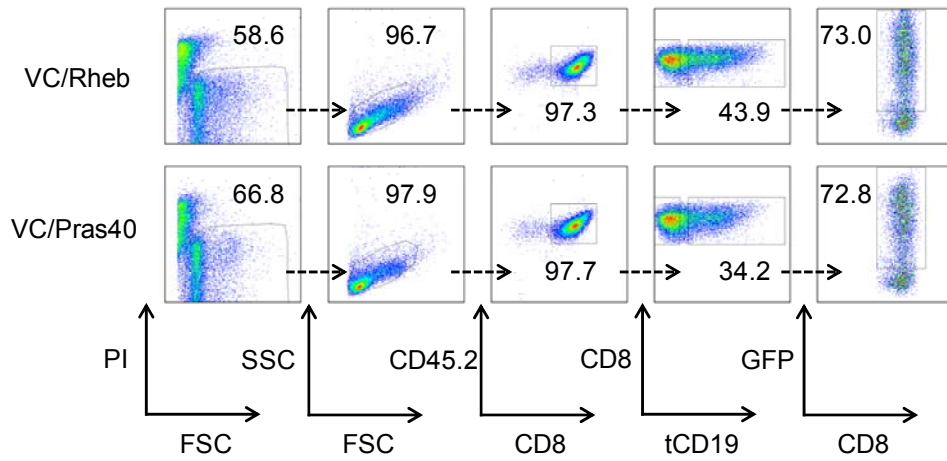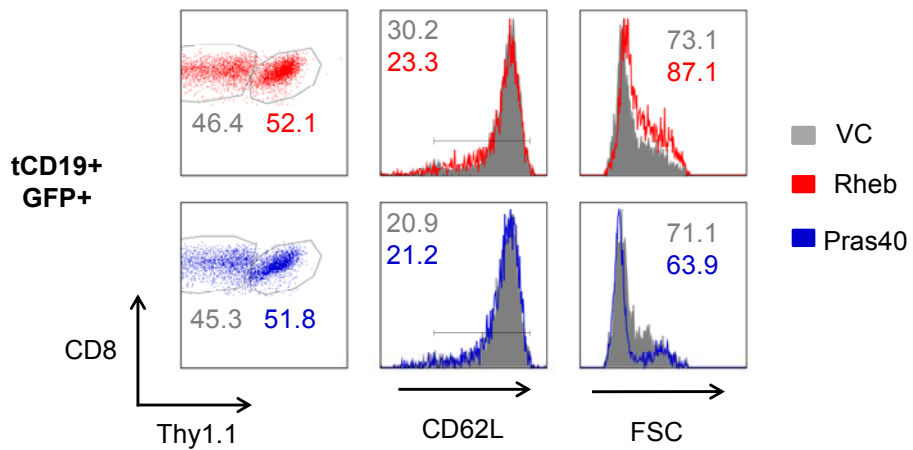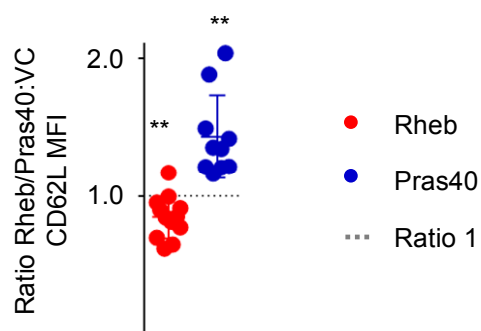
Figure 44: Pre-injection profile

A) Pre-injection FACS profile 3 days post transduction. CD8 sorted Thy1.1 congenic T cells were co-transduced with the F5 TCR and either Rheb or Pras40. CD8 sorted Thy1.2 congenic T cells were co-transduced with the F5 TCR and VC. It was gated on PI-lymphocytes (defined by FSC/SSC profile) to detect the CD45.2+ cells. F5 TCR transduction was determined by looking at the tCD19 marker. Arrows in plots show gating. Numbers inside of gates represent percentage.

B) mTOR modified (Rheb or Pras40 transduced) and VC transduced cells could be distinguished by the expression of Thy1.1. Rheb and Pras40 transduced cells expressed Thy1.1, VC transduced cells did not express Thy1.1. CD62L profile was also determined. Grey dotted line in summary graph marks the hypothetical ratio of 1, everything above means that cells express more, everything below means that cells express less CD62L than VC. Numbers in plots represent percentage (CD8/Thy1.1 dot plot), MFI x10^3 (CD62L) or median of the FSC index x10^3 (FSC). Statistical test: Wilcoxon Signed Rank test (calculates p-value of the difference from the hypothetical value 1). Statistical significance defined as p-value < 0.05. TD=Transduction. Grey represents VC, red represents Rheb and blue represents Pras40.

0.4x10^6 total F5+ CD8 T cells were injected i.v. in both groups (n=4 per group). Two days post injection, a tailbleed was done to confirm engraftment of the transferred T cells, mice were then vaccinated with irradiated EL4-NP cells.

Figure 45A shows expression of the F5 TCR in the 2 groups (Rheb:VC and Pras40:VC) post vaccination as well as re-challenge and gives an idea of the expansion and contraction over time without looking at VC or mTOR modified cells in detail. Figure 45B summarizes these data. Expansion of F5 TCR+ cells is displayed as relative to total CD8+ cells in the blood since determining absolute numbers by tailbleeds was not possible. Because recipient mice were irradiated before T cell injection, some of the expansion can probably also be attributed to homeostatic rather than antigen driven proliferation. To get an idea of the rate of homeostatic proliferation, the expansion of F5 TCR- cells relative to the total CD8 pool is also displayed on the left hand side. It is obvious that some expansion is going on in this group of cells, albeit when compared to the F5 TCR+ cells (right graph), it is very small. Overall F5 TCR driven expansion, not distinguishing between Rheb/Pras40 and VC, followed a very similar pattern and to a very similar extent in both groups (Rheb:VC and Pras40:VC). The peak of the response was seen 7 days post vaccination, after which the contraction phase began and cells returned slowly back to baseline between 20 and 40 days post vaccination, not without leaving behind a number of F5 specific T cells as memory cells.

Upon re-challenge on day 41 post vaccination, the cells expanded again, though it seems to a smaller extent than at the initial antigen encounter. One must not forget, however, that in absolute numbers, the second response may in fact be higher and that this may be masked by looking at relative expansions only. Again, the peak of

the response was seen 7 days post EL4-NP injection, after which the cells slowly returned back to baseline, leaving behind an even bigger pool of F5 specific T cells than after the first vaccination. F5 TCR- cells did not respond to the re-challenge which highlights the specificity of the response.

Figure 46 is similar to Figure 45, except that in this case, the total F5 T cell response is further sub-divided into a $mTOR_{hi}$ (Rheb transduced cells) versus $mTOR_{no}$ (normal mTOR activation; VC transduced cells) for the former and, respectively, a $mTOR_{lo}$ (Pras40 transduced cells) versus $mTOR_{no}$ response for the latter case. Looking at the Rheb:VC group first, one can see that 7 days post vaccination (effector phase), Rheb transduced cells (Thy1.1+) expand better than VC transduced cells (Thy1.2+). After that, however, VC cells take over the majority of the niche occupied by the F5 TCR+ cells, at the expense of Rheb transduced cells. Upon re-challenge, Rheb transduced cells catch up again a little bit but overall, they perform worse than VC transduced cells. In the case of the Pras40:VC group, on the other hand, Pras40 transduced cells do not seem to expand at all, VC transduced cells take up the majority of the niche occupied by the F5 TCR+ cells. They remain low over the whole course of the experiment and upon re-challenge even seem to slightly further decrease. The whole data are summarized in Figure 46B.

It is noteworthy to point out that the *overall* F5 T cell response is similar in both groups (Rheb:VC and Pras40:VC) (see Figure 45) and that the mTOR modifying constructs (Rheb/Pras40) seem to confer a relative advantage/disadvantage for the competition of the niche the F5 T cells take up within the whole CD8 T cell pool. In fact, the F5+VC transduced cells in the Pras40:VC group expand more than the F5+VC and at least the same as the F5+Rheb transduced cells in the Rheb:VC group. But it is in direct competition with a "stronger" group of cells that the F5+VC transduced cells do worse- at least within the first 7 days post vaccination. This is important to know in relation to some of the issues encountered in the last results chapter of this thesis (Chapter 6).

A)

Total F5 CD8 T cell response in peripheral blood over time
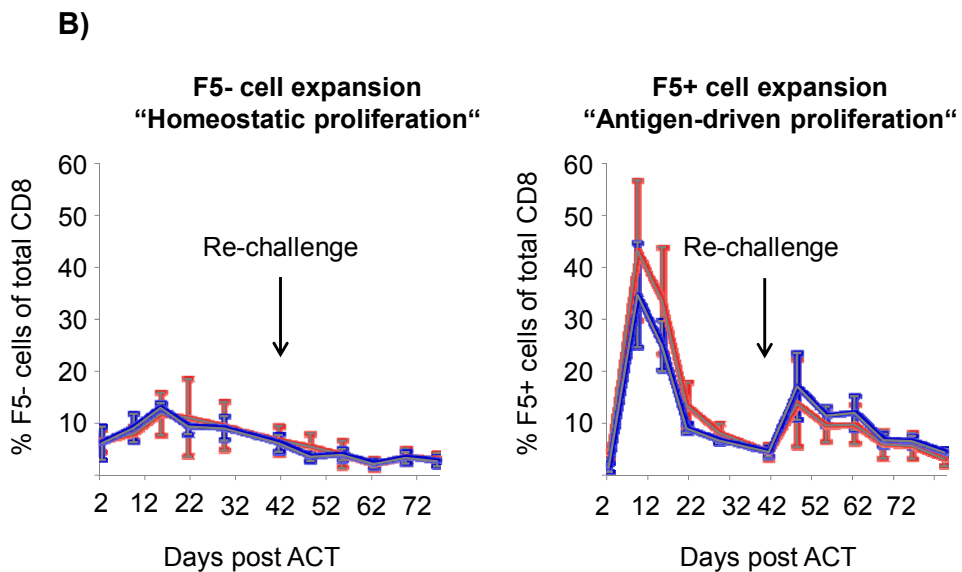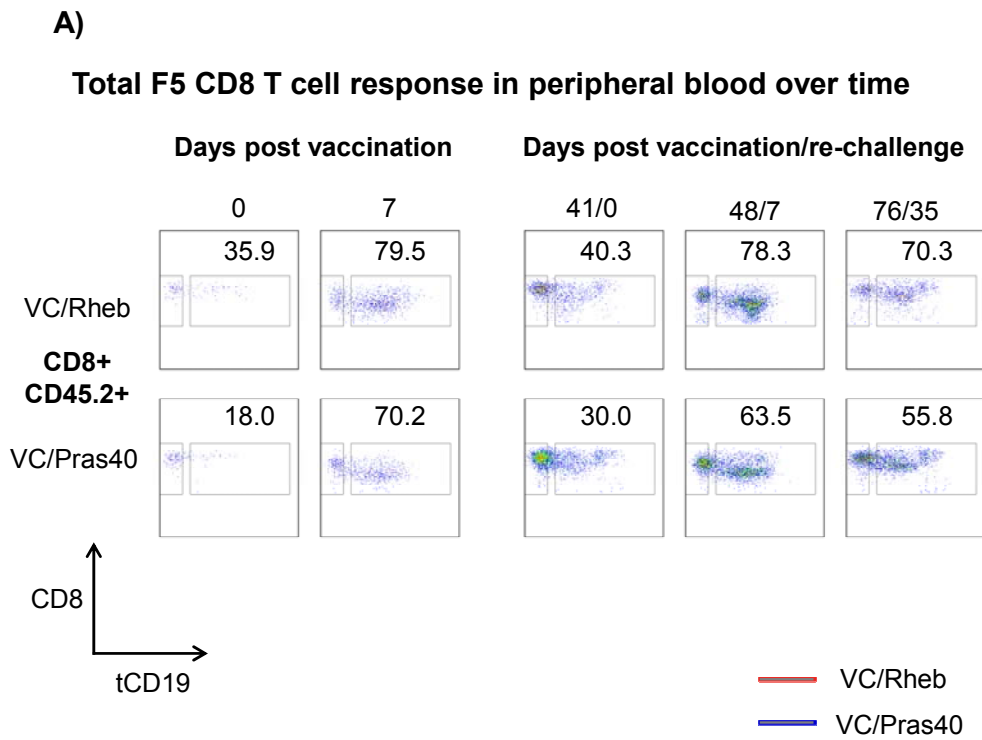
Figure 45: Total F5 response over time

A) Expression of the tCD19 marker (= F5 TCR marker) after antigen re-challenge in peripheral blood over time. It was gated on CD8+CD45.2+ cells. Two gates are shown in the plots, one highlighting the tCD19+, one the tCD19- cells. Numbers in plots represent percentage of the tCD19+ cells only. For both groups (Rheb:VC and Pras40:VC), one representative example is shown.

B) Summary data of the expansion of F5 TCR- (left) - representing homeostatic proliferation - and F5 TCR+ (right) – representing antigen driven proliferation - CD8 T cells in peripheral blood over time. Arrow in graph indicates time point of re-challenge with EL4-NP cells (day 43 post ACT). X-axis shows days after ACT and Y-axis shows level of F5 independent (F5 TCR-, left graph) or F5 specific (F5 TCR+, right graph) T cell response relative to total CD8 T cells. Mean and standard deviation are indicated. Red-grey line represents Rheb:VC group, blue-grey line represents Pras40:VC group.
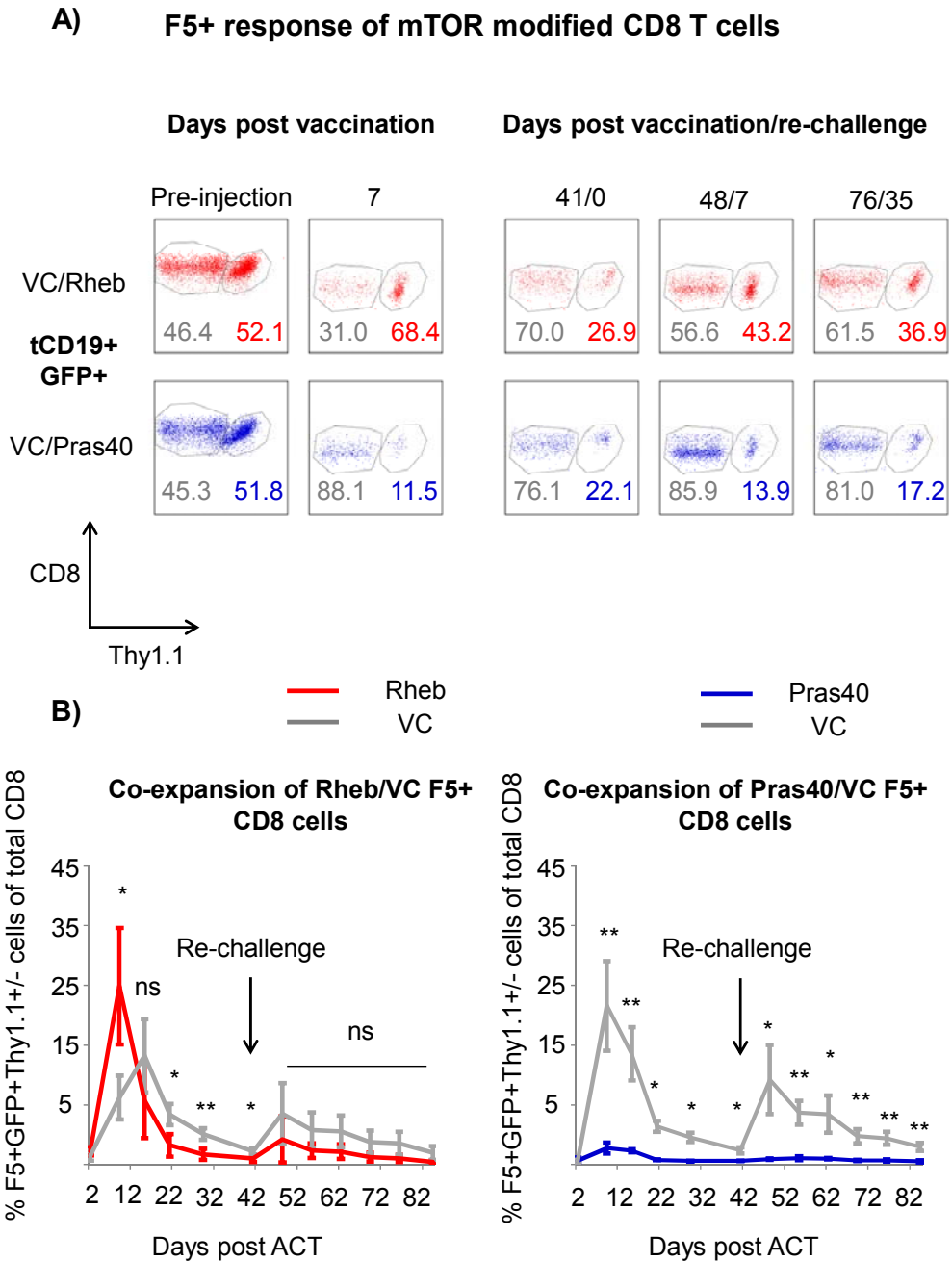
Figure 46: F5 T cell response of mTOR modified T cells

A) Ratios of mTOR modified T cells to VC transduced cells after antigen re-challenge in peripheral blood over time. It was gated on CD8+CD45.2+tCD19+GFP+ cells. Two gates are shown in the plots, one highlighting the Thy1.1+ (Rheb or Pras40 transduced), one the Thy1.1- (VC transduced) cells. Grey represents percentage of VC, red represents percentage of Rheb and blue represents percentage of Pras40 transduced cells. For both groups (Rheb:VC and Pras40:VC), one representative example is shown.

B) Summary data of the expansion of Rheb transduced and VC transduced cells (left graph; n=4) as well as Pras40 and VC transduced cells (right graph; n=4) in peripheral blood over time. Arrow in graph indicates time point of re-challenge with EL4-NP cells (day 42 post ACT). X-axis shows days after ACT and Y-axis shows level of tCD19+GFP+ T cell response relative to total CD8 T cells. Mean and standard deviation are indicated. Statistical test: Paired student's t test. Statistical significance defined as p-value < 0.05. Grey represents VC, red represents Rheb and blue represents Pras40 transduced cells. ns=not significant.

129

In addition to the change of F5 TCR+ T cells as a ratio of total CD8 T cells, Figure 47 displays the change of ratios of mTOR modified to VC transduced cells over time. Again, for the Rheb:VC group, the ratio changes in favor of Rheb initially but then this relation switches over and remains like this for the rest of the experiment. In case of the Pras40:VC group, the ratio changes in favor for VC early on and it remains like this for the whole course of the experiment. Even the re-challenge changes very little.
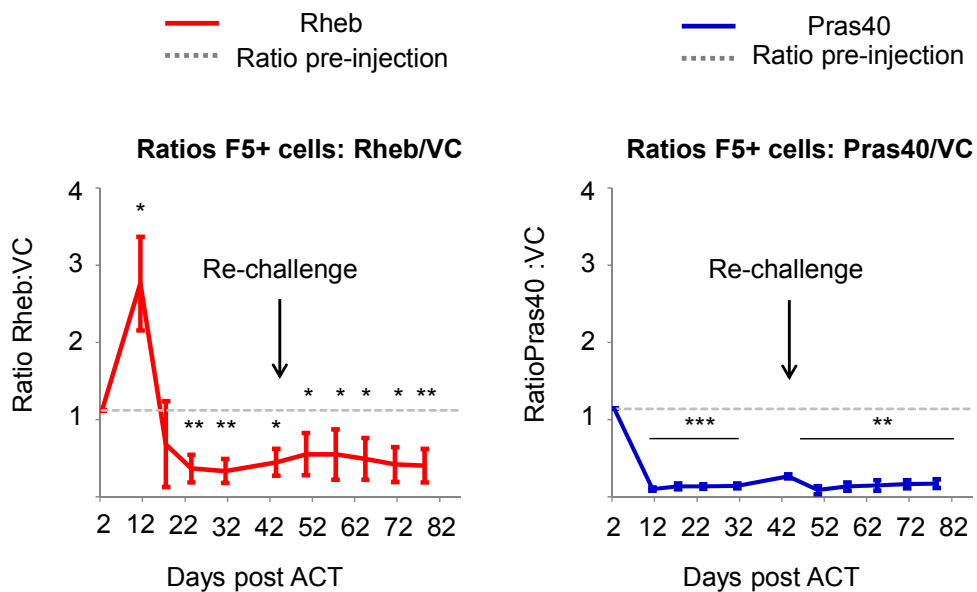
Figure 47 Ratios Rheb:VC and Pras40:VC over time

Indicated at each time point are the ratios of either Rheb:VC (left graph; n=4) or Pras40:VC (right graph; n=4) in peripheral blood over time. Arrow in graph indicates time point of re-challenge with EL4-NP cells (day 42 post ACT).Mean and standard deviation are indicated. Statistical test: Wilcoxon Signed Rank test (calculates p-value of the difference from the ratio pre-injection). Statistical significance defined as p-value < 0.05. Grey dotted line represents ratio pre-injection, red represents ratio of Rheb:VC and blue represents ratio of Pras40:VC.

It was difficult to evaluate absolute numbers during these responses as the data were derived from peripheral blood which was collected through tailbleeds. But since mTOR modified and VC transduced cells were injected into the same mice, it is clear that the magnitude of response by Rheb transduced cells relative to co-transferred VC transduced cells must be reflected in absolute numbers.

In addition to the F5 T cell response, we wanted to investigate the effects of mTOR modification on CD62L expression. CD62L is an important molecule that guides T cell homing, serves as a marker of T cell activation and T cell memory (Mora and von Andrian 2006) and has been shown to be down-regulated by mTOR activity. Sinclair et al. (2008) have demonstrated that while phosphatidylinositol-3-OH kinase (PI3K) is responsible for the immediate early proteolysis of CD62L, mTOR activity, through regulation (mTOR induced CD62L mRNA reduction) of the transcription factor Kruppel like factor 2 (KLF2), controls the expression of CD62L on a transcriptional level. Treatment with rapamycin could maintain expression of CD62L significantly. In addition, D. K. Finlay et al. (2012) were able to show that HIF1β-/- CD8 T cells maintain high expression of CD62L after peptide specific stimulation *in vitro*. Since HIF activity is regulated by mTOR, CD62L expression can also be influenced through the mTOR-HIF axis.

Figure 48A shows the expression of CD62L as a percentage of GFP+ cells over time. In each case, CD62L is down-regulated upon vaccination and re-challenge. For the Rheb:VC group, the initial down-regulation of CD62L is greater for Rheb than for VC transduced cells whereas during the rest of the experiment, no differences could be seen between the two groups of cells, not even after EL4-NP re-challenge. With regards to the Pras40:VC group, even though Pras40 transduced cells do initially lose expression of CD62L upon vaccination and re-challenge, the rate of down-regulation is much lower than for VC transduced cells. CD62L expression of Pras40 transduced cells also remains higher during the whole course of the experiment. The observed differences are further exemplified in Figure 48B. The greater decrease in CD62L down-regulation by Rheb transduced cells in direct comparison to VC transduced cells on day 7 after re-challenge is shown and, respectively, the high increase in CD62L expression by Pras40 transduced cells on day 40 post vaccination. Summarized data are pooled from 2 independent experiments.

A)

CD62L profile over time

B)
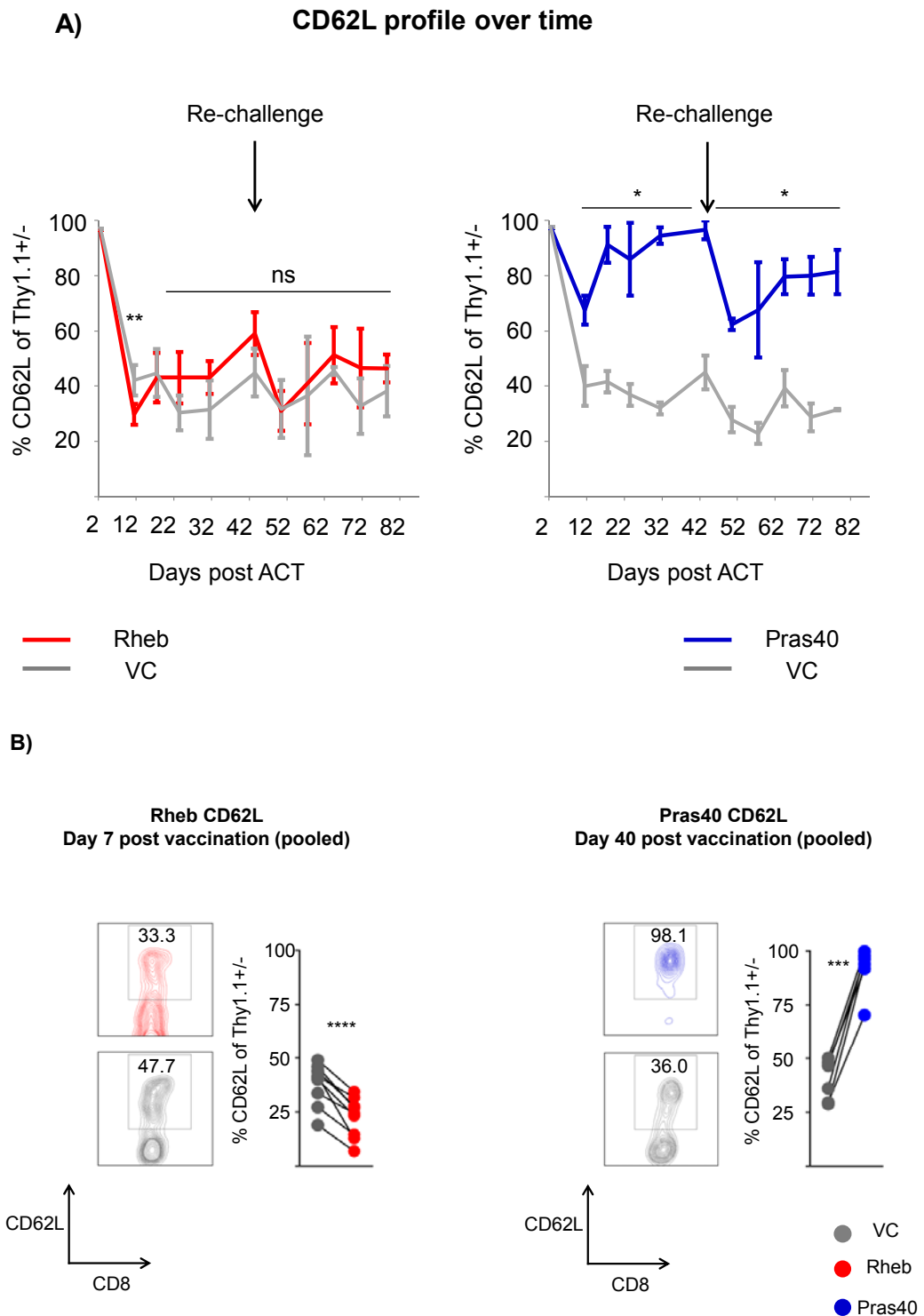
Figure 48: CD62L expression over time

A) Summary data of the expression of CD62L by Rheb and VC transduced cells (left graph; n=4) as well as Pras40 and VC transduced cells (right graph; n=4) in peripheral blood over time. Arrow in graph indicates time point of re-challenge with EL4-NP cells (day 42 post ACT). X-axis shows days after adoptive cell therapy (ACT) and Y-axis shows the expression of CD62L in percentage relative to Thy1.1+ or Thy1.1- cells, respectively. Mean and standard deviation are indicated. Statistical test: Paired student's t test. Statistical significance defined as p-value < 0.5. Grey line represents VC, red line represents Rheb and blue line represents Pras40 transduced cells. ns=not significant.

B) CD62L expression of Rheb compared to VC transduced cells on day 7 post vaccination and of Pras40 compared to VC transduced cells on day 40 post vaccination is shown. For both groups (Rheb:VC and Pras40:VC), one representative contour plot is shown. Numbers inside of gates represent percentage. It was gated on Thy1.1+ (Rheb or Pras40 transduced cells) and Thy1.1- (VC transduced cell) cells. Summary data are pooled from 2 independent experiments. Statistical test: Paired student's *t* test. Statistical significance defined as p-value < 0.05. Grey represents VC, red represents Rheb and blue represents Pras40 transduced cells.

In a repeat of the just described experiment, 2 things have been slightly modified:

1) F5 co-transduction with RQ64L was included as an own group to see if the above mentioned effects of Rheb transduced cells can be further enhanced.

2) More F5 TCR+ CD8 T cells were injected (1.5×10^6 as opposed to 0.4×10^6) to increase the quality of the FACS data, especially prior to vaccination when the number of events of transferred cells is still very low.

This latter change had a significant and noteworthy impact on the experimental outcome, particularly with regards to the initial expansion upon vaccination, as shown in Figure 49. Due to the lower number of injected cells in the first experiment (left graph), they had more room to expand and occupy the CD8 T cell niche upon vaccination (~9.9 mean fold change of F5 frequency relative to pre-injection). In contrast, when more cells were injected (right graph), the level of F5 TCR+ T cells relative to total CD8 T cells was already higher prior to vaccination, leaving less room for the cells to expand (~1.7 mean fold change of F5 frequency relative to pre-injection). The bar graph below exemplifies that. Nonetheless, as it was the case for the first experiment, all 3 groups (Rheb:VC, RQ64L:VC and Pras40:VC) followed a very similar response pattern. The peak of the response was again seen 7 days post vaccination, after which the contraction phase began and cells returned slowly back to baseline between 20 and 50 days post vaccination.

What is interesting is that there seems to be an intrinsic threshold above which the F5 TCR+ T cells cannot expand and this threshold is a function of the whole CD8 T cell compartment. In both experiments, the F5 TCR+ T cells took up a maximum between 55 and 70 % of the whole CD8 T cell niche in a very similar manner. The re-call response in the repeat experiment was much higher than in the first experiment. Gerlach et al. (2013) and Buchholz et al. (2013) independently made the observation that cells that respond poorly at the initial antigen encounter can nonetheless make a high memory re-call response (discussed in chapter 5.4). If cells respond poorly, this may allow them to maintain in higher number due to a

reduced contraction response, resulting in a highly potent re-call response. Nonetheless, even at this second memory response, the F5 TCR+ T cells again did not breach the maximum threshold of 70 % of total CD8 T cells.

Exactly because of this internal threshold above which the F5 TCR+ cells cannot expand, Rheb transduced cells were not able to show their full potential. If T cells cannot expand optimally, modifications such as increasing the mTOR signaling pathway are probably not providing any advantages. As shown in Figure 50, Rheb transduced cells did not show any advantage in the expansion phase as compared to VC transduced cells 7 days post vaccination in the repeat experiment. Nonetheless, they did show increased contraction and worse persistence just like in the first experiment. In general, except of the expansion phase, the rest of the experiment progressed in a very similar way, including the kinetic profile of CD62L expression (not shown).

Interestingly, RQ64L transduced cells show an even more dramatic contraction response, worse persistence and a poor re-call response relative to VC transduced cells which is in accordance with published data. Yang et al. (2011) have extensively shown that survival of T cells with a constitutively high mTOR pathway is poor in the periphery and that these cells are more likely to undergo apoptosis. Just like Rheb transduced cells, RQ64L transduced cells down-regulate CD62L in an increased manner compared to VC transduced cells 7 days post vaccination but after that, the levels of CD62L expression are very similar to VC transduced cells (result not shown).

Pras40 transduced cells again do not seem to expand at all and remain at low levels throughout the course of the experiment. The results are very similar to the first experiment.

Although the rate of expansion was much lower in the repeat than in the first experiment, when the ratios of Rheb:VC cells at day 7 post vaccination were pooled from both experiments, Rheb transduced cells still showed a statistically significant advantage over VC transduced cells (Figure 50B).

Impact of number of injected cells on experimental outcome
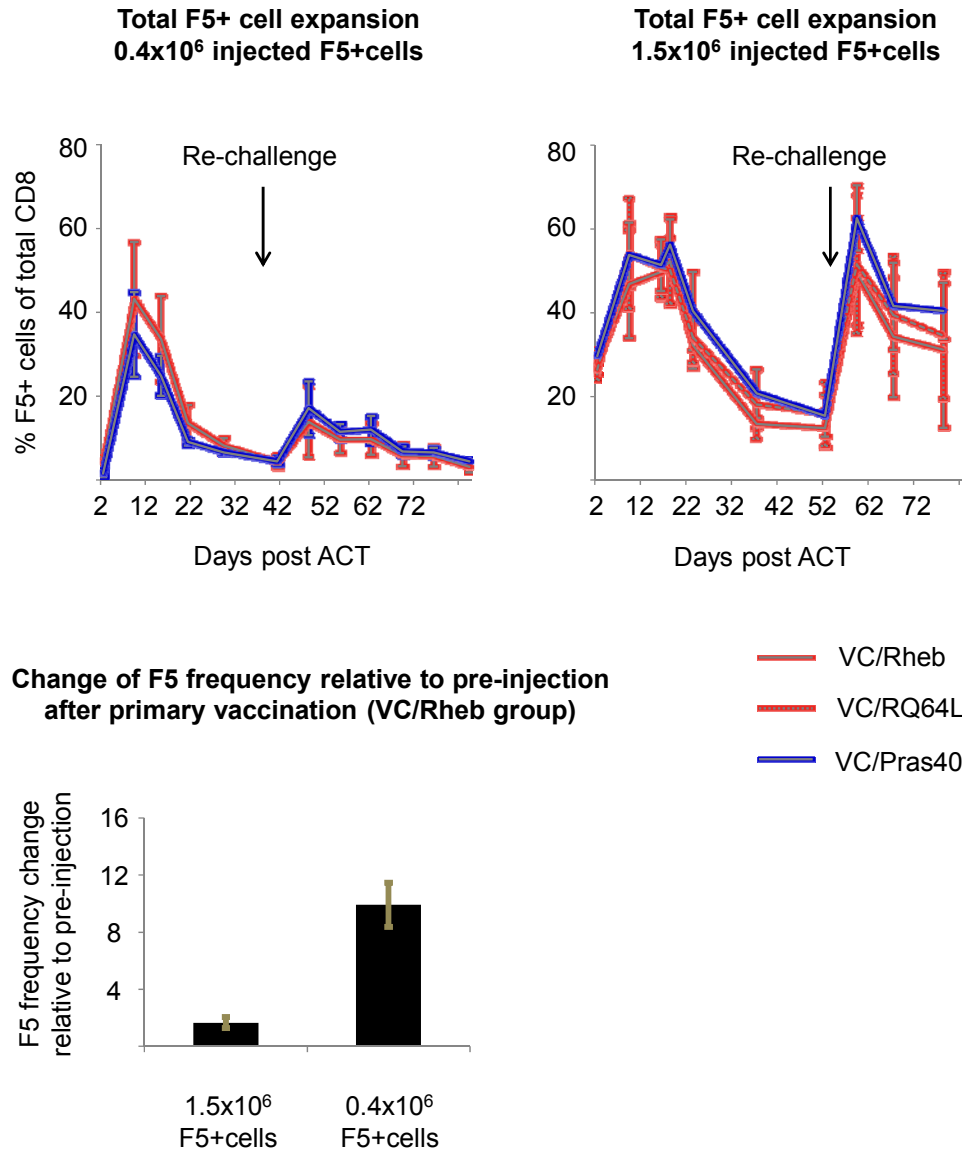
Figure 49: Number of injected F5 TCR+ T cells determines experimental outcome

Total F5 T cell responses in peripheral blood over time in the first experiment (left graph; n=4/group) and the repeat experiment (right graph; n=5/group) are compared side-by-side. Arrows in graphs indicate time point of re-challenge with EL4-NP cells (day 52 post ACT). X-axis shows days after ACT and Y-axis shows level of F5 specific (F5 TCR+) T cell response relative to total CD8 T cells. Mean and standard deviation are indicated. Red-grey line represents Rheb:VC group, dotted red-grey line represents RQ64L:VC group and blue-grey line represents Pras40:VC group. The bar graph below shows the relative change of F5 TCR+ frequency relative to pre-vaccination in both experiments (Rheb:VC group shown as example).

A)

B)
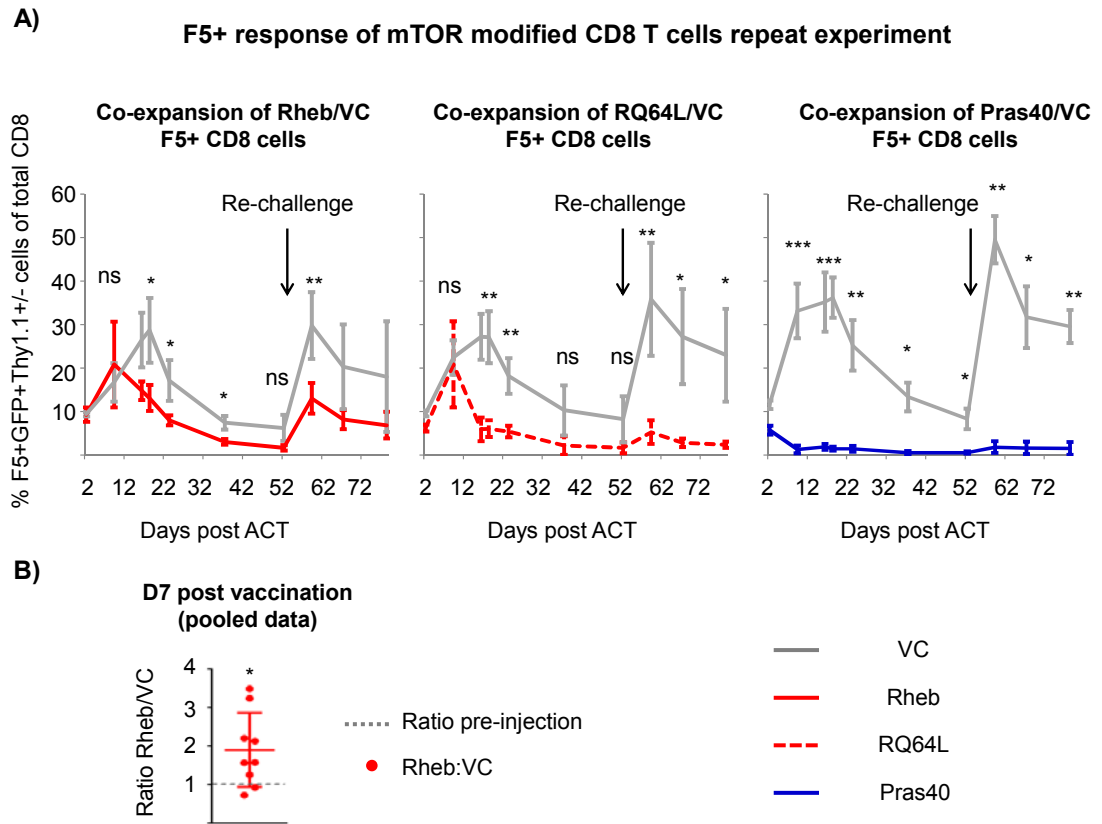
Figure 50 Repeat experiment: VC:Rheb, VC:RQ64L, VC:Pras40

A) Summary data of the expansion of Rheb transduced and VC transduced cells (left top graph; n=5), RQ64L transduced and VC transduced cells (middle top graph; n=5) as well as Pras40 and VC transduced cells (right top graph; n=5) in peripheral blood over time. Arrows in graphs indicate time point of re-challenge with EL4-NP cells (day 52 post ACT). X-axis shows days after ACT and Y-axis shows level of tCD19+GFP+ T cell response relative to total CD8 T cells. Mean and standard deviation are indicated. Statistical test: Paired student's t test. Statistical significance defined as p-value < 0.5. Grey line represents VC, red line represents Rheb, red dotted line represents RQ64L and blue line represents Pras40 transduced cells.

B) Pooled data from 2 independent experiments (n=9), showing ratio of Rheb to VC transduced cells 7 days post vaccination. Mean and standard deviation are indicated. Statistical test: Wilcoxon Signed Rank test (calculates p-value of the difference from the ratio pre-injection). Statistical significance defined as p-value < 0.05. Grey dotted line represents ratio pre-injection, red represents ratio of Rheb:VC.

5.3 Lymphoid Tissue Infiltration and Phenotype of Antigen Experienced MTOR Modified CD8 T Cells

After following the immunological and memory re-call response of mTOR modified (Rheb, RQ64L and Pras40 transduced) F5 TCR+ T cells *in vivo* in direct comparison with VC transduced cells for more than 3 months, mice were culled, their spleen, lymph nodes and bone marrow were collected, cells were counted and ratios as well as CD62L/CD127 phenotype were determined. It was decided to look at CD127, rather than CD44 since CD44 expression is unlikely to change after the initial activation process for the transduction procedure. CD127 together with CD62L represent good markers to characterize CD8 T cells (Bachmann et al. 2005): CD62L+CD127+ cells are considered central memory, CD62L-CD127+ cells effector memory and CD62L-CD127- effector T cells.

Figure 51 shows representative example plots of ratios of mTOR modified F5 TCR+ and VC transduced T cells in spleen, lymph nodes and bone marrow, the data (pooled from 2 independent experiments) are summarized in Figure 52. The ratios of Rheb:VC and RQ64L:VC are reduced in spleens and lymph nodes but not in bone marrow. This may be related to the result shown in chapter 5.1 where Rheb transduced T cells in mice which have not been challenged with antigen showed slightly better engraftment in bone marrow compared to VC transduced cells.

The ratios of Pras40:VC are reduced only in spleen and bone marrow, not in lymph nodes. This may be explained by the very high CD62L expression by Pras40 transduced cells which allows those cells to migrate and persist efficiently in the lymph nodes.

The change in ratios again reflects the differences in absolute cell numbers (results not shown).

With regards to the CD62L/CD127 profile, Figure 53 shows representative example plots and data (pooled from 2 independent experiments) are summarized in detail in Figure 54. Rheb and RQ64L transduced cells show no difference in their CD62L/CD127 profile compared to VC transduced cells in any of the 3 compartments (spleen, lymph nodes, bone marrow). Pras40 transduced cells, however, predominantly show a CD62L+CD127+ double positive phenotype in all 3 compartments. In other words, they resemble very much CD8 T cells of a central memory phenotype.

Take down: Engraftment in lymphoid tissues
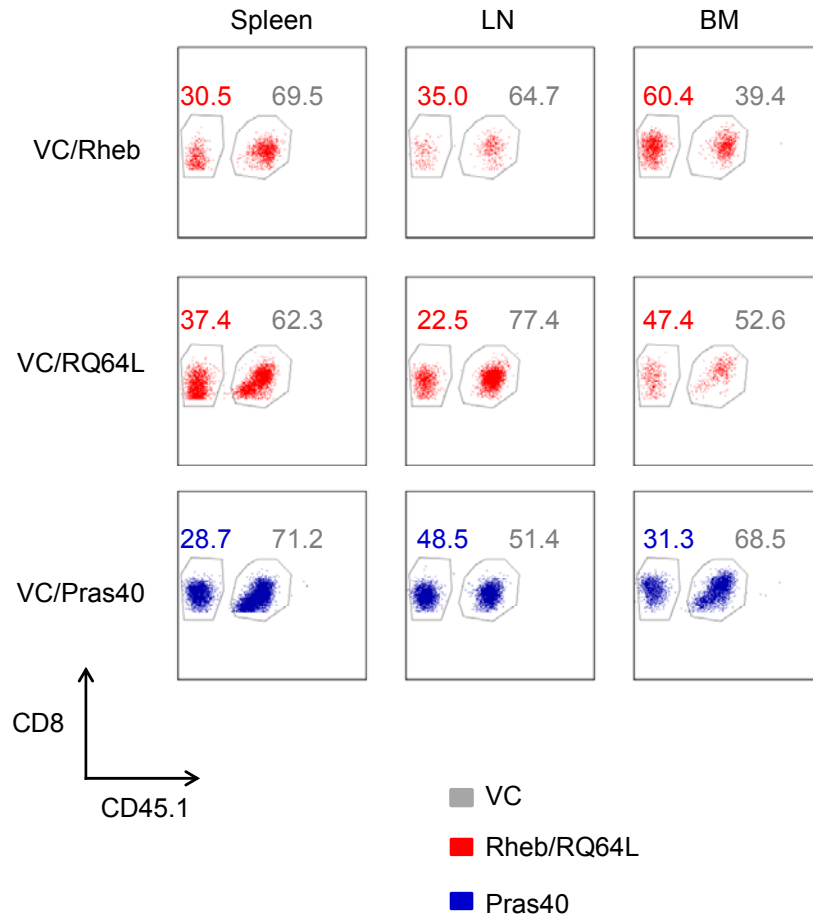
Figure 51: Ratios in different lymphoid compartments (1)

At the end of the experiment (day 135 post ACT), mice were taken down, spleen, lymph nodes and bone marrow were collected and the ratios of mTOR modified to VC transduced F5 TCR+ T cells were determined. One representative dot plot from each group shows the ratios of Rheb:VC, RQ64L:VC and Pras40:VC. The plots were taken from the repeat experiment where the strategy to distinguish Rheb/RQ64L/Pras40 from VC transduced cells is different than described in Figure 43: Rheb/RQ64L/Pras40 transduced cells are CD45.1- (and CD45.2+), VC transduced cells are CD45.1+. It was gated on tCD19+GFP+ cells. Numbers in gates represent percentage. Grey represents VC, red represents Rheb and, where indicated, RQ64L and blue represents Pras40. LN=lymph nodes. BM=bone marrow.
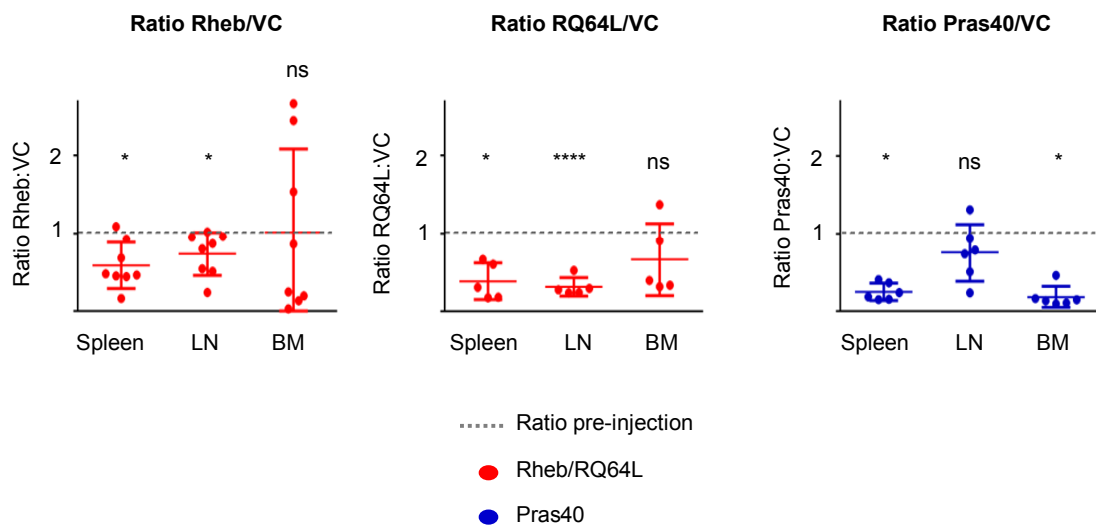
Figure 52: Ratios in different lymphoid compartments (2)

Ratios of mTOR modified to VC transduced F5 TCR+ T cells in the different lymphoid compartments (spleen, lymph nodes, bone marrow) are shown. The results were pooled from 2 independent experiments (Rheb:VC n=8; RQ64L:VC n=5; Pras40:VC n=6). Mean and standard deviation are indicated. Statistical test: One sample t test (calculates p-value of the difference from the ratio pre-injection). Statistical significance defined as p-value < 0.05. Grey dotted line represents ratio pre-injection, red represents ratio of Rheb:VC and, where indicated, RQ64L:VC and blue represents ratio of Pras40:VC. LN=lymph nodes. BM=bone marrow. ns=not significant.

Memory profile: CD62L/CD127
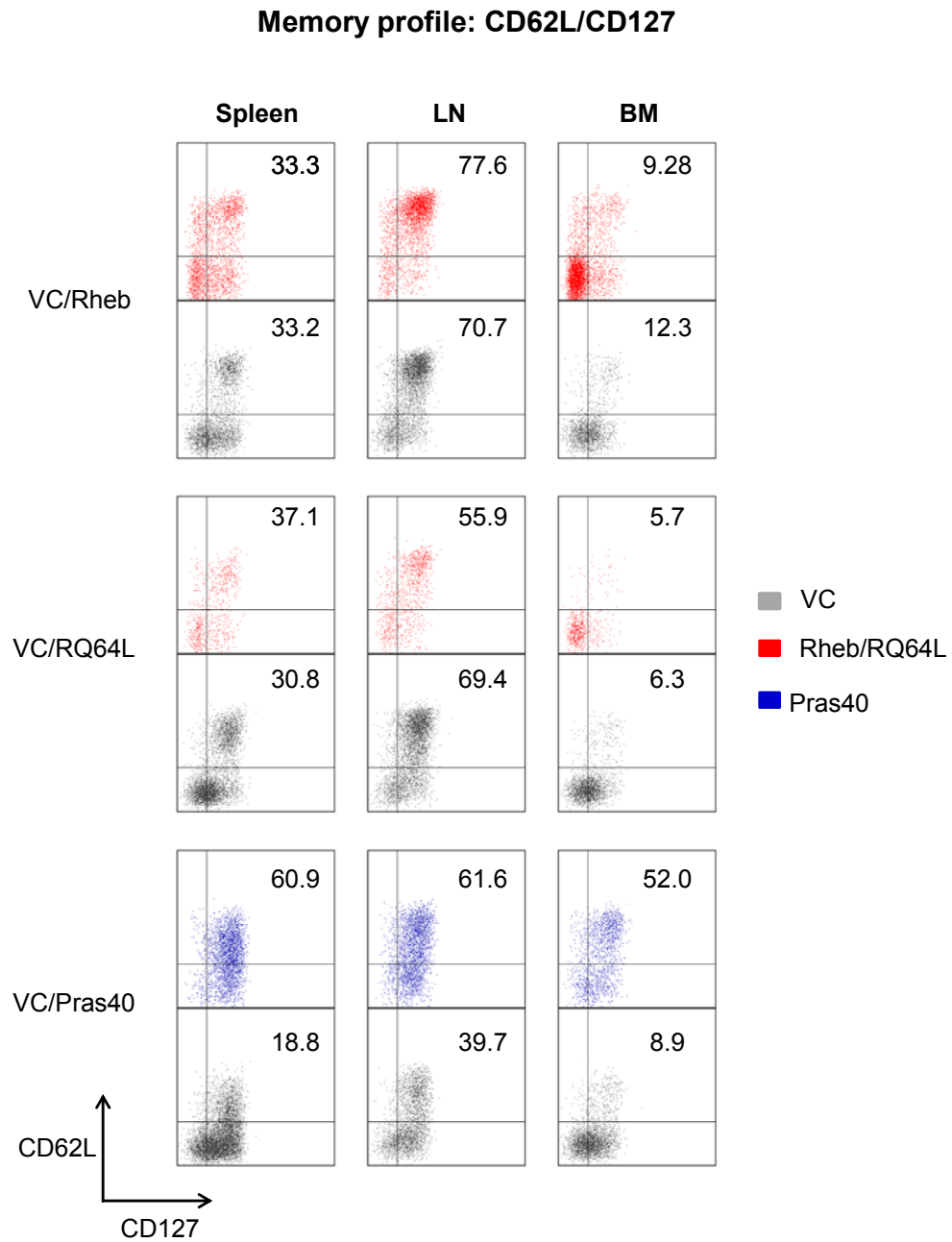
Figure 53: CD62L/CD127 profile in lymphoid compartments (1)

One representative dot plot from each group shows CD62L/CD127 profile in the different lymphoid compartments after take down (day 135 post ACT). Numbers inside the gates represent percentage of CD62L+CD127+ double positive T cells. It was gated on CD45.1- (Rheb, RQ64L and Pras40 transduced) and CD45.1+ (VC transduced) cells. Grey represents VC, red represents Rheb and, where indicated RQ64L and blue represents Pras40. LN=lymph nodes. BM=bone marrow.
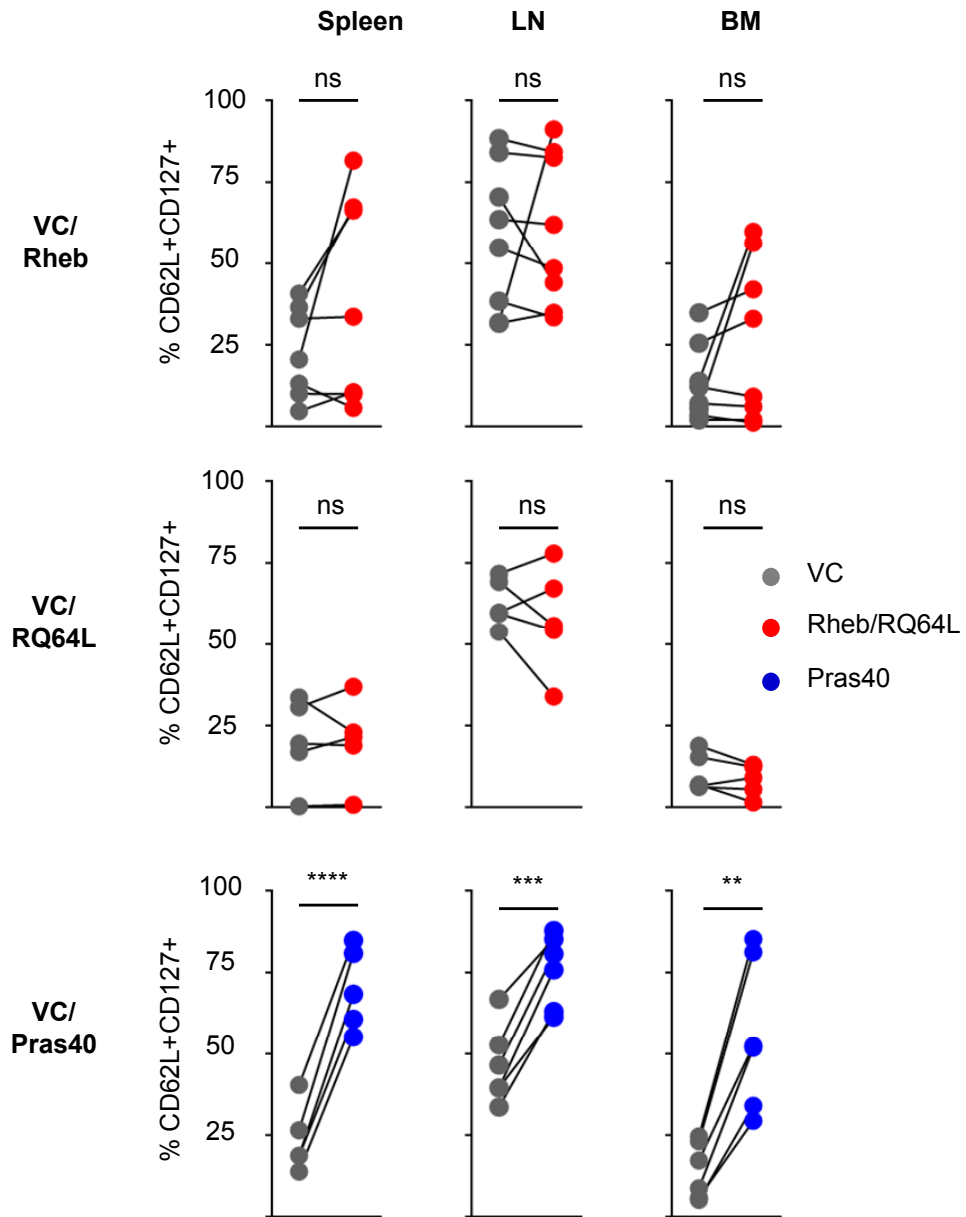
Figure 54: CD62L/CD127 profile in lymphoid compartments (2)

Summary data from 2 independent experiments, displaying the percentage of CD62L+CD127+ double positive cells for mTOR modified and VC transduced F5 TCR+ T cells in the different lymphoid compartments (Rheb:VC n=8; RQ64L:VC n=5; Pras40:VC n=6). Mean and standard deviation are indicated. Statistical test: Paired student's t test. Statistical significance defined as p-value < 0.05. Grey represents VC, red represents Rheb and, where indicated, RQ64L and blue represents Pras40 transduced cells. LN=lymph nodes. BM=bone marrow. ns=not significant.

5.4 Summary and Conclusion

The data shown in this chapter complement the *in vitro* data discussed in Chapter 4. The main results are:

1) When transferred Rheb transduced CD8 T cells are not stimulated by antigen, these cells engraft in the same manner as VC transduced cells in the 3 lymphoid compartments spleen, lymph nodes and bone marrow. Rheb transduced cells even show a small engraftment advantage in bone marrow. In addition, Rheb transduced cells show a trend to spontaneous differentiation into effector or effector memory like CD8 T cells (CD62L-CD44+) which is statistically significant in spleen.

2) During the effector phase of an immunological response, Rheb transduced CD8 T cells compete better for the CD8 T cell niche which is occupied by the F5 TCR+ T cells upon vaccination. In other words, during the expansion (effector) phase of a T cell response (7 days post vaccination), Rheb transduced cells show a superiority over VC transduced cells. Pras40 transduced cells, on the other hand, do not seem to expand at all and therefore show an inferiority over VC transduced cells.

3) After the expansion phase, Rheb transduced CD8 T cells contract more dramatically than VC transduced cells (days 7-40 post vaccination), they remain low during the rest of the experiment but can still mount a re-call response. They engraft worse than VC transduced cells in spleen and lymph nodes but not in bone marrow. The contraction is further increased and engraftment further decreased when T cells are transduced with RQ64L. These cells also show an impaired re-call response. Pras40 transduced cells remain low during the whole course of an immunological response and engraft at low percentage in spleen and bone marrow. However, in lymph nodes they are present at similar percentage than control T cells.

4) Rheb transduced cells down-regulate CD62L in a greater manner than VC transduced cells during the effector phase of an immunological response. However, during all other phases of the immune response (contraction and memory) no differences in CD62L expression can be detected. In addition, no differences in CD62L+CD127+ double positive phenotype can be detected in spleen, lymph nodes or bone marrow. Pras40 transduced cells, on the other hand, although they do show down-regulation upon vaccination (indicating that they do actually encounter antigen), maintain high CD62L expression throughout the whole course of the response (expansion,

contraction and memory). In addition, they predominantly present with a CD62L+CD127+ double positive phenotype in spleen, lymph nodes and bone marrow.

It is interesting to see that the only difference in CD62L expression by Rheb transduced T cells coincides with their peak of expansion. It is likely that the strong effector response conferred by an increase in mTOR signaling through Rheb drives the T cells into end stage $CD62L_{lo}$ effectors which will later on die and hence leave behind less total Rheb transduced cells. It is known that at the peak of an effector response, there are end stage effector cells ($CD127_{lo}$ $KLRG1_{hi}$) which eventually die off and memory pre-cursor cells ($CD127_{hi}$ $KLRG1_{lo}$) with the potential to enter the long term memory pool (Kaech et al. 2003; Sarkar et al. 2008). Rheb overexpression may tip the balance towards the former and against the latter. The cells, which manage to enter the pool of cells that persist long term, may have re-tuned their mTOR activation profile in a way that allows them to maintain. Because RQ64L cannot re-tune in the same way, these cells persist worse, not even allowing them to mount a re-call response due to their inability to go back to a quiescent state – similar to TSC1-/- T cells (Yang et al. 2011). Overall, it is tempting to speculate that the effects of Rheb transduction are only seen early on during an effector response while they become negligible when this phase has passed.

Gerlach et al. (2013) and Buchholz et al. (2013) have shown that an overall T cell response consists of several disparate ones, some of which are higher, others are lower than the average response. It is interesting that the level of effector responses of these individual T cell groups does not correlate with the level of memory re-call responses, i.e. a high initial effector response does not predict an equally high memory re-call response and vice versa. In addition, they showed that the level of CD62L down-regulation correlates with the size of the initial effector response. The authors did not comment on the persistence of the individual groups of cells.

It is conceivable that persistence of cells may be inversely correlated with the rate of the effector T cell response, as this was observed for Rheb transduced T cells. If this is true, one factor that may contribute to the observations made by Gerlach et al. (2013) and Buchholz et al. (2013), is the activation of the mTOR pathway within the individual groups of cells. In other words, high mTOR activation may lead to high effector responses, increased CD62L downregulation and subsequent worse persistence in the "strong responders" of the initial response but it does not

necessarily preclude a memory response later on, as this was observed in Figure 46. This means that some of the progenies of T cell families that respond highly initially simply disappear. Low mTOR activation during effector responses, on the other hand, may confer better memory characteristics phenotypically but if inhibition is permanent, these cells cannot realize their full potential upon antigen encounter. Under other conditions, they would potentially be potent memory T cells. This assumption is supported by the fact that a short and transient high dose treatment with rapamycin during the expansion phase of a T cell response (days 0-7) can result in the production of potent and highly functional memory cells whereas long term treatment abrogates this effect (Q. Li et al. 2012). Possible strategies to address this problem are discussed further below (Chapter 7).

In conclusion, Rheb transduced CD8 T cells show increased effector functions both *in vitro* as well as *in vivo*. They do persist worse than VC transduced cells but can nonetheless mount a memory re-call response. Pras40 transduced CD8 T cells show a dramatic lack of effector response, whereby the results are more dramatic *in vivo* than *in vitro*. At the same time, they maintain a phenotype, reminiscent of central memory T cells which are, however, not functional.

In the next and final chapter of this thesis (Chapter 6), the question is going to be addressed which of the so far described modifications confers better protection from live tumour *in vivo*.

Chapter 6   Tumour Protection Experiments

The aims of this chapter were:

1) To investigate whether increasing or inhibiting mTOR signaling results in any benefits or disadvantages in tumour protection.
2) To elaborate the mechanisms behind the observed outcomes.

6.1 Effects of MTOR Modified T Cells on Tumour Growth and Survival

The principles of the following experiment are outlined in Figure 55. In short, C57BL/6 mice were irradiated with 5.5 Gy before they received a subcutaneous injection of EL4-NP cells. They then received either un-transduced or F5 TCR transduced T cells which were co-transduced with Rheb, Pras40 or VC. The mice were monitored for the following weeks, i.e. tumour size and weight changes were documented.

Figure 56 shows a representative example of T cells co-transduced with the F5 TCR and the mTOR modifying constructs or VC. The CD8 sorted T cells are of Thy1.1 origin (recipient mice are Thy1.2), so they could be identified when this was required. tCD19 expression (=F5 TCR transduction) is lower for the Pras40 group than for the VC and Rheb groups, possibly because of a lack of expansion *in vitro* relative to un-transduced cells. Nonetheless, co-transduction was usually very high. In the example shown here, most of the cells transduced with the F5 TCR also expressed GFP (80.0 % for Rheb, 87.1 % for Pras40 and 70.8 % for VC). To guarantee comparability amongst the groups (so that the mice of the different groups do not receive different total numbers of F5 TCR transduced cells which has a major impact on tumour control, as shown by Abad et al. [2008]) as well as to avoid the need for FACS sorting, the same number of F5 TCR+ instead of the same number of F5 TCR+GFP+ double positive cells were injected. The mock group received a number of CD8 T cells equal to the highest total T cell number injected in the other groups. So the sole difference amongst the 3 groups was the expression of the co-transduced constructs. Again, Rheb transduced cells were larger and Pras40 transduced cells were smaller than VC transduced cells.

Before the tumour challenged mice were irradiated, their original weight was documented. After adoptive T cell transfer, the weight of the treated mice was

monitored and the change relative to pre-irradiation was documented. Most of the mice showed an initial drop in body weight which can probably be assigned to the pre-conditioning. When the mice lost >20 % of their original weight, they had to be sacrificed due to home office regulations and were excluded from the experiment. No differences between the groups in weight related deaths could be observed (result not shown).

Experimental layout:
Protection from tumour

Day 0

Total body irradiation 5.5 Gray
EL4-NP 1x10^6
tumour injection s.c.

Day 1, 5 or 10

I.v. injection of 0.003-0.3x10^6
F5+ cells

Tumour measurements

EL4-NP

Group 1: Mock (no F5 TCR)

Group 2: F5 TCR + VC

Group 3: F5 TCR + Rheb

Group 4: F5 TCR + Pras40

Take down criteria

- Tumour >15 mm in any dimension
- Ulceration
- Wait loss >20 % (excluded from analysis)
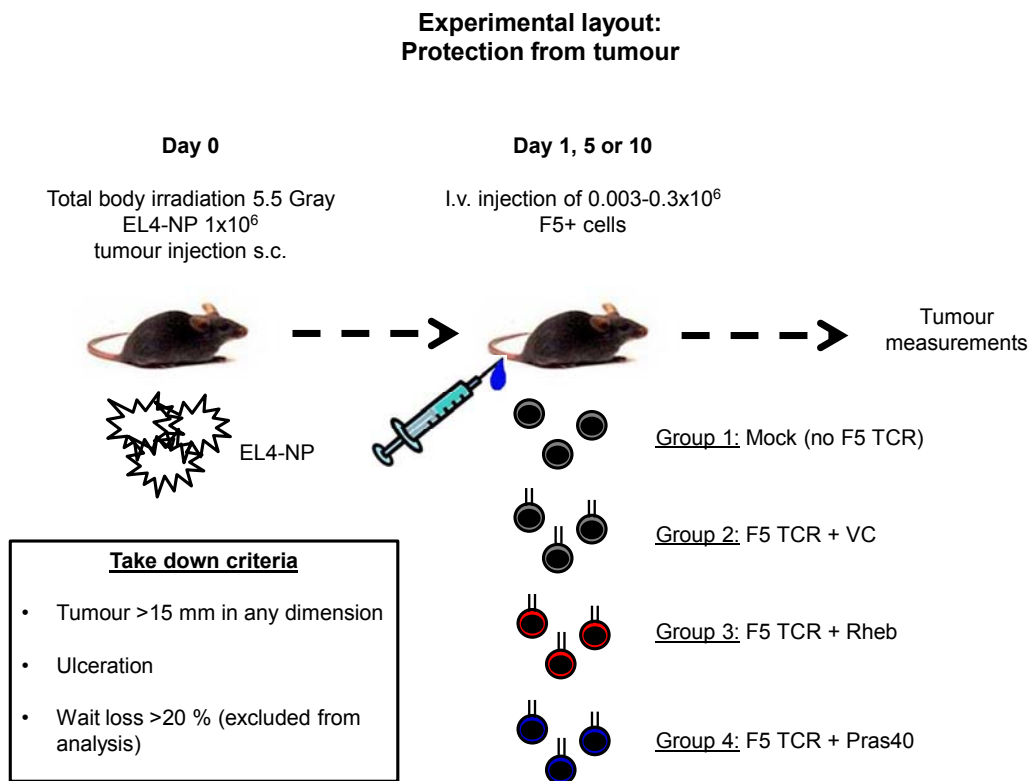
Figure 55: Tumour protection experiment

Four hours before C57BL/6 mice (Thy1.2) received 1x10^6 EL4-NP (immersed in 100 µl of matrigel containing suspension) subcutaneously, they were irradiated with 5.5 Gy. They were then adoptively transferred with either mock transduced (group 1) or between 0.003 and 0.3 x10^6 F5 TCR transduced CD8 T cells that were co-transduced with VC (group 2), Rheb (group 3) or Pras40 (group 4). The T cells (Thy1.1) were injected either on day 1, 5 or 10 post tumour challenge. Mice that lost >20 % of their original weight were culled and excluded from analysis because in this case, cause of death could not exclusively be assigned to tumour growth. Mice were culled when tumour exceeded 15 mm of size in any dimension, when the tumour was ulcerated or when they appeared sick. Tumour was measured manually in a vertical (a) and horizontal (b) dimension with a caliber and tumour surface was calculated using the formula: $\frac{a \times b \times \pi}{4}$ (see also Ahmadi et al. 2011). s.c.=subcutaneous. i.v.=intravenous.

Representative transduction efficiency
Tumour protection experiment
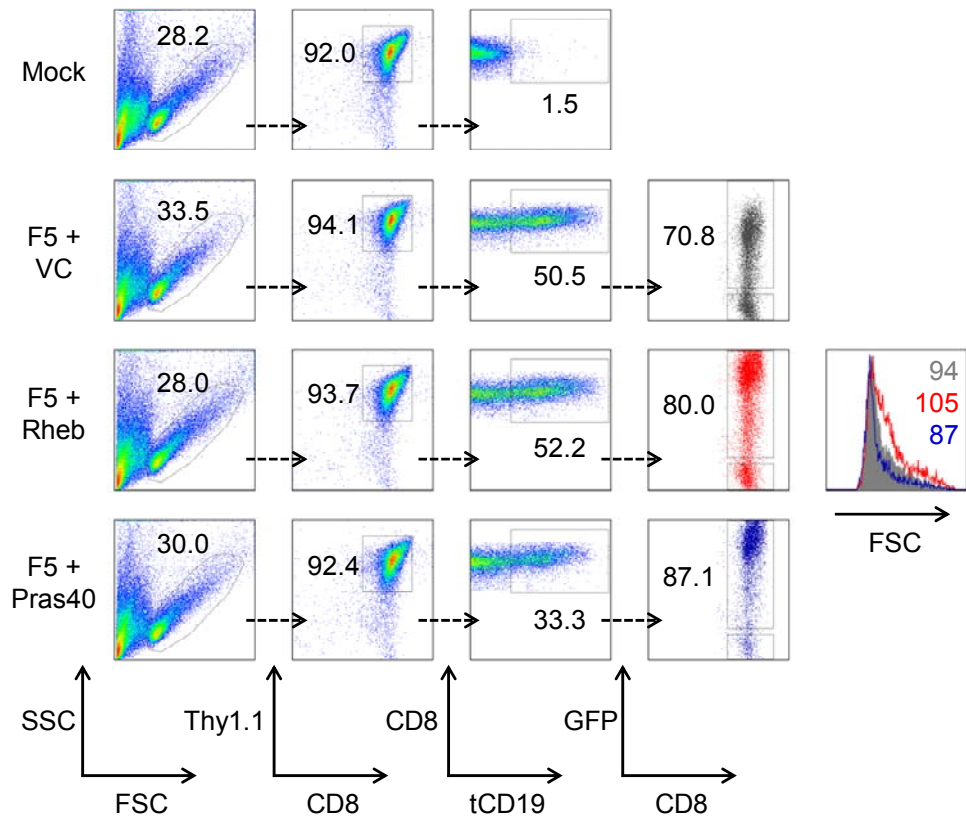
Figure 56: Transduction profile of transferred T cells

CD8 T cells from Thy1.1 mice were co-transduced with the F5 TCR (tCD19+) and Rheb, Pras40 or VC (GFP+). FACS analysis was done 3 days post transduction (= day of T cell injection). Arrows in plots show gating. Numbers in dot plots represent percentage. Numbers in the histogram plot represent the median of the FSC $x10^3$. Grey represents VC, red represents Rheb and blue represents Pras40.

Figure 57A shows tumour growth kinetics over time. Each line represents one individual mouse.

1st group: Mice receiving mock transduced cells very quickly succumb to tumour.

2nd group: Mice receiving F5+VC transduced cells show a very distinct growth pattern: most of the mice control the tumour, ~19 % die because of this initial tumour outgrowth. However, ~40 % of these survivors show a second outgrowth of tumour and ~20 % of the survivors die because of that.

3rd group: Mice receiving F5+Rheb transduced cells show a similar but slightly less dramatic picture. Again, most of the mice control the tumour and only ~4 % die because of this initial tumour outgrowth. Only ~23 % of these survivors show a second outgrowth of tumour (and if they do so, it's to a lesser extent than in the F5+VC group) and ~9 % of the survivors succumb to this second outgrowth.

4th group: The tumour growth pattern of mice receiving F5+Pras40 transduced cells on the other hand very much resembles the group receiving mock transduced cells. All of the mice die due to tumour burden very early on.

These multi-faceted data are summarized in a table in Figure 57B. A Kaplan-Meier survival curve is shown in Figure 58. Mice receiving F5+Rheb transduced CD8 T cells overall survive significantly better compared to mice receiving F5+VC transduced CD8 T cells (p-value [Log rank test] = 0.046). As already mentioned, mice receiving F5+Pras40 transduced CD8 T cells all succumb to tumour very early on (p-value [Log rank test] < 0.001).

A)
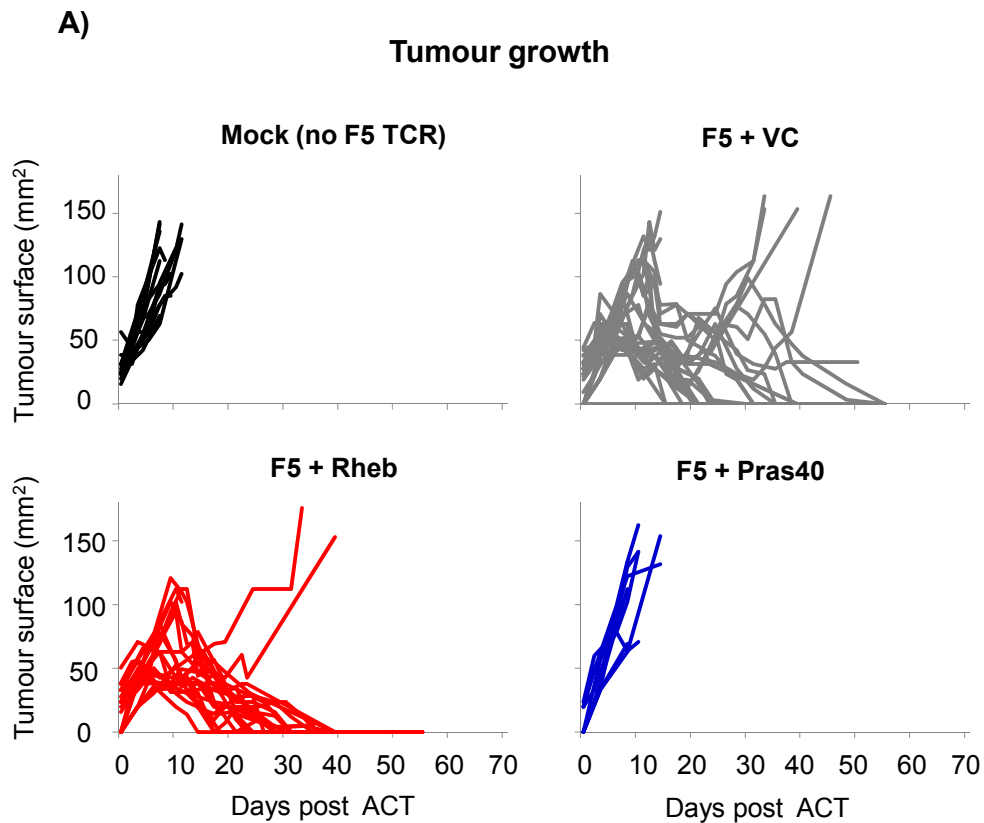
B)

Summary tumour growth

	n (graph)	Deaths 1st outgrowth	Re-growth	Deaths re-growth
Mock	13	13 (100 %)	/	/
F5 + VC	31	6 (~19 %)	10 (40 %)	5 (20%)
F5 + Rheb	23	1 (~4 %)	5 (~23 %)	2 (9%)
F5 + Pras40	9	9 (100 %)	/	/

Figure 57: Tumour growth and deaths due to tumour

A) Tumour growth over time. Pooled data from several experiments (Mock n=13; VC n=31; Rheb n=23; Pras40 n=9). Each line represents one individual mouse. X-axis shows time post ACT and Y-axis shows tumour surface as calculated by the formula described in the text (mm^2). Black lines represent mock, grey lines represent VC, red lines represent Rheb and blue lines represent Pras40 groups.

B) Table summarizing the data. Tumour re-growth is defined as clear and visible re-appearance upon previous rejection. Percentages in brackets relate to the number of mice (n) entering the experiment ("Deaths 1st outgrowth") and, respectively, to the number of survivors of the 1st outgrowth ("Re-growth" and "Deaths re-growth").

Overall death due to tumour
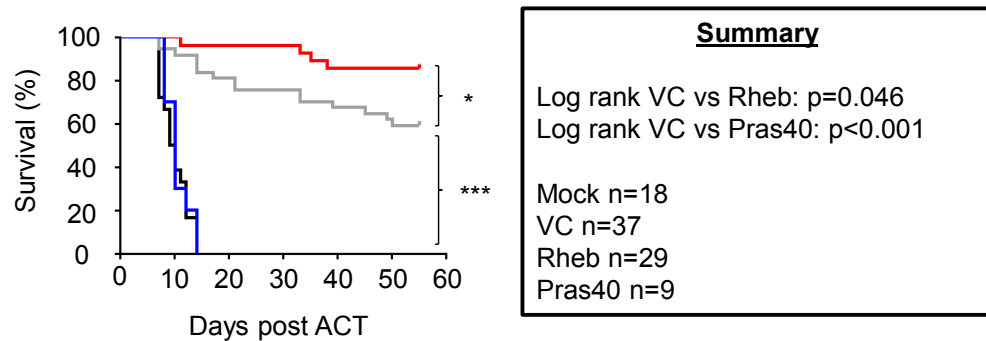
Figure 58: Kaplan-Meier survival curve

Kaplan-Meier survival curve which shows tumour related deaths in the individual groups. Pooled data from several experiments (Mock n=18; VC n=37; Rheb n=29; Pras40 n=9). Statistical test: Log rank test (VC vs Rheb; VC vs Pras40). Statistical significance defined as p-value < 0.05. Black line represents mock, grey line represents VC, red line represents Rheb and blue line represents Pras40 groups.

Tumours from mice that had to be culled because of re-appearance of the tumours were isolated to see if they had lost MHC expression - a common strategy by tumours to escape immune responses (Rabinovich, Gabrilovich, and Sotomayor 2007) - or the NP antigen against which the transferred T cells reacted. Figure 59A shows staining of *in vitro* cultured EL4-NP as well as of the *ex vivo* isolated tumour for H-2D^b, in context of which the NP peptide is presented (see also chapter 2.2.2). In addition to this staining, the isolated cells were compared to *in vitro* cultured cells in their ability to elicit a F5 specific CD8 T cell response (Figure 59B).

While *ex vivo* isolated tumours still expressed H-2D^b, they were unable to stimulate F5 TCR transduced CD8 T cells to produce IFNγ or IL2. This suggests that some of the tumours could escape the immune response because 1) they either lost expression or presentation of the NP peptide or because a small group of of NP negative cell variants which were co-injected into mice was selected out or 2) they acquired characteristics enabling them to suppress a CD8 T cell response. The former explanation is more likely, as cells that do not express the NP peptide should also not be resistant to G418 (see chapter 2.2.2 – EL4-NP cells are EL4 cells stably transfected with an expression cassette encoding the NP peptide as well as a G418 resistance gene and are therefore selected *in vitro* with the antibiotic G418). When

we exposed some of the *ex vivo* isolated tumour cells to G418, they all died within 24 hours (result not shown), suggesting that they do not express the NP peptide.

We could observe that the cells isolated from the F5+Rheb transduced CD8 T cells treated mice showed less tumour re-appearance than mice treated with F5+VC transduced cells, suggesting that the strong effector response elicited by F5+Rheb transduced CD8 T cells helps to prevent tumour escape due to antigen loss or NP-variant selection. Nonetheless, the tumours of the few F5+Rheb treated mice that died due to secondary outgrowth were also not able to elicit a NP specific T cell response after *ex vivo* isolation.

A)

Ex vivo isolation of tumour outgrowth variants
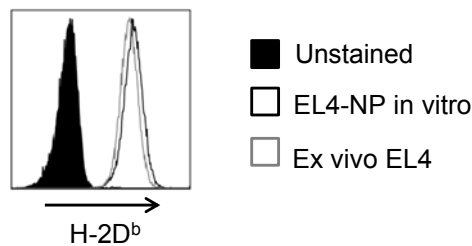
B)

F5 TCR transduced CD8 T cells + ex vivo isolated tumour
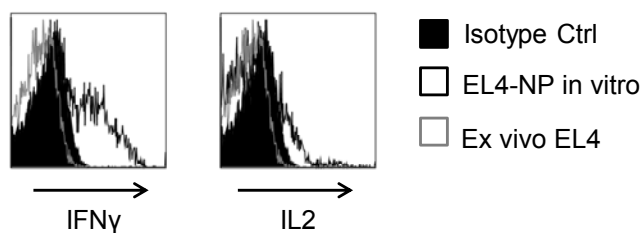
Figure 59: Characteristics of isolated tumour escape variants

A) Tumours of mice which succumbed to a secondary tumour outgrowth were isolated and analyzed for the expression of H-2D^b. One representative example is shown. Filled black histogram represents the unstained control, black line represents *in vitro* cultured EL4-NP cells and grey line represents *ex vivo* isolated tumour cells.

B) Tumours of mice which succumbed to a secondary tumour outgrowth were isolated and analyzed for their ability to elicit a cytokine response in F5 TCR transduced CD8 T cells. It was gated on tCD19+ (F5 TCR+) CD8 T cells. Filled black histogram represents staining with isotype control, black line represents T cells stimulated with *in vitro* cultured EL4-NP cells and grey line represents T cells stimulated with *ex vivo* isolated tumour cells.

Finally, we wanted to know how well T cells persist in tumour survivors. From what was shown in chapter 5.2, it was expected that persistence in survivors that received Rheb transduced T cells was lower compared to those who received VC transduced T cells. Figure 60 shows the summary data of F5+GFP+ cells relative to total CD8 T cells in peripheral blood before and after the mice received an i.p. injection of irradiated EL4-NP cells to provoke a memory re-call response. Although both Rheb and VC transduced cells efficiently mount such a re-call response, over time, Rheb transduced cells are present in lower levels than VC transduced cells.

In summary, F5+Rheb transduced CD8 T cell cells protect better from live EL4-NP tumour *in vivo* than F5+VC transduced, while Pras40 transduction impair the tumour protective functions of F5 TCR+ T cells so severely that mice treated with this type of cells all succumb to tumour. Similar to what was reported in chapter 5.2, Rheb transduced cells are present in lower numbers in peripheral blood post re-challenge with irradiated EL4-NP cells, suggesting that their ability to enter the CD8 T cell memory pool is reduced. In a next instance it was crucial to know how well mTOR modified F5 TCR+ T cells can infiltrate tumour mass.

Engraftment and re-call rsponse in tumour survivors
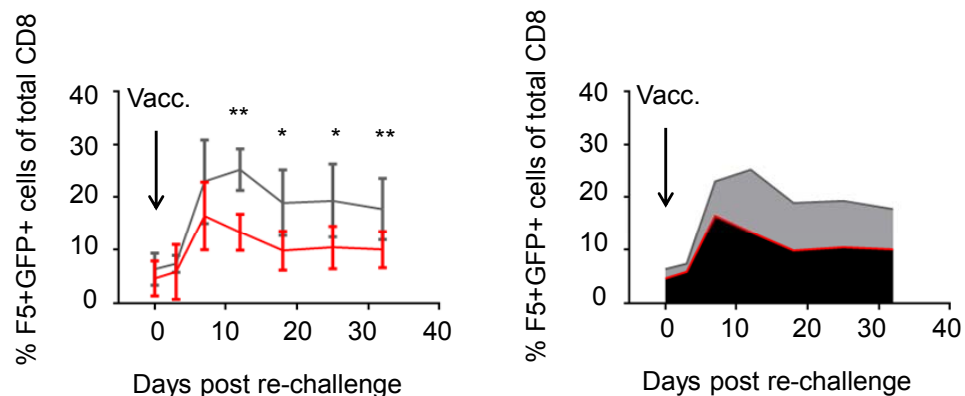
Figure 60 Persistence of T cells in tumour survivors

Summary data showing tailbleeds of tumour survivors pooled from 3 independent experiments (Rheb n=8; VC n=11). Blood was collected at least 3 months post tumour rejection, mice then received an i.p. injection of $1x10^6$ irradiated EL4-NP cells to provoke a memory re-call response (i.p. vaccination). The level of F5+GFP+ relative to total CD8 T cells in peripheral blood over time is shown. Arrow indicates time point of vaccination (re-challenge). Mean and standard deviations are indicated in left graph, right graph shows area under the curve (only indicating mean). Statistical test: Mann-Whitney U test. Statistical significance defined as p-value < 0.05. Grey line represents VC, red line represents Rheb. Vacc=vaccination.

6.2 T Cell Infiltration into Tumour

Figure 61 shows the setup of the following experiment. Like in Figure 55, mice received tumours, followed by adoptive T cell therapy 5 days later. However, this time T cells from luciferase transgenic mice were used (Zeiser et al. 2007). The cells were FACS sorted for GFP before injection in order to guarantee that only GFP+ cells enter the tumour and that the analysis is not distorted by F5+GFP- cells. Luciferase is an enzyme that oxidizes the substrate luciferin, which is injected into tumour bearing mice i.p., in an ATP dependent matter into a bluish-green light emitting product which can be detected by a bioluminescence imaging (BLI) camera. The strength of the emitted light signal correlates with the rate of T cell infiltration. In addition, mice were culled, tumours and spleens were isolated and blood was collected to determine the rate of tumour infiltration and engraftment *ex vivo*.

Figure 62 shows BLI of infiltrating T cells. It is clear from the picture on the left that the main site of T cell accumulation is the tumour which was injected into the right flank as this is where most of the signal is emitted from. One mouse of the F5+VC group died during the procedure and was therefore omitted from the analysis. The graph on the right shows infiltration expressed as emitted photons per second. No difference between the F5+Rheb and the F5+VC groups could be detected but the F5+Pras40 treated mice showed significantly less T cell infiltration.

Figure 63 shows *ex vivo* rate of tumour infiltration as well as level of engraftment in blood and spleen relative to total CD8 T cells. No difference between the F5+Rheb and the F5+VC groups could be detected in blood, spleen and tumour but the F5+Pras40 treated mice showed significantly less T cells in all 3 compartments.

As shown in Chapter 5, Rheb transduced CD8 T cells show an advantage in a competitive setting while F5+VC transduced cells can expand to a different extend depending on which type of cells are co-transferred with them (see Figure 46). So the reason why no difference in tumour infiltration was seen may simply be that in a non-competitive setting F5+VC transduced cells can just as well expand up to the internally set threshold discussed in chapter 5.3 as F5+Rheb transduced cells. This is why it was necessary to see if Rheb transduced F5 TCR+ T cells can infiltrate tumour better in a competitive setting. To these ends, an equal number of GFP sorted F5+Rheb (CD45.1+) and F5+VC (Thy1.1+) transduced CD8 T cells were mixed in a ratio close to 1:1 (see Figure 64A) and were injected into mice (Thy1.2+) bearing 5 days old tumours. Seven days post injection, mice were taken down,

tumours were collected and rate of infiltrating T cells together with the ratios of Rheb:VC transduced F5 TCR+ T cells were determined. As shown in Figure 64B, Rheb transduced T cells showed no advantage in tumour infiltration over VC transduced T cells.

Experimental layout:
Bioluminescence imaging (BLI)

Figure 61: T cell tumour infiltration experiment

Four hours before C57BL/6 mice (Thy1.2+; n=5/group) received $1x10^6$ EL4-NP (immersed in 100 µl of matrigel containing suspension) subcutaneously, they were irradiated with 5.5 Gy. They were adoptively transferred with $0.03 x10^6$ F5 TCR transduced CD8 T cells that were co-transduced with VC (group 1), Rheb (group 2) or Pras40 (group 3) which have been FACS sorted for GFP beforehand. The T cells (Thy1.1+) were taken from luciferase transgenic C57BL/6 mice and were injected on day 5 post tumour challenge. Eight days after ACT, mice received an i.p. injection of luciferin (100 µl) before the mice were anaesthesized and put under a BLI camera to measure *in vivo* T cell infiltration. On day 9 post ACT, mice were culled, their tumours and spleens were collected and infiltration was determined *ex vivo.*

A)

Pre-injection

B)

Tumour infiltration: Bioluminescence Imaging
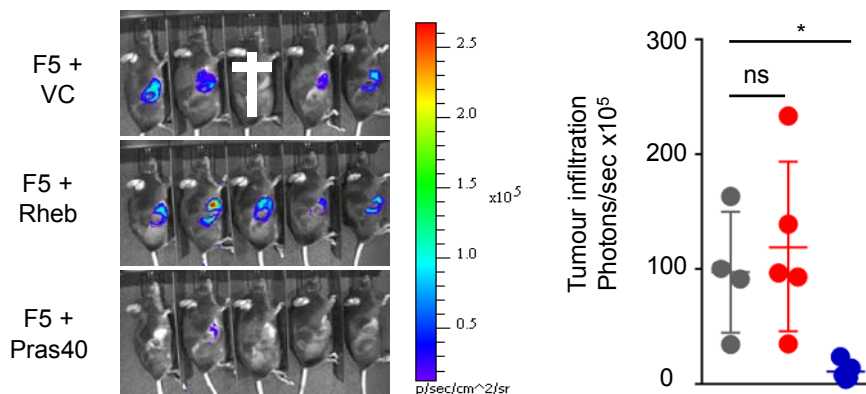
Figure 62: BLI infiltrating T cells

A) CD8 T cells from luciferase transgenic mice were co-transduced with the F5 TCR and Rheb, Pras40 or VC. The cells were sorted for GFP before a total of 0.05×10^6 F5 TCR+ T cells were injected i.v. (n=5/group). Pre- and post-sort tCD19/GFP profiles are shown. In a previous experiment, the observation was made that when bulk T cells were injected, only F5 TCR expressing cells infiltrated the tumour (result not shown) which is why only GFP+ cells were sorted. Numbers in plots represent percentage. It was gated on CD8+ T cells. Black represents mock, grey represents VC, red represents Rheb and blue represents Pras40.

B) On day 8 post tumour challenge, mice received 100 µl of luciferin i.p. and were anaesthesized before they were exposed under the bioluminescence camera for 5 minutes. One mouse of the F5+VC group died during the procedure and was omitted from the analysis. The enzyme luciferase which is expressed by the transferred T cells oxidizes the substrate luciferin into a bluish-green light emitting product which can be detected by the BLI camera. Data were analyzed using the software "Living Image 3.2". The rate of T cell infiltration correlates with the strength of the emitted light signal which is indicated as photons per second. Statistical test: Mann-Whitney U test. Statistical significance defined as p-value < 0.05. Grey filled circles represent VC, red filled circles represent Rheb and blue filled circles represent Pras40 groups. ns=not significant.
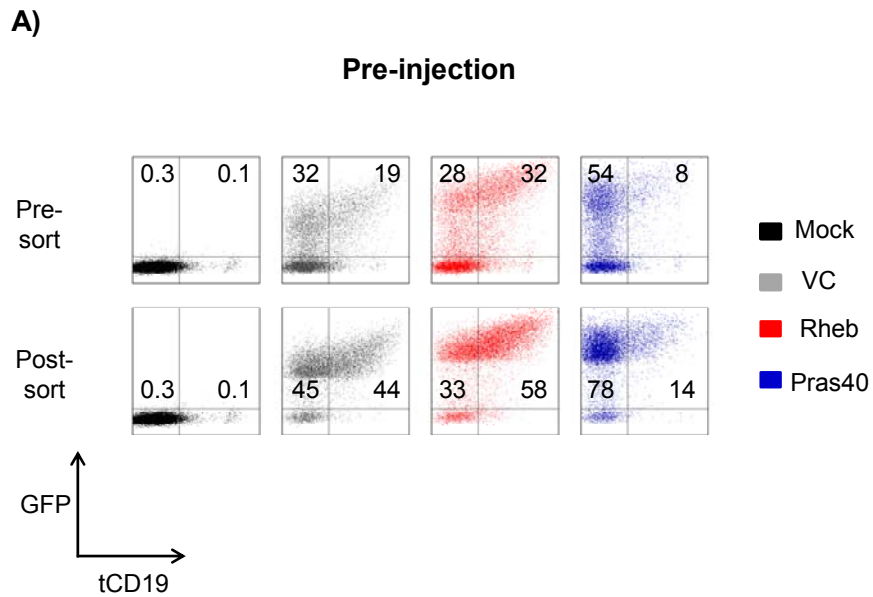
Engraftment lymphoid organs and TILs
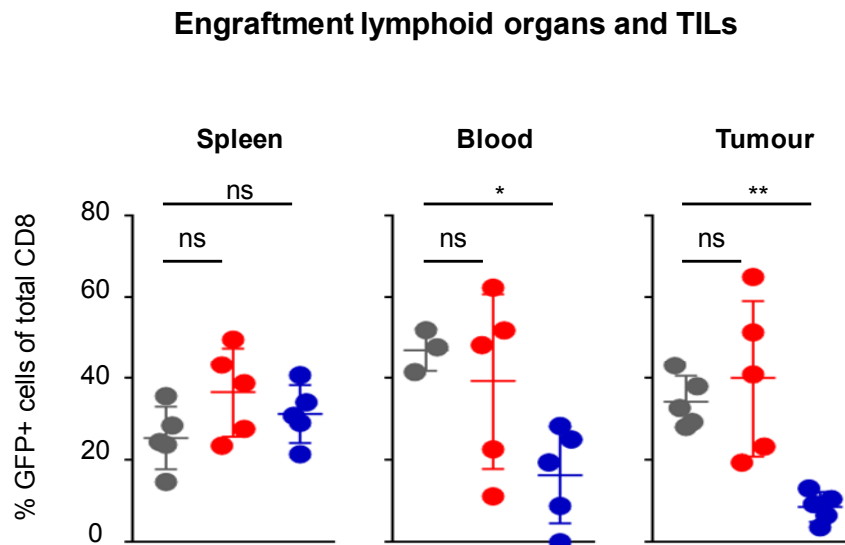
Figure 63: Ex vivo tumour infiltrating lymphocytes (TILs)

On day 9 post tumour challenge, mice were culled and blood, spleens and tumours were collected. Tumours were treated with a mix of enzymes to release the tumour infiltrating lymphocytes (TILs) making them available for FACS analysis (see chapter 2.5.7). Engraftment of cells relative to total CD8 T cells in the individual compartments is indicated. Statistical test: Mann-Whitney U test. Statistical significance defined as p-value < 0.05. Grey filled circles represent VC, red filled circles represent Rheb and blue filled circles represent Pras40 groups. ns=not significant.

A)

**Competitive engraftment in tumour:
Post-sort and pre-injection**

B)

TILs 7 days post injection
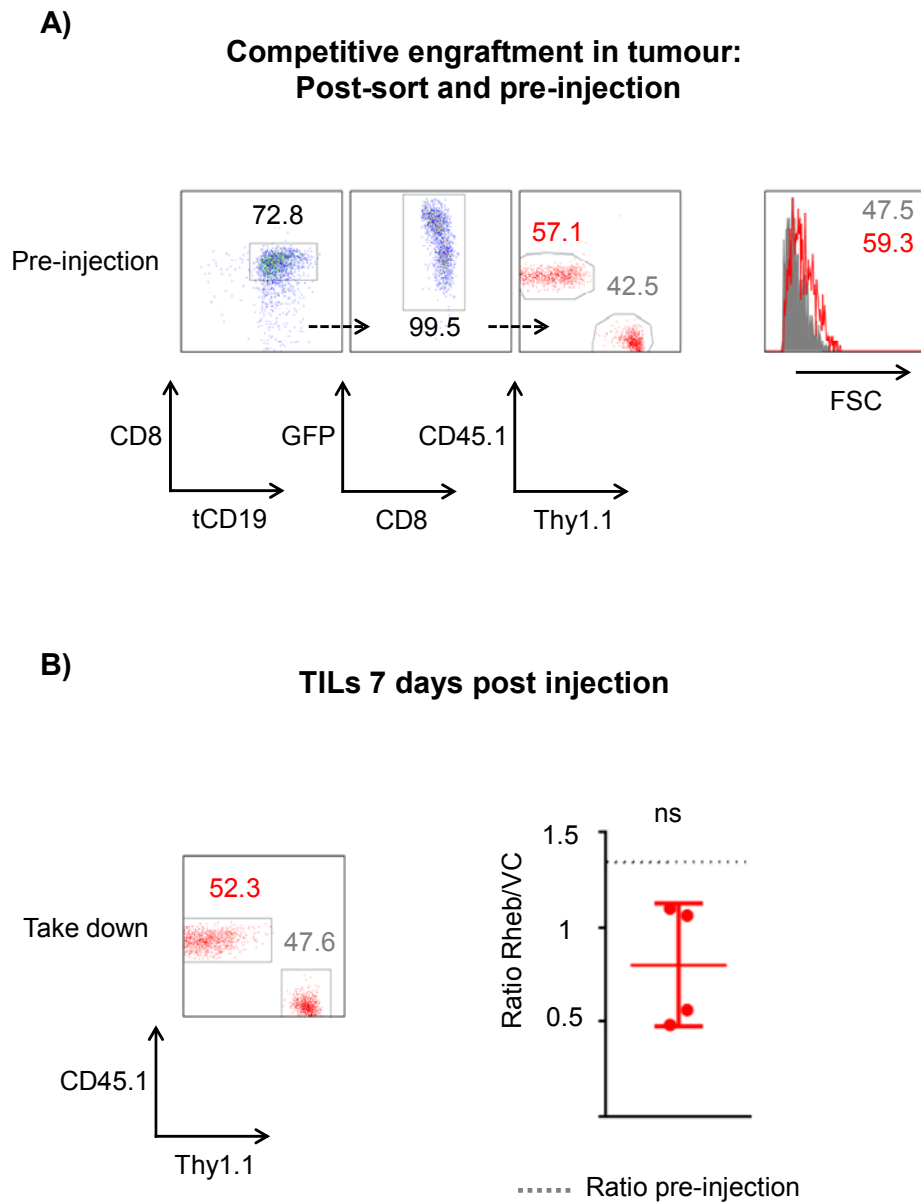
Figure 64: Competitive T cell infiltration

A) F5+Rheb (CD45.1+) and F5+VC (Thy1.1+) co-transduced CD8 T cells were FACS sorted for GFP, mixed together in a ratio 1:1 and 0.03×10^6 total F5 TCR+ T cells were injected into mice (Thy1.2+) bearing 5 days old tumours (n=6). Arrows in plots represent gating. Numbers inside of dot plots represent percentage, numbers inside of histogram plot represents median of FSC $x10^3$. Grey represents VC and red represents Rheb.

B) On day 7 post ACT, mice were culled and tumours were collected. One representative dot plot showing ratio of Rheb and VC is displayed. It was gated on tCD19+GFP+ cells. Data are summarized on the right. Statistical test: Wilcoxon signed rank test. Statistical significance defined as p-value < 0.05. Grey dotted line represents ratio pre-injection and red filled circles represent ratio Rheb:VC. Grey dotted line represents ratio pre-injection. ns=not significant.

Stimulation of T cells *in vivo* through i.p. vaccination is different than treating mice already bearing tumour with anti-tumour T cells and hence the outcome can be different as well. T cells need to infiltrate tumour at first before they can expand and exert their effector functions. This can take up to 2 days (Breart et al. 2008), so the ideal time point of take down may be somewhere between 7 and 10 days post ACT. In addition, antigen is presented at a different site, in larger quantities and for a longer time. All of this can impact on the outcome of the experiment.

6.3 Summary and Conclusion

In summary, tumour bearing mice treated with Rheb transduced F5 TCR+ T cells show a better survival rate than mice treated with VC transduced cells. Pras40 transduction impairs the anti-tumour functions of F5 TCR+ T cells so severely that all the mice treated with this type of cells succumb to tumour. The protective function of Rheb transduced T cells seems to be 2-fold:

1) Rheb transduced cells provide better protection from death due to an initial tumour outgrowth.

2) Rheb transduced cells prevent tumour escape due to NP loss or selection of NP- variants.

It was not possible to show increased tumour infiltration by Rheb transduced F5 TCR+ T cells compared to VC transduced cells, neither through *in vivo* BLI nor *ex vivo* analysis. However, it was possible to show that Pras40 transduced cells were unable to accumulate at the tumour site in sufficient numbers.

Hence, the question remains: how do Rheb transduced F5 TCR+ CD8 T cells confer better tumour protection than VC transduced cells? Several answers are possible:

1) As shown in Chapter 4, Rheb transduction results in a number of improved effector functions *in vitro*, each of which can contribute to the superior ability of these cells to protect from tumour *in vivo.* For example, EL4 cells have been shown to express TGFβ which enables them to suppress T cell responses directed towards against them. T cells insensitive to TGFβ were able to overcome these negative effects (Gorelik and Flavell 2001). As shown in chapter 4.5, Rheb transduction confers partial resistance to TGFβ which may be a possible mechanism why these cells protect better from tumour. But also the facts that Rheb transduced cells produce more IFNγ and are more functional at low arginine conditions can contribute to the observed effects. EL4 tumours were shown to attract arginase expressing tumour associated macrophages (TAMs) which can deplete arginine within the tumour microenvironment (Kusmartsev and Gabrilovich 2005) and IFNγ is known to be a crucial cytokine for tumour protection (Shankaran et al. 2001).

2) Rheb over-expression confers a protective advantage but this effect is very discrete and VC transduced cells also show a remarkable ability to protect from tumour. Many experiments had to be carried out to see positive effects

by Rheb transduction. The differences in tumour infiltration may therefore be equally discrete and may not be picked up by one experiment.

3) As shown in Chapter 5, Rheb revealed its *in vivo* superior effector function primarily in a competitive setting and within a small time frame. The better ability to expand within the first 7 days post ACT may reflect an increased sensitivity to cytokines and other stimuli, rendering these cells better effectors. In the end, this may enable them to efficiently clear tumour. If so, this difference is not picked up by merely comparing infiltration into tumour side by side, as in a non-competitive setting VC transduced cells occupy the CD8 T cell niche to a similar extent as Rheb transduced cells. However, the fact that in a competitive setting Rheb transduced cells did not infiltrate the tumour better than VC transduced cells was surprising. Nonetheless, as already mentioned, the time window within which Rheb exerts its increased effector functions is fairly narrow and it may well be that the right time point to pick up differences was missed out.

The negative effects on tumour protection by mTOR inhibition through Pras40 transduction are easier to explain:

1) Pras40 transduced F5 TCR+ T cells fail to efficiently accumulate at the tumour site.

2) Pras40 transduced F5 TCR+ T cells fail to mount an effector response *in vivo* upon antigen encounter.

3) Pras40 transduced F5 TCR+ T show decreased *in vitro* effector functions.

The combination of these factors is probably sufficient to explain the detrimental effects on tumour protection by Pras40 transduction. It remains to determine under which conditions mTOR inhibition may be beneficial. Amongst other things, this will be a topic in the "Discussion" (Chapter 7).

Chapter 7　General Discussion

Adoptive T cell therapy for tumour patients represents a promising therapeutic option. However, there are still obstacles to overcome. The immunosuppressive tumour microenvironment can impair T cell functions and the question if effector or memory T cells confer better protection has not been conclusively answered yet. In this PhD project, it was attempted to develop a strategy to render T cells resistant to amino acid depleted conditions. However, previously reported data on the role of GCN2 in mediating T cell inhibition could not be replicated. Instead, a strategy, based on the tuning of the mTOR pathway, was developed with the goal to manufacture potent effector and memory T cells. While enhancing mTOR signaling resulted in an increase in CD8 T cell effector functions, both *in vitro* as well as *in vivo*, inhibition of mTOR proved detrimental to the function of T cells but maintained a phenotype reminiscent of central memory T cells. In this final chapter, some open questions shall be addressed.

7.1　Permanent versus Transient MTOR Inhibition

Treatment of mice with rapamycin during a T cell response can enhance the formation of memory cells. However, this is very much dependent on the dose used as well as the duration of treatment. Whereas high rapamycin doses over a long time course impair T cell responses as this is expected from a routinely used immunosuppressant, a short high dose during the expansion phase of an effector response (Q. Li et al. 2012) as well as a low dose over a longer period (Araki et al. 2009) can yield high and powerful memory T cells.

Rapamycin treatment was not only shown to favor memory differentiation in CD8 T cells but also to drive CD4 T cells to become Foxp3 expressing Tregs (Haxhinasto, Mathis, and Benoist 2008, 3; Sauer et al. 2008). Treg recruitment (Curiel et al. 2004; Dürr et al. 2010, 12) and conversion of conventional CD4 into Treg cells in tumours (Ai et al. 2009) represent a serious obstacle to tumour immunology as this has been discussed in chapter 1.2.3. Systemic administration of rapamycin therefore not only provides the chance to favor memory formation but also poses the risk of increasing the Treg burden in tumours which could eventually make T cell therapy difficult. Henceforth, to avoid systemic administration of rapamycin and the accompanying risks of Treg formation, we developed a strategy which allows to intrinsically commit

T cells to the memory lineage, based on the transduction of the negative mTOR regulator Pras40. However, the fact that this causes a permanent block in mTOR signaling is probably the reason for the observed lack of anti-tumour functions by Pras40 transduced cells. It is likely that this mimics the observations with long term and high dose rapamycin treatment.

Taken together, it seems as if Pras40 transduction induces a stop in the differentiation of CD8 T cells. The cells acquire a phenotype reminiscent of central memory T cells. They are not stem memory T cells because even though they show high stem cell antigen 1 (Sca1) expression they also express CD44 (results not shown). Murine stem memory T cells, on the contrary, were shown to be $Sca1_{hi}$ and $CD44_{lo}$ (Luca Gattinoni et al. 2009). The cells expressing Pras40 have therefore undergone the transition from naïve to stem cell memory to central memory T cells but are then stopped from further differentiating into effector memory and effector T cells. In other words, Pras40 stores the "potential energy" of T cells without being able to transform it into "kinetic energy".

**Effects of Pras40 on T cell
differentiation**

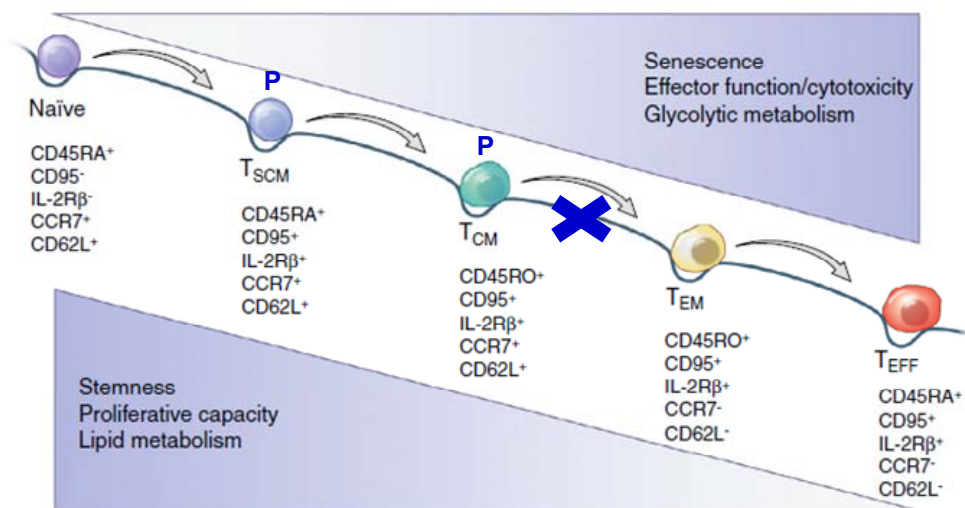**Figure 65: Effects of Pras40 on T cell differentiation**

Pras40 overexpression (indicated by a blue "P" over T_{SCM} and T_{CM} cells) prevents CD8 T cells from undergoing differentiation into effector memory and effector T cells (indicated by a blue cross). The cells acquire a phenotype reminiscent of central memory T cells. Permission to reproduce this picture has been granted by Restifo and Gattinoni (2013).

162

If this is the case, releasing the inhibition on mTOR after the initial expansion phase during a T cell response should result in a high yield of potent memory T cells which can mount a powerful re-call response. To achieve that, Pras40 expression requires regulation.

One way of controlling the expression of a transgene is by using a tetracycline inducible expression cassette. Heinz et al. (2011) have developed a pSERS retrovirus harboring a tetracycline sensitive transactivator protein (rtTA-M2) which is expressed under the hPGK promoter. When tetracycline is present, this transactivator can bind to a second promoter (TetO) within the vector, initiating the expression of the transgene of interest, in this case GFP (Tet-ON system). This vector has been slightly modified by Dr Pedro Velica from the UCL Research Department of Haematology such that a truncated marker derived from human CD34 (Q8) was linked through a FMD-2A sequence to the transactivator. Upstream of GFP, connected through P-2A, the mTOR modifying constructs (Pras40, Rheb and RQ64L) were inserted. Transduced cells can be recognized by Q8 expression and upon addition of tetracycline, induced cells express GFP. It could be shown *in vitro* that induction of Pras40 results in an inhibition of the mTOR signal, as this was observed for the MP71 vector (Figure 66).

Oral administration of tetracycline supplemented drinking water (2 mg/ml) also results in the induction of transgene expression in adoptively transferred T cells transduced with the inducible Pras40 vector *in vivo* (results not shown). In close collaboration with Dr Pedro Velica, we set up an experiment in which mice were subcutaneously challenged with EL4-NP tumour, as described in Chapter 6. Five days later, mice received CD8 T cells co-transduced with the F5 TCR and the inducible Pras40 vector. One group received tetracycline through drinking water (Pras40 induced) for the first 30 days after T cell injection, the other group received normal drinking water throughout the course of the experiment. Both groups rejected tumour in the same manner. After 30 days, tetracycline was withdrawn, thereby releasing the inhibition on mTOR. Mice were re-challenged with irradiated EL4-NP tumour cells on day 45 post T cell injection, as described in Chapter 5. Mice who had previously received tetracycline and whose mTOR pathway therefore had been inhibited during the T cell expansion phase mounted a statistically significantly greater re-call response than mice that didn't receive anything (results not shown). This suggests that transient intrinsic mTOR inhibition results in a higher yield of potent memory CD8 T cells. It was surprising to see that T cells with induced Pras40

were able to reject tumour because, as shown in Chapter 6, inhibition of mTOR during the effector phase by Pras40 is detrimental to the function of tumour specific T cells. However, tetracycline induction *in vivo* is less potent than *in vitro*. Consequently, the expression of Pras40 is not as high as in T cells transduced with the conventional MP71 vector, mTOR inhibition is therefore attenuated and the function of T cells is maintained. Nonetheless, low level mTOR inhibition over a longer time period had a significant impact on the re-call functions of the T cells which is in accordance with the results on long term and low dose rapamycin treatment reported by Araki et al. (2009).

Inducible Pras40 in BW cells
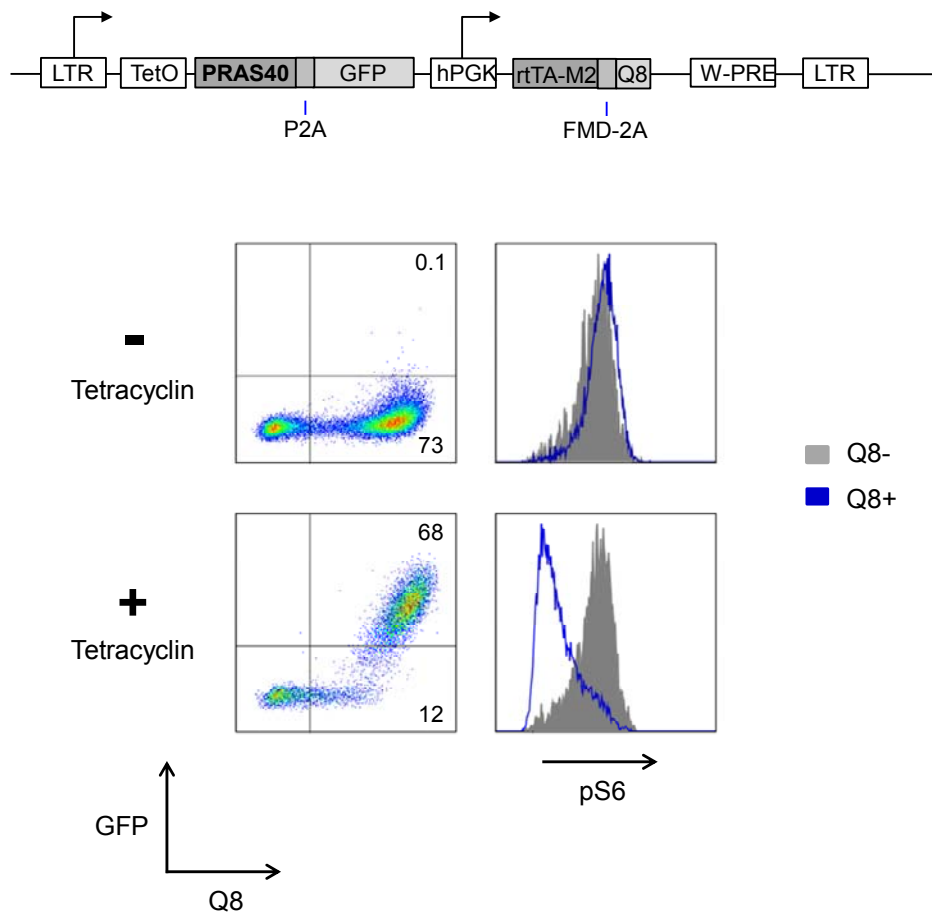
Figure 66: Inducible Pras40 in BW cells

The vector with its different components is schematically represented on the top (description in text). The FACS plots show transduction of BW cells with the inducible Pras40 vector. It was gated on FSC/SSC live cells. Q8 serves as a marker of transduction, GFP is a marker for induction. Cells were cultured overnight in medium with or without tetracycline (0.5 µg/ml). Cells were then harvested, fixed and stained for pS6. Grey represents untransduced (Q8-), blue represents transduced cells (Q8+). Numbers in dot plots represent percentage.

Further tests need to be carried out to confirm these results. While we know that permanent mTOR inhibition by Pras40 transduction results in a phenotype reminiscent of central memory T cells, it is still unclear how induced Pras40 expression affects markers such as CD62L and CD127. It would also be of interest to see if these cells persist better upon secondary transfer into antigen free mice as one key characteristic of memory T cells is their ability to persist without the need for continuous TCR stimulation (Murali-Krishna et al. 1999) which would only be guaranteed in an antigen un-experienced host.

7.2 Permanent versus Transient MTOR Enhancement

Constitutive activation of the mTOR pathway by knocking out one of its key negative regulator, TSC1, has detrimental effects on CD4 and CD8 T cell function, as described in detail in chapter 1.6.2 (O'Brien et al. 2011, 1; Yang et al. 2011). We therefore sought to design a strategy that would allow us to enhance mTOR signaling whilst reducing its detrimental effects. The *in vivo* competition experiment discussed in chapter 5.3 confirmed our suspicion that RQ64L transduction which mimics the situation in TSC1-/- T cells deteriorates T cell function as cells that overexpress RQ64L did not persist well and were hardly able to mount a re-call memory response. Furthermore, preliminary tumour protection experiments using CD8 T cells co-transduced with the F5 TCR and RQ64L showed a trend towards reduced protection by T cells with a constitutively activated mTOR pathway, reminiscent of the reports by Yang et al. (2011) (see chapter 1.6.2).

Rheb transduction, on the other hand, creates an entirely different situation. Un-mutated Rheb remains subject to regulation by the TSC. But because the original ratio of Rheb:TSC is increased, inhibition of Rheb is impaired, mTOR signaling therefore enhanced and prolonged. In this situation, cells do not constitutively activate the mTOR pathway but are still dependent on activation signals. More specifically this means that even though upon T cell activation Rheb transduced cells show increased and prolonged mTOR signaling, once the activation signals have faded, some of the cells can re-tune their mTOR pathway back to normal and henceforth enter the long term memory pool. Nonetheless, because Rheb expression probably drives the end stage effector differentiation of cells – which represents a dead end road if the "Developmental Model" of T cell differentiation is correct (see chapter 1.4.1) – this pool is overall smaller compared to control cells. While Pras40 transduction halts differentiation of T cells at the memory stage, Rheb transduction boosts this differentiation but in a controlled manner and to a lesser extent than RQ64L. In other words, Rheb releases "kinetic energy" and is less able to store "potential energy."

**Effects of Rheb on T cell
differentiation**
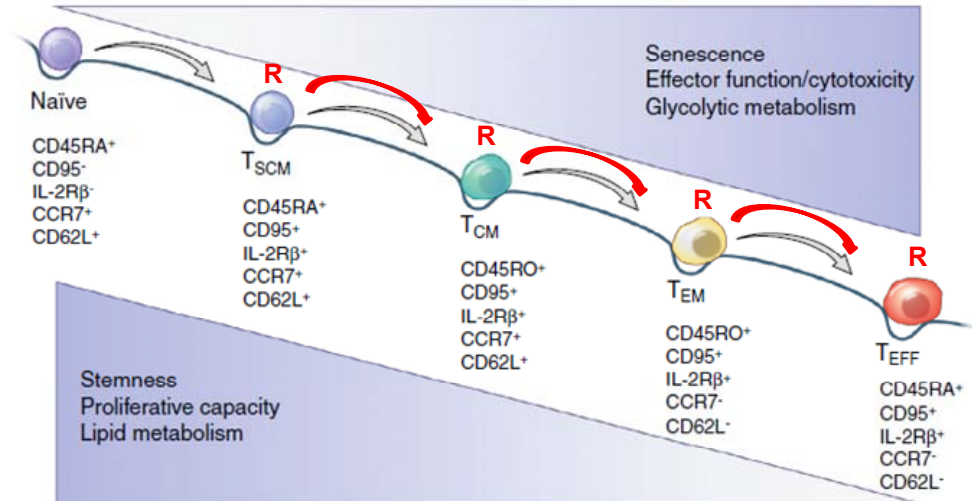
Figure 67: Effects of Rheb on T cell differentiation

Rheb overexpression (indicated by a red "R" over the T_{SCM}, T_{CM}, T_{EM} and T_{EFF} cells) boosts CD8 T cell differentiation into effector memory and effector T cells (indicated by red arrows).

It remains to be examined if Rheb transduction in fact results in the production of end stage effector cells. High KLRG1 and low CD127 expression are two key signs of these cells (Kaech et al. 2003, 127; Sarkar et al. 2008). Next to the enhanced CD62L downregulation reported in chapter 5.2, staining for these markers at the peak of the T cell response would probably help answering this question. In addition, we have designed inducible Rheb vectors but not tested them *in vivo* yet. It remains to be explored if transient Rheb expression during the beginning of a T cell response results in superior expansion and if a stop of expression reduces the level of contraction. However, if Rheb increases end stage effector commitment, this seems unlikely because once T cells have achieved this last stage of differentiation they will simply die off, regardless of their mTOR activation level.

Rheb overexpression (Lu et al. 2010) and increased mTOR signaling in general (Gerlinger et al. 2012) has been associated with carcinogenesis. Rheb can therefore be considered an oncogene and its transduction harbors the potential of malignantly transforming T cells. In addition, insertional mutagenesis poses a general risk

associated with retrovirus mediated gene modifications. The strong promoters of the introduced vector genome can, if inserted in close vicinity to oncogenes, turn on or increase the expression of these molecules and initiate oncogenesis. Indeed, some of the severe combined deficiency patients (SCID) patients who have been treated with an autologous stem cell transplantation post gene re-construction (IL2 receptor γ chain) developed acute T cell leukemia due to insertion near the oncogene LIM domain only 2 (LMO2) (Hacein-Bey-Abina et al. 2003; Nienhuis, Dunbar, and Sorrentino 2006). However, stem cells are pluripotent and have a higher potential to become malignant than differentiated T cells. Despite that, it has been recently reported that retroviral T cell transduction can in fact cause clonal transformation of T cells through vector integration close to the IL2 and IL15 receptor genes (Newrzela et al. 2011). Even though this is a very rare event, it is conceivable that the risk of malignancy is further increased through Rheb transduction. Therefore, an inducible expression system, as introduced previously, provides an additional level of safety to this type of approach.

In the end, the best strategy for adoptive T cell tumour therapy, in terms of the effector and memory T cell responses and in the light of the "Developmental Model" of T cell differentiation, probably consists in the transfer of 2 subsets of tumour specific T cells. One subset with an inducible high mTOR activity could mount the crucial initial effector response while a second subset with inducible mTOR inhibition could increase the yield of potent memory T cells. This requires further testing, ideally in a tumour model in which effector responses are suppressed and where long term persistence of T cells is impaired.

7.3 Effects of MTOR Tuning on Metabolism

The role of mTOR as a metabolic switch has been extensively discussed in chapter 1.6.1. T cell activation is accompanied by increased glycolysis which, on the one hand, serves to prepare the cells for the massive clonal expansion during a T cell response and, on the other hand, is an integral component of T cell function, as it can affect the expression of effector molecules such as IFNγ (Chang et al. 2013), perforin and granzyme molecules (D. K. Finlay et al. 2012). It is therefore important to know how Rheb and Pras40 transduction impacts on overall T cell metabolism.

The following parameters can be used to measure a cell's metabolism:
1) The oxidative consumption rate (OCR) is an indicator of OXPHOS.
2) The extracellular acidification rate (EAR) and the proton production rate (PPR) are indicators of glycolysis.
3) Low ratios of OCR/EAR are found during glycolysis, high ratios during OXPHOS.

The change of metabolism from OXPHOS to glycolysis in the presence of oxygen is called aerobic glycolysis or "Warburg effect". Otto Warburg made the observation that tumour cells predominantly use the glycolytic pathway, even in the presence of enough oxygen (WARBURG 1956). In this respect, activated T cells behave similarly to tumour cells. The reason for that is still under debate but it is thought that glucose is a good carbon source for the synthesis of nucleic acids and other components required for cell expansion (D. Finlay and Cantrell 2011; Wang and Green 2012). Because of the increased use of the glycolytic pathway, pyruvate levels rise which can be further converted by the lactate dehydrogenase (LDH) into lactate when oxygen is lacking. This is accompanied by a decrease in the pH of the cell medium, hence EACR and PPR rise.

Just because activated and effector T cells predominantly use the glycolytic pathway does not mean they don't consume oxygen at all. In absolute quantities they even consume more oxygen than naïve T cells and are still dependent on mitochondrial ATP production, as shown by Chang et al. (2013). At the same time, however, they also show higher EACR rates and lower OCR/EACR ratios meaning they use the glycolytic pathway more than they use OXPHOS. Therefore, the more activated a cell is, the higher their absolute OCR and EACR and the lower their OCR/EACR ratio (Sukumar et al. 2013).

Using the "seahorse machine" which allows deriving all of these parameters from *in vitro* cultured cells, Dr Pedro Velica and Dr Sian Henson from the Research Department of Immunology (UCL) were able to demonstrate that basal levels of OCR, EACR and PPR are increased for Rheb and decreased for Pras40 transduced CD8 T cells compared to VC transduced cells. When the cells get stimulated through CD3, all 3 groups decrease OCR and increase EACR but the Rheb transduced cells do this to an increased and Pras40 transduced cells to a lower extent. The OCR/EACR ratios are not different under resting conditions between the 3 groups, but once the cells get activated with CD3 antibodies, Rheb transduced cells decrease and Pras40 transduced cells increase their OCR/EACR ratios compared to VC transduced cells (results not shown).

In summary, Rheb transduced CD8 T cells show higher metabolic activity during resting and activated conditions while Pras40 transduced cell show the exact opposite. It remains to be determined which glycolytic enzymes specifically contribute to these changes and how the mTOR modifying constructs affect the expression of these molecules.

7.4 Effects of MTOR Tuning on Cytotoxicity and Apoptosis

The metabolic aspects of CD8 T cells are tightly linked to their cytotoxic functions along the mTOR-HIF axis as discussed in detail in chapter 1.6.3. HIF not only controls the transcription of glycolytic enzymes, it was also shown to induce the expression of perforin and granzyme molecules (D. K. Finlay et al. 2012). In addition, it was shown that inhibition of the glycolytic pathway results in a decrease of perforin 1 and granzyme B expression (Sukumar et al. 2013).

Given that Rheb transduction results in an increase and Pras40 transduction in a decrease of effector functions and metabolic activity, it would be interesting to assess their cytotoxic profile. We have not done cytotoxicity assays yet but we did look at the expression of granzyme B pre- and post T cell activation through intracellular FACS staining. Rheb transduced cells so far did not show any differences in expression whilst Pras40 transduced cells showed clear reductions post activation compared to VC transduced cells (results not shown). Further functional tests need to be carried out to gain more insight in the killer potentials of mTOR modified T cells (e.g. a chromium release cytotoxicity assay).

Finally, mTOR hyperactivation is associated with a decrease in CD4 and CD8 T cell survival due to increased production of ROS and reduced expression of the anti-apoptotic factor bcl2 as overexpression of bcl2 is able to prolong T cell survival. This is probably also the reason why Rheb transduced T cells contract more and persist worse than control cells, as shown in chapters 5.2 and 6.1. We have not carried out the respective tests yet to confirm that. Annexin 5 is an anticoagulant which binds with high affinity to phosphatidlyserine that appears in the cell membrane only in apoptotic cells. The combination of propidium iodide (PI), a fluorescent dye which dissociates through disintegrated cell membranes into necrotic cells and stains nucleic acid, and fluorochrome conjugated annexin 5 staining is a possibility to assess the tendency of Rheb and Pras40 transduced to undergo cell death. In addition, it would be interesting to look at the expression of bcl2.

Another explanation for the lack of persistence of Rheb transduced cells is that they show less homeostatic proliferation during the memory phase. However, this is unlikely as Yang et al. (2011) observed even higher homeostatic turnover rates upon conditional TSC1 deletion in peripheral T cells which enhances their mTOR signaling. We have done bromdesoxyuridin (Brdu) staining on cells isolated from tumour survivor mice which have been treated with Rheb or Pras40 transduced cells

171

and received Brdu supplemented drinking water for 7 days during the T cell memory phase. Brdu integrates into the genome as cells undergo division and its expression correlates with the rate of cellular proliferation. We couldn't observe any differences in Brdu expression between Rheb and VC transduced cells but Pras40 transduced cells showed a trend to integrate less Brdu, suggesting that functional mTOR signaling is required for the homeostatic proliferation of cells (results not shown).

So far, we have not got an explanation yet for the observed lack of persistence of Rheb transduced cells but it seems likely that these cells are more prone to apoptosis.

7.5 Translational Aspects

The primary goal of this PhD project was to establish a strategy to improve current adoptive T cell therapy approaches. Therefore, this thesis closes with some final remarks about translational aspects of the here presented results. Several observations are clinically relevant and the developed strategy of mTOR tuning is theoretically applicable in the clinic.

Firstly, it could be shown that mTOR acts as a rheostat to control T cell lineage commitment at the intersection of effector and memory differentiation. Even though some memory characteristics can be preserved when mTOR is inhibited, it is crucial to know that permanent mTOR inhibition deteriorates T cell function, in particular with regards to efforts to promote memory at the expense of effector functions (e.g. through rapamycin treatment). One lesson learnt from the here presented data is that mTOR inhibition may only be beneficial if this can be achieved transiently. Preserving and sustaining mTOR signaling, on the other hand, can be useful, even if this is achieved at the expense of memory formation. The advantage of a hyperactive mTOR pathway *in vivo* has not been reported before.

Secondly, even though T cell memory formation may be facilitated when mTOR is inhibited, memory T cells require a functional mTOR pathway to carry out their function. Hence, mTOR is not expendable once memory formation has been completed but it is a crucial and integral component of T cell function, regardless of the differentiation state. The second lesson learnt therefore is that when an effector function is needed, be it in the context of a primary or secondary T cell response, inhibition of mTOR should be avoided.

Thirdly, the here presented strategy of mTOR tuning through Rheb and Pras40 transduction, is ideally implemented in the clinic via inducible or transient expression systems due to the detrimental effects of permanent mTOR inhibition on tumour protection and the oncogenic potential of Rheb. Using a tetracycline inducible system, as discussed above, represents one possibility of achieving that goal. The path for the clinical use of tetracycline inducible vectors has already been paved (VanderVeen et al. 2013). However, tetracycline depot formation *in vivo* (Anders et al. 2012) as well as the ubiquity of antibiotics in modern day food may impair the possibility of tightly regulating gene expression. Therefore, another possibility represents the transient transfection of Rheb and Pras40 into T cells, e.g. through RNA electroporation. In this system, high Rheb expression would boost the initial

cell activation while Pras40 expression would attenuate activation in the initial phases of antigen encounter, just as this was observed for retrovirus transduced cells. However, because RNA is not integrated into the genome, with every cell division, Rheb and Pras40 expression will be diluted out on a per cell basis. This allows the T cells to slowly retune their mTOR pathway back to normal, not without having guided the differentiation of the cells towards potent effector (Rheb) and memory (Pras40) cells.

In conclusion, mTOR represents a fascinating pathway for the manipulation of T cell responses. This thesis has explored the possibility of mTOR tuning, revealed advantages and disadvantages of this approach and created a platform for potential future applications.

Bibliography

Abad, John D, Claudia Wrzensinski, Willem Overwijk, Moniek A De Witte, Annelies Jorritsma, Cary Hsu, Luca Gattinoni, et al. 2008. 'T-Cell Receptor Gene Therapy of Established Tumors in a Murine Melanoma Model'. *Journal of Immunotherapy (Hagerstown, Md.: 1997)* 31 (1) (January): 1–6.

Ahmadi, Maryam, Judith W King, Shao-An Xue, Cécile Voisine, Angelika Holler, Graham P Wright, Jonathan Waxman, Emma Morris, and Hans J Stauss. 2011. 'CD3 Limits the Efficacy of TCR Gene Therapy in Vivo'. *Blood* 118 (13) (September 29): 3528–3537.

Ai, Weiyun Z, Jing-Zhou Hou, Robert Zeiser, Debra Czerwinski, Robert S Negrin, and Ronald Levy. 2009. 'Follicular Lymphoma B Cells Induce the Conversion of Conventional CD4+ T Cells to T-Regulatory Cells'. *International Journal of Cancer. Journal International Du Cancer* 124 (1) (January 1): 239–244.

Anders, Kathleen, Christian Buschow, Jehad Charo, and Thomas Blankenstein. 2012. 'Depot Formation of Doxycycline Impairs Tet-Regulated Gene Expression in Vivo'. *Transgenic Research* 21 (5) (October): 1099–1107.

Araki, Koichi, Alexandra P Turner, Virginia Oliva Shaffer, Shivaprakash Gangappa, Susanne A Keller, Martin F Bachmann, Christian P Larsen, and Rafi Ahmed. 2009. 'mTOR Regulates Memory CD8 T-Cell Differentiation'. *Nature* 460 (7251) (July 2): 108–112.

Aruga, A, E Aruga, K Tanigawa, D K Bishop, V K Sondak, and A E Chang. 1997. 'Type 1 versus Type 2 Cytokine Release by Vbeta T Cell Subpopulations Determines in Vivo Antitumor Reactivity: IL-10 Mediates a Suppressive Role'. *Journal of Immunology (Baltimore, Md.: 1950)* 159 (2): 664–673.

Atkins, M B, M T Lotze, J P Dutcher, R I Fisher, G Weiss, K Margolin, J Abrams, et al. 1999. 'High-Dose Recombinant Interleukin 2 Therapy for Patients with Metastatic Melanoma: Analysis of 270 Patients Treated between 1985 and 1993'. *Journal of Clinical Oncology: Official Journal of the American Society of Clinical Oncology* 17 (7): 2105–2116.

Bibliography

Bachmann, Martin F, Petra Wolint, Katrin Schwarz, Petra Jäger, and Annette Oxenius. 2005. 'Functional Properties and Lineage Relationship of CD8+ T Cell Subsets Identified by Expression of IL-7 Receptor Alpha and CD62L'. *Journal of Immunology (Baltimore, Md.: 1950)* 175 (7): 4686–4696.

Bai, Ailin, Hui Hu, Mandy Yeung, and Jianzhu Chen. 2007. 'Kruppel-like Factor 2 Controls T Cell Trafficking by Activating L-Selectin (CD62L) and Sphingosine-1-Phosphate Receptor 1 Transcription'. *Journal of Immunology (Baltimore, Md.: 1950)* 178 (12): 7632–7639.

Bobisse, Sara, Maria Rondina, Anna Merlo, Veronica Tisato, Susanna Mandruzzato, Mario Amendola, Luigi Naldini, et al. 2009. 'Reprogramming T Lymphocytes for Melanoma Adoptive Immunotherapy by T-Cell Receptor Gene Transfer with Lentiviral Vectors'. *Cancer Research* 69 (24) (December 15): 9385–9394.

Boshoff, Chris, and Robin Weiss. 2002. 'AIDS-Related Malignancies'. *Nature Reviews. Cancer* 2 (5) (May): 373–382.

Boyman, Onur, and Jonathan Sprent. 2012. 'The Role of Interleukin-2 during Homeostasis and Activation of the Immune System'. *Nature Reviews. Immunology* 12 (3): 180–190.

Brahmer, Julie R, Scott S Tykodi, Laura Q M Chow, Wen-Jen Hwu, Suzanne L Topalian, Patrick Hwu, Charles G Drake, et al. 2012. 'Safety and Activity of Anti-PD-L1 Antibody in Patients with Advanced Cancer'. *The New England Journal of Medicine* 366 (26) (June 28): 2455–2465.

Breart, Béatrice, Fabrice Lemaître, Susanna Celli, and Philippe Bousso. 2008. 'Two-Photon Imaging of Intratumoral CD8+ T Cell Cytotoxic Activity during Adoptive T Cell Therapy in Mice'. *The Journal of Clinical Investigation* 118 (4) (April): 1390–1397.

Brentjens, Renier J, Marco L Davila, Isabelle Riviere, Jae Park, Xiuyan Wang, Lindsay G Cowell, Shirley Bartido, et al. 2013. 'CD19-Targeted T Cells Rapidly Induce Molecular Remissions in Adults with Chemotherapy-Refractory Acute Lymphoblastic Leukemia'. *Science Translational Medicine* 5 (177) (March 20): 177ra38.

Bronte, Vincenzo, and Paola Zanovello. 2005. 'Regulation of Immune Responses by L-Arginine Metabolism'. *Nat Rev Immunol* 5 (8): 641–654.

Bibliography

Brown, E J, M W Albers, T B Shin, K Ichikawa, C T Keith, W S Lane, and S L Schreiber. 1994. 'A Mammalian Protein Targeted by G1-Arresting Rapamycin-Receptor Complex'. *Nature* 369 (6483) (June 30): 756–758.

Brugarolas, James B, Francisca Vazquez, Archana Reddy, William R Sellers, and William G Kaelin Jr. 2003. 'TSC2 Regulates VEGF through mTOR-Dependent and -Independent Pathways'. *Cancer Cell* 4 (2): 147–158.

Bubeck Wardenburg, J, C Fu, J K Jackman, H Flotow, S E Wilkinson, D H Williams, R Johnson, G Kong, A C Chan, and P R Findell. 1996. 'Phosphorylation of SLP-76 by the ZAP-70 Protein-Tyrosine Kinase Is Required for T-Cell Receptor Function'. *The Journal of Biological Chemistry* 271 (33): 19641–19644.

Buchholz, Veit R, Michael Flossdorf, Inge Hensel, Lorenz Kretschmer, Bianca Weissbrich, Patricia Gräf, Admar Verschoor, Matthias Schiemann, Thomas Höfer, and Dirk H Busch. 2013. 'Disparate Individual Fates Compose Robust CD8+ T Cell Immunity'. *Science (New York, N.Y.)* (March 14): 630-635.

Buerger, Claudia, Ben DeVries, and Vuk Stambolic. 2006. 'Localization of Rheb to the Endomembrane Is Critical for Its Signaling Function'. *Biochemical and Biophysical Research Communications* 344 (3) (June 9): 869–880.

Bunpo, Piyawan, Judy K Cundiff, Rachel B Reinert, Ronald C Wek, Carla J Aldrich, and Tracy G Anthony. 2010. 'The eIF2 Kinase GCN2 Is Essential for the Murine Immune System to Adapt to Amino Acid Deprivation by Asparaginase'. *The Journal of Nutrition* 140 (11) (November): 2020–2027.

Burnet, F M. 1970. 'The Concept of Immunological Surveillance'. *Progress in Experimental Tumor Research* 13: 1–27.

Burnet, Macfarlane. 1957. 'Cancer--A Biological Approach'. *British Medical Journal* 1 (5022): 779–786.

Bushati, Natascha, and Stephen M Cohen. 2007. 'microRNA Functions'. *Annual Review of Cell and Developmental Biology* 23: 175–205.

Carpenito, Carmine, Michael C Milone, Raffit Hassan, Jacqueline C Simonet, Mehdi Lakhal, Megan M Suhoski, Angel Varela-Rohena, et al. 2009. 'Control of Large, Established Tumor Xenografts with Genetically Retargeted Human T Cells Containing CD28 and CD137 Domains'. *Proceedings of the National Academy of Sciences of the United States of America* 106 (9) (March 3): 3360–3365.

Bibliography

Carswell, E A, L J Old, R L Kassel, S Green, N Fiore, and B Williamson. 1975. 'An Endotoxin-Induced Serum Factor That Causes Necrosis of Tumors'. *Proceedings of the National Academy of Sciences of the United States of America* 72 (9): 3666–3670.

Cerwenka, A, and L L Lanier. 2001. 'Natural Killer Cells, Viruses and Cancer'. *Nature Reviews. Immunology* 1 (1) (October): 41–49.

Chan, A C, M Iwashima, C W Turck, and A Weiss. 1992. 'ZAP-70: A 70 Kd Protein-Tyrosine Kinase That Associates with the TCR Zeta Chain'. *Cell* 71 (4): 649–662.

Chang, Chih-Hao, Jonathan D. Curtis, Leonard B. Maggi Jr., Brandon Faubert, Alejandro V. Villarino, David O'Sullivan, Stanley Ching-Cheng Huang, et al. 2013. 'Posttranscriptional Control of T Cell Effector Function by Aerobic Glycolysis'. *Cell* 153 (6) (June 6): 1239–1251.

Chaturvedi, Anil K, Ruth M Pfeiffer, Leonard Chang, James J Goedert, Robert J Biggar, and Eric A Engels. 2007. 'Elevated Risk of Lung Cancer among People with AIDS'. *AIDS (London, England)* 21 (2) (January 11): 207–213.

Cieri, Nicoletta, Barbara Camisa, Fabienne Cocchiarella, Mattia Forcato, Giacomo Oliveira, Elena Provasi, Attilio Bondanza, et al. 2013. 'IL-7 and IL-15 Instruct the Generation of Human Memory Stem T Cells from Naive Precursors'. *Blood* 121 (4) (January 24): 573–584.

Clay, T M, M C Custer, J Sachs, P Hwu, S A Rosenberg, and M I Nishimura. 1999. 'Efficient Transfer of a Tumor Antigen-Reactive TCR to Human Peripheral Blood Lymphocytes Confers Anti-Tumor Reactivity'. *Journal of Immunology (Baltimore, Md.: 1950)* 163 (1): 507–513.

Cobbold, Stephen P, Elizabeth Adams, Claire A Farquhar, Kathleen F Nolan, Duncan Howie, Kathy O Lui, Paul J Fairchild, Andrew L Mellor, David Ron, and Herman Waldmann. 2009. 'Infectious Tolerance via the Consumption of Essential Amino Acids and mTOR Signaling'. *Proceedings of the National Academy of Sciences of the United States of America* 106 (29) (July 21): 12055–12060.

Coley, W B. 1991. 'The Treatment of Malignant Tumors by Repeated Inoculations of Erysipelas. With a Report of Ten Original Cases. 1893'. *Clinical Orthopaedics and Related Research*, no. 262 (January): 3–11.

Bibliography

Curiel, Tyler J, George Coukos, Linhua Zou, Xavier Alvarez, Pui Cheng, Peter Mottram, Melina Evdemon-Hogan, et al. 2004. 'Specific Recruitment of Regulatory T Cells in Ovarian Carcinoma Fosters Immune Privilege and Predicts Reduced Survival'. *Nature Medicine* 10 (9) (September): 942–949.

Curtsinger, Julie M, and Matthew F Mescher. 2010. 'Inflammatory Cytokines as a Third Signal for T Cell Activation'. *Current Opinion in Immunology* 22 (3): 333–340.

Delgoffe, Greg M, Thomas P Kole, Yan Zheng, Paul E Zarek, Krystal L Matthews, Bo Xiao, Paul F Worley, Sara C Kozma, and Jonathan D Powell. 2009. 'The mTOR Kinase Differentially Regulates Effector and Regulatory T Cell Lineage Commitment'. *Immunity* 30 (6) (June 19): 832–844.

Delgoffe, Greg M, Kristen N Pollizzi, Adam T Waickman, Emily Heikamp, David J Meyers, Maureen R Horton, Bo Xiao, Paul F Worley, and Jonathan D Powell. 2011. 'The Kinase mTOR Regulates the Differentiation of Helper T Cells through the Selective Activation of Signaling by mTORC1 and mTORC2'. *Nature Immunology* 12 (4) (April): 295–303.

Delgoffe, Greg M, and Jonathan D Powell. 2009. 'mTOR: Taking Cues from the Immune Microenvironment'. *Immunology* 127 (4) (August): 459–465.

Delisle, J-S, M Giroux, G Boucher, J-R Landry, M-P Hardy, S Lemieux, R G Jones, B T Wilhelm, and C Perreault. 2013. 'The TGF-B-Smad3 Pathway Inhibits CD28-Dependent Cell Growth and Proliferation of CD4 T Cells'. *Genes and Immunity* (January 17): 115-126.

Dong, Haidong, Scott E Strome, Diva R Salomao, Hideto Tamura, Fumiya Hirano, Dallas B Flies, Patrick C Roche, et al. 2002. 'Tumor-Associated B7-H1 Promotes T-Cell Apoptosis: A Potential Mechanism of Immune Evasion'. *Nature Medicine* 8 (8) (August): 793–800.

Dowling, Ryan J O, Ivan Topisirovic, Tommy Alain, Michael Bidinosti, Bruno D Fonseca, Emmanuel Petroulakis, Xiaoshan Wang, et al. 2010. 'mTORC1-Mediated Cell Proliferation, but Not Cell Growth, Controlled by the 4E-BPs'. *Science (New York, N.Y.)* 328 (5982) (May 28): 1172–1176.

Dudley, Mark E. 2011. 'Adoptive Cell Therapy for Patients with Melanoma'. *Journal of Cancer* 2: 360–362.

Bibliography

Dudley, Mark E, James C Yang, Richard Sherry, Marybeth S Hughes, Richard Royal, Udai Kammula, Paul F Robbins, et al. 2008. 'Adoptive Cell Therapy for Patients with Metastatic Melanoma: Evaluation of Intensive Myeloablative Chemoradiation Preparative Regimens'. *Journal of Clinical Oncology: Official Journal of the American Society of Clinical Oncology* 26 (32) (November 10): 5233–5239.

Dudley, Mark E., John R. Wunderlich, Paul F. Robbins, James C. Yang, Patrick Hwu, Douglas J. Schwartzentruber, Suzanne L. Topalian, et al. 2002. 'Cancer Regression and Autoimmunity in Patients After Clonal Repopulation with Antitumor Lymphocytes'. *Science* 298 (5594) (October 25): 850–854.

Dunn, Gavin P, Lloyd J Old, and Robert D Schreiber. 2004. 'The Immunobiology of Cancer Immunosurveillance and Immunoediting'. *Immunity* 21 (2) (August): 137–148.

Dürr, Christoph, Dietmar Pfeifer, Rainer Claus, Annette Schmitt-Graeff, Ulrike V Gerlach, Ralph Graeser, Sophie Krüger, et al. 2010. 'CXCL12 Mediates Immunosuppression in the Lymphoma Microenvironment after Allogeneic Transplantation of Hematopoietic Cells'. *Cancer Research* 70 (24) (December 15): 10170–10181.

Düvel, Katrin, Jessica L Yecies, Suchithra Menon, Pichai Raman, Alex I Lipovsky, Amanda L Souza, Ellen Triantafellow, et al. 2010. 'Activation of a Metabolic Gene Regulatory Network Downstream of mTOR Complex 1'. *Molecular Cell* 39 (2) (July 30): 171–183.

Eisenhauer, E A, P Therasse, J Bogaerts, L H Schwartz, D Sargent, R Ford, J Dancey, et al. 2009. 'New Response Evaluation Criteria in Solid Tumours: Revised RECIST Guideline (version 1.1)'. *European Journal of Cancer (Oxford, England: 1990)* 45 (2) (January): 228–247.

Engels, Boris, Hakan Cam, Thomas Schüler, Stefano Indraccolo, Monika Gladow, Christopher Baum, Thomas Blankenstein, and Wolfgang Uckert. 2003. 'Retroviral Vectors for High-Level Transgene Expression in T Lymphocytes'. *Human Gene Therapy* 14 (12) (August 10): 1155–1168.

Ferradini, L, A Mackensen, C Genevée, J Bosq, P Duvillard, M F Avril, and T Hercend. 1993. 'Analysis of T Cell Receptor Variability in Tumor-Infiltrating

Lymphocytes from a Human Regressive Melanoma. Evidence for in Situ T Cell Clonal Expansion'. *The Journal of Clinical Investigation* 91 (3) (March): 1183–1190.

Finlay, David, and Doreen A Cantrell. 2011. 'Metabolism, Migration and Memory in Cytotoxic T Cells'. *Nature Reviews. Immunology* 11 (2) (February): 109–117.

Finlay, David K, Ella Rosenzweig, Linda V Sinclair, Carmen Feijoo-Carnero, Jens L Hukelmann, Julia Rolf, Andrey A Panteleyev, Klaus Okkenhaug, and Doreen A Cantrell. 2012. 'PDK1 Regulation of mTOR and Hypoxia-Inducible Factor 1 Integrate Metabolism and Migration of CD8+ T Cells'. *The Journal of Experimental Medicine* 209 (13) (December 17): 2441–2453.

Flavell, Richard A., Shomyseh Sanjabi, Stephen H. Wrzesinski, and Paula Licona-Limón. 2010. 'The Polarization of Immune Cells in the Tumour Environment by TGFβ'. *Nat Rev Immunol* 10 (8): 554–567.

Förster, Reinhold, Ana Clara Davalos-Misslitz, and Antal Rot. 2008. 'CCR7 and Its Ligands: Balancing Immunity and Tolerance'. *Nature Reviews. Immunology* 8 (5) (May): 362–371.

Gabrilovich, Dmitry I., and Srinivas Nagaraj. 2009. 'Myeloid-Derived Suppressor Cells as Regulators of the Immune System'. *Nat Rev Immunol* 9 (3) (March): 162–174.

Galon, Jérôme, Helen K Angell, Davide Bedognetti, and Francesco M Marincola. 2013. 'The Continuum of Cancer Immunosurveillance: Prognostic, Predictive, and Mechanistic Signatures'. *Immunity* 39 (1) (July 25): 11–26.

Galon, Jérôme, Anne Costes, Fatima Sanchez-Cabo, Amos Kirilovsky, Bernhard Mlecnik, Christine Lagorce-Pagès, Marie Tosolini, et al. 2006. 'Type, Density, and Location of Immune Cells within Human Colorectal Tumors Predict Clinical Outcome'. *Science (New York, N.Y.)* 313 (5795) (September 29): 1960–1964.

Gao, L, I Bellantuono, A Elsässer, S B Marley, M Y Gordon, J M Goldman, and H J Stauss. 2000. 'Selective Elimination of Leukemic CD34(+) Progenitor Cells by Cytotoxic T Lymphocytes Specific for WT1'. *Blood* 95 (7): 2198–2203.

Gattinoni, L. 2005. 'Acquisition of Full Effector Function in Vitro Paradoxically Impairs the in Vivo Antitumor Efficacy of Adoptively Transferred CD8+ T Cells'. *Journal of Clinical Investigation* 115 (6) (June): 1616–1626.

Bibliography

Gattinoni, Luca, Steven E Finkelstein, Christopher A Klebanoff, Paul A Antony, Douglas C Palmer, Paul J Spiess, Leroy N Hwang, et al. 2005. 'Removal of Homeostatic Cytokine Sinks by Lymphodepletion Enhances the Efficacy of Adoptively Transferred Tumor-Specific CD8+ T Cells'. *The Journal of Experimental Medicine* 202 (7) (October 3): 907–912.

Gattinoni, Luca, Enrico Lugli, Yun Ji, Zoltan Pos, Chrystal M Paulos, Máire F Quigley, Jorge R Almeida, et al. 2011. 'A Human Memory T Cell Subset with Stem Cell-like Properties'. *Nature Medicine* 17 (10) (October): 1290–1297.

Gattinoni, Luca, Xiao-Song Zhong, Douglas C Palmer, Yun Ji, Christian S Hinrichs, Zhiya Yu, Claudia Wrzesinski, et al. 2009. 'Wnt Signaling Arrests Effector T Cell Differentiation and Generates CD8+ Memory Stem Cells'. *Nat Med* 15 (7) (July): 808–813.

Genot, E, and D A Cantrell. 2000. 'Ras Regulation and Function in Lymphocytes'. *Current Opinion in Immunology* 12 (3): 289–294.

Gerlach, Carmen, Jan C Rohr, Leïla Perié, Nienke van Rooij, Jeroen W J van Heijst, Arno Velds, Jos Urbanus, et al. 2013. 'Heterogeneous Differentiation Patterns of Individual CD8+ T Cells'. *Science (New York, N.Y.)* (March 14): 635-639.

Gerlinger, Marco, Andrew J Rowan, Stuart Horswell, James Larkin, David Endesfelder, Eva Gronroos, Pierre Martinez, et al. 2012. 'Intratumor Heterogeneity and Branched Evolution Revealed by Multiregion Sequencing'. *The New England Journal of Medicine* 366 (10) (March 8): 883–892.

Gerner, Michael Y, Lynn M Heltemes-Harris, Brian T Fife, and Matthew F Mescher. 2013. 'Cutting Edge: IL-12 and Type I IFN Differentially Program CD8 T Cells for Programmed Death 1 Re-Expression Levels and Tumor Control'. *Journal of Immunology (Baltimore, Md.: 1950)* 191 (3) (August 1): 1011–1015.

Ghorashian, Sara, Emma Nicholson, and Hans J Stauss. 2011. 'T Cell Gene-Engineering to Enhance GVT and Suppress GVHD'. *Best Practice & Research. Clinical Haematology* 24 (3) (September): 421–433.

Gill, Saar, and David L Porter. 2013. 'CAR-Modified Anti-CD19 T Cells for the Treatment of B-Cell Malignancies: Rules of the Road'. *Expert Opinion on Biological Therapy* (November 21): 37-49.

Bibliography

Gorelik, L, and R A Flavell. 2001. 'Immune-Mediated Eradication of Tumors through the Blockade of Transforming Growth Factor-Beta Signaling in T Cells'. *Nature Medicine* 7 (10) (October): 1118–1122.

GREEN, H N. 1954. 'An Immunological Concept of Cancer: A Preliminary Report'. *British Medical Journal* 2 (4901): 1374–1380.

Grohmann, Ursula, and Vincenzo Bronte. 2010. 'Control of Immune Response by Amino Acid Metabolism'. *Immunological Reviews* 236 (July): 243–264.

Grupp, Stephan A, Michael Kalos, David Barrett, Richard Aplenc, David L Porter, Susan R Rheingold, David T Teachey, et al. 2013. 'Chimeric Antigen Receptor-Modified T Cells for Acute Lymphoid Leukemia'. *The New England Journal of Medicine* 368 (16) (April 18): 1509–1518.

Hacein-Bey-Abina, S, C Von Kalle, M Schmidt, M P McCormack, N Wulffraat, P Leboulch, A Lim, et al. 2003. 'LMO2-Associated Clonal T Cell Proliferation in Two Patients after Gene Therapy for SCID-X1'. *Science (New York, N.Y.)* 302 (5644) (October 17): 415–419.

Hamid, Omid, Caroline Robert, Adil Daud, F. Stephen Hodi, Wen-Jen Hwu, Richard Kefford, Jedd D. Wolchok, et al. 2013. 'Safety and Tumor Responses with Lambrolizumab (Anti–PD-1) in Melanoma'. *New England Journal of Medicine* 369(2) (July 11):134-44.

Han, Jung Min, Seung Jae Jeong, Min Chul Park, Gyuyoup Kim, Nam Hoon Kwon, Hoi Kyoung Kim, Sang Hoon Ha, Sung Ho Ryu, and Sunghoon Kim. 2012. 'Leucyl-tRNA Synthetase Is an Intracellular Leucine Sensor for the mTORC1-Signaling Pathway'. *Cell* 149 (2): 410–424.

Hanahan, D, and R A Weinberg. 2000. 'The Hallmarks of Cancer'. *Cell* 100 (1): 57–70.

Hanahan, Douglas, and Robert A Weinberg. 2011. 'Hallmarks of Cancer: The next Generation'. *Cell* 144 (5) (March 4): 646–674.

Harding, H P, I Novoa, Y Zhang, H Zeng, R Wek, M Schapira, and D Ron. 2000. 'Regulated Translation Initiation Controls Stress-Induced Gene Expression in Mammalian Cells'. *Molecular Cell* 6 (5): 1099–1108.

Bibliography

Haxhinasto, Sokol, Diane Mathis, and Christophe Benoist. 2008. 'The AKT-mTOR Axis Regulates de Novo Differentiation of CD4+Foxp3+ Cells'. *The Journal of Experimental Medicine* 205 (3) (March 17): 565–574.

He, T C, S Zhou, L T da Costa, J Yu, K W Kinzler, and B Vogelstein. 1998. 'A Simplified System for Generating Recombinant Adenoviruses'. *Proceedings of the National Academy of Sciences of the United States of America* 95 (5): 2509–2514.

Heinz, Niels, Axel Schambach, Melanie Galla, Tobias Maetzig, Christopher Baum, Rainer Loew, and Bernhard Schiedlmeier. 2011. 'Retroviral and Transposon-Based Tet-Regulated All-in-One Vectors with Reduced Background Expression and Improved Dynamic Range'. *Human Gene Therapy* 22 (2) (February): 166–176.

Hinrichs, Christian S, Zachary A Borman, Lydie Cassard, Luca Gattinoni, Rosanne Spolski, Zhiya Yu, Luis Sanchez-Perez, et al. 2009. 'Adoptively Transferred Effector Cells Derived from Naive rather than Central Memory CD8+ T Cells Mediate Superior Antitumor Immunity'. *Proceedings of the National Academy of Sciences of the United States of America* 106 (41) (October 13): 17469–17474.

Hinrichs, Christian S, Zachary A Borman, Luca Gattinoni, Zhiya Yu, William R Burns, Jianping Huang, Christopher A Klebanoff, et al. 2011. 'Human Effector CD8+ T Cells Derived from Naive rather than Memory Subsets Possess Superior Traits for Adoptive Immunotherapy'. *Blood* 117 (3) (January 20): 808–814.

Hinrichs, Christian S, and Nicholas P Restifo. 2013. 'Reassessing Target Antigens for Adoptive T-Cell Therapy'. *Nature Biotechnology* (October 20): 999-1008.

Hodi, F Stephen, Steven J O'Day, David F McDermott, Robert W Weber, Jeffrey A Sosman, John B Haanen, Rene Gonzalez, et al. 2010. 'Improved Survival with Ipilimumab in Patients with Metastatic Melanoma'. *The New England Journal of Medicine* 363 (8) (August 19): 711–723.

Hohenstein, Peter, and Nicholas D Hastie. 2006. 'The Many Facets of the Wilms' Tumour Gene, WT1'. *Human Molecular Genetics* 15 Spec No 2 (October 15): R196–201.

Holst, Jeff, Kate M Vignali, Amanda R Burton, and Dario A A Vignali. 2006. 'Rapid Analysis of T-Cell Selection in Vivo Using T Cell-Receptor Retrogenic Mice'. *Nature Methods* 3 (3) (March): 191–197.

Bibliography

Hombach, Andreas A, Gunter Rappl, and Hinrich Abken. 2013. 'Arming Cytokine-Induced Killer Cells With Chimeric Antigen Receptors: CD28 Outperforms Combined CD28-OX40 "Super-Stimulation"'. *Molecular Therapy: The Journal of the American Society of Gene Therapy* (August 28): 2268-2277.

Horowitz, M M, R P Gale, P M Sondel, J M Goldman, J Kersey, H J Kolb, A A Rimm, O Ringdén, C Rozman, and B Speck. 1990. 'Graft-versus-Leukemia Reactions after Bone Marrow Transplantation'. *Blood* 75 (3): 555–562.

Inoki, Ken, Hongjiao Ouyang, Tianqing Zhu, Charlotta Lindvall, Yian Wang, Xiaojie Zhang, Qian Yang, et al. 2006. 'TSC2 Integrates Wnt and Energy Signals via a Coordinated Phosphorylation by AMPK and GSK3 to Regulate Cell Growth'. *Cell* 126 (5) (September 8): 955–968.

Intlekofer, Andrew M, Naofumi Takemoto, E John Wherry, Sarah A Longworth, John T Northrup, Vikram R Palanivel, Alan C Mullen, et al. 2005. 'Effector and Memory CD8+ T Cell Fate Coupled by T-Bet and Eomesodermin'. *Nature Immunology* 6 (12) (December): 1236–1244.

Irving, B A, and A Weiss. 1991. 'The Cytoplasmic Domain of the T Cell Receptor Zeta Chain Is Sufficient to Couple to Receptor-Associated Signal Transduction Pathways'. *Cell* 64 (5): 891–901.

Itzhaki, Orit, Daphna Levy, Dragoslav Zikich, Avraham J Treves, Gal Markel, Jacob Schachter, and Michal J Besser. 2013. 'Adoptive T-Cell Transfer in Melanoma'. *Immunotherapy* 5 (1) (January): 79–90.

Iwai, Yoshiko, Masayoshi Ishida, Yoshimasa Tanaka, Taku Okazaki, Tasuku Honjo, and Nagahiro Minato. 2002. 'Involvement of PD-L1 on Tumor Cells in the Escape from Host Immune System and Tumor Immunotherapy by PD-L1 Blockade'. *Proceedings of the National Academy of Sciences of the United States of America* 99 (19) (September 17): 12293–12297.

Johnson, Laura A, Richard A Morgan, Mark E Dudley, Lydie Cassard, James C Yang, Marybeth S Hughes, Udai S Kammula, et al. 2009. 'Gene Therapy with Human and Mouse T-Cell Receptors Mediates Cancer Regression and Targets Normal Tissues Expressing Cognate Antigen'. *Blood* 114 (3) (July 16): 535–546.

Joshi, Nikhil S, Weiguo Cui, Anmol Chandele, Heung Kyu Lee, David R Urso, James Hagman, Laurent Gapin, and Susan M Kaech. 2007. 'Inflammation Directs

Memory Precursor and Short-Lived Effector CD8(+) T Cell Fates via the Graded Expression of T-Bet Transcription Factor'. *Immunity* 27 (2) (August): 281–295.

Kaech, Susan M, Joyce T Tan, E John Wherry, Bogumila T Konieczny, Charles D Surh, and Rafi Ahmed. 2003. 'Selective Expression of the Interleukin 7 Receptor Identifies Effector CD8 T Cells That Give Rise to Long-Lived Memory Cells'. *Nature Immunology* 4 (12) (December): 1191–1198.

Kalos, Michael, Bruce L Levine, David L Porter, Sharyn Katz, Stephan A Grupp, Adam Bagg, and Carl H June. 2011. 'T Cells with Chimeric Antigen Receptors Have Potent Antitumor Effects and Can Establish Memory in Patients with Advanced Leukemia'. *Science Translational Medicine* 3 (95) (August 10): 95ra73.

Kang, Jong Seok, Cheng Liu, and Rik Derynck. 2009. 'New Regulatory Mechanisms of TGF-Beta Receptor Function'. *Trends in Cell Biology* 19 (8): 385–394.

Kaplan, D H, V Shankaran, A S Dighe, E Stockert, M Aguet, L J Old, and R D Schreiber. 1998. 'Demonstration of an Interferon Gamma-Dependent Tumor Surveillance System in Immunocompetent Mice'. *Proceedings of the National Academy of Sciences of the United States of America* 95 (13): 7556–7561.

Kawakami, Y, S Eliyahu, C H Delgado, P F Robbins, L Rivoltini, S L Topalian, T Miki, and S A Rosenberg. 1994. 'Cloning of the Gene Coding for a Shared Human Melanoma Antigen Recognized by Autologous T Cells Infiltrating into Tumor'. *Proceedings of the National Academy of Sciences of the United States of America* 91 (9): 3515–3519.

Kehrl, J H, L M Wakefield, A B Roberts, S Jakowlew, M Alvarez-Mon, R Derynck, M B Sporn, and A S Fauci. 1986. 'Production of Transforming Growth Factor Beta by Human T Lymphocytes and Its Potential Role in the Regulation of T Cell Growth'. *The Journal of Experimental Medicine* 163 (5): 1037–1050.

Kerkar, Sid P, Romina S Goldszmid, Pawel Muranski, Dhanalakshmi Chinnasamy, Zhiya Yu, Robert N Reger, Anthony J Leonardi, et al. 2011. 'IL-12 Triggers a Programmatic Change in Dysfunctional Myeloid-Derived Cells within Mouse Tumors'. *The Journal of Clinical Investigation* 121 (12) (December): 4746–4757.

Kerkar, Sid P, Anthony J Leonardi, Nicolas van Panhuys, Ling Zhang, Zhiya Yu, Joseph G Crompton, Jenny H Pan, et al. 2013. 'Collapse of the Tumor Stroma Is

Bibliography

Triggered by IL-12 Induction of Fas'. *Molecular Therapy: The Journal of the American Society of Gene Therapy* (April 9): 1369-1377.

Kerkar, Sid P, Pawel Muranski, Andrew Kaiser, Andrea Boni, Luis Sanchez-Perez, Zhiya Yu, Douglas C Palmer, et al. 2010. 'Tumor-Specific CD8+ T Cells Expressing Interleukin-12 Eradicate Established Cancers in Lymphodepleted Hosts'. *Cancer Research* 70 (17) (September 1): 6725–6734.

Kershaw, Michael H, Jennifer A Westwood, and Phillip K Darcy. 2013. 'Gene-Engineered T Cells for Cancer Therapy'. *Nature Reviews. Cancer* 13 (8) (August): 525–541.

Kessels, H W, M D van Den Boom, H Spits, E Hooijberg, and T N Schumacher. 2000. 'Changing T Cell Specificity by Retroviral T Cell Receptor Display'. *Proceedings of the National Academy of Sciences of the United States of America* 97 (26) (December 19): 14578–14583.

Kessels, H W, M C Wolkers, M D van den Boom, M A van der Valk, and T N Schumacher. 2001. 'Immunotherapy through TCR Gene Transfer'. *Nature Immunology* 2 (10) (October): 957–961.

Kilberg, Michael S, Jixiu Shan, and Nan Su. 2009. 'ATF4-Dependent Transcription Mediates Signaling of Amino Acid Limitation'. *Trends in Endocrinology and Metabolism: TEM* 20 (9) (November): 436–443.

King, Carolyn G, Sabrina Koehli, Barbara Hausmann, Mathias Schmaler, Dietmar Zehn, and Ed Palmer. 2012. 'T Cell Affinity Regulates Asymmetric Division, Effector Cell Differentiation, and Tissue Pathology'. *Immunity* 37 (4) (October 19): 709–720.

Kirk, Gregory D, Christian Merlo, Peter O' Driscoll, Shruti H Mehta, Noya Galai, David Vlahov, Jonathan Samet, and Eric A Engels. 2007. 'HIV Infection Is Associated with an Increased Risk for Lung Cancer, Independent of Smoking'. *Clinical Infectious Diseases: An Official Publication of the Infectious Diseases Society of America* 45 (1) (July 1): 103–110.

Klebanoff, Christopher A, Luca Gattinoni, Parizad Torabi-Parizi, Keith Kerstann, Adela R Cardones, Steven E Finkelstein, Douglas C Palmer, et al. 2005. 'Central Memory Self/tumor-Reactive CD8+ T Cells Confer Superior Antitumor Immunity Compared with Effector Memory T Cells'. *Proceedings of the National Academy of Sciences of the United States of America* 102 (27) (July 5): 9571–9576.

Bibliography

Klebanoff, Christopher A, Hung T Khong, Paul A Antony, Douglas C Palmer, and Nicholas P Restifo. 2005. 'Sinks, Suppressors and Antigen Presenters: How Lymphodepletion Enhances T Cell-Mediated Tumor Immunotherapy'. *Trends in Immunology* 26 (2) (February): 111–117.

Kochenderfer, James N, and Steven A Rosenberg. 2013. 'Treating B-Cell Cancer with T Cells Expressing Anti-CD19 Chimeric Antigen Receptors'. *Nature Reviews. Clinical Oncology* 10 (5) (May): 267–276.

Kochenderfer, James N, Wyndham H Wilson, John E Janik, Mark E Dudley, Maryalice Stetler-Stevenson, Steven A Feldman, Irina Maric, et al. 2010. 'Eradication of B-Lineage Cells and Regression of Lymphoma in a Patient Treated with Autologous T Cells Genetically Engineered to Recognize CD19'. *Blood* 116 (20) (November 18): 4099–4102.

Koebel, Catherine M., William Vermi, Jeremy B. Swann, Nadeen Zerafa, Scott J. Rodig, Lloyd J. Old, Mark J. Smyth, and Robert D. Schreiber. 2007. 'Adaptive Immunity Maintains Occult Cancer in an Equilibrium State'. *Nature* 450 (7171) (December 6): 903–907.

Koren, Itay, Eran Reem, and Adi Kimchi. 2010. 'Autophagy Gets a Brake: DAP1, a Novel mTOR Substrate, Is Activated to Suppress the Autophagic Process'. *Autophagy* 6 (8) (November): 1179–1180.

Kreis, H, J M Cisterne, W Land, L Wramner, J P Squifflet, D Abramowicz, J M Campistol, et al. 2000. 'Sirolimus in Association with Mycophenolate Mofetil Induction for the Prevention of Acute Graft Rejection in Renal Allograft Recipients'. *Transplantation* 69 (7): 1252–1260.

Kulkarni, A B, C G Huh, D Becker, A Geiser, M Lyght, K C Flanders, A B Roberts, M B Sporn, J M Ward, and S Karlsson. 1993. 'Transforming Growth Factor Beta 1 Null Mutation in Mice Causes Excessive Inflammatory Response and Early Death'. *Proceedings of the National Academy of Sciences of the United States of America* 90 (2): 770–774.

Kunert, Andre, Trudy Straetemans, Coen Govers, Cor Lamers, Ron Mathijssen, Stefan Sleijfer, and Reno Debets. 2013. 'TCR-Engineered T Cells Meet New Challenges to Treat Solid Tumors: Choice of Antigen, T Cell Fitness, and Sensitization of Tumor Milieu'. *Frontiers in Immunology* 4: 363.

Bibliography

Kusmartsev, Sergei, and Dmitry I Gabrilovich. 2005. 'STAT1 Signaling Regulates Tumor-Associated Macrophage-Mediated T Cell Deletion'. *Journal of Immunology (Baltimore, Md.: 1950)* 174 (8): 4880–4891.

Landsberg, Jennifer, Judith Kohlmeyer, Marcel Renn, Tobias Bald, Meri Rogava, Mira Cron, Martina Fatho, et al. 2012. 'Melanomas Resist T-Cell Therapy through Inflammation-Induced Reversible Dedifferentiation'. *Nature* (October 10): 412-416.

Laplante, Mathieu, and David M Sabatini. 2009. 'An Emerging Role of mTOR in Lipid Biosynthesis'. *Current Biology: CB* 19 (22) (December 1): R1046–1052.

Laplante, Mathieu, and David M Sabatini. 2012. 'mTOR Signaling in Growth Control and Disease'. *Cell* 149 (2) (April 13): 274–293.

Li, Ming O, Yisong Y Wan, Shomyseh Sanjabi, Anna-Karin L Robertson, and Richard A Flavell. 2006. 'Transforming Growth Factor-Beta Regulation of Immune Responses'. *Annual Review of Immunology* 24: 99–146.

Li, Qingsheng, Rajesh Rao, Joseph Vazzana, Peter Goedegebuure, Kunle Odunsi, William Gillanders, and Protul A Shrikant. 2012. 'Regulating Mammalian Target of Rapamycin To Tune Vaccination-Induced CD8+ T Cell Responses for Tumor Immunity'. *Journal of Immunology (Baltimore, Md.: 1950)* (February 29): 3080-3087.

Liao, Wei, Jian-Xin Lin, and Warren J Leonard. 2013. 'Interleukin-2 at the Crossroads of Effector Responses, Tolerance, and Immunotherapy'. *Immunity* 38 (1): 13–25.

Linette, Gerald P, Edward A Stadtmauer, Marcela V Maus, Aaron P Rapoport, Bruce L Levine, Lyndsey Emery, Leslie Litzky, et al. 2013. 'Cardiovascular Toxicity and Titin Cross-Reactivity of Affinity-Enhanced T Cells in Myeloma and Melanoma'. *Blood* 122 (6) (August 8): 863–871.

Linsley, P S, J L Greene, W Brady, J Bajorath, J A Ledbetter, and R Peach. 1994. 'Human B7-1 (CD80) and B7-2 (CD86) Bind with Similar Avidities but Distinct Kinetics to CD28 and CTLA-4 Receptors'. *Immunity* 1 (9): 793–801.

Long, Xiaomeng, Yenshou Lin, Sara Ortiz-Vega, Kazuyoshi Yonezawa, and Joseph Avruch. 2005. 'Rheb Binds and Regulates the mTOR Kinase'. *Current Biology: CB* 15 (8) (April 26): 702–713.

Bibliography

Lu, Zhi Hong, Mark B Shvartsman, Andrew Y Lee, Jenny M Shao, Mollianne M Murray, Raleigh D Kladney, Dong Fan, et al. 2010. 'Mammalian Target of Rapamycin Activator RHEB Is Frequently Overexpressed in Human Carcinomas and Is Critical and Sufficient for Skin Epithelial Carcinogenesis'. *Cancer Research* 70 (8) (April 15): 3287–3298.

Macintyre, Andrew N, David Finlay, Gavin Preston, Linda V Sinclair, Caryll M Waugh, Peter Tamas, Carmen Feijoo, Klaus Okkenhaug, and Doreen A Cantrell. 2011. 'Protein Kinase B Controls Transcriptional Programs That Direct Cytotoxic T Cell Fate but Is Dispensable for T Cell Metabolism'. *Immunity* 34 (2) (February 25): 224–236.

Mamalaki, C, T Norton, Y Tanaka, A R Townsend, P Chandler, E Simpson, and D Kioussis. 1992. 'Thymic Depletion and Peripheral Activation of Class I Major Histocompatibility Complex-Restricted T Cells by Soluble Peptide in T-Cell Receptor Transgenic Mice'. *Proceedings of the National Academy of Sciences of the United States of America* 89 (23): 11342–11346.

Martínez-Estrada, Ofelia M, Laura A Lettice, Abdelkader Essafi, Juan Antonio Guadix, Joan Slight, Víctor Velecela, Emma Hall, et al. 2010. 'Wt1 Is Required for Cardiovascular Progenitor Cell Formation through Transcriptional Control of Snail and E-Cadherin'. *Nature Genetics* 42 (1) (January): 89–93.

Matsushita, Hirokazu, Matthew D Vesely, Daniel C Koboldt, Charles G Rickert, Ravindra Uppaluri, Vincent J Magrini, Cora D Arthur, et al. 2012. 'Cancer Exome Analysis Reveals a T-Cell-Dependent Mechanism of Cancer Immunoediting'. *Nature* 482 (7385) (February 16): 400–404.

Ménasché, Gaël, Stefanie Kliche, Natalie Bezman, and Burkhart Schraven. 2007. 'Regulation of T-Cell Antigen Receptor-Mediated inside-out Signaling by Cytosolic Adapter Proteins and Rap1 Effector Molecules'. *Immunological Reviews* 218: 82–91.

Metz, Richard, Sonja Rust, James B Duhadaway, Mario R Mautino, David H Munn, Nicholas N Vahanian, Charles J Link, and George C Prendergast. 2012. 'IDO Inhibits a Tryptophan Sufficiency Signal That Stimulates mTOR: A Novel IDO Effector Pathway Targeted by D-1-Methyl-Tryptophan'. *Oncoimmunology* 1 (9) (December 1): 1460–1468.

Bibliography

Michalek, Ryan D, Valerie A Gerriets, Sarah R Jacobs, Andrew N Macintyre, Nancie J MacIver, Emily F Mason, Sarah A Sullivan, Amanda G Nichols, and Jeffrey C Rathmell. 2011. 'Cutting Edge: Distinct Glycolytic and Lipid Oxidative Metabolic Programs Are Essential for Effector and Regulatory CD4+ T Cell Subsets'. *Journal of Immunology (Baltimore, Md.: 1950)* 186 (6) (March 15): 3299–3303.

Moloney, F J, H Comber, P O'Lorcain, P O'Kelly, P J Conlon, and G M Murphy. 2006. 'A Population-Based Study of Skin Cancer Incidence and Prevalence in Renal Transplant Recipients'. *The British Journal of Dermatology* 154 (3) (March): 498–504.

Mora, J Rodrigo, and Ulrich H von Andrian. 2006. 'T-Cell Homing Specificity and Plasticity: New Concepts and Future Challenges'. *Trends in Immunology* 27 (5) (May): 235–243.

Morgan, Richard A, Mark E Dudley, John R Wunderlich, Marybeth S Hughes, James C Yang, Richard M Sherry, Richard E Royal, et al. 2006. 'Cancer Regression in Patients after Transfer of Genetically Engineered Lymphocytes'. *Science (New York, N.Y.)* 314 (5796) (October 6): 126–129.

Mueller, Daniel L. 2010. 'Mechanisms Maintaining Peripheral Tolerance'. *Nature Immunology* 11 (1): 21–27.

Müller, Martin R, and Anjana Rao. 2010. 'NFAT, Immunity and Cancer: A Transcription Factor Comes of Age'. *Nature Reviews. Immunology* 10 (9): 645–656.

Munn, David H, and Andrew L Mellor. 2007. 'Indoleamine 2,3-Dioxygenase and Tumor-Induced Tolerance'. *The Journal of Clinical Investigation* 117 (5) (May): 1147–1154.

Munn, David H, Madhav D Sharma, Babak Baban, Heather P Harding, Yuhong Zhang, David Ron, and Andrew L Mellor. 2005. 'GCN2 Kinase in T Cells Mediates Proliferative Arrest and Anergy Induction in Response to Indoleamine 2,3-Dioxygenase'. *Immunity* 22 (5) (May): 633–642.

Munn, David H., Min Zhou, John T. Attwood, Igor Bondarev, Simon J. Conway, Brendan Marshall, Corrie Brown, and Andrew L. Mellor. 1998. 'Prevention of Allogeneic Fetal Rejection by Tryptophan Catabolism'. *Science* 281 (5380) (August 21): 1191–1193.

Bibliography

Murali-Krishna, K, L L Lau, S Sambhara, F Lemonnier, J Altman, and R Ahmed. 1999. 'Persistence of Memory CD8 T Cells in MHC Class I-Deficient Mice'. *Science (New York, N.Y.)* 286 (5443): 1377–1381.

Newrzela, Sebastian, Kerstin Cornils, Tim Heinrich, Julia Schläger, Ji-Hee Yi, Olga Lysenko, Janine Kimpel, Boris Fehse, and Dorothee von Laer. 2011. 'Retroviral Insertional Mutagenesis Can Contribute to Immortalization of Mature T Lymphocytes'. *Molecular Medicine (Cambridge, Mass.)* 17 (11-12): 1223–1232.

Nienhuis, Arthur W, Cynthia E Dunbar, and Brian P Sorrentino. 2006. 'Genotoxicity of Retroviral Integration in Hematopoietic Cells'. *Molecular Therapy: The Journal of the American Society of Gene Therapy* 13 (6) (June): 1031–1049.

O'Brien, Thomas F, Balachandra K Gorentla, Danli Xie, Sruti Srivatsan, Ian X McLeod, You-Wen He, and Xiao-Ping Zhong. 2011. 'Regulation of T-Cell Survival and Mitochondrial Homeostasis by TSC1'. *European Journal of Immunology* 41 (11) (November): 3361–3370.

Ohtani, Masashi, Shigenori Nagai, Shuhei Kondo, Shinta Mizuno, Kozue Nakamura, Masanobu Tanabe, Tsutomu Takeuchi, Satoshi Matsuda, and Shigeo Koyasu. 2008. 'Mammalian Target of Rapamycin and Glycogen Synthase Kinase 3 Differentially Regulate Lipopolysaccharide-Induced Interleukin-12 Production in Dendritic Cells'. *Blood* 112 (3) (August 1): 635–643.

Pagès, Franck, Anne Berger, Matthieu Camus, Fatima Sanchez-Cabo, Anne Costes, Robert Molidor, Bernhard Mlecnik, et al. 2005. 'Effector Memory T Cells, Early Metastasis, and Survival in Colorectal Cancer'. *The New England Journal of Medicine* 353 (25) (December 22): 2654–2666.

Papagno, Laura, Celsa A Spina, Arnaud Marchant, Mariolina Salio, Nathalie Rufer, Susan Little, Tao Dong, et al. 2004. 'Immune Activation and CD8+ T-Cell Differentiation towards Senescence in HIV-1 Infection'. *PLoS Biology* 2 (2) (February): E20.

Park, Yoon, Hyung-Seung Jin, Justine Lopez, Chris Elly, Gisen Kim, Masako Murai, Mitchell Kronenberg, and Yun-Cai Liu. 2013. 'TSC1 Regulates the Balance between Effector and Regulatory T Cells'. *The Journal of Clinical Investigation* (November 25): 5165-5178.

Bibliography

Patsoukis, Nikolaos, Julia Brown, Victoria Petkova, Fang Liu, Lequn Li, and Vassiliki A Boussiotis. 2012. 'Selective Effects of PD-1 on Akt and Ras Pathways Regulate Molecular Components of the Cell Cycle and Inhibit T Cell Proliferation'. *Science Signaling* 5 (230): ra46.

Pearce, Erika L, Matthew C Walsh, Pedro J Cejas, Gretchen M Harms, Hao Shen, Li-San Wang, Russell G Jones, and Yongwon Choi. 2009. 'Enhancing CD8 T-Cell Memory by Modulating Fatty Acid Metabolism'. *Nature* 460 (7251) (July 2): 103–107.

Perro, M, J Tsang, S-A Xue, D Escors, M Cesco-Gaspere, C Pospori, L Gao, et al. 2010. 'Generation of Multi-Functional Antigen-Specific Human T-Cells by Lentiviral TCR Gene Transfer'. *Gene Therapy* 17 (6) (June): 721–732.

Plumlee, Courtney R, Brian S Sheridan, Basak B Cicek, and Leo Lefrançois. 2013. 'Environmental Cues Dictate the Fate of Individual CD8+ T Cells Responding to Infection'. *Immunity* 39 (2) (August 22): 347–356.

Pogulis, R J, and L R Pease. 1998. 'A Retroviral Vector That Directs Simultaneous Expression of Alpha and Beta T Cell Receptor Genes'. *Human Gene Therapy* 9 (15) (October 10): 2299–2304.

Porter, David L, Bruce L Levine, Michael Kalos, Adam Bagg, and Carl H June. 2011. 'Chimeric Antigen Receptor-Modified T Cells in Chronic Lymphoid Leukemia'. *The New England Journal of Medicine* 365 (8) (August 25): 725–733.

Powell, Jonathan D, Emily B Heikamp, Kristen N Pollizzi, and Adam T Waickman. 2013. 'A Modified Model of T-Cell Differentiation Based on mTOR Activity and Metabolism'. *Cold Spring Harbor Symposia on Quantitative Biology* (October 7).

Qureshi, Omar S, Yong Zheng, Kyoko Nakamura, Kesley Attridge, Claire Manzotti, Emily M Schmidt, Jennifer Baker, et al. 2011. 'Trans-Endocytosis of CD80 and CD86: A Molecular Basis for the Cell-Extrinsic Function of CTLA-4'. *Science (New York, N.Y.)* 332 (6029) (April 29): 600–603.

Rabinovich, Gabriel A, Dmitry Gabrilovich, and Eduardo M Sotomayor. 2007. 'Immunosuppressive Strategies That Are Mediated by Tumor Cells'. *Annual Review of Immunology* 25: 267–296.

Rachmilewitz, Jacob. 2008. 'Serial Triggering Model'. *Advances in Experimental Medicine and Biology* 640: 95–102.

Bibliography

Ralph, P. 1973. 'Retention of Lymphocyte Characteristics by Myelomas and Theta + -Lymphomas: Sensitivity to Cortisol and Phytohemagglutinin'. *Journal of Immunology (Baltimore, Md.: 1950)* 110 (6): 1470–1475.

Rao, Rajesh R, Qingsheng Li, Kunle Odunsi, and Protul A Shrikant. 2010. 'The mTOR Kinase Determines Effector versus Memory CD8+ T Cell Fate by Regulating the Expression of Transcription Factors T-Bet and Eomesodermin'. *Immunity* 32 (1) (January 29): 67–78.

Restifo, Nicholas P, Mark E Dudley, and Steven A Rosenberg. 2012. 'Adoptive Immunotherapy for Cancer: Harnessing the T Cell Response'. *Nature Reviews. Immunology* 12 (4) (April): 269–281.

Restifo, Nicholas P, and Luca Gattinoni. 2013. 'Lineage Relationship of Effector and Memory T Cells'. *Current Opinion in Immunology* 25 (5) (October): 556–563.

Riese, Matthew J, Liang-Chuan S Wang, Edmund K Moon, Rohan P Joshi, Anjana Ranganathan, Carl H June, Gary A Koretzky, and Steven M Albelda. 2013. 'Enhanced Effector Responses in Activated CD8+ T Cells Deficient in Diacylglycerol Kinases'. *Cancer Research* 73 (12) (June 15): 3566–3577.

Robbins, Paul F, Richard A Morgan, Steven A Feldman, James C Yang, Richard M Sherry, Mark E Dudley, John R Wunderlich, et al. 2011. 'Tumor Regression in Patients with Metastatic Synovial Cell Sarcoma and Melanoma Using Genetically Engineered Lymphocytes Reactive with NY-ESO-1'. *Journal of Clinical Oncology: Official Journal of the American Society of Clinical Oncology* 29 (7) (March 1): 917–924.

Roccio, M, J L Bos, and F J T Zwartkruis. 2005. 'Regulation of the Small GTPase Rheb by Amino Acids'. *Oncogene* 25 (5): 657–664.

Rodriguez, Paulo C, David G Quiceno, and Augusto C Ochoa. 2007. 'L-Arginine Availability Regulates T-Lymphocyte Cell-Cycle Progression'. *Blood* 109 (4) (February 15): 1568–1573.

Rodriguez, Paulo C., David G. Quiceno, Jovanny Zabaleta, Blair Ortiz, Arnold H. Zea, Maria B. Piazuelo, Alberto Delgado, et al. 2004. 'Arginase I Production in the Tumor Microenvironment by Mature Myeloid Cells Inhibits T-Cell Receptor Expression and Antigen-Specific T-Cell Responses'. *Cancer Research* 64 (16): 5839 –5849.

Bibliography

Rosenberg, S A, B S Packard, P M Aebersold, D Solomon, S L Topalian, S T Toy, P Simon, M T Lotze, J C Yang, and C A Seipp. 1988. 'Use of Tumor-Infiltrating Lymphocytes and Interleukin-2 in the Immunotherapy of Patients with Metastatic Melanoma. A Preliminary Report'. *The New England Journal of Medicine* 319 (25) (December 22): 1676–1680.

Rosenberg, S A, P Spiess, and R Lafreniere. 1986. 'A New Approach to the Adoptive Immunotherapy of Cancer with Tumor-Infiltrating Lymphocytes'. *Science (New York, N.Y.)* 233 (4770): 1318–1321.

Rosenberg, Steven A, James C Yang, Richard M Sherry, Udai S Kammula, Marybeth S Hughes, Giao Q Phan, Deborah E Citrin, et al. 2011. 'Durable Complete Responses in Heavily Pretreated Patients with Metastatic Melanoma Using T-Cell Transfer Immunotherapy'. *Clinical Cancer Research: An Official Journal of the American Association for Cancer Research* 17 (13) (July 1): 4550–4557.

Roux, Philippe P., David Shahbazian, Hieu Vu, Marina K. Holz, Michael S. Cohen, Jack Taunton, Nahum Sonenberg, and John Blenis. 2007. 'RAS/ERK Signaling Promotes Site-Specific Ribosomal Protein S6 Phosphorylation via RSK and Stimulates Cap-Dependent Translation'. *Journal of Biological Chemistry* 282 (19) (November 5): 14056–14064.

Sabatini, D M, H Erdjument-Bromage, M Lui, P Tempst, and S H Snyder. 1994. 'RAFT1: A Mammalian Protein That Binds to FKBP12 in a Rapamycin-Dependent Fashion and Is Homologous to Yeast TORs'. *Cell* 78 (1): 35–43.

Salmond, Robert J, Juliet Emery, Klaus Okkenhaug, and Rose Zamoyska. 2009. 'MAPK, Phosphatidylinositol 3-Kinase, and Mammalian Target of Rapamycin Pathways Converge at the Level of Ribosomal Protein S6 Phosphorylation to Control Metabolic Signaling in CD8 T Cells'. *Journal of Immunology (Baltimore, Md.: 1950)* 183 (11): 7388–7397.

Sancak, Yasemin, Liron Bar-Peled, Roberto Zoncu, Andrew L Markhard, Shigeyuki Nada, and David M Sabatini. 2010. 'Ragulator-Rag Complex Targets mTORC1 to the Lysosomal Surface and Is Necessary for Its Activation by Amino Acids'. *Cell* 141 (2): 290–303. doi:10.1016/j.cell.2010.02.024.

Sancak, Yasemin, Timothy R Peterson, Yoav D Shaul, Robert A Lindquist, Carson C Thoreen, Liron Bar-Peled, and David M Sabatini. 2008. 'The Rag GTPases Bind

Raptor and Mediate Amino Acid Signaling to mTORC1'. *Science (New York, N.Y.)* 320 (5882) (June 13): 1496–1501.

Sancak, Yasemin, Carson C Thoreen, Timothy R Peterson, Robert A Lindquist, Seong A Kang, Eric Spooner, Steven A Carr, and David M Sabatini. 2007. 'PRAS40 Is an Insulin-Regulated Inhibitor of the mTORC1 Protein Kinase'. *Molecular Cell* 25 (6) (March 23): 903–915.

Sanjabi, Shomyseh, Munir M Mosaheb, and Richard A Flavell. 2009. 'Opposing Effects of TGF-Beta and IL-15 Cytokines Control the Number of Short-Lived Effector CD8+ T Cells'. *Immunity* 31 (1): 131–144.

Sarkar, Surojit, Vandana Kalia, W Nicholas Haining, Bogumila T Konieczny, Shruti Subramaniam, and Rafi Ahmed. 2008. 'Functional and Genomic Profiling of Effector CD8 T Cell Subsets with Distinct Memory Fates'. *The Journal of Experimental Medicine* 205 (3) (March 17): 625–640.

Saucedo, Leslie J, Xinsheng Gao, Dominic A Chiarelli, Ling Li, Duoija Pan, and Bruce A Edgar. 2003. 'Rheb Promotes Cell Growth as a Component of the insulin/TOR Signalling Network'. *Nature Cell Biology* 5 (6) (June): 566–571.

Sauer, Stephan, Ludovica Bruno, Arnulf Hertweck, David Finlay, Marion Leleu, Mikhail Spivakov, Zachary A Knight, et al. 2008. 'T Cell Receptor Signaling Controls Foxp3 Expression via PI3K, Akt, and mTOR'. *Proceedings of the National Academy of Sciences of the United States of America* 105 (22) (June 3): 7797–7802.

Schenten, Dominik, and Ruslan Medzhitov. 2011. 'The Control of Adaptive Immune Responses by the Innate Immune System'. *Advances in Immunology* 109: 87–124.

Schreiber, Robert D, Lloyd J Old, and Mark J Smyth. 2011. 'Cancer Immunoediting: Integrating Immunity's Roles in Cancer Suppression and Promotion'. *Science (New York, N.Y.)* 331 (6024) (March 25): 1565–1570.

Sena, Laura A, Sha Li, Amit Jairaman, Murali Prakriya, Teresa Ezponda, David A Hildeman, Chyung-Ru Wang, et al. 2013. 'Mitochondria Are Required for Antigen-Specific T Cell Activation through Reactive Oxygen Species Signaling'. *Immunity* 38 (2) (February 21): 225–236.

Serafini, Paolo, Kristen Meckel, Michael Kelso, Kimberly Noonan, Joseph Califano, Wayne Koch, Luigi Dolcetti, Vincenzo Bronte, and Ivan Borrello. 2006. 'Phosphodiesterase-5 Inhibition Augments Endogenous Antitumor Immunity by

Reducing Myeloid-Derived Suppressor Cell Function'. *The Journal of Experimental Medicine* 203 (12) (November 27): 2691–2702.

Serrone, L, M Zeuli, F M Sega, and F Cognetti. 2000. 'Dacarbazine-Based Chemotherapy for Metastatic Melanoma: Thirty-Year Experience Overview'. *Journal of Experimental & Clinical Cancer Research: CR* 19 (1): 21–34.

Shankaran, V, H Ikeda, A T Bruce, J M White, P E Swanson, L J Old, and R D Schreiber. 2001. 'IFNgamma and Lymphocytes Prevent Primary Tumour Development and Shape Tumour Immunogenicity'. *Nature* 410 (6832) (April 26): 1107–1111.

Sharma, Madhav D, Babak Baban, Phillip Chandler, De-Yan Hou, Nagendra Singh, Hideo Yagita, Miyuki Azuma, Bruce R Blazar, Andrew L Mellor, and David H Munn. 2007. 'Plasmacytoid Dendritic Cells from Mouse Tumor-Draining Lymph Nodes Directly Activate Mature Tregs via Indoleamine 2,3-Dioxygenase'. *The Journal of Clinical Investigation* 117 (9) (September): 2570–2582.

Silva, Jose M, Mamie Z Li, Ken Chang, Wei Ge, Michael C Golding, Richard J Rickles, Despina Siolas, et al. 2005. 'Second-Generation shRNA Libraries Covering the Mouse and Human Genomes'. *Nature Genetics* 37 (11) (November): 1281–1288.

Simpson, Tyler R, Fubin Li, Welby Montalvo-Ortiz, Manuel A Sepulveda, Katharina Bergerhoff, Frederick Arce, Claire Roddie, et al. 2013. 'Fc-Dependent Depletion of Tumor-Infiltrating Regulatory T Cells Co-Defines the Efficacy of Anti-CTLA-4 Therapy against Melanoma'. *The Journal of Experimental Medicine* 210 (9) (August 26): 1695–1710.

Sinclair, Linda V, David Finlay, Carmen Feijoo, Georgina H Cornish, Alex Gray, Ann Ager, Klaus Okkenhaug, Thijs J Hagenbeek, Hergen Spits, and Doreen A Cantrell. 2008. 'Phosphatidylinositol-3-OH Kinase and Nutrient-Sensing mTOR Pathways Control T Lymphocyte Trafficking'. *Nature Immunology* 9 (5) (May): 513–521.

Sinclair, Linda V, Julia Rolf, Elizabeth Emslie, Yun-Bo Shi, Peter M Taylor, and Doreen A Cantrell. 2013. 'Control of Amino-Acid Transport by Antigen Receptors Coordinates the Metabolic Reprogramming Essential for T Cell Differentiation'. *Nature Immunology* 14 (5) (May): 500–508.

Bibliography

Smith-Garvin, Jennifer E., Gary A. Koretzky, and Martha S. Jordan. 2009. 'T Cell Activation'. *Annual Review of Immunology* 27 (1) (April): 591–619.

Spranger, Stefani, Robbert M Spaapen, Yuanyuan Zha, Jason Williams, Yuru Meng, Thanh T Ha, and Thomas F Gajewski. 2013. 'Up-Regulation of PD-L1, IDO, and Tregs in the Melanoma Tumor Microenvironment Is Driven by CD8+ T Cells'. *Science Translational Medicine* 5 (200) (August 28): 200ra116.

Stemberger, Christian, Katharina M Huster, Martina Koffler, Florian Anderl, Matthias Schiemann, Hermann Wagner, and Dirk H Busch. 2007. 'A Single Naive CD8+ T Cell Precursor Can Develop into Diverse Effector and Memory Subsets'. *Immunity* 27 (6) (December): 985–997.

Stocker, Hugo, Thomas Radimerski, Benno Schindelholz, Franz Wittwer, Priyanka Belawat, Pierre Daram, Sebastian Breuer, George Thomas, and Ernst Hafen. 2003. 'Rheb Is an Essential Regulator of S6K in Controlling Cell Growth in Drosophila'. *Nature Cell Biology* 5 (6) (June): 559–565.

Stutman, O. 1974. 'Tumor Development after 3-Methylcholanthrene in Immunologically Deficient Athymic-Nude Mice'. *Science (New York, N.Y.)* 183 (4124): 534–36.

Sukumar, Madhusudhanan, Jie Liu, Yun Ji, Murugan Subramanian, Joseph G Crompton, Zhiya Yu, Rahul Roychoudhuri, et al. 2013. 'Inhibiting Glycolytic Metabolism Enhances CD8+ T Cell Memory and Antitumor Function'. *The Journal of Clinical Investigation* 123 (10) (October 1): 4479–4488.

Szabo, Susanne J, Brandon M Sullivan, Claudia Stemmann, Abhay R Satoskar, Barry P Sleckman, and Laurie H Glimcher. 2002. 'Distinct Effects of T-Bet in TH1 Lineage Commitment and IFN-Gamma Production in CD4 and CD8 T Cells'. *Science (New York, N.Y.)* 295 (5553) (January 11): 338–342.

Takemoto, Naofumi, Andrew M Intlekofer, John T Northrup, E John Wherry, and Steven L Reiner. 2006. 'Cutting Edge: IL-12 Inversely Regulates T-Bet and Eomesodermin Expression during Pathogen-Induced CD8+ T Cell Differentiation'. *Journal of Immunology (Baltimore, Md.: 1950)* 177 (11): 7515–7519.

Terabe, Masaki, and Jay A Berzofsky. 2004. 'Immunoregulatory T Cells in Tumor Immunity'. *Current Opinion in Immunology* 16 (2) (April): 157–162.

Bibliography

Tey, Siok-Keen, Gianpietro Dotti, Cliona M Rooney, Helen E Heslop, and Malcolm K Brenner. 2007. 'Inducible Caspase 9 Suicide Gene to Improve the Safety of Allodepleted T Cells after Haploidentical Stem Cell Transplantation'. *Biology of Blood and Marrow Transplantation: Journal of the American Society for Blood and Marrow Transplantation* 13 (8) (August): 913–924.

Thomas, Sharyn, Shao-An Xue, Charles R M Bangham, Bent K Jakobsen, Emma C Morris, and Hans J Stauss. 2011. 'Human T Cells Expressing Affinity-Matured TCR Display Accelerated Responses but Fail to Recognize Low Density of MHC-Peptide Antigen'. *Blood* 118 (2) (July 14): 319–329.

Thoreen, Carson C, Lynne Chantranupong, Heather R Keys, Tim Wang, Nathanael S Gray, and David M Sabatini. 2012. 'A Unifying Model for mTORC1-Mediated Regulation of mRNA Translation'. *Nature* 485 (7396) (May 3): 109–113.

Travis, Mark A, and Dean Sheppard. 2013. 'TGF-B Activation and Function in Immunity'. *Annual Review of Immunology*, December. Online publication.

Uyttenhove, Catherine, Luc Pilotte, Ivan Théate, Vincent Stroobant, Didier Colau, Nicolas Parmentier, Thierry Boon, and Benoît J Van den Eynde. 2003. 'Evidence for a Tumoral Immune Resistance Mechanism Based on Tryptophan Degradation by Indoleamine 2,3-Dioxygenase'. *Nature Medicine* 9 (10) (October): 1269–1274.

Vajdic, Claire M, Stephen P McDonald, Margaret R E McCredie, Marina T van Leeuwen, John H Stewart, Matthew Law, Jeremy R Chapman, Angela C Webster, John M Kaldor, and Andrew E Grulich. 2006. 'Cancer Incidence before and after Kidney Transplantation'. *JAMA: The Journal of the American Medical Association* 296 (23) (December 20): 2823–2831.

Van der Bruggen, P, C Traversari, P Chomez, C Lurquin, E De Plaen, B Van den Eynde, A Knuth, and T Boon. 1991. 'A Gene Encoding an Antigen Recognized by Cytolytic T Lymphocytes on a Human Melanoma'. *Science (New York, N.Y.)* 254 (5038): 1643–1647.

Van Houdt, Inge S, Berbel J R Sluijter, Laura M Moesbergen, Wim M Vos, Tanja D de Gruijl, Barbara G Molenkamp, Alfons J M van den Eertwegh, et al. 2008. 'Favorable Outcome in Clinically Stage II Melanoma Patients Is Associated with the Presence of Activated Tumor Infiltrating T-Lymphocytes and Preserved MHC Class I Antigen Expression'. *International Journal of Cancer. Journal International Du Cancer* 123 (3) (August 1): 609–615.

Bibliography

Van Pel, A, F Vessière, and T Boon. 1983. 'Protection against Two Spontaneous Mouse Leukemias Conferred by Immunogenic Variants Obtained by Mutagenesis'. *The Journal of Experimental Medicine* 157 (6): 1992–2001.

VanderVeen, Nathan, Christopher Paran, Jonathan Krasinkiewicz, Lili Zhao, Donna Palmer, Shawn Hervey-Jumper, Philip Ng, Pedro R Lowenstein, and Maria G Castro. 2013. 'Effectiveness and Preclinical Safety Profile of Doxycycline to Be Used "off-Label" to Induce Therapeutic Transgene Expression in a Phase I Clinical Trial for Glioma'. *Human Gene Therapy. Clinical Development* 24 (3) (September): 116–126.

Vesely, Matthew D, Michael H Kershaw, Robert D Schreiber, and Mark J Smyth. 2011. 'Natural Innate and Adaptive Immunity to Cancer'. *Annual Review of Immunology* 29 (April 23): 235–271.

Waickman, Adam T, and Jonathan D Powell. 2012. 'mTOR, Metabolism, and the Regulation of T-Cell Differentiation and Function'. *Immunological Reviews* 249 (1) (September): 43–58.

Wang, Ruoning, Christopher P Dillon, Lewis Zhichang Shi, Sandra Milasta, Robert Carter, David Finkelstein, Laura L McCormick, et al. 2011. 'The Transcription Factor Myc Controls Metabolic Reprogramming upon T Lymphocyte Activation'. *Immunity* 35 (6): 871–882.

Wang, Ruoning, and Douglas R Green. 2012. 'Metabolic Checkpoints in Activated T Cells'. *Nature Immunology* 13 (10) (September 18): 907–915.

WARBURG, O. 1956. 'On Respiratory Impairment in Cancer Cells'. *Science (New York, N.Y.)* 124 (3215): 269–270.

Weichhart, Thomas, Giuseppina Costantino, Marko Poglitsch, Margit Rosner, Maximilian Zeyda, Karl M Stuhlmeier, Thomas Kolbe, et al. 2008. 'The TSC-mTOR Signaling Pathway Regulates the Innate Inflammatory Response'. *Immunity* 29 (4) (October 17): 565–577.

Wells, Andrew D. 2009. 'New Insights into the Molecular Basis of T Cell Anergy: Anergy Factors, Avoidance Sensors, and Epigenetic Imprinting'. *Journal of Immunology (Baltimore, Md.: 1950)* 182 (12): 7331–7341.

Bibliography

Weninger, W, M A Crowley, N Manjunath, and U H von Andrian. 2001. 'Migratory Properties of Naive, Effector, and Memory CD8(+) T Cells'. *The Journal of Experimental Medicine* 194 (7): 953–966.

Wilkie, Scott, May C I van Schalkwyk, Steve Hobbs, David M Davies, Sjoukje J C van der Stegen, Ana C Parente Pereira, Sophie E Burbridge, Carol Box, Suzanne A Eccles, and John Maher. 2012. 'Dual Targeting of ErbB2 and MUC1 in Breast Cancer Using Chimeric Antigen Receptors Engineered to Provide Complementary Signaling'. *Journal of Clinical Immunology* 32 (5) (October): 1059–1070.

Williams, Matthew A, and Michael J Bevan. 2007. 'Effector and Memory CTL Differentiation'. *Annual Review of Immunology* 25: 171–192.

Willimsky, Gerald, and Thomas Blankenstein. 2005. 'Sporadic Immunogenic Tumours Avoid Destruction by Inducing T-Cell Tolerance'. *Nature* 437 (7055) (September 1): 141–146.

Willimsky, Gerald, Melinda Czéh, Christoph Loddenkemper, Johanna Gellermann, Karin Schmidt, Peter Wust, Harald Stein, and Thomas Blankenstein. 2008. 'Immunogenicity of Premalignant Lesions Is the Primary Cause of General Cytotoxic T Lymphocyte Unresponsiveness'. *The Journal of Experimental Medicine* 205 (7) (July 7): 1687–1700.

Wolchok, Jedd D., Harriet Kluger, Margaret K. Callahan, Michael A. Postow, Naiyer A. Rizvi, Alexander M. Lesokhin, Neil H. Segal, et al. 2013. 'Nivolumab plus Ipilimumab in Advanced Melanoma'. *New England Journal of Medicine* 369 (2) (July 11): 122-133.

Xie, Dan-Li, Jinhong Wu, Yong-Liang Lou, and Xiao-Ping Zhong. 2012. 'Tumor Suppressor TSC1 Is Critical for T-Cell Anergy'. *Proceedings of the National Academy of Sciences of the United States of America* 109 (35) (August 28): 14152–14157.

Xue, S, L Gao, R Gillmore, G Bendle, A Holler, A M Downs, A Tsallios, et al. 2004. 'WT1-Targeted Immunotherapy of Leukaemia'. *Blood Cells, Molecules & Diseases* 33 (3) (December): 288–290.

Yang, Kai, Geoffrey Neale, Douglas R Green, Weifeng He, and Hongbo Chi. 2011. 'The Tumor Suppressor Tsc1 Enforces Quiescence of Naive T Cells to Promote Immune Homeostasis and Function'. *Nature Immunology* 12 (9): 888–897.

Bibliography

Yao, Shuyu, Bruno Fernando Buzo, Duy Pham, Li Jiang, Elizabeth J Taparowsky, Mark H Kaplan, and Jie Sun. 2013. 'Interferon Regulatory Factor 4 Sustains CD8(+) T Cell Expansion and Effector Differentiation'. *Immunity* (November 6): 833-845.

Yu, Yadong, Sheng Li, Xiang Xu, Yong Li, Kunliang Guan, Eddy Arnold, and Jianping Ding. 2005. 'Structural Basis for the Unique Biological Function of Small GTPase RHEB'. *The Journal of Biological Chemistry* 280 (17): 17093–17100.

Zaborske, John M, Jana Narasimhan, Li Jiang, Sheree A Wek, Kimberly A Dittmar, Florien Freimoser, Tao Pan, and Ronald C Wek. 2009. 'Genome-Wide Analysis of tRNA Charging and Activation of the eIF2 Kinase Gcn2p'. *The Journal of Biological Chemistry* 284 (37) (September 11): 25254–25267.

Zea, Arnold H, Paulo C Rodriguez, Michael B Atkins, Claudia Hernandez, Sabina Signoretti, Jovanny Zabaleta, David McDermott, et al. 2005. 'Arginase-Producing Myeloid Suppressor Cells in Renal Cell Carcinoma Patients: A Mechanism of Tumor Evasion'. *Cancer Research* 65 (8) (April 15): 3044–3048.

Zeiser, Robert, Vu H Nguyen, Jing-Zhou Hou, Andreas Beilhack, Elizabeth Zambricki, Martin Buess, Christopher H Contag, and Robert S Negrin. 2007. 'Early CD30 Signaling Is Critical for Adoptively Transferred CD4+CD25+ Regulatory T Cells in Prevention of Acute Graft-versus-Host Disease'. *Blood* 109 (5) (March 1): 2225–2233.

Zeng, Yan, Eric J Wagner, and Bryan R Cullen. 2002. 'Both Natural and Designed Micro RNAs Can Inhibit the Expression of Cognate mRNAs When Expressed in Human Cells'. *Molecular Cell* 9 (6): 1327–1333.

Zhang, L, Z Yu, P Muranski, D C Palmer, N P Restifo, S A Rosenberg, and R A Morgan. 2012. 'Inhibition of TGF-B Signaling in Genetically Engineered Tumor Antigen-Reactive T Cells Significantly Enhances Tumor Treatment Efficacy'. *Gene Therapy* (September 13): 575-580.

Zhang, Lin, Jose R Conejo-Garcia, Dionyssios Katsaros, Phyllis A Gimotty, Marco Massobrio, Giorgia Regnani, Antonis Makrigiannakis, et al. 2003. 'Intratumoral T Cells, Recurrence, and Survival in Epithelial Ovarian Cancer'. *The New England Journal of Medicine* 348 (3) (January 16): 203–213.

Zhang, Ling, Sid P Kerkar, Zhiya Yu, Zhili Zheng, Shicheng Yang, Nicholas P Restifo, Steven A Rosenberg, and Richard A Morgan. 2011. 'Improving Adoptive T

Cell Therapy by Targeting and Controlling IL-12 Expression to the Tumor Environment'. *Molecular Therapy: The Journal of the American Society of Gene Therapy* 19 (4) (April): 751–759.

Zhang, W, J Sloan-Lancaster, J Kitchen, R P Trible, and L E Samelson. 1998. 'LAT: The ZAP-70 Tyrosine Kinase Substrate That Links T Cell Receptor to Cellular Activation'. *Cell* 92 (1): 83–92.

Zheng, Yan, Greg M Delgoffe, Christian F Meyer, Waipan Chan, and Jonathan D Powell. 2009. 'Anergic T Cells Are Metabolically Anergic'. *Journal of Immunology (Baltimore, Md.: 1950)* 183 (10) (November 15): 6095–6101.

Zheng, Yong, Claire N Manzotti, Fiona Burke, Laure Dussably, Omar Qureshi, Lucy S K Walker, and David M Sansom. 2008. 'Acquisition of Suppressive Function by Activated Human CD4+ CD25- T Cells Is Associated with the Expression of CTLA-4 Not FoxP3'. *Journal of Immunology (Baltimore, Md.: 1950)* 181 (3): 1683–1691.

Zoncu, Roberto, Liron Bar-Peled, Alejo Efeyan, Shuyu Wang, Yasemin Sancak, and David M Sabatini. 2011. 'mTORC1 Senses Lysosomal Amino Acids through an inside-out Mechanism That Requires the Vacuolar H^+-ATPase'. *Science (New York, N.Y.)* 334 (6056): 678–683.

Zoncu, Roberto, Alejo Efeyan, and David M Sabatini. 2011. 'mTOR: From Growth Signal Integration to Cancer, Diabetes and Ageing'. *Nature Reviews. Molecular Cell Biology* 12 (1) (January): 21–35.

Zorn, E, and T Hercend. 1999. 'A Natural Cytotoxic T Cell Response in a Spontaneously Regressing Human Melanoma Targets a Neoantigen Resulting from a Somatic Point Mutation'. *European Journal of Immunology* 29 (2) (February): 592–601.